AUTOMATED SAFETY ANALYSIS OF CONSTRUCTION SITE ACTIVITIES USING SPATIO-TEMPORAL DATA

A Dissertation
Presented to
The Academic Faculty

by

Tao Cheng

In Partial Fulfillment
of the Requirements for the Degree
Doctor of Philosophy in the
School of Civil and Environmental Engineering

Georgia Institute of Technology
May 2013

AUTOMATED SAFETY ANALYSIS OF CONSTRUCTION SITE ACTIVITIES USING SPATIO-TEMPORAL DATA

Approved by:

Dr. Jochen Teizer, Advisor
School of Civil and Environmental Engineering
Georgia Institute of Technology

Dr. Patricio A. Vela
School of Electrical and Computer Engineering
Georgia Institute of Technology

Dr. Lawrence F. Kahn
School of Civil and Environmental Engineering
Georgia Institute of Technology

Dr. Ioannis Brilakis
Department of Engineering
University of Cambridge

Professor Charles M. Eastman
Colleges of Computing and Architecture
Georgia Institute of Technology

Date Approved: March 22, 2013

To my mother, Guohua Li

ACKNOWLEDGEMENTS

I would like to sincerely and heartily express my gratitude to my advisor, Professor Jochen Teizer, for the support he gave me throughout my doctoral research. I am sure it would have not been possible without his help. The days we spent together collecting various data from numerous construction sites at Cliffside NC, Savannah GA, and on Georgia Tech campus are the ones that immediately come to my mind. These valuable data laid the foundation of this research work. Another mentor who has contributed a lot through his ideas and detailed feedback is Professor Patricio A. Vela. His feedback and expertise in computing and data processing techniques inspired me thoroughly in the development of several key algorithms in this research. I would also like to thank the other members of my doctoral committee, Professors Lawrence F. Kahn, Charles Eastman, and Ioannis Brilakis, for their constant encouragement, insightful comments and constructive criticism, which has helped me to considerably improve this dissertation.

Studying at a top institution like Georgia Tech is very demanding and one cannot survive without having friends. I thoroughly enjoyed my time I spent working with construction engineering students at Rapids Lab, especially Sijie Zhang, Soumitry Jagadev Ray, Nipesh Pradhananga, Eric Marks, Manu Venugopal, and Ben Allread among others. They were always around whenever I needed any technical help. The field trips and social activities that we undertook have bonded us into a family and I look forward to continuing this relationship. Besides my labmates, I could not have asked for better roommates than Laxman Pandey and Yihai Fang with whom I had delightful times as we shared the same favorite soccer team, created our own cooking recipes, and competed in games. I consider myself extremely lucky to have known Yu Liu, Pengzi Yu, Dandan Zheng, Shanshan Zou, Yu Zhu, Bingxian Luo, Jun Yang, and Nan Zhao. Without them, I could not have had fantastic journeys to numerous attractions and national parks inside and outside the US. Spending time and traveling with them helped me relax and unwind after tough work.

I would like to extend my heartfelt gratitude to my uncle Qing Zhao, aunt Jiali Tao, my cousins Michael Zhao, Zhongyuan Yu, and Xi Du Woo. Their continuous

encouragements and supports helped me go through the perplex situation when I questioned myself. During my absence, my brothers Yang Liu and Yufei Zhang took care of my family back in Beijing. Personally, I would like to specially thank my beloved girlfriend Xiaoxi Liu who has been a source of constant support. Without them, I could not have devoted myself wholeheartedly to pursue my doctoral study.

Finally, I would like to thank my mother and grandparents for their blessings and support. I was born to a family with a long history of having excellent educators and researchers in the past century in China. They had an expectation of me to continue the family tradition. Meeting their expectations by accomplishing my doctoral degree has instilled a sense of pride and to them I dedicate this thesis.

TABLE OF CONTENTS

LIST OF TABLES

LIST OF FIGURES

LIST OF SYMBOLS OR ABBREVIATIONS

AOA	Angle of Arrival
ASME	American Society of Mechanical Engineers
BBS	Behavior-Based Safety
BIM	Building Information Modeling
BLS	Bureau of Labor Statistics
CDC	Centers for Disease Control and Prevention
CFOI	Census of Fatal Occupational Injuries
CMU	Concrete Masonry Unit
CPMS	Construction Productivity Metric System
CPWR	Center to Protect Workers' Right
CQS	Craftsman Questionnaire Sampling
CVE	Collaborative Virtual Environment
DQI	Data Quality Indicator
DBSCAN	Density-Based Spatial Clustering of Applications with Noise
ECG	Electrocardiograph
EMG	Electromyography
ENR	Engineering News Record
FDS	Forman Delay Survey
FOV	Field of View
GPS	Global Positioning System
GVA	Gross Value Added
IIF	Injuries, Illness and Fatalities
ILO	International Labour Organization
IR	OSHA recordable Injury Rate
JHA	Jobsite Hazard Analysis
KLEMS	Capital, Labor, Energy, Materials, and Services
LADAR	Light Detection And Ranging
LODs	Level of Details
LOS	Line of Sight

LTC	Lost Time Cast Rate
MFP	Multi Factor Productivity
MMH	Manual Material Handling
MPDM	Method Productivity Delay Model
MSIs	Musculoskeletal Injuris
NIOSH	National Institute for Occupational Safety and Health
OSHA	Occupational Safety and Health Administration
PCL	Point Clouds Library
PHI	Proximity Hazard Indicator
PIMs	Productivity Improving Methods
PMMs	Productivity Measuring Methods
PPE	Personal Protection Equipment
PSM	Physiological Status Monitoring
QA/QC	Quality Assessment and Quality Control
RFID	Radio Frequency Identification
RMS	Root Mean Square
RSSI	Received Signal Strength Indication
RTLS	Real-time Locate Sensing
RTS	Robotic Total Station
SFP	Single Factor Productivity
SNs	Sensor Networks
TDOA	Time Difference of Arrival
TOA	Time of Arrival
UTC	Coordinated Universal Time
UWB	Ultra Wideband
VE	Virtual Environment
VMU	Vector Magnitude Unit
VR	Virtual Reality
VRML	Virtual Reality Modeling Language
WSNs	Wireless Sensor Networks

SUMMARY

During the past 10 years, construction was the leading industry of occupational fatalities when compared to other goods producing industries in the US. This is partially attributed to ineffective safety management strategies, specifically lack of automated construction equipment and worker monitoring. Currently, worker safety performance is measured and recorded manually, assessed subjectively, and the resulting performance information is infrequently shared among selected or all project stakeholders. Accurate and emerging remote sensing technology provides critical spatio-temporal data that have the potential to automate and advance the safety monitoring of construction processes.

This doctoral research focuses on pro-active safety utilizing radio-frequency location tracking (Ultra Wideband) and real-time three-dimensional (3D) immersive data visualization technologies. The objective of the research is to create a model that can automatically analyze the spatio-temporal data of the main construction resources (personnel, materials, and equipment), and automatically measure, assess, and visualize worker's safety performance. The research scope is limited to human-equipment interaction in a complex construction site layout where proximities among construction resources are omnipresent. In order to advance the understanding of human-equipment proximity issues, extensive data have been collected in various field trials and from projects with multiple scales. Computational algorithms developed in this research process the data to provide spatio-temporal information that is crucial for construction activity monitoring and analysis. Results indicate that worker's safety performance of selected activities can be automatically and objectively measured using the developed model.

The major contribution of this research is the creation of a proximity hazards assessment model to automatically analyze spatio-temporal data of construction resources, and measure, evaluate, and visualize their safety performance. This research has potential to complement the current safety measures in construction industry, as it can determine and communicate automatically safe and unsafe conditions to various project participants located on the field or remotely.

CHAPTER I

INTRODUCTION

This chapter introduces the overview and challenge in construction safety. The motivation of this dissertation is explained, followed by a brief definition of the problem. Then the research scope and contribution are stated. At the end of this chapter, an outline of the thesis is provided to help the readers understand the flow of the thesis.

1.1 Overview

In 2010, the Gross Value Added (GVA) of the construction industry in the US was $510.5 billion, 3.5% of the gross domestic product at purchaser's prices [1]. After shedding about 2.5 million jobs since the economic recession, the construction industry offered employment to approximately 6% of the total civilian employed population in 2010 [2]. In the meantime, the construction industry is one of the most dangerous industries, which has witnessed continually injury and fatality during the last decades. According to the Bureau of Labor Statistics (BLS), construction workers account for more than 16% of total fatal occupational injuries of the overall industry in the same year [3]. During year 2006-2010, more than 10 workers out of 100,000 were killed in construction, a figure twice that of general industry [4]. Within a ten years period (1992-2002), a total of 12,075 fatalities have resulted in approximately a $10 billion loss to the American construction industry [5]. A conservative report by the International Labor Organization (ILO) estimates that globally, there are an annual 60,000 fatalities related to construction work, and many hundreds of thousands more suffer serious injuries, as well as ill health [6].

1.2 Motivation and Problem Definition

This research intends to improve the understanding and measurement of workers' safety performances in the construction industry.

Even though the safety performance has been improved during the last decade, the construction industry is still leading in work related fatalities relative to other industries [7]. Apart from the high occupational fatality and injury rates, what is absent is

a systematic and proactive approach to deriving measures of the on-site safety performance and how they link to the risk control process [8]. Therefore, it is necessary to have a reliable measuring approach for safety performance, which should give an indication of how well a construction activity, task and even the entire project is being executed in the aspect of safety. Moreover, certain changes of the level of safety performance should be able to be reflected by this measure [9].

There are a variety of safety performance measures that have been in usage and/or introduced in the construction industry, which fall into two major categories: Lagging and Leading Indicators. In economics, these two terms are defined as [10]:

- *Lagging (or Trailing, Downstream) Indicators* are indicators that usually change after the economy as a whole changes.
- *Leading (or Upstream) Indicators* are indicators that usually change before the economy as a whole does.

The lagging indicators to measuring safety performance are based on the fatality and injury statistics. Examples include: lost workday/restricted work activity injuries, and Occupational Safety and Health Administration (OSHA) recordable injuries. Although this type of indicators can accurately reflect the trend of safety performance, it can neither be used to prevent the occurrence of injuries, nor reflect the potential severity of an event, merely the consequence [11]. The other type of safety performance measures, leading indicators, are able to predict the future safety performance based on selected criteria [12]. Typical Examples include: Safety training survey, safety meeting survey, and Behavior-Based Safety (BBS). Instead of focusing on the end result, the use of leading indicators emphasize on the monitoring of work processes. Hence, modifications or improvements can be made before injuries actually occur if indicators show unacceptable result [12].

The implementation of leading indicators relies on the data to be collected from on-site inspections. Since the data collection is only performed manually in the current construction industry [13], the nature of resulting safety measurement is subjective and varies considerably from inspector to inspector [9]. Therefore, there needs to be a method

that can measure the construction safety performances in an objective, consistent and reliable manner. Accurate and emerging remote sensing technology provides critical spatio-temporal data that have the potential to automate and advance the safety measurement of construction processes.

1.3 Research Questions

The central theme of this thesis is:

How to implement emerging sensing technologies in combination with innovative data processing techniques to automatically and reliably detect, record, analyze, and assess the on-site safety, health as well as productivity performance of selected activities, thereby proactively improving the understanding and monitoring of construction process.

Five major research questions raised in this research and investigated are as follows:

- *What hazards exist on a construction site?*
  Workers are always exposed to various hazardous conditions on a construction site. It is essential to identify and focus on those hazards that result in significant fatal and nonfatal injuries.
- *Can technologies be reliably used to collect data from construction resources?*
  In order to be implemented for activity monitoring, the performance of sensing technology in harsh construction environment has to be evaluated, lack of which causes uncertainty and frustrates the accuracy of the result.
- *What type of hazards can be detected using remote sensing technology?*
  Accurate safety performance measuring requires a comprehensive understanding of the construction site settings. Automatic identification of the potential hazards rapidly allocates the situations that unsafe performance will likely to occur.
- *How to detect and measure the interactions between workers and identified hazards?*

There is a need to analyze the interaction between workers and hazards. An automated approach to analyze crucial spatio-temporal information is required for generating new measures of safety performance.

- *How to reproduce the detected unsafe behavior share the information among project participants?*

  When the safety performance information has been achieved, there is a need to rapidly share such information among project participants. Unsafe behavior can be corrected so as to prevent the occurrence of severe consequence. In addition, such information can be used for safety training and educations.

1.4 Contribution

This thesis focuses on proactive safety utilizing automated construction site sensing and information technology. This thesis comes at a crucial juncture, since the measures of safety performance of construction site work have hardly been objective. The major contributions of the thesis are introduced as follow:

- This research creates an assessment model that leverages various sensing technologies to automatically analyze spatio-temporal data of construction resources (workers, equipment and materials), and automatically identify, evaluate, and visualize their safety performance. The framework is also extended for the study of work ergonomic analysis and continuous labor productivity analysis
- A test-bed is developed to evaluate the performance of various real-time tracking technologies in harsh construction environment. It is demonstrated in this thesis, a commercial-available active Radio Frequency Identification (RFID) technology, Ultra Wideband (UWB), can reliably record real-time spatio-temporal data of construction resources from the construction site.
- A data processing algorithm is developed that can automatically detect object from the large point cloud dataset collected by Light Detection And Ranging (LADAR) technology, and furthermore identify potential hazards, especially the blind spaces from the equipment operators' perspective on the job site.

- A leading indicator, Proximity Hazard Index (PHI), is created to continuously assess the on-site proximity issue that workers are closed to various identified hazards. This factor generates a metric to evaluate the proximity hazards not only on individual level, but also for the entire crew. A safety benchmarking system can be further developed.
- A framework is developed to combine real-time tracking data with a virtual environment for construction safety monitoring purpose. It enables the information such as measures of safety performance to be rapidly exchanged among project participants. It can be further used to reconstruct the detected unsafe behaviors. Such information can be applied in the construction safety training and education program.

1.5 Organization of the Thesis

This thesis describes an investigation into the use of various sensing technologies for the assessment of construction safety, health and productivity performance. The following is an outline of how this thesis is set-up.

Chapter 1 introduces the overview of construction safety. The industry is facing the issue of safety measures being subjective, error-prone, and inconsistent due to the manual inspection. Hence, the motivation for this research is to improve the understanding and measuring of workers' safety performances in the construction industry.

Chapter 2 gives a brief account about the causations of fatalities and accidents in the construction industry. Various approaches attempting to improve the job site safety performance is reviewed. The applications of several emerging sensing technologies, that are available to the construction engineering discipline and will be implemented in this thesis, are introduced to the reader. The gaps in current research are summarized at the end of this chapter.

Chapter 3 presents the hypothesis and objectives of this thesis, followed by the definition of research scopes. Then, the framework of research methodology is explained in detail.

Chapter 4 evaluates the performance of real-time tracking technology, especially the Ultra Wideband (UWB), when it is implemented in harsh construction environment. The result demonstrates that this technology can be used to reliably collect spatial and temporal data of the construction resources from job site.

Chapter 5 explains the analysis of a special type of on-site hazards, the blind space to equipment operators. The result shows that this type of hazard can be automatically measured based on the existing construction site settings using LADAR technology.

Chapter 6 demonstrates an approach of analyzing human-equipment interactions, especially proximity hazards, using a new safety measurement. The measurement is established upon the identification of on-site hazard detection and spatio-temporal reasoning of collected trajectory data.

Chapter 7 fuses spatio-temporal data into workers' physiological information for construction ergonomic analysis, with the special emphasis on locating the spot that associates to most frequent non-ergonomic material handling activities.

Chapter 8 shows the possible extension of the research framework on worker productivity analysis by implementing the same data fusion technique to the physiological data.

Chapter 9 establishes a framework that facilitates the exchange of the derived safety information among distributed project participant using real-time visualization technology. This chapter also explains the potential application of such framework to be deployed in construction training and education program.

Chapter 10 concludes the thesis and also summarizes the findings. Also discussed are the future extension and limitations of this thesis research.

CHAPTER II

BACKGROUND

Construction industry has been experiencing high occupational fatal injury rates during the past decades. Many research efforts have been investigated to explore the causations of on-site accidents. Approaches and techniques attempting to prevent accidents have been studied, some of which have been in wide usage. In addition, pro-active real-time safety using emerging technologies are recently introduced in the construction industry.

2.1 A Closer Look at the Construction Fatality Statistics

The safety statistics have been published by the Census of Fatal Occupational Injuries (CFOI) for the overall industry sectors of the entire U.S. since 1992. The CFOI is the official federal count of occupational fatalities in U.S. The Injuries Illnesses and fatalities (IIF) program of CFOI provides annual statistics of the fatal and nonfatal data. The data are collected from a number of different sources, including OSHA reports, death certificates, worker's compensation reports, and media reports [14]. The CFOI defines occupational fatality and nonfatal (OSHA recordable) injuries and illness as follow:

Occupational Fatality *is a death that occurs while a person is at work or performing work related tasks*

Nonfatal (OSHA recordable) Injury and Illness *are an injury or illness that is work-related if an event or exposure in the work environment either caused or contributed to the resulting condition or significantly aggravated a pre-existing condition.*

According to CFOI, construction industry has been leading the occupational fatality number since 2003 among goods producing industries in the private industry division. Good producing industries include agriculture, construction, manufacturing, mining, and forestry. Table 1 summarizes the occupational fatality statistics between 2003 and 2012 of construction industry by exposure type. In 2008, 1,192 Construction workers were killed during the work related activities [15], and over 150,070 nonfatal

injury cases were filed to the Bureau of Labor Statistics [16]. According to the National Safety Council, the fatal and nonfatal injuries in 2008 were associated to over $10 billion annual cost [17]. As an average, a substantial fraction (35%) of the overall fatalities during this period was due to falls, followed by transportation (25%), contact with objects and equipment (19%), exposure to harmful substances (15%), and others (6%).

Table 1. Occupational fatalities by exposure, 2003-2012

Exposure types	2003	2004	2005	2006	2007	2008	2009	2010
Falls	364	445	394	433	447	336	283	260
Contact with objects and equipment	231	267	244	216	206	201	151	136
Exposure to harmful substances	179	170	164	191	182	132	132	126
Transportation incidents	290	287	318	323	296	241	231	173
Others	67	65	72	76	73	65	55	56
Total fatalities	1131	1234	1192	1239	1204	975	834	751

CFOI also sample the fatality data according to the primary and secondary sources involved in accidents.

Primary source *of injury identifies the object, substance, or exposure that directly produced or inflicted the injury.*

Secondary source *of injury identifies the object, substance, or person that generated the source of injury or that contributed to the event or exposure.*

Table 2 lists the fatal injuries that are produced by several sub-categories of primary sources that are associated to proximity issue. This closer look at the fatal injuries by primary and secondary source indicates that there is significant portion (on average 40%, shown in Figure 1) of fatalities account for personnel being proximate to various hazards.

Table 2 Fatal occupational injuries by primary source, 2003-2010.

Year	2003	2004	2005	2006	2007	2008	2009	2010
(1) Contact with objects and equipment	231	267	244	216	206	201	151	136
- Machinery	139	150	140	149	123	118	87	77
- Building materials	58	57	66	63	52	40	31	31
- Others	34	60	38	4	31	43	33	28
(2) Fall from floors	100	139	111	113	152	105	68	72
(3) Chemicals and containers	47	36	52	55	45	38	36	42
(4) Struck by vehicle	84	78	97	91	73	73	62	44
Subtotal: (1)+(2)+(3)+(4)	462	520	504	475	476	417	317	294
Total fatalities	1131	1234	1192	1239	1204	975	834	751
Percentage of proximity issue	41%	42%	42%	38%	40%	43%	38%	39%

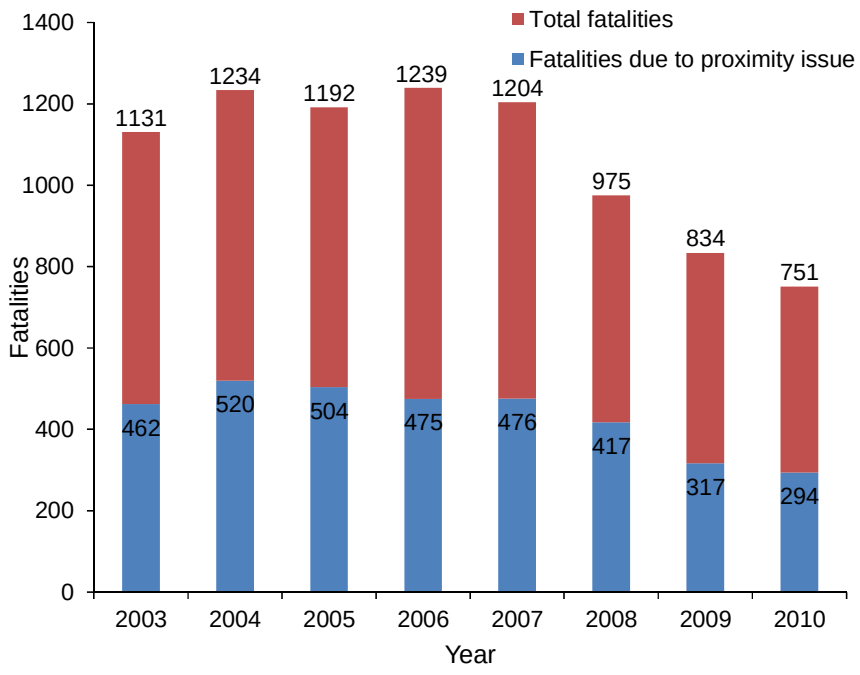

Figure 1 Fatalities due to proximity issue vs. total fatalities.

One of the distinct safety problems has been identified as the proximity of workers-on-foot to heavy construction equipment [18]. Over six hundred fatalities on the site were related to construction equipment and contact collisions during the inclusive years of 2004 to 2006 [19]. However, the causation and specific safety needs on this type of fatalities have yet to be sufficiently identified, since the knowledge of specific risk

factor to the contact collision problem is lacking, and no real-time information is gathered during the incidents [20]. Therefore, a special emphasis of this research is placed on the understanding of human-equipment interactions on job site.

2.2 Overview of Safety Performance Measures

The previous subchapter gives a number of safety statistics of the recent years. Despite reductions in injury and fatality rates, the safety records in the construction industry have been frustrated by the inability to make a step-change improvement [21], which can be achieved, according to many safety professionals, by careful selection, measurement and response to leading indicators of safety performance [22]. The safety statistics given in the previous chapter are considered as one type of measures/metrics of safety performance. There are various other safety measures for construction projects. Some of the metrics have been widely used in the industry, including Recordable Incident Rate (IR) and Lost Time Cast Rate (LTC). Both are defined by OSHA as following [23]:

$$\textbf{\textit{Recordable Incident Rate}}\ (\textbf{\textit{IR}}) = \frac{Number\ of\ OSHA\ recordable\ cases\ \times 200{,}000}{Number\ of\ employee\ labor\ hour\ worked}$$

$$\textbf{\textit{Lost Time Case Rate}}\ (\textbf{\textit{LTC}}) = \frac{Number\ of\ Lost\ Time\ Cases\ \times 200{,}000}{Number\ of\ Employee\ Labor\ Hour\ Worked}$$

Since these factors together with injury statistics measure the safety performance after event to assess outcomes and occurrences, they are lagging indicators. This type of indicators characteristically [24]:

- Identify the trends in past safety performance
- Have a long history of use, and so are accepted standards
- Are easy to calculate
- Are good for self-comparison

Researches have been conducted to demonstrate the effectiveness, efficiency, and reliability of various lagging indicators when they are implemented in construction safety [25][26][27]. However, its disadvantage in reflecting the safety performance on complex and dynamic construction site is also prominent. One of the major distinct disadvantage

of this type of measures is it focuses on the negative aspects of safety performance, which means there must have been an injury in order to get a data point [9]. Some other problems with the lagging indicators include [28]:

- Not being able to reflect whether or not a hazard is under control
- Fail to reflect the potential severity of an event, merely the consequence
- Not being able to reflect causation of event

Because of the drawbacks associated with the implementation of lagging indicators, research efforts have been investigated on proactive activities that identify hazards and assess, eliminate, minimize and control risk [29]. That is developing high-impact leading indicators for construction safety, which can precede an undesirable event and that have value in predicting the arrival of the event [30].

Leading and lagging indicators differ by scope [31]. Leading indicators are primarily focuses at the individual level and analysis at small units (behaviors). In contrast, a broader scope makes the lagging indicators focuses on organizational measures. This difference has important implications for data collection, analysis and measurement of leading indicator [30].

The safety leading indicators are furthermore classified into two categories: passive and active. An indicator that does not have a meaningful (actionable) metric is referred as a passive leading indicator [32]. In general, passive leading indicators only have True/False value to whether a practice or program is implemented [33]. Example of passive leading indicators include: drug testing, incident investigations, and worker recognition. As a contrast, an indicator with a metric that prompts a proactive response relative to the process it measures is known as an active leading indicator [32]. One example of active leading indicator is jobsite safety audit.

In order to provide meaningful (actionable) safety information, an active leading indicator must have the following key features [34]:

- Data must be numeric – they can be translated as a “score”.
- Data must be easily understood.

- Data must be perceived as credible; they must be objective rather than subjective.
- Data must signal the need for action, when indicate a deviation from expectation.
- Data may be related to other indicator.
- Data must not be easily manipulated.

As the requirements of an active safety leading indicator have been defined, an appropriate measurement process has to be developed, which requires the following [32]:

- Consistency in the measures obtained by various individuals
- A defined mechanism for information/data collection
- Tools formatted for the consistent data processing
- A repository for the information/data

Several techniques to measure leading safety indicators are listed as follow:

- **Behavior Based Safety (BBS)** is the application of behavioral research on human performance to the problems of safety in the workplace [35]. This technique is based on the site observations and individual feedback after the observation period. Observing data gathered from the job site are entered in a database with a prepared checklist to flag out the trends of at-risk behaviors. A report is generated for analysis and certain recommendations of modification are given [36]. The performances of BBS applied for construction safety has been studied and documented in many previous researches [37][38][39][40].
- **Jobsite Hazard Analysis (JHA)** is the on-site risk assessment technique that focuses on job tasks as a way to identify hazards before they occur, and serves to bring foreman and workers' attention to these potential hazards [9]. This technique is always associated to on-site safety inspections, which are made to assess physical working conditions. A cross-level (administrative, engineering and personal protective) emergency control system is suggested by OSHA [41].
- **Near misses reporting**. A near miss is an event, or a chain of events, that under slightly different circumstances could have resulted in an accident, injury, damage,

or loss of personnel, or equipment [24]. Investigation of near miss occurrences is a very useful measure of health and safety performance as well as enabling organizations to learn from such errors [42]. A common industry problem is that the accuracy of the estimation of near-miss largely depends on voluntary report.

- **Safety training**. Two types of measures of training are available [43]. The first is measuring the number of attendance. The second is measuring the number of people that can perform tasks they have been trained.
- **Safety audits** attempt to assess safety management and safety culture by measuring whether safety performance indicators are present or not [44]. This technique is useful to gauge the extent to which the organization's policies and rules are being followed and how they might be improved. However, the effectiveness of a safety audit can be influenced by the organization's safety culture itself [45].
- **Worker safety perception survey** is a mechanism of obtaining generic data about the safety condition on a construction site. These surveys can be conducted monthly, quarterly, or even annually [46].

Since the above techniques focus on the process, not the end result, if the performance indicators show unacceptable performance, modifications or changes can be made before accidents actually occur, which becomes the distinct advantage of implementing the leading indicator. However, since these indicators are measured based on manual observation or survey-based, the measures are inconsistent, subjective and error-prone [12].

2.3 Causation of Construction Accidents

It has been widely agreed that there is no perfect safety measure that can be to every situation. The selection of a proper safety measure relies on the causation of accidents [43]. Studies have been conducted to find out the major causes of construction accidents. Accident causal model provided strong and consistent evidence that most of the accidents were the result of human errors and mistakes [47]. According to Reason [48], human error occurs in a limited number of forms including unintentional errors

(slips and lapses) and intentional mistaken actions (mistakes and violations). The fundamental difference between these two forms is that errors cause results in failures of execution (e.g., inattentiveness, distraction); and mistakes are planning errors (e.g., intentionally choosing an unsafe pathway through a worksite).

Errors in judgment, decision making, and physical actions result in loss of productivity, the need for rework in industrial operations, and occupational injuries. In order to prevent human error organizations conduct training sessions, provide feedback to workers, and conduct inspections [49]. However, these prevention activities rarely occur in real-time. That is, organizations rarely have the capability to systematically warn workers of their erroneous actions before negative consequences are realized. This is especially true in work environments where conditions continually change, mobile equipment is integrated within the workspace, and many distractions are present. Therefore, there is a clear need for a reliable real-time information providing system that specifically targets the cessation of erroneous behavior.

Mistakes are defined by Reason as, "deficiencies or failures in the judgmental and/or inferential process involved in the selection of an objective or in the specification of the means to achieve it, irrespective of whether or not the actions directed by this decision scheme run according to plan [48]." Mistakes are relatively common and exist in three categories [50]: Skill-based, rule-based, and knowledge-based. Skill-based mistake refers to the failure of applying learned routine skill in normal situations. A typical example is a skilled driver of a dump truck stepping on the accelerator instead of brake. Rule-based mistake involves the incorrect application of a rule or inadequacy of the plan, for example unauthorized personnel invades a restricted area. Knowledge-based mistakes associates to the actions which are intended but do not achieve the intended outcome due to knowledge deficit. The knowledge-based mistake always occurs due to the incomplete and inaccurate understanding of system, environment, and job setting. An example of knowledge-based mistake can be a worker is hit by a reversing dozer inside its blind area.

A sequential model of occurrence combining human errors and mistakes is illustrated in Figure 2, which shows accidents always start with unexpected exposure to a hazardous situation in the workplace. Insufficient situational awareness and perceptual skills of work participants escalate the risk that an accident could happen. Other human

errors and mistakes including unexpected workers' risk-taking tendencies, failures in physical, psychological and physiological responses eventually contribute to the occurrence of an accident.

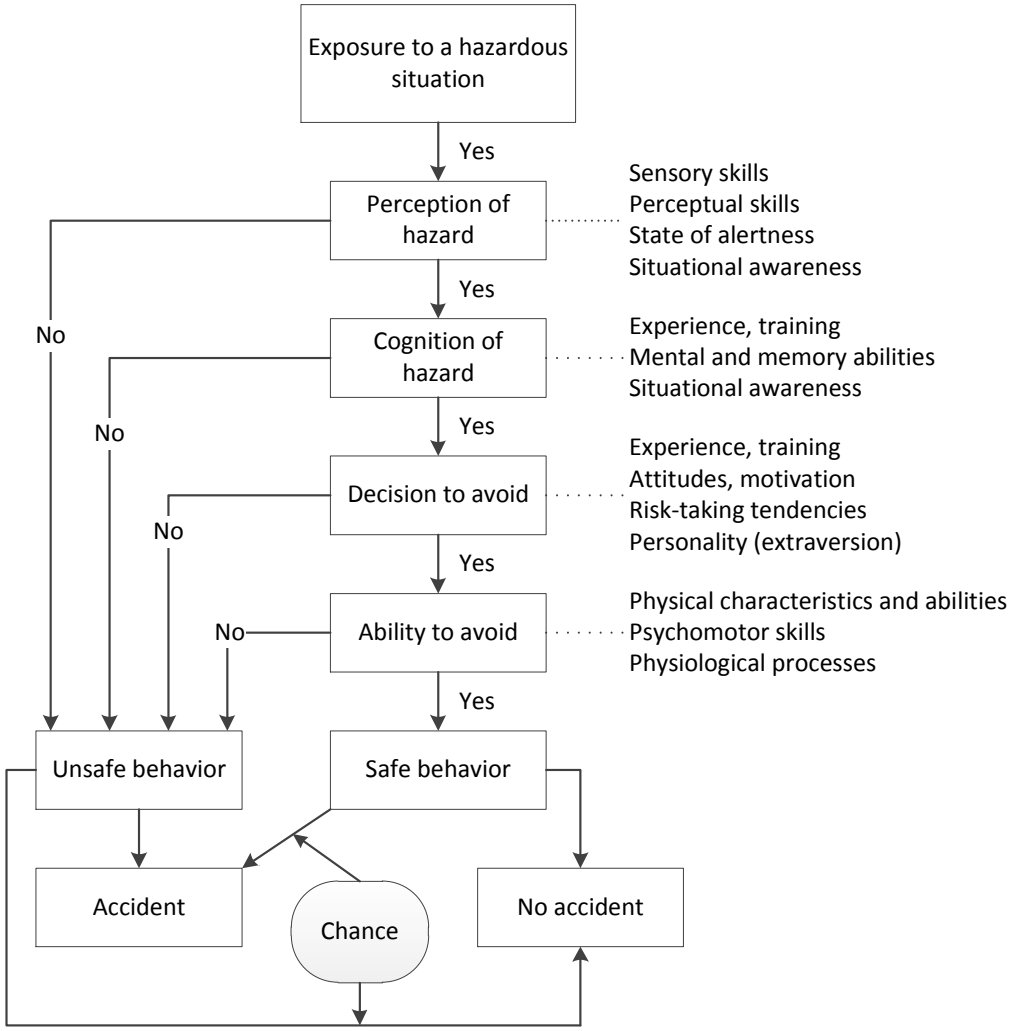

Figure 2 Sequential model of accident occurrence [51]

However, negative consequences resulting from these errors and mistakes are generally preventable when workers obtain feedback when they are exposed to hazards and when they are involved in erroneous behaviors before accident could occur [52]. Hence, there is a clear need for an advanced understanding of such erroneous behavior so as to specifically reproduces and corrects them. In construction industry, safety defenses

and barriers have been addressed in many layers: some rely on people (personal protective equipment, and safety supervising), others depend on procedures and administrative controls (safety standards and regulations, safety training and education). However, an engineered layer based on the applications of technology has not been considered as one of the key solutions for the construction safety. Therefore, a modified causation model (Figure 3) is presented that emerging safety technologies are applied to first prevent the potential accident by giving workers real-time warning, and secondly to collect data and derive information and knowledge from previous recorded events, such as close-calls [19]. This new information leads to significant promotion of understanding and measuring the safety.

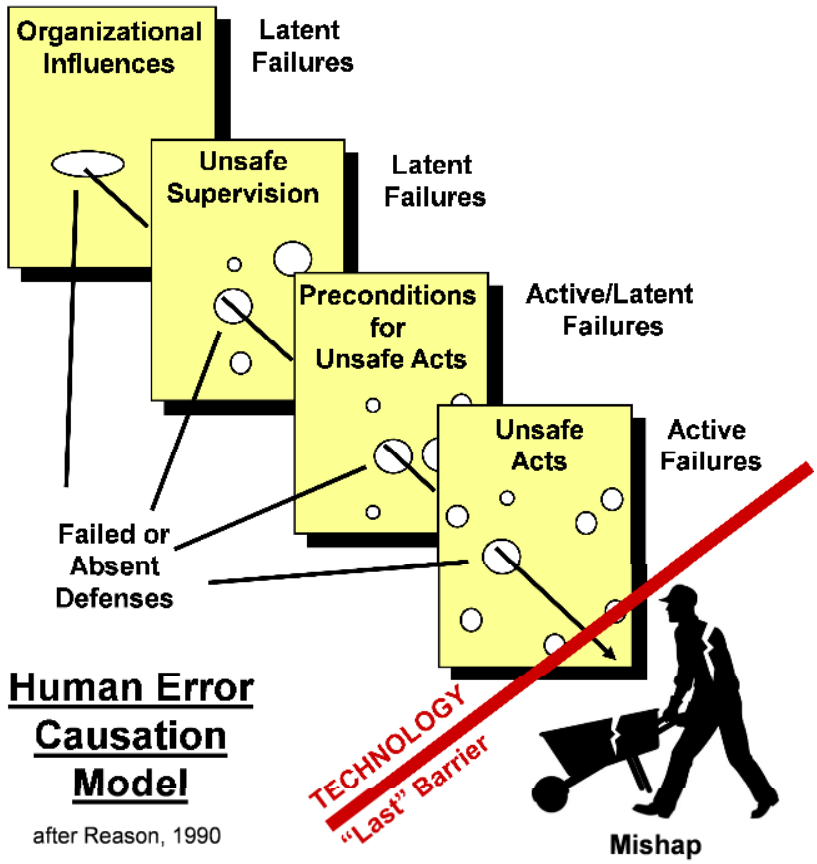

Figure 3 Human error causation model including technology as an extra barrier [19]

2.4 Focus of this Research

In general, a safety management system deals with the performance measurement on two levels. The first focuses on organizational mechanisms such as safety culture, safety climate, policies and regulations. The second moves down to the individual level and deals specifically with the issues of the performance based approach and its impacts to organizational level safety management [53]. This research focuses on the analysis and measures of daily-based individual safety performances. It aims to research about how safety performance of individual can be effectively measured and how to improve the understanding of the worker's at-risk behavior are the major motivations of this research.

As mentioned in the previous sections, two types of measures are used for safety measures, which are varied from the scopes. Existing safety measures on individual level have various drawbacks, which has been described in the previous sections. This research aims to generate a new measure that should:

- Enable to track small improvements in safety performance
- Measure both positive and negative events
- Enable rapid and frequent feedback to all stakeholders
- Be consistent, objective and robust to observers as well as to performers
- Be predictive

CHAPTER III

RESEARCH HYPOTHESIS AND METHODOLOGY

This chapter explains the research methodology and framework for human-equipment proximity hazard assessment using real-time sensing and visualization technology in combination to processing techniques. The first several sections state the research hypothesis, research objectives and scopes, followed by an overview of the research framework. The subsequent sections describe the different phases of the research, including evaluation of technology, operator visibility analysis, worker-equipment proximity algorithm, data fusion for worker's physiology and activity level analysis, and real-time virtual environment.

3.1 Introduction

The goal of this research is to build and test a framework measuring the safety and productivity performance in construction operations. The methodology can be envisioned as involving three major steps: real-time data collection, parametric information generation, and work performance analysis. A brief overview of the three steps and their corresponding goals are shown in Figure 4.

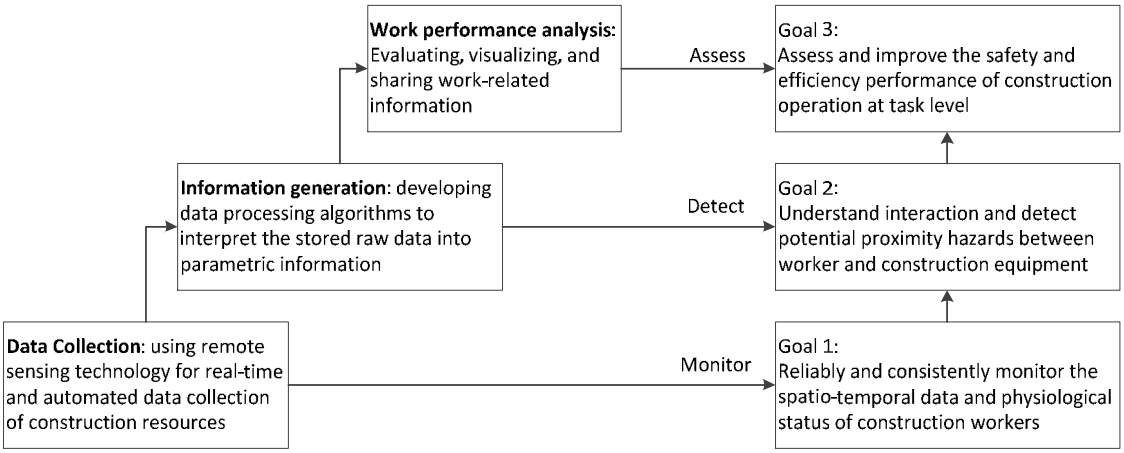

Figure 4 Research steps: Compartmentalizing the research methodology into three phases

The data collection phase aims to gather real-time spatio-temporal data as well as the worker's physiological status (e.g. heart rate, breath rate, and body temperature) from the job site. The performance of remote sensing technology has been evaluated. In this phase, it demonstrates that the selected sensing technology is capable to continuously, consistently, reliably monitor work activities in a harsh construction environment. During the information generation phase, gathered raw data are processed through a series of developed data processing algorithms. Parametric information related to the work activities as well as the construction environment is derived from the raw data. The parametric information is implemented to detect potential hazardous conditions on a construction site, as well as to understand the interaction between construction resources. As a sequence, this information is utilized to analyze and assess the worker's safety and efficiency performance at work task level. The results are evaluated and shared via a virtual environment.

3.2 Hypothesis

Despite the significant reduction of fatal and nonfatal injuries during the past decades, the safety performance in the construction industry continues to lag behind other industrial sectors. Moreover, most of the safety performance measures are based on survey and manual observations, which are inconsistent, labor intensive and error prone. In addition to the traditional management approach to improve construction safety performance, another option is to add a technology barrier using real-time remote sensing and visualization technology as a pro-active solution to protect workers from potential hazards. Therefore, two important research questions were put forth during the development effort of the research framework that formed the basis for initiating this research and are central to answering this hypothesis. These are as follow:

Research Questions:

1. *Can real-time remote sensing and visualization technology be implemented to detect, record, and visualize the construction safety performance?*
2. *How to develop a hazard detection model that automatically analyze gathered data, and accurately measure construction safety performances?*

3.3 Objectives and Scopes

Applications of real-time monitoring and controlling of construction site progress is of both managerial and technological interests. From a management perspective, accurate and emerging remote sensing technology, with a particular emphasis on real-time detection and tracking of construction resources (personnel, equipment, and material), can provide critical spatio-temporal information. Once gathered data are processed, information has the potential to advance the understanding of construction processes, including the level of productivity and safety performance. From a technical perspective, the development and evaluation of various electronic sensors for applications in the harsh construction environment, as well as the exploration of their potential as a valuable aid in project management, enables tighter control of project progress.

Therefore, this research investigates the crossover into nearby engineering disciplines. The goal is to design, test, and validate new methods that improve construction safety and productivity measurement. In order to achieve this goal, several research objectives have been set as follow:

- To create a test-bed to evaluate the performance of real-time locate sensing (RTLS) technology when implemented in harsh construction environment
- To develop data processing algorithms that can automatically identify potential safe/unsafe site conditions to equipment operators, ground workers, and decision makers.
- To create an assessment technique that can automatically analyze spatio-temporal data of workers, equipment, and materials, and automatically identify, evaluate, and visualize their safety and productivity performance.

- To develop a framework that provides real-time information sharing and visualization of the construction safety performance for training and education purpose.

As is summarized in Chapter 2.1, a large fraction of the construction fatalities (40%) were due to construction personnel work proximately to various hazards. In this research, the proximity hazard is defined as follow:

> A **Proximity Hazard** in construction operation is a situation that poses a potential level of threat to a worker's safety, which occurs only when the worker approaches to such a situation.

Several typical proximity hazards are considered in this dissertation, which include but are not limited to:

- Contacting with objects and equipment (machinery, materials, and structures)
- Falling from elevations (e.g. close to the edge of floor and openings)
- Struck by a vehicle
- Working close to chemical, flammable, and toxic substances
- Unauthorized intrusion to access-controlled space

Therefore, this research focuses on the selected construction activities such that the construction personnel are repeatedly exposed and/or close to various above-mentioned hazards on a construction site, with a particular emphasis on human-equipment interactions. Moreover, this research aims to quantify the assessment of the above-mentioned hazards, as these hazards can be only reported as binary values by the current manual observing approaches.

3.4 Overview of Framework

This research creates a framework that connects the raw data collected from the construction activities to relevant knowledge, which is required in construction productivity level and safety performance measurements. The framework involves three phase: data collection, data processing, and applications. An overview of the research framework is given in Figure 5.

The first phase of this research is to collect realistic construction site data by utilizing remote sensing technology in multiple field trials. The gathered data can be

divided into two categories: ranging data and tracking data. The ranging data, collected by LADAR or laser scanner in this research, is utilized to represent geometric and topologic information of the construction site environment. Tracking data, recorded by real-time location sensing (RTLS) and physiological status monitoring sensor, provides spatio-temporal data and the human physiological status of monitored construction resources.

In the second phase, the raw data are processed to derive parametrical information through the development of computing algorithms. The data processing phase consists of several modules: the error associated with tracking data are evaluated to demonstrate the appropriate selection of the technology; selected safety rules and regulations are interpreted as various parameters which later becomes constraints and thresholds in the developed computing algorithms; construction activities related zones and onsite objects are identified, which forms various hazardous conditions such as blind spaces to the equipment operator; kinetic and dynamic information is derived from spatio-temporal data for proximity analysis; and a virtual environment is created from the ranging data. In the last phase, the parametric information is applied to measure the safety, health and productivity performance.

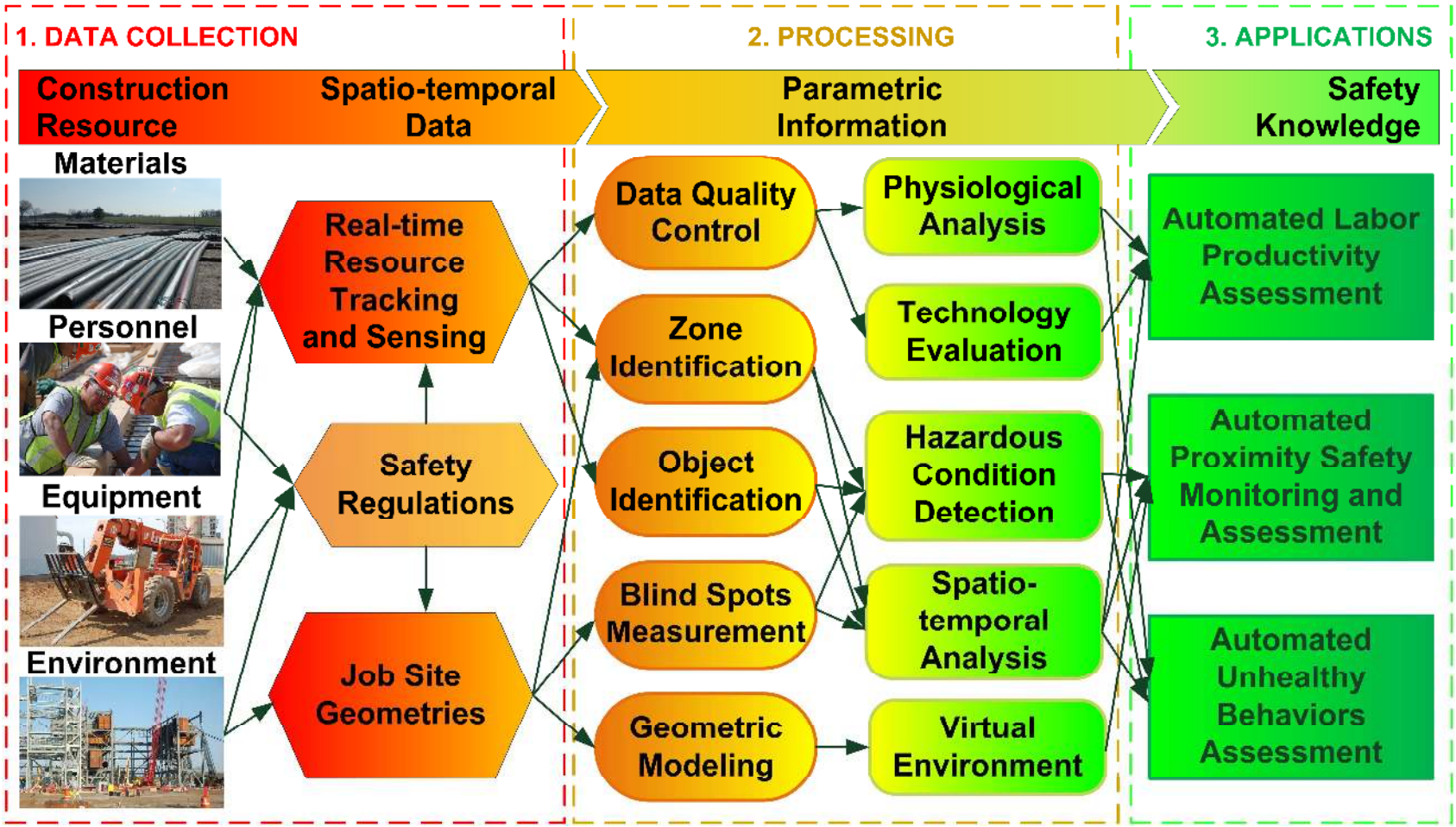

Figure 5 Framework of research methodology

3.5 Technology Evaluation

Emerging wireless remote sensing technologies offer significant potential to advance the management of construction processes by providing real-time access to the locations of workers, materials, and equipment. Unfortunately, existing research provides limited knowledge regarding the accuracy, reliability, and practical benefits of an emerging technology when it is deployed in a complex construction site, effectively impeding widespread adoption. Evaluation of a commercially-available Ultra Wideband (UWB) system for real-time, mobile resource location tracking in harsh construction environments is very necessary. A focus of Chapter IV is to measure the performance of the UWB technology for tracking mobile resources in real-world construction settings. To assess tracking accuracy, location error rates for select UWB track signals are obtained by automatically tracking a single entity using a Robotic Total Station (RTS) for ground truth. Furthermore, to demonstrate the benefits of UWB technology, the chapter provides case studies of resource tracking for analysis of worksite operations including safety and productivity. It also demonstrates the applicability of UWB for the design of construction management support tools.

3.6 Job Site Hazard Detection

As is mentioned in Chapter 2.1, 40% of the construction fatalities were due to personnel being proximate to various hazards. Chapter V focuses on detecting selected hazardous conditions and generating corresponding hazardous zones in the existing construction site setting.

Hazardous conditions such as the existence of chemical, flammable and toxic substances are detected and processed based-on real-time location data. Utilizing the polygon buffering algorithm, zones associated to these hazards are generated which only authorized workforces are allowed to enter.

Furthermore, many construction fatalities involving cranes and ground workers are caused by contact with objects and equipment, in particular struck-by crane loads and parts. Another hazardous condition is the limited visibility of the equipment operator. An approach is presented that aims at increasing the situational awareness of a tower crane

operator by aligning enhanced understanding of construction site layout with increased operator visibility of ground level operations. The developed method uses sensors to collect two data types: first, a laser scanner measures the as-built conditions and geometry of a construction site, and secondly, real-time location tracking technology gathers the mostly dynamic location of workers on the ground. Several algorithms are presented to (1) identify blind spaces from the collected point cloud data that limit the visibility of a crane operator, (2) process real-time location tracking data of workers on the ground, and (3) fuse the resulting data to create information that allows the quantitative assessment of the situational awareness of a tower crane operator. Results to a field trial are presented and show that a tower crane operator using the developed approach can increase understanding of where and when occluded spaces and ground level operations occur. The developed methods for creating safety information from range point cloud and trajectory data are a promising approach in significantly improving the currently unsafe operation of one of the most utilized pieces of equipment in construction: tower cranes.

3.7 Spatio-temporal Analysis

This session focuses on analyzing the interaction between workers and construction site hazards. The considered hazards are classified as dynamic and static. The dynamic hazards include mobile ground vehicles and equipment, and revolving crane components. The static hazards generally have fixed position on a construction site. Examples includes but not are not limited to: flammable, chemical, and toxic substances, floor edge, openings at elevation (associated to fall hazards), and any pre-defined areas that are only accessible to authorized personnel.

The goal of this session is to develop an algorithm that can evaluate and measure the safety performance of construction personnel especially when they are conducting activity proximate to the abovementioned hazardous conditions. In order to achieve this goal, two sub-objectives have been defined. The first objective is to automatically generate hazardous areas surrounding the existing static and dynamic hazards on the specific construction site settings. The second objective is to automatically analyze the spatio-temporal conflicts between each worker and each considered hazard. A proximity

hazard detection model is therefore established based on the achievement of both sub-objectives.

3.8 Virtual Environment

This session integrates the safety information and measurements to an immersive virtual reality world that represents the accurate construction site. The assumption was that any project stakeholder (equipment operator, worker on the ground, safety control command) with access rights and who could view live and processed field data in an immersive Virtual Reality (VR) could make more informed decisions in shorter times and at lower cost. This session consists of four central research phases: (1) data collection, (2) data processing, (3) information visualization, and (4) decision making and application in the field, education, and training.

An accurate spatial world of the construction environment (e.g. site layout and terrain) was created using commercially-available laser scanning and modeling techniques. The immersive VR world then integrated data from real-time location tracking sensors (GPS and/or UWB) that collected trajectory data of resources present within the construction site. A user was then able to create safety rules, and based on the information output, see and observe results, and even interact within the immersive world but from a safe distance.

3.9 Physiological Analysis

This session extends the developed spatio-temporal analysis algorithm for labor productivity analysis and ergonomic working behavior assessment. It demonstrates that location sensing and worker's physiological data can be fused to automatically identify the dynamic zones associated to the work activities as well as to categorize the work activities for the purpose of activity and ergonomic assessment.

The results show that current technology is satisfactorily reliable in autonomously and remotely monitoring participants during simulated construction activities. In addition, the data from various sensing sources can be successfully fused to augment real-time knowledge of construction activity assessment, which would reduce, if not avoid, the

shortcomings of traditional approach of estimating productivity rates and working healthy level based on manual observation.

CHAPTER IV

SELECTION OF TECHNOLOGY FOR REAL-TIME SPATIAL AND TEMPORAL DATA COLLECTION AND DATA ERROR ANALYSIS

This Chapter reviews the needs for real-time location tracking in construction industry. It also summarizes the current available tracking technologies and their applications. In order to select a reliable technology for spatio-temporal data collection for this dissertation, a test-bed which evaluates the performance of Ultra Wideband technology in harsh construction environment is developed and tested.

4.1 Introduction

The dynamic nature of construction activities, in comparison to the manufacturing industry and its mostly stationary fabrication plants and assembly environments, presents a significant challenge towards realizing the goal of understanding construction site activities. Hindering this understanding is the fact that production control protocols in the construction industry are labor intensive, manual, and error prone [54]. Recent developments in remote sensing and automated data acquisition technology promise to improve upon existing material management strategies [55][56][57][58][59][60]. Similar benefits are anticipated for process management strategies.

To date, many barriers exist that prevent owners and contractors from deploying data acquisition technology in construction. These include the risk of failure during the initial implementation phase and the high cost of implementation. An additional barrier is the lack of demonstrated benefits associated with emerging technology, e.g. the inability of the owner and/or contractor organization to exploit the information collected. When faced with known costs but unknown returns on investment, adoption of emerging technology can be nonexistent. Utilization of the technology is then limited to scattered implementations in various engineering subfields until more precise cost-benefit

valuations are determined [61]. It is, therefore, important to investigate how promising real-time location tracking technology may advance construction practices and enhance production control procedures in the construction industry. Two key areas closely tied to the economics of construction projects are productivity and safety [62]; lapses in both are responsible for significant losses in the construction industry.

With regards to productivity, one key area identified as a critical need is the localization and tracking of assets that are linked to work tasks, including workforce, equipment, and materials [63][64]. For example, material handling and transport has been identified as a critical work task in construction [64][65]. Recent studies report significant amounts of time spent on materials searches in lay down yards [66]. The material flow for a steel erection process at industrial job sites may involve the delivery of the material component from the fabrication plant to a temporary lay down yard. A lay down yard is an important temporal space in the assembly process of material components, as it allows for storing and sorting the components in the correct order, and provides a healthy temporal buffer to ensure parts availability when needed. Prior research has shown that the current process of material handling on large industrial job sites is inefficient [67].

Within the context of safety, significant time and economic resources are lost when workers are injured or killed by loads during work tasks [19][68]. Current construction best practices in material handling prescribe the foremen to blow a whistle or the equipment operator to activate the horn of a crane at the beginning of a material lift. Such manually activated signals are effective in alerting the surrounding workers to pay attention to where the load is swinging. Many workers or crane operators have difficulty, though, in relating their own location to the position of the load. Incorrect spatial awareness could lead to accidental injury. The importance of spatial awareness is emphasized by the fact that 25% of all construction fatalities relate to the unsafe proximity of ground workers and equipment [69].

To more concretely understand worker behavior and activities for improving the understanding of construction site operations, it is necessary to analyze observations of construction work in progress. For example, one way of improving current work practices

is by observing work tasks and generating manual evaluations. This practice is commonly known as 'work sampling' [70][71][72]. Any technology that can reliably, accurately, and automatically record the location of construction resources for work sampling could significantly simplify previously conducted manual assessments and improve confidence in the measurements. Likewise, technological systems that track project critical resources (e.g., people, equipment, material) and provide information on resource utilization can enhance current work practices. Such systems are popular in robotics and telecommunications by the name of context aware systems. The existence of a context aware system in construction that tracks the location of construction resources, and identifies and measures the status of work tasks, would improve project performance [73][74].

Wireless, non-destructive, and reflector-less sensor technologies applied to construction have been identified as key breakthroughs [65] for both construction practitioners and researchers in terms of reducing non-value-added activities, responding quickly to safety hazards, and automating and rapidly generating as-built and project documentation. In both cases, technological adoption is lagging due to uncertain benefits. Further investigation and control is needed to improve on these fronts.

This chapter presents research findings on the evaluation of a commercially-available Ultra Wideband (UWB) system, which is a radio-frequency based real-time location tracking technology, in several harsh construction environments. The error rate of the real-time location tracking technology is measured and evaluated. Results of experimental field validation studies are presented, along with technology application scenarios analyzing the field data.

The goal of this chapter is to evaluate the capabilities of a commercially-available Ultra Wideband (UWB) system to record work tasks that occur frequently on construction and infrastructure sites. The first objective is to measure the performance of the real-time tracking technology for mobile resources in realistic job sites. The second objective is to illustrate work tasks that would benefit from such real-time location data. Both research objectives include technology performance testing in live construction environments. The environments were a large and relatively flat lay down yard for

handling large pieces of steel material and a construction pit that was classified as a confined space by construction safety professionals. Both had multiple workers, pieces of equipment, material, and other obstructions present at the time of the experiments. Typical scenarios that were observed included heavy construction equipment operating in close proximity to workers. The location measurement error rate of UWB technology in these environments is computed, while the utility of UWB technology is discussed and brought into context to existing best work practices with regards to a specific safety or productivity task.

Since extended UWB performance evaluation in the various construction environments has not been performed in previous research, the particular scope of the remainder of this paper is to explore and test the technical feasibility of operating the UWB system in large-scale open construction environments. This paper does not address the social, legal, or behavioral impacts on workers using UWB technology, the sensor node layout and its effect on measurements, nor the comparison of commercially-available UWB systems. The following sections present the methodology, experiments, and results of performance measurements of tracking the real-time location of assets (workers, equipment, material), in open (lay down yard) and dense (object cluttered and confined spaces) construction environments. Demonstration of the UWB signal for safety metrics and work sampling follows.

4.2 Remote Construction Resource Tracking

Arguments in favor of using automated remote tracking technology in construction are to increase tracking efficiency, to reduce errors caused by human transcription, and to reduce labor costs. A variety of sensors and sensing technologies with automated tracking capabilities are available for use in construction and infrastructure projects [59]. Selection of one particular technology depends on the application, the line-of-sight (LOS) access between sensors and sensed objects, the required signal strength, the data provided, and the calibration requirements. Moreover, the prevailing legal framework regarding the permitted bandwidth and associated availability, and the implementation costs associated with each technology add further

constraints [18][75][76][77]. These characteristics must be weighed against the benefits provided.

Many existing technologies for localization and tracking fall within the broader category known as sensor networks (SNs) or wireless sensor networks (WSNs). Sensor networks consist of a collection of sensing nodes used to compute position from location-based measurements via triangulation. When a resource is tagged with an electronic tag capable of generating the necessary signals, a sensor network provides location information of the tagged resource. The three predominant location-based variables of a wirelessly transmitted signal are the received-signal-strength indicator (RSSI), the angle-of-arrival (AoA), the time-of-arrival (ToA), and the time-distance-of-arrival (TDoA). Given measurements of one of these variables by a collection of distributed sensor nodes, triangulation leads to estimates of the associated signal source position.

In RSSI models, the effective signal propagation loss is calculated based on the power of received signals at the nodes. Several theoretical and empirical models are implemented to translate this loss into distance [55][56][57][78]. However, the disadvantage of this technique is that convergence from data collection to information may take time, which leads to post real-time positioning [79].

In AoA models, sensor nodes estimate the angle direction from which the signals originate. Based on simple geometric relationships it calculates the position of the nodes. Studies show that high accuracy can be achieved by several advanced approaches [80][81]. Implementation of an AoA-based sensor network requires antenna arrays with directional antennae for triangulation. Deployment of the antennae for complete coverage can be costly for many temporary projects and for object cluttered environments, such as those found in indoor construction environments [82][83].

In ToA and TDoA models, the propagation time of a signal is translated directly into distance if the propagation speed is known. The most popular localization system using ToA techniques is Global Positioning Systems (GPS), which relies on communication with Earth orbiting satellites for triangulation. Cost and size make high precision GPS prohibitive for tracking every asset on a construction site [55][56][59][60]. An alternative emerging TDoA technology is active RFID, which employs an on-board

power source for the signaling electronics, together with locally installed antennae. One form of active RFID is Ultra Wideband RFID, which was initially developed for military use in the 1960s. FCC approval led to UWB being explored for monitoring of civil applications [84][85][86], including construction in 2007 [76].

Several case studies exist in construction applications that describe the successful use or combination of more than one of these principles in association of technology such as GPS, RFID, bar codes, laser scanning, and ultrasound. Other researchers experimented successfully fusing active RFID and GPS technology to predict the location of metal pipe spools and other industrial construction assets[60][87]. Passive RFID technology has been tested to track construction assets in a high-rise renovation project [88]. Others focused on radio frequency in combination with ultrasound signals in a wireless sensor network [89].

Alternative (non-sensor networked) tracking technologies include Robotic Total Station (RTS) and vision-based technologies. An RTS can only track single entities, thus its utility is limited to specific scenarios. Tracking construction resources using vision cameras can make work sampling more objective by automatically recording and reviewing the performance of selected work tasks. Although recent progress has been made in automated vision data processing [90][91][92][93], fully automated vision tracking of multiple resources in dynamic environments is far from being solved.

Although any of the previously offered tracking principles and their associated data gathering devices could be selected to monitor the trajectories of construction resources, few studies have focused on evaluating technology that is capable of simultaneously monitoring multiple, mobile resources at high data collection rates. To be of interest to the construction industry, the tracking technology should meet as many of the criteria listed as follows:

- Cost and maintenance: Low implementation and maintenance cost, while rugged enough to withstand a harsh environment and project lengths of up to several years;

- Device form factor: Small enough to fit on any asset (as needed) without interrupting the completion of work objectives;
- Scalability: Robust in a variety of site layouts (open, closed, and/or cluttered space(s), and small to large spaces);
- Reliability: Capable of accurately and precisely recording the activities that are associated to monitored work tasks;
- Data update rate: High data frequency provided in real-time (greater or equal 1 Hz); and
- Social impact: Less invasive technology, but providing highest possible safety and security standards for all project stakeholders while at work (in particular workers that face risks directly).

Existing UWB research in construction applications has focused on evaluating real-time resource location tracking of workers, equipment, and materials in outdoor and indoor environments [18][76][82][83] and first responder tracking applications [77]. Recent research has shown the use of UWB in construction potentially offers a solution to the aforementioned requirements. Compared to other technologies like RFID or ultrasound, UWB has shown to possess unique advantages including: longer range, higher measurement rate, improved measurement accuracy, and immunity to interference from rain, fog, or clutter. This study focuses on the performance capabilities of UWB in real-world settings while also demonstrating the operations analysis possible with UWB track signals from multiple project entities.

4.3 Test-bed of Evaluating UWB tracking technology

This research utilized a commercially-available UWB localization system consisting of a central processing unit, called the hub, which triangulates the positions of incoming Time-Distance-of-Arrival (TDoA) streams from multiple UWB receivers deployed in the construction environment. The UWB signal receivers connect to the hub via shielded CAT5e cables. The TDoA streams originate from actively signaling UWB tags, which are attached to construction resources of interest (worker, equipment, material). In addition, the UWB system requires the placement of a static reference tag in

the scene to improve the position measurements of UWB tags. A typical UWB setup and installation with tags on construction assets, including workers, equipment, and materials, is shown in Figure 6.

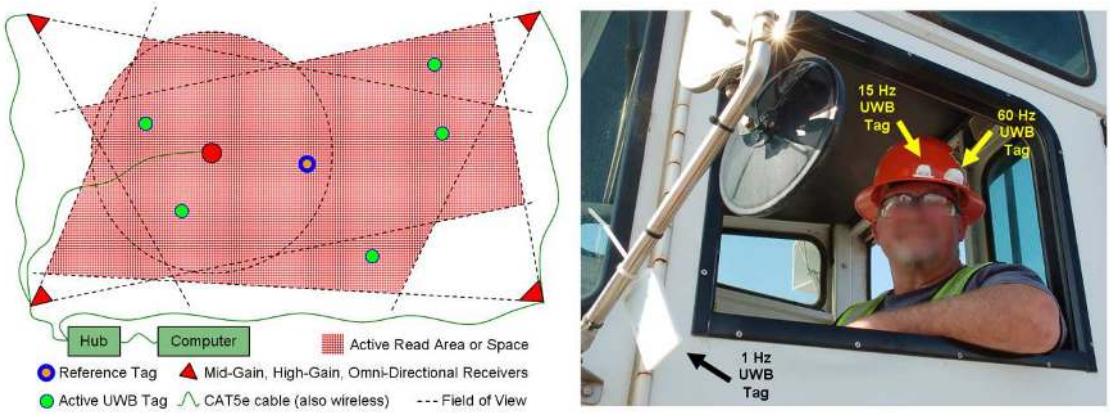

Figure 6 Triangulation of UWB tags using UWB receivers that overlap the coverage area/space and application to construction assets (yard dog and construction worker) inside a lay down yard.

The accuracy of the distance measurements will depend on the geometric configuration of the reference point and the receivers deployed in the field. Best practices were followed to ensure a functional setup. The methodology to evaluate the performance of UWB technology in live construction environments included the following tasks:

1. Coordinate field trial with field personnel and construction schedule prior to test day and identify test location.
2. Performa laser scan of test site to capture existing as-built conditions.
3. Install mid-gain (30° field-of-view) or high gain (60° field-of-view) UWB receivers to cover maximum observation space, while maintaining maximum distance from each other, and facing as few obstructions as possible (at least three receiver TDoA measurements are needed in one plane to measure two-dimensional (2D) tag locations readings, at least 4 receivers are needed at different elevations to measure three-dimensional (3D location readings).

4. Utilize a total station to measure the receiver locations and register them in the UWB hub. Define the RTS and UWB coordinate systems with reference to a common frame.
5. Attach 1 Hz, 15 Hz, 30 Hz, or 60 Hz UWB tags on assets, e.g., workers, equipment, and materials. Choose higher frequency tags for highly dynamic assets, e.g., workers. Document the material, the piece of equipment, or the worker's trade and work task that each tag is attached to.
6. Utilize a Robotic Total Station (RTS) to measure the ground truth location of one asset.
7. Gather real-time UWB and RTS location data.
8. Visualize the information in real-time using a 2D user interface.
9. Use data in post-processing analysis, e.g., for error and proximity analysis.

The first two tasks are part of the 'preparation phase', which should occur in advance of the actual experiment. Tasks three to five describe the 'installation and registration phase', which should occur immediately prior to the experiment. Tasks six and seven are the 'data collection phase,' which is the experiment proper. Tasks eight and nine form the 'data visualization and analysis phase'. As one focus of this paper is the performance evaluation of a commercially available UWB system in live construction environments, emphasis in the next section is on explaining of the steps associated to task nine.

4.4 Evaluation of Ultra Wideband Data Error

This section describes the procedure followed to assess UWB tracking performance. The default data output stream provided by the UWB system consists of data packets of three types which are differentiated by their packet headers: position data associated to a sensed tag, status information regarding the receivers, and reference tag information. The data packet associated to tag position data is of the form:

<Data Header>,<TagID>,<X>,<Y>,<Z>,<Battery Power>,<Timestamp>,<Unit>,<DQI>.

Each position data packet represents a triangulated position from unique tag identification (ID). In addition to the tag identification number and the time-stamped spatial data(x, y, z, t) for the UWB tag, the UWB system (a Sapphire DART, Model H651) collects additional status information regarding the tag. Status information includes the battery power level, a message unit, and a Data Quality Indicator (DQI). Sample data and their corresponding paths are illustrated in Figure 7.

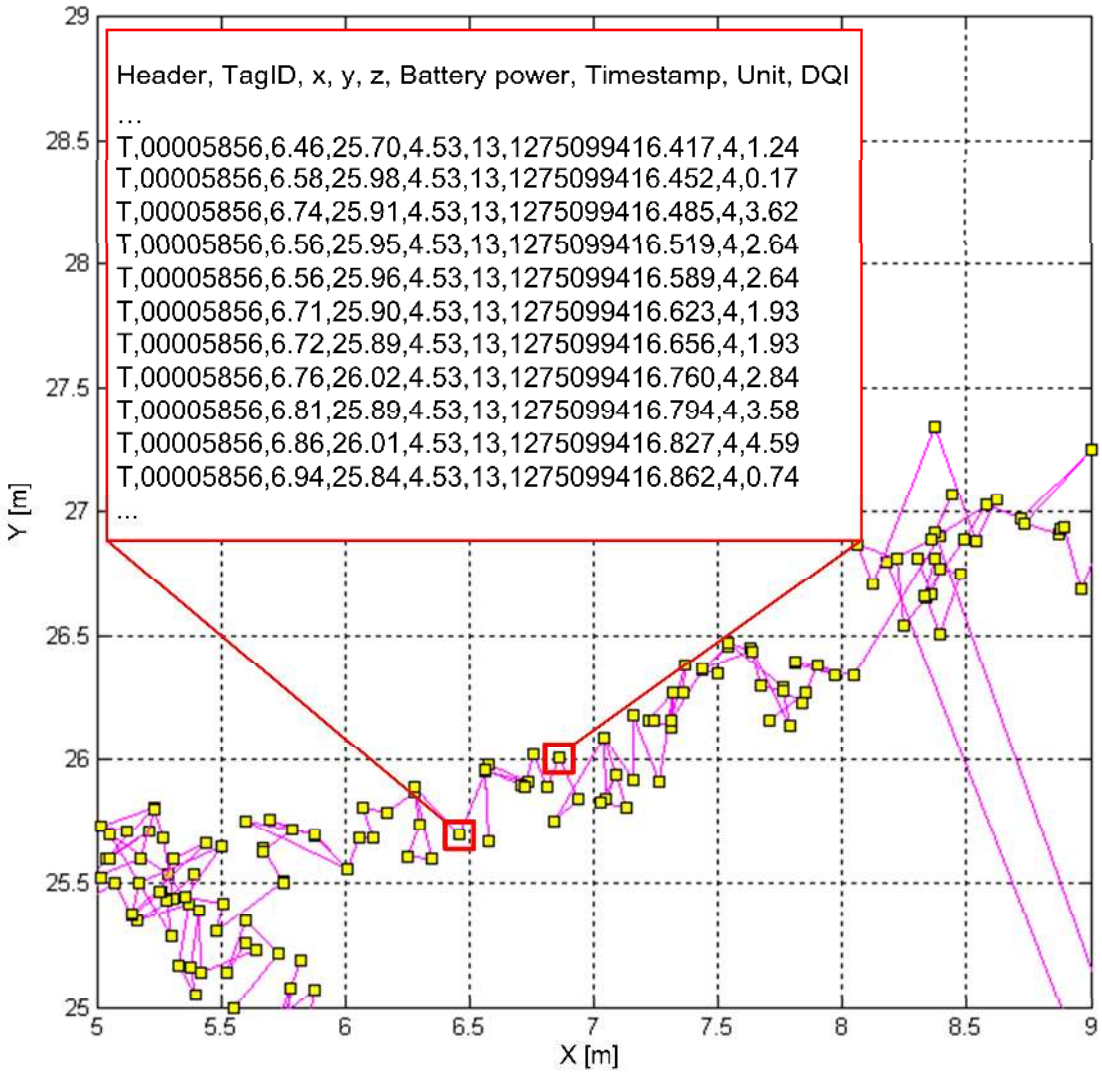

Figure 7 Sample and format of raw UWB data.

The data header “T” of each row means that two-dimensional data are collected. The time stamp is in the UNIX timestamp format. The tag, whose ID is 00005856, has

variable X and Y coordinates, and a fixed Z coordinate. The battery level is 13 out of 14 (14 means full). In general, low DQI value means higher data quality.

Previous experiments have shown that the data quality indicator provides values that are insufficient when estimating the error rate of a UWB system in construction environments [18][82][83]; they do not correlate to error. For this reason, a commercially-available 1" construction Robotic Total Station (RTS) was selected to provide real-time ground truth location data. A 360° (mini-) prism was mounted on a worker's helmet, which was also tagged with UWB tags. The relative height distance between the center of the RTS prism and UWB tag was less than 3 cm and subsequently insignificant for practical tracking applications in a construction environment. Both RTS and UWB systems record real-time spatial and temporal data to prism and tags, respectively. Since the UWB signal are noisy with occasional outliers, the UWB signal was filtered with a Robust Kalman filter [94]. In addition to signal smoothing, the robust Kalman filter rejects outlier measurements so that the outliers do not corrupt the filtered signal estimate. Figure 8 depicts a UWB track signal filtered by the Robust Kalman filter. Once the temporal correspondence between the two data series is established, the UWB is interpolated and the measurement error is computed with RTS data as the reference.

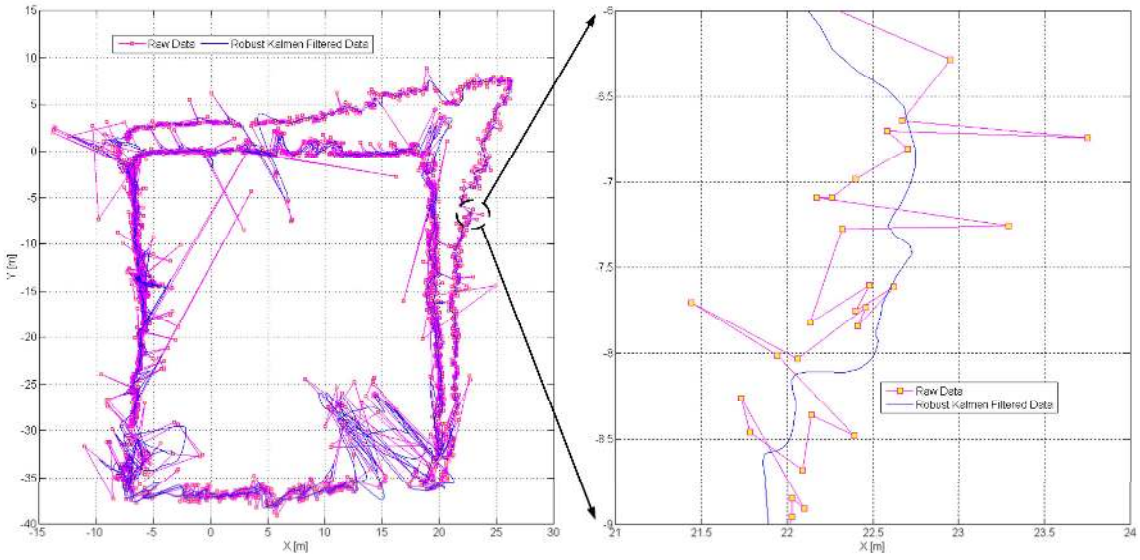

Figure 8 Raw UWB data (left) and sample of Robust Kalman Filtered UWB data (right).

4.4.1 Signal Synchronization

The UWB system was set up in the same Cartesian coordinate system as the RTS, but operated at different measurement rates, thus comparison of the two signals required signal synchronization. The procedure first consists of resampling the two signals to the same frequency. The frequency chosen was that of the UWB sensor since it required up-sampling of the RTS signal (and, consequently, no loss of information). Time synchronization consisted of maximizing the cross-correlation, where the cross-correlation is a measure of the similarity between two signals as a function of a time-shift applied to one of the signals. When the features of both data series (UWB and RTS) match, the cross-correlation is maximized at the time-shift aligning the two signals. Because the cross-correlation can be sensitive to missing or incorrect signal segments, the time synchronizing shifts were computed for several signal subsets.

The two data series from both tracking technologies were divided into several signals, each with different time intervals. The cross-correlation and maximizing time-shift were computed for each interval. The cross-correlation computation process for one UWB and RTS interval is:

$$C(\tau_j) \overset{def}{=} (R \cdot U)[\tau_j] = \sum_{i=1}^{n} R[\tau_j] U[\tau_j + t_i] \qquad \text{(Eq. 4 - 1)}$$

where the $C(\tau_j)$ denotes the similarity between two data streams at time lag τ_j^*, while $R[\tau]$ and $U[t]$ denote the RTS and UWB data respectively. After the time lag, maximizing the cross-correlation for each data subset is found, the average time lag τ_j is implemented as the synchronization time lag for the complete data series.

4.4.2 Error Analysis

Once synchronized to the ground truth signal (here, the RTS signal), the UWB measurement error is computable through comparison with the ground truth data. Rather than compare the UWB signal directly to the resampled RTS signal, the method from [44] is used to generate the signal error. In this method, the error associated to a given ground truth location measurement is computed through a weighted average of several UWB measurements (recall that the UWB tag operates at a higher frequency). Given the *i-th* RTS measurement occurring at time t_i, define $t_{i-1/2}$ to be the time halfway between t_i and

t_{i-1}, and similarly define $t_{i+1/2}$. The index set *J(i)* consists of all indices of UWB measurements occurring between $t_{i-1/2}$ and $t_{i+1/2}$, e.g., $J(i)=\{j|t_j \text{ in } [t_{i-1/2}, t_{i+1/2}]\}$. All of the measurements associated to the index set are valid measurements to compare against the *i-th* RTS measurement. Rather than compare one of the UWB measurements to arrive at the error, a weighted average of the UWB errors of elements in the associated index set is computed,

$$Error[t_i] = \sum_{j \in J(i)} W_{i,j} Error[t_i, t_j] \qquad \text{(Eq. 4 - 2)}$$

where

$$Error[t_i, t_j] = \left\| U[x, y, t_j] - R[x, y, t_i] \right\| \qquad \text{(Eq. 4 - 3)}$$

and

$$W_{i,j} = \frac{4t_j - 4t_i + 2}{\Delta T^2} \text{ with } \sum_{j \in J(i)} W_{i,j} = 1 \qquad \text{(Eq. 4 - 4)}$$

At the time t_i, the RTS data can be directly retrieved from the records, while the error of UWB measurement is computed by the weighted average of the errors between the UWB data found within one RTS data collection period ΔT to the RTS data at the time t_i. The weight factor $W_{i,j}$ is a function of time, with a greater contribution to the average error when the UWB data are recorded at the time closer to t_i. Figure 9 depicts the error computation with the weight factors represented by circles of differing radii.

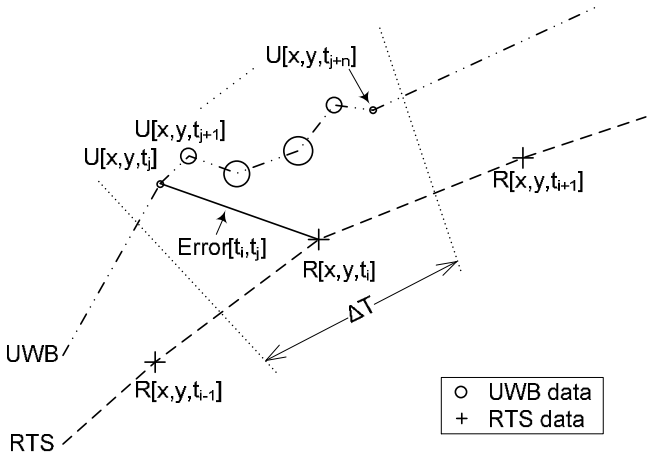

Figure 9 Schematic or error computation: UWB location track signal and visualization of comparison with RTS signal.

4.5 Experiment and Results

This section consists of four major subsections. The first details the experiments performed and their overall characteristics. The second collects the experimental data and examines the expected error rates of UWB when deployed for real-time tracking. The last two demonstrate practical benefits of having the real-time UWB track data for analysis. In particular, the coordinated activities of workers moving a load is assessed from a safety perspective, and the time trajectories of a worker are analyzed to demonstrate automated work sampling.

4.5.1 Description of the Experimental Environments

There were a total of three experimental environments, one controlled and two real-world construction areas. The controlled area was an open field. The two construction areas were located on a large industrial job site (see Figure 10). They were a construction pit (classified as a confined space by construction safety professionals) and a lay down yard for temporarily placing steel materials. To understand resource flow visually and connect the trajectories to their surrounding environment, a commercially-available laser scanner gathered the three-dimensional (3D) point cloud and a camera documented the as-built conditions prior to the experiments. The focus of data capturing was on recording resource location from naturally occurring work tasks in harsh (i.e., resource rich, spatially challenging, object cluttered, metal) construction environments. Thus, the experiments lasted several days to make the workforce familiar with the presence of UWB, RTS, and laser scanning technology.

Figure 10 Layout of experiments: construction pit (left), lay down yard (middle), and UWB tag and RTS prism on helmet (right).

Each resource entering the work zone was tagged. Here, a resource refers to either a worker, a piece of equipment, or material. Available UWB tags varied from low to high frequency (1 Hz to 60 Hz) and from low to high power (5mW to 1W). The decision on which tag type was applied to each of the resources was made based on the resource, its velocity, and its operational environment. For example, a badge type UWB tag was attached to steel material as the form factor (length/width/height=7.4/4.2/0.7 cm) and high power (1W) were best suited for attachment to the metal material. High frequency tags were (15/30/60 Hz) were attached to the helmets of workers as their movements required more frequent location monitoring. In some cases, multiple tags were attached to a single resource. All UWB tag locations were simultaneously tracked at update rates of at least 1 Hz. A 1 Hz tag was designated to be the static reference tag for the UWB receivers. As previously described, a commercial 1" Robotic Total Station (RTS) measured the ground truth (x, y, z, and timestamp) of UWB tag(s) using a 360° mini-reflector-prism that was installed on the helmet of one worker or on a prism rod (see Figure 10).

Open Field

In order to provide a more complete picture of the tracking performance characteristics associated to UWB as a function of the site diameter, several controlled experiments were conducted in an open field. Four UWB receivers were placed in a square configuration. Within the primary sensing zone (where there were at least three receivers within the field-of-view), a person equipped with UWB tags and an RTS prism (all helmet mounted), was tasked to walk in a rectangular pattern. The same experiment was repeated for four UWB receiver diameters (20, 40, 60, and 70 meters). The trajectory of the person was scaled accordingly with the receiver configuration diameter (the diameter is the maximum pair wise distance between two installed receivers when considering all possible receiver pairings). Figure 11 depicts the square UWB receiver layout and the location of the reference tag. Unlike industrial site environments, the open field provides the ideal environment for UWB sensing as there were no obstructions.

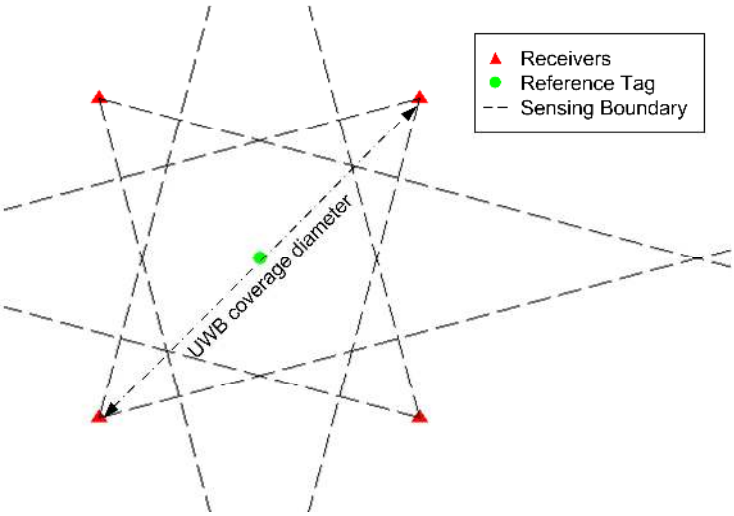

Figure 11 Open field receiver layout.

Construction Pit

This experiment was conducted in a confined work area of approximately 2400m^2. The registered 3D point cloud of the as-built conditions at the time of the experiment can be seen in Figure 12. The red triangles represent the location and orientation of the UWB receivers (short edges indicate the direction), while the green circle represents the location of the static reference tag. UWB trajectory data for a few of the tracked resources are overlaid in the image. Of note, two access points (ramps for equipment and workers) allowed entry into the confined space. The south side of the pit was specified as a confined space (a 20 meter long, three meter wide, and five meter high space, with unstable walls and a repose angle of greater than 45^o).

The work crew consisted of several workers (six carpenters, ten rod busters, eight form workers, 2 foremen, and one crane operator) and equipment (one mobile crane, one tractor and two material hauling trailers). Although location data of the entire crew were collected, the following observations include (for illustration purposes) data to one carpenter erecting formwork, two rod busters tying rebar, one foreman supervising, and crane operator hoisting materials with the crane. The work task of the day was to erect formwork and rebar to all sides of a four meter tall rectangular reinforced concrete structure (close to the center of the excavated pit). Although the work activities and locations of resources were recorded for the entire work day, only a sample (43 minutes

and 22 seconds) of the entire UWB data set will be analyzed. The data sample includes events linked to the crane unloading rebar into the pit.

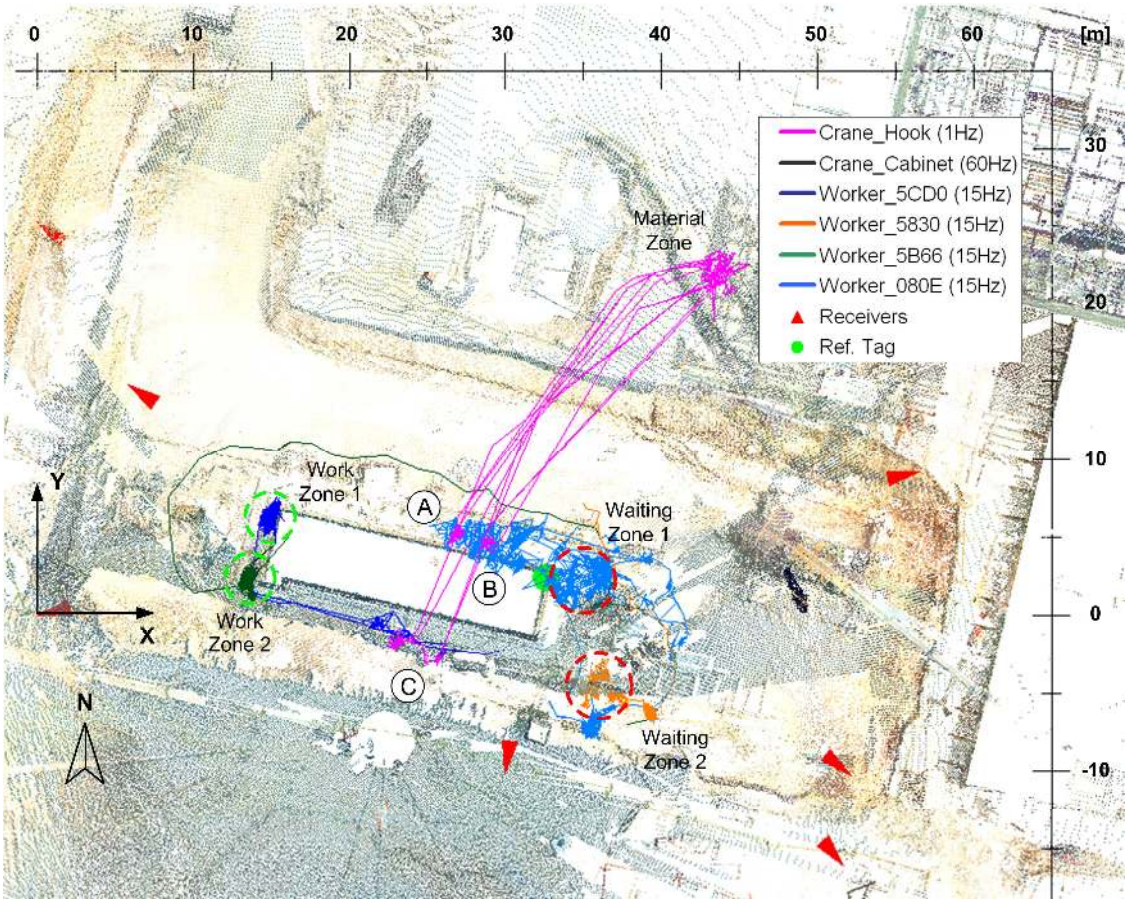

Figure 12 Plan view of construction pit: UWB resource trajectory data mapped on the registered range point cloud from a 3D laser scanner.

Lay Down Yard

The second field trial environment included monitoring resource locations in a large lay down yard which had significant quantities of metal steel pipe and girder objects present. The size of the lay down yard and available UWB receivers limited the observation area to approximately 65,000 m^2. The major material bays comprised mostly of custom fabricated steel pieces, which were well laid out for workers and equipment to move around. At the time of the experiment, equipment and ground workers had only one access point available to the yard and one tool and restroom area. Nine UWB receivers

were set up at the boundaries (fences) of the lay down yard. A reference tag (green circle) in the line-of-sight of all receivers was placed on a 2.5 m high pole overlooking all steel materials. The location of important control points such as material bays, fence, road, and other installments in the lay down area were recorded using the RTS. These measurements were used to develop an approximated plan view of the lay down yard. The plan view of the lay down yard, access gate, work and tool box areas, and other facilities, including the UWB receiver locations (red triangles) are illustrated in Figure 13. The dark areas are the material bays where material was frequently placed or picked up. A 34 minute subset of the data was elected for analysis.

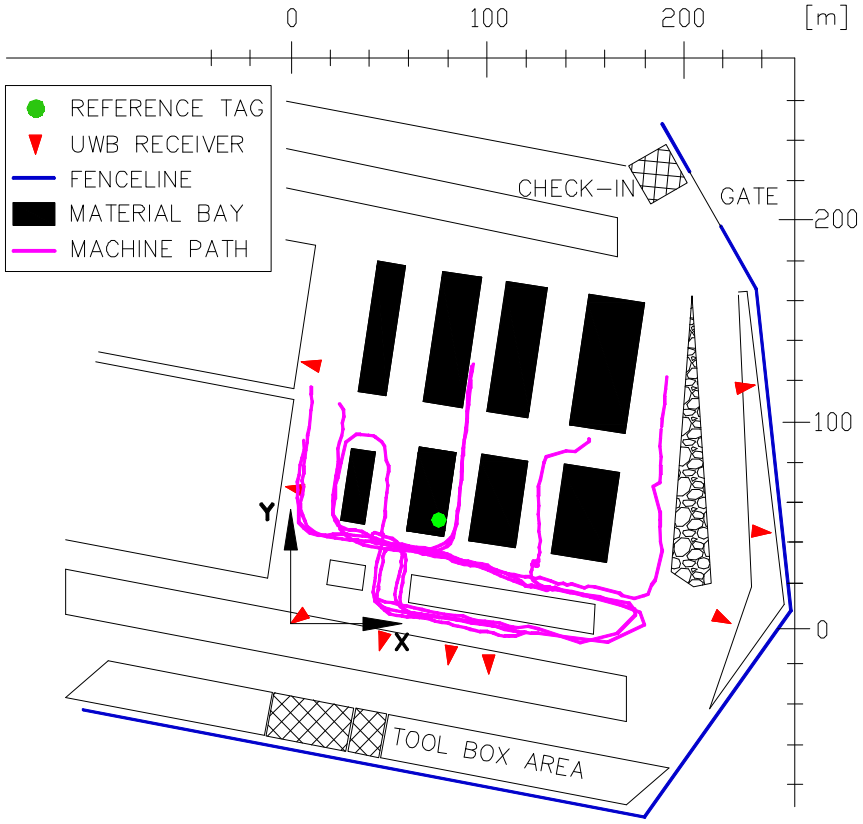

Figure 13 Lay down yard with overlaid sample of the UWB trajectory data of a yard dog (a construction vehicle to transport material).

4.5.2 Tracking Performance Analysis of Ultra Wideband

This section analyzes the error between the ground truth RTS signal and the UWB signal. We must first acknowledge that different tasks require different levels of accuracy.

For the tasks being examined here, high fidelity (on the order of centimeters or millimeters) is not necessary. What is essential is that personnel utilizing the track data can effectively use it for analysis and operations purposes. With this in mind, an opinion based worker survey was taken. For materials discovery in large lay down yards, those surveyed identified the ability to "quickly locate materials within a two meter radii" would assist in the efficiency of their work. This is consistent with other research indicating that meter accuracy is sufficient for the majority of work tasks [57][59][83].

Performance in the Construction Pit

The track signals of a worker fitted with a 60 Hz UWB tag and the RTS prism are plotted in Figure 14(a). The observation period collected 603 synchronized samples for the 1 Hz tag and 2654 synchronized samples for the 60 Hz tag. The average error of the 1 Hz tag was 0.48 m for raw data and 0.41 m for the filtered data. The average error of the 60 Hz tag was 0.36 m for raw data, and 0.34 m for the filtered data. The low average error coupled with a standard deviation of 0.35m/0.20 m for 1 Hz/60 Hz, respectively, means that real-time location tracking utilizing UWB technology in similar construction environments is feasible.

Performance in the Lay Down Yard

The track signals of a worker fitted with 1 Hz and 60 Hz tags, and he RTS prism are plotted in Figure 14(b). The observation period led to 1023 synchronized samples for the 1 Hz UWB tag and 4370 synchronized samples for the 60 Hz UWB tag. The average error of the 1 Hz tag was 1.82 m for raw data, and 1.26 m for the filtered data. The average error of the 60 Hz tag was 1.64 m for raw data, and 1.23 m for the filtered data. In this experiment, the larger covered area required to separate the UWB receiver distances to the upper limits of the suggested receiver configurations for some of the receiver pairings. Given that the error rates were within the suggested range for locating materials, and low standard deviations of 0.72m/0.66 m for 1 Hz/60 Hz, respectively, UWB localization technology in large, open, outdoor areas is feasible. Detailed results are shown in Table 3 and Table 4.

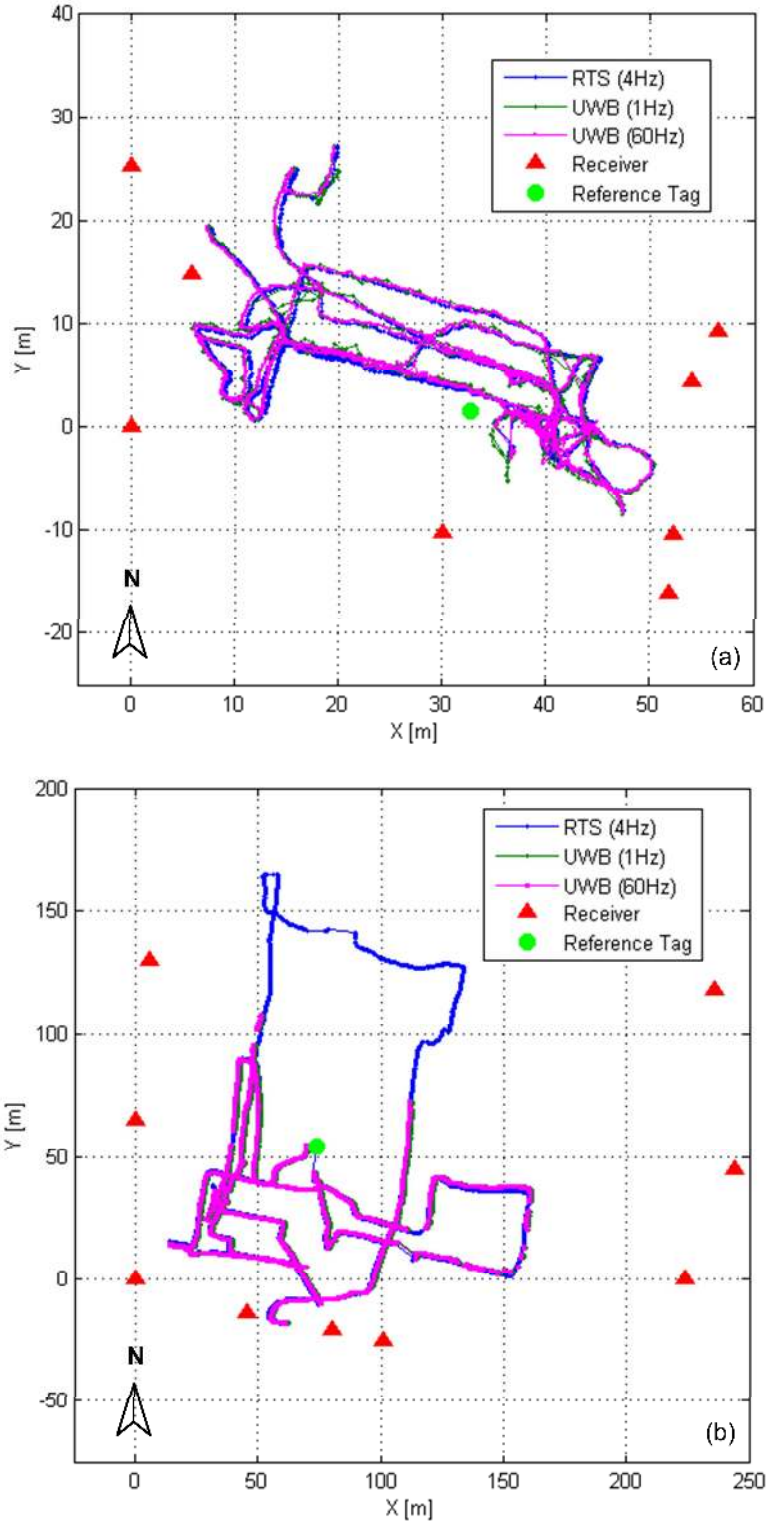

Figure 14 Synchronized UWB and RTS trajectories: (a) construction pit, and (b) lay down yard.

Table 3 Statistical results of experiment in construction pit.

Summary of Construction Pit Experiment			
UWB data collected (1 Hz) [No.]	620	UWB data points collected (60 Hz) [No.]	39,275
Duration [mm:ss]	14:25	RTS data points collected [No.]	2,724
Synchronized data pairs (1 Hz) [No.]	603	Synchronized data pairs (60 Hz) [No.]	2,654
Raw Data		**Filtered Data**	
Average Error (1Hz) [m]	0.48	Average Error (1Hz) [m]	0.41
Standard Deviation (1 Hz) [m]	0.37	Standard Deviation (1 Hz) [m]	0.35
Average Error (60 Hz) [m]	0.36	Average Error (60 Hz) [m]	0.34
Standard Deviation (60 Hz) [m]	0.21	Standard Deviation (60 Hz) [m]	0.20

Table 4 Statistical results of experiment in lay down yard.

Summary of Construction Lay Down Yard			
UWB data collected (1 Hz) [No.]	1,287	UWB data points collected (60 Hz) [No.]	64,128
Duration [mm:ss]	31:14	RTS data points collected [No.]	4,919
Synchronized data pairs (1 Hz) [No.]	1,023	Synchronized data pairs (60 Hz) [No.]	4,370
Raw Data		**Filtered Data**	
Average Error (1Hz) [m]	1.82	Average Error (1Hz) [m]	1.26
Standard Deviation (1 Hz) [m]	1.67	Standard Deviation (1 Hz) [m]	0.72
Average Error (60 Hz) [m]	1.64	Average Error (60 Hz) [m]	1.23
Standard Deviation (60 Hz) [m]	1.23	Standard Deviation (60 Hz) [m]	0.66

Discussion of Ultra Wideband Tracking Errors

The data from the open field experiments and two site experiments were collected and plotted in the form of several error box-plots and organized by increasing diameter (see Figure 15). The box diagram shows the lower quartile, median and upper quartile of the computed tracking errors. The lowest and highest errors within a factor of 1.5 of the inter-quartile range lie are demarcated by the horizontal bars below and above the box. Points that have errors beyond the quartiles by 1.5 of the inter-quartile range are considered as outliers, which are demarcated by "+" symbols. Most of the outliers are caused by the fact that the radio frequency signals generated by the UWB tags were blocked by the obstructions which are omnipresent on construction sites. In this case, the UWB tag cannot be detected by sufficient number of receivers (at least 3 receivers are

required to collect 2D data and 4 receivers are required to collect 3D data), which ultimately results in discrete positioning records with high errors.

To be noticed, even though Figure 15 indicates a rising trend of the tracking errors when the UWB coverage diameter increases, the error distribution with respect to the distance between UWB receivers remains uncertain. As the tracking errors are represented by the quadratic mean (Root Mean Square, RMS) instead of directional vectors, they only have positive values and may not follow a common and standard distribution. Study on understanding the correlations between tracking errors and coverage distance is not within the scope of this dissertation and can be explored in the future research.

Figure 15 also demonstrates that the distributions of errors are skewed in some cases (when UWB coverage diameter is 60 m, 70 m and 270 m). This is caused by the layout of the UWB receivers. The UWB receivers are installed at the beginning of each experiment and they must not be moved during the data collection phase, which means each experiment has a unique and fixed layout. During the data collection phase, if the UWB tags are always detected by sufficient number of receivers, the average and variance of tracking errors are small, and the error distribution will have a positive skew (UWB coverage diameter is 60 m and 70 m in Figure 15). Otherwise if the UWB tags are frequently outside the view of receivers, the tracking error increases and the error distribution will have a negative skew (UWB coverage diameter is 270 m in Figure 15). In summary, the layout of the UWB receivers has to be designed properly to ensure continuous communications between UWB tags and receivers.

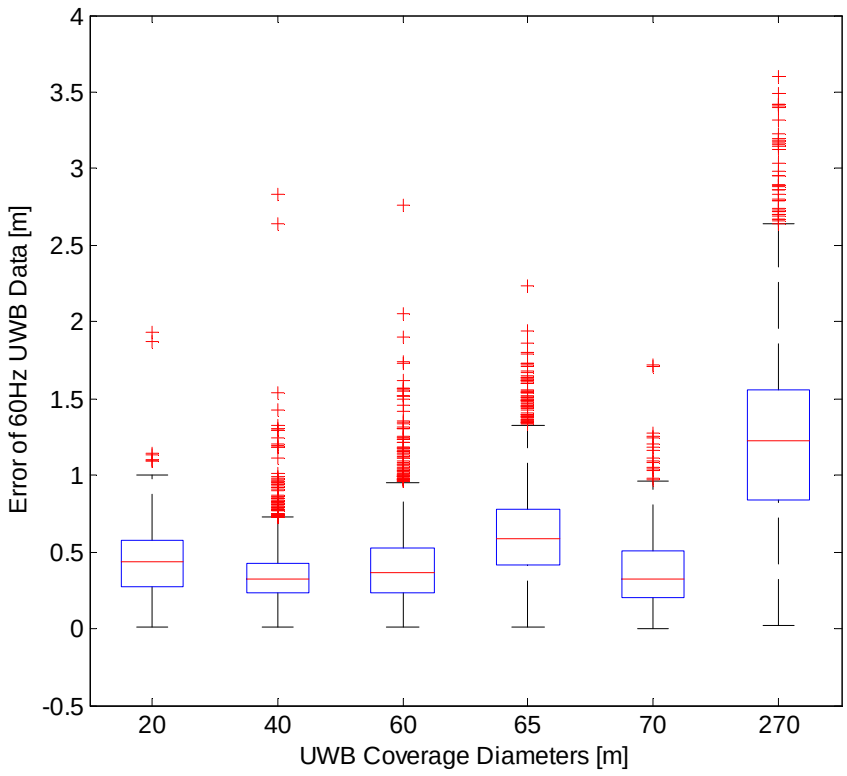

Figure 15 Error box plots of UWB signal as UWB configuration diameter increases.

Up to the 70 m diameter measured, the error rates are well within the tolerances expected by workers for the majority of their work tasks. Note further, that the construction pit scenario (diameter of 65 m) lies between two best-case, controlled scenarios (45 m and 70 m). Comparison of the error rates shows that performance does not degrade significantly, thus construction environments similar to the construction pit should lead to similar performance. When the diameter increases to 270 m, as in the case of the lay down yard, the error rate grows, however it is low enough to perform materials search. Importantly, for the 270 m distance setup 99.9% of reported UWB data lies within four meters of associated the RTS measurement, while over 75% of the reported UWB data lies within two meters.

4.5.3 Safety Analysis in the Construction Pit

Since 25% of all construction fatalities relate to too close proximity of pedestrian workers to equipment [19][69], a particular emphasis in the experiment was to study the interaction of workers with equipment. To demonstrate how UWB tracking could assist,

consider one of the hoisting operations. The last of the three hoists ("A", "B", and "C") is associated with the drop-off zone labeled by a "C" in Figure 12. The rebar load was attached to the hook of the mobile crane at "C1", in Figure 16. The crane and its attached load started swinging toward the drop location "C3" at timestamp 108 (seconds) and arrived at timestamp 267 (seconds). Detaching the load from the crane hook took the worker (5CD0) 224 seconds before the crane swung back to its original load location "C1". This one material delivery cycle lasted approximately 10 minutes.

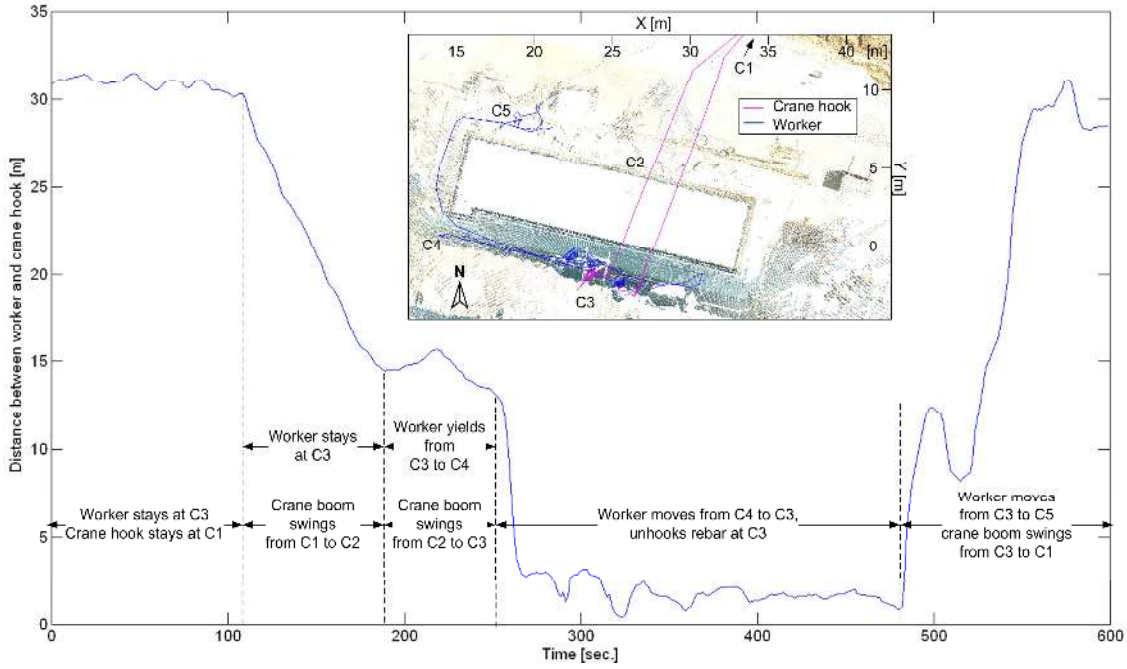

Figure 16 In-depth look at worker-crane interaction (distances) during a material host.

A spatio-temporal analysis of the worker assisting the process provides clues into the worker's behavior. For safety purposes, the worker should maintain a safe distance from the moving load until it has been safely lowered. While the crane boom was swinging, the worker (5CD0) originally occupied the drop location "C". As the crane was swinging toward him, the worker-to-crane hook distance decreased continuously from over 30 meters to 13.4 meters. Being warned by the horn of the crane and realizing the load was getting closer to the worker, he stepped outside the potential path of the crane load and moved temporarily to "C4". As shown in Figure 16, a safe distance of about 14

meters was maintained between the worker and the crane hook. As soon as the crane stopped swinging, the worker returned to unhook the load from the crane. The worker-to-crane hook distance then dropped to less than three meters. After completion, the crane swung back using path "C2" and the worker moved to another work location "C5".

4.5.4 Automated Productivity Analysis and Work Sampling

Another application example demonstrating the utility of UWB location tracking data are for automated productivity analysis. Based on pre-defined work and wait areas, location tracking data can be used to analyze the worker's activities. The sampling of work, travel, and wait time on a more detailed level and over longer temporal durations becomes feasible when it is automated. Typically, the data are obtained manually, which places an upper limit on the frequency and duration of data collected, while also placing limits on accuracy given the subjective nature of the measurements [64][96].

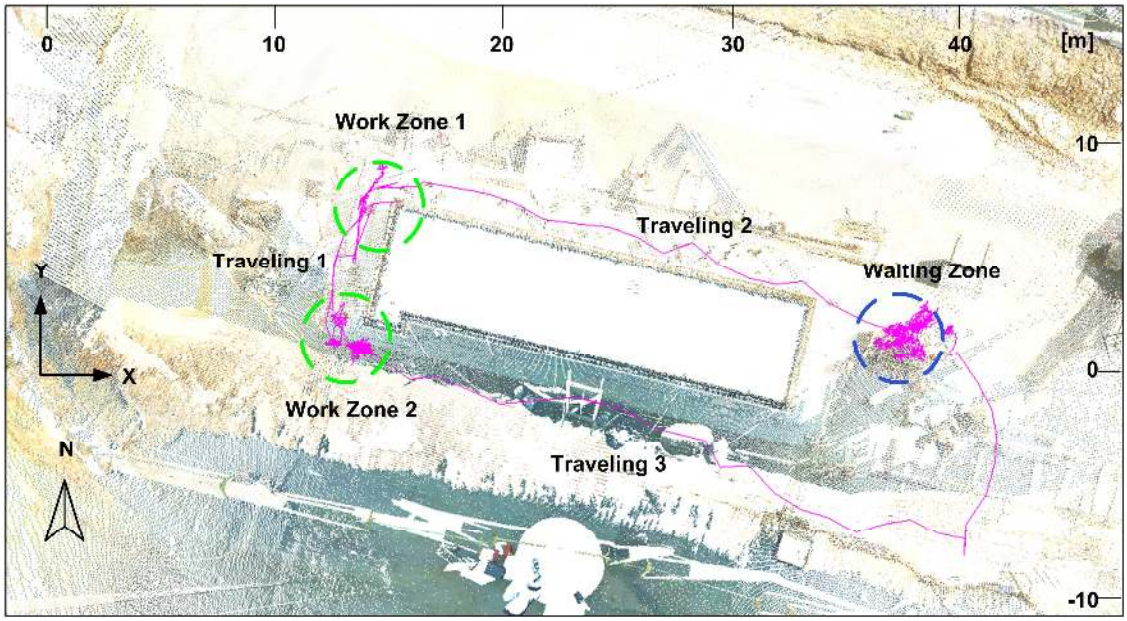

Figure 17 Job site zone depictions for automated work sampling analysis.

Ten minutes of trajectory data of a worker (0BC6) are illustrated in Figure 17. The graphs in Figure 18 show the traveling speed of a worker and his distance to two work related zones and one wait zone. The dashed lines represent thresholds below which the worker is presumed to be not moving in the case of a velocity threshold, or

within the confines of a defined zone in the case of a distance threshold. Assuming a worker traverses at a velocity similar to the walking speed of pedestrians which is about one meter per second [97], similar or greater speeds can account for changing the work position, while slower speeds (in combination with absolute location position over time) imply a constant work position. Thus, a speed threshold of 0.5 m/s is defined. For work/wait zones, a radius of 3 m defines the work area given a coordinate location for the zone.

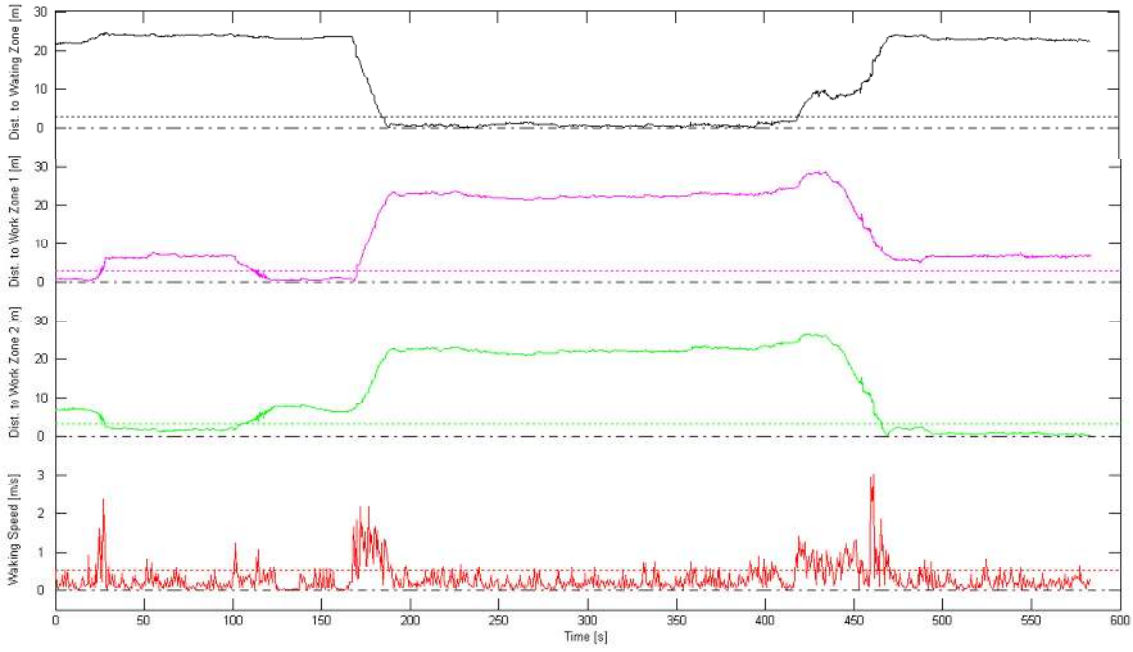

Figure 18 Automated work sampling for a worker based on UWB track signal: worker traveling speed and distances to work/wait zones.

In this example, the worker started in "Work Zone 1" and traveled to "Work Zone 2". After staying in "Work Zone 1" for about 170 seconds, the worker moved within 30 seconds to the "Waiting Zone", where he spent more than 200 seconds. The worker then returned to "Work Zone 2" within 30 seconds and remained there for 130 seconds before the observation period ended. The pie-chart in Figure 19 illustrates the results of automated work sampling as determined automatically from the data in Figure 18.

Even with complete information regarding the work process and product such as would be provided in a building information model [98], location based monitoring of

construction work activities can only be conclusive concerning the amount of time spent in a given zone. Additional inspection is required to estimate the work completed, and thereby the value added. Combining automated work sampling with additional (possibly occasional) inspection would enable productivity analysis [64][66][70].

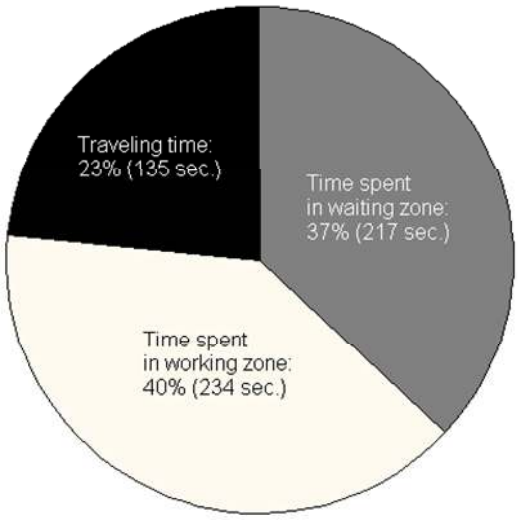

Figure 19 Automated work sampling for a worker based on UWB track signal: activity decomposition based on pre-defined work zones.

4.6 Conclusion

Rapid technological advances have made it possible to implement Ultra Wideband (UWB) real-time localization and tracking systems in construction applications. While possible, the capabilities and benefits of UWB deployment require further study, which is the aim of this investigation. This paper demonstrated that, in field trials, a commercially-available UWB system is able to provide real-time location data of construction resources thereby resolving the capability question. Validation occurred through performance measurements utilizing a Robotic Total Station (RTS) for ground truth measurements.

Aside from being able to collect reliable spatio-temporal data from job sites, it is also highly imperative to understand the benefits of promising real-time location tracking technology so as to increase adoption and advance production control procedures in the construction industry. Thus, the field data were analyzed from safety and productivity

perspectives. The safety application demonstrates the benefits of applying location tracking data for better documenting, analyzing, understanding, and correcting best safety practices as they are executed in the field. In this particular case, successfully computing the distance between two dynamic construction resources (worker and crane hook) allows the analysis for too-close proximity of resources, and eventually preventing struck-by incidents [19]. The productivity application exposed the benefit of applying location tracking data to automated conventional work sampling techniques. Automated work sampling, however, may demand more details than the location tracking data provides; for example, is the worker carrying a tool (productive task) or not (unproductive task)? Automated location tracking data and work sampling has tremendous utility for productivity analysis of long term work tasks involving multiple resources that possibly traverse the job site.

In summary, UWB technology in large open space construction environments achieves sufficient accuracy as to be practical for many open environment construction application areas. Overall, the presented work showed that real-time location tracking has potential construction applications in assisting the safety and productivity management of job sites and other areas requiring monitoring and control. Further, construction engineering and management concepts would benefit from the real-time location tracking data that UWB, and other, technologies provide.

CHAPTER V

OPERATOR VISIBILITY AND EQUIPMENT BLIND SPACE ANALYSIS

Many construction fatalities involving cranes and ground workers are caused by contact with objects and equipment, in particular struck-by crane loads and parts. This chapter presents an approach that detects and measures the possible blind spaces to crane operators. This approach includes two steps: The first step is to design an algorithm that can detect the on-site obstructions from as-built spatial data collected with a laser scanner; the second step is to optimize and reduce the blind spaces by alternating the crane location.

5.1 Introduction

A crane is an important hoisting resource in construction operations making it a key factor for enabling mobility of project resources. Unfortunately cranes are also often associated to accidents that lead to injuries or even fatalities. From 1992 to 2006, 307 crane accidents in the private construction industry sector caused the death of 323 workers [99]. In 2006, cranes contributed both as primary and secondary source of injuries to 72 of the fatal occupational injuries in the United States. This number is slightly lower than the average number of 78 fatalities per year between 2003 and 2005. 61% of these fatalities were categorized as "contact with objects or equipment" [100]. In 2012, ENR published results to a case study stating that 'worker contact' was the cause of accidents in 46.7% of over 700 investigated crane-related accidents. As many of these statistics indicate, safe crane operation requires well-coordinated activity planning including all related processes and resources, such as involving the workers that rig material and the equipment [101].

Due to the dynamic and complex nature of the building process, multiple of these resources perform on construction projects simultaneously. The interaction of these typically requires sophisticated construction activity planning [102]. As hoisting capacity

and availability often determines how quickly material resources can be moved or placed, the selection and placement of a tower crane on a job site is one of the first and most important tasks for field engineers in optimizing job sites [103].

Although safety of tower crane operation has become more important in recent years due to some high profile accidents, operator visibility is typically not a main criterion for selecting its position on the construction site. Typically, cranes are mobilized on sites based on productivity concerns. Another factor for planning a safe location of a crane is the input of an operator's experience, for example, how well an operator can see operations at lower levels.

In fact, as crane cabins are elevated at great height, it often prevents operators to observe the ground level activities in three dimensions (3D). Thus, any object on the ground, whether static or dynamic, is often experienced as a flat (two dimensional) object. This is the main reason why feedback from ground workers back to the crane operator is needed. Communicating the perspective or field-of-view (FOV) of ground workers give tower crane operators additional information, especially when obstructions such as as-built structures limit a crane operator's FOV.

As construction sites become increasingly congested as the project progresses, FOV limitations can become severe limitations for crane operators. These limitations often result in lower safety and productivity performance.

The most effective method for communication between crane operators and ground level workers to date has been hand or radio signaling. Few cranes possess a video camera system in the crane trolley that increases the visibility of ground level operations underneath a load. Recent research studies have made quite some progress on developing visualization and simulation tools that provide safer crane operation [104][105]. However, they do not utilize the potential of as-built information and real-time location tracking of ground resources for planning safe crane operation. In addition, cranes employ other safety technologies which have existed for years. These warn crane operators from collision with other cranes or parts, or heavy loads reaching out too far.

Although the application of such safety systems help improving the operator's perception and potentially enable real-time measurement and feedback from other crane

components (Rosenfeld 1995), crane operator visibility remains very limited. Being not seen by a crane operator and being struck-by loads is one of the most severe threats to workforce on the ground, leading to death, injury, and/or collateral damage [101].

Many of the recommendations issued by the construction industry, equipment manufacturers, or regulators indicate that safer crane performance could be achieved by enhancing the training of crane operators [106] and by increasing their situational awareness [107]. Another suggestion was to advance site planning to avoid potential risks related to crane operation, mobilization, and demobilization [108].

One key factor – identified by many researchers and practitioners – that impacts operational safety of cranes is to increase the operator's situational awareness. The initial basis for optimizing the visibility of a crane operator is to plan a safe site layout and equipment location. Multiple alternatives typically exist to determine the most efficient and productive position of a tower crane. However, setting up a safe location of a crane from construction drawings is often a challenging and time consuming task. This is in particular true for setting up a crane in existing built environments, including construction sites that have already progressed. In addition to available spatial information of the construction space, resource flow of material routes, and worker trajectories should be taken into account during planning of safe construction site layouts.

Most recently, the American Society of Mechanical Engineers has set up a committee (ASME P30) for the development and maintenance of a new standard that supports lift planning activities of cranes and other lifting support equipment [101]. It has recognized that the operation of a tower crane is constrained to the environment it operates in [108].

One of the elements is the construction space itself. It can be classified into three categories: resource space, topology space, and process space [109]. The resource space is defined as the space that workers, equipment, and materials occupy to perform their construction tasks. The topology space represents the built environment and site layout. The topology space is time-dependent and changes as a project evolves. The process space is related to any spatial requirements that are needed to perform a construction task. The process space thus includes potential hazardous spaces, such as blind spaces,

protected spaces, and post-processing spaces. The spatial constraints generated by construction spaces are always interdependent.

An example of the spatial constraints is the blind spaces to the crane operators. Blind spaces are caused by objects that obstruct the operator's FOV. This type of spatial constraint can be derived from the geometric dimensions of the respective objects that are present in the work environment.

The blind spaces can then be projected to the process space such as the necessary working path that ground workers need to accomplish a work task. A crane load swinging directly above workers and/or inside blind spaces, for example, is considered an unsafe process. This paper aims to address the risks that limited situational awareness of tower crane operations cause. It presents a method to detect work spaces that are not in the FOV of crane operators, for example, as-built structures that obstruct the FOV and cause blind spaces at the work levels of a high-rise building under construction. Further results to studies are presented that map the location data of workers to the blind spaces. Lastly, an optimization of crane location is presented.

5.2 Background

5.2.1 Crane Safety in Construction

Compared to mobile cranes, tower crane cabins mounted at height offer a wide field-of-view (FOV) and typically a nearly complete view of the entire site. This is in particular helpful for varieties of crane-related work activities such as rigging, loading, and unloading [110]. As past studies have shown, with the purpose of improving productivity and safety, cranes were suggested to be installed at locations where clear and non-obstructed line-of-sight (LOS) can be provided [111]. To date, selecting the location for a tower crane is often performed in manual trial-and-error analysis. Reach of the crane jib to cover the building envelope and other productivity factors play a key role in selecting a crane's position.

Existing researches utilized mathematical prescriptive models to evaluate the locations of a single crane in order to minimize the transportation cost of materials a crane moves on a project [112]. In contrast, a mixed-integer linear programming method

was used to optimize the location of a tower crane to improve the productivity and reduce the time it required to hoist material [113]. Another study developed a computerized model to optimize location of a group of cranes to balance its workload and minimize likelihood of conflicts [114].

Numerous studies have been conducted to ensure the safe operation of the tower cranes once their locations are determined. Although requirements and guidelines for safe crane operation exist [115], accident investigation reports often lack detail to the root cause(s) [116][117][118][119][106][120]. Thus, recent research has focused on a multi-attribute decision making tool as it can be implemented to formalize the specific safety factors that relate to tower crane activity [121]. In their research, data from several case studies indicated that two project conditions remain at the top of the causes for crane-related accidents: (1) obstructions that force blind lifts, and (2) human factors and operator performance. Although both accident causes are inherently different from each other, good understanding of the work environment and surrounding cranes is always necessary to further eliminate crane accidents [122].

A different study in the United Kingdom concluded similarly: A competent person must operate lifting equipment and should be familiar with work environment and processes [123]. Most of these studies concluded that safety in lifting operations can be improved through proper planning, training, and inspection. Safety, as an abstract concept, may not be quantifiable but could lend itself to a direct measuring of specific hazards so that it enables the comparison of risk levels on different sites [110].

In addition, reliable and rapid communication between crane operators and ground workers becomes crucial for project safety. Infrequent or inadequate communication between a crane operator and ground level personnel can significantly degrade a crane operator's situational awareness and understanding of operations at lower work heights. Previous researches suggested several approaches to improve the situational awareness of tower crane operators. 3D interactive, animation, and visualization systems have been heavily used on projects that can provide the budget to simulate crane utilization and load erection sequences. These tools also assist in better understanding any related constructability issues. Simulation ahead of time and special

conflicts benefit site planning and decision making, as risks can be identified ahead of time [105][124][125].

Other research shows that image data from a video camera installed on a crane trolley observing the space underneath, can be transmitted to a crane cabin. The access of such live video streams can increase the crane operator's visibility of operations that happen on the ground level [126][127]. Although the implementation of such cameras is beneficial and further limits previously discussed crane operator blind spots, some limitations to the use of such technology exist, for example, cameras mounted on the trolley generally do not provide good images when crane loads are large or swinging. The implementation of a video camera system can also be limited in situations with insufficient illumination as well as the lack of the visual depth perception. Besides, video streams cannot provide accurate and overall views of the lifted object in the context of the construction site settings.

A tower crane navigation system has been developed and tested to assist a crane operator during blind lift [104]. This system uses a laser sensor to acquire mechanical data of a crane such as boom angle, slewing angle, and cable length. It also uses a video camera for capturing the vertical field-of-view of a load. The approach uses a BIM model to visualize the load in the surrounding building environment, which also enables the operator to navigate through the building model. However, this approach is not able to accurately locate, quantify and evaluate the blind spaces as they physically exist in the built or dynamic environment. A ground worker, for example, would not benefit from the approach because the position information of the ground worker and equipment is not gathered accordingly to the crane load location. In addition, the visualization system relies on a BIM that is hardly updated in the field. Although the overall integration of positioning and camera technology significantly improves the operation of maneuvering crane loads, it does not take blind spaces generated by temporal structures such as dumpsters, trailers, scaffolding, and ground equipment into consideration.

5.2.2 Remote Sensing Technologies

Limited research has been conducted on exploring how a construction site layout and progress influence a crane operators' situational awareness. Approaches yet have to

be developed that allow rapid assessment and control of site safety conditions at the pre-task planning or operational level [75]. In addition, pro-active safety that anticipates and tries to prevent blind spaces requires effective and efficient communication of visible and non-visible spaces to all project stakeholders, in particular (crane) equipment operators and pedestrian workers [69].

Various emerging remote sensing and ranging technologies can be utilized to assess the conditions of a construction site at the operational level. Laser detection and ranging (LADAR) technology, as an optical remote sensing technology, has been widely utilized for range measurement [128]. One of the major applications of the LADAR focuses on implementing the 3D as-designed and as-built information project performance control tasks including construction progress tracking [129], productivity tracking [130], construction quality assessment and quality control (QA/QC) [131][132] and construction safety and health monitoring [69]. 3D terrestrial laser scanning provides very high dense point cloud data which can benefit the rapid, detailed, and large-scale topographic mapping especially for large building construction sites. In spite of the wide applications of laser scanning technology, filtering, organizing, and segmenting laser scanned data is currently a complex, manual, and time-consuming task. Several computer-aided point cloud data segmentation processes have been developed in modeling construction objects from laser scan data [133][134][135]. Although other very promising techniques have recently evolved in generating point cloud and object data using (video) camera approaches [136][137], these may require a surveyor to access the interior of potentially hazardous project and may only work at certain ambient conditions.

The next sections will explain the steps taken to achieve the objectives. The first step was to design an algorithm that can detect the on-site obstructions from as-built spatial data collected with a laser scanner. The second step was to optimize and reduce the blind spaces by alternating the crane location.

Both tasks included technology performance testing and a demonstration in a live construction environment. The selected experimental site was a multi-story building under construction with one tower crane on site. The site included multiple trades and workers, and pieces of materials and equipment present at the time of the experiment. For

simplicity reasons, the laser scan was performed from the ground on two locations. This ensured that enough spatial points were collected from all objects and all sides. Ultra Wideband (UWB) sensing infrastructure was installed to track ground workers' location and the position of the crane hook.

Previous research has not focused on blind space analysis for cranes at buildings under construction. As generally numerous as-built and temporary objects (defined as concrete slabs, walls, columns, dumpster and any other static objects taller than 0.7 meters) are present on the top floor of a dynamic construction site, they can limit the FOV of tower crane operators. The next section presents the algorithm that determines blind spaces.

5.3 Algorithm for Measuring the Field-of-View of a Crane Operator

This chapter focuses on estimating the blind spaces of a crane operator which are generated by large-size objects at the top level of a construction building site. The objects represent obstacles in the field-of-view (FOW) of a crane operator. These are located within the construction environment and include in addition to structural building elements such as walls, columns and slabs, also temporal structures such as formwork, dumpsters, and material palettes. Since the geometry and position information of these temporal components may not be necessarily available from engineering drawings and/or building information modeling [114], this chapter utilized a commercially-available time-of-flight pulsed laser scanner for as-built and topographic surveys. The artifacts such as noise and outliners in the collected point cloud data are manually removed. Once the point cloud data have been cleaned, the developed algorithm first detected the present job-site objects on the top floor of the building. Afterwards the blind space analysis was started. The tracking data of construction resources was finally integrated into the blind spots map to identify any potential unsafe worker behavior.

The data processing algorithms were developed in Matlab^{TM}. The results were plotted using a CAD software package. A flowchart of the research methodology is shown in Figure 20. The major components of the approach are detailed in the following sessions.

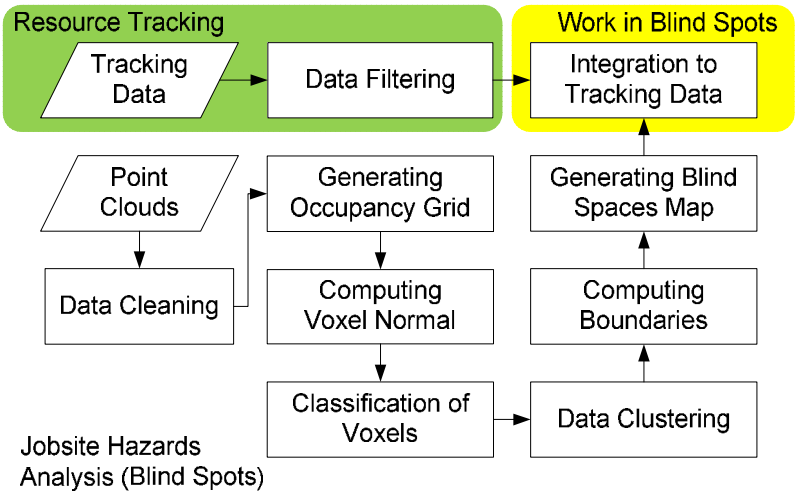

Figure 20 Flowchart of computing blind spaces and identify unsafe work behaviors.

5.3.1 Point Cloud Data Noise Removal

Two types of data noise in the as-built data that are collected by a 3D laser scanner were considered: (a) mixed pixels and (b) noise caused by frequently moving objects on the job site's top floor. Mixed pixels are artifacts in most laser scan data. They are caused by the laser spot straddling two surfaces that lie at distinctly different distances from the sensor [138]. Mobile objects also cause noise in laser scan data as multiple points of the same object would be collected as the object traverses. Examples are moving equipment and/or personnel. Fast laser scanners though can help reduce such noise artifacts.

Several noise removal technique and outlier detection methods for point cloud data have been studied [139][140][141]. Some of the noise reduction tools exist in the literature are Point Cloud DeNoiser^{TM} 3D, Point Clouds Library (PCL), and Pointshop 3D. However, the effectiveness and performance of these techniques is very much constrained by the complexity of the scanned scene [139]. The presented algorithm does not focus on the automation of noise removal in point clouds. Furthermore, the scale of the area that was scanned was large (20m x 40m). Thus, noise (artifacts in the air; trees and bushes outside of the construction space; the shape of larger pieces of moving equipment on a road) was manually removed from the point cloud. This task included drawing a bounding box around larger noise objects and deleting the points inside of it,

takes a few minutes per object for an experienced user. Noise removal largely depends on the laser scanning equipment that is used (measurement errors) as well as on the complexity of the environment (space and ambient conditions) that needs to be scanned.

5.3.2 Building a 3D Occupancy Grid Representation of the Point Cloud

The point cloud from the laser scanner is exported as a text file containing the spatial information. The exported spatial information is stored in a matrix "index, x, y, z". The spatial information is then utilized to construct a 3D occupancy grid, which is established along the X, Y, and Z axis. The grid has a consistent user-defined size (length, width, height) which determines the resolution of the blind space map [142]. A cell in the grid is called a voxel (volume pixel). The fill factor of a voxel can be measured by counting the points of the laser scan point cloud which is within the voxel. Otherwise, a grid cell is empty and does not further impact the calculation of the blind space. Fine grids result in more accurate blind space calculation, but may lead to higher computational complexity, for example, the time needed to process the point cloud data.

5.3.3 Computing the Surface Directions of Voxels

Generating complex solid model based on point cloud data of surfaces is generally challenging [58]. As detailed solid modeling is not necessary for the purpose of this study (computing blind spaces), surface estimation based on features which relate to specific height levels of objects is performed. A simplistic but computationally efficient geometric approach to locate entities and estimate the blind spaces was used. It relies on representing as-built objects with basic geometric representations (extrusions; convex hulls). When the size of the each voxel is set significantly smaller than the scale of the object, the surface of the object can be fitted by an array of fitting planes of the points contained in each voxel. The surface direction of each fitting plane is computed using a multiple-regression method.

The directions in the occupancy grid are sorted into three types: (1) horizontal surfaces which have vertical normal vectors of the fitting plane (align to Z-axis with a ±5 degree tolerance); (2) vertical surfaces which have horizontal normal vectors (align to X-axis or Y-axis with a ±5 degree tolerance); and (3) arbitrary surfaces which have a random surface direction.

The surface directions of the n x m x p occupancy grid are indexed and saved to a 3D matrix A(n x m x p). The 3D matrix is called the surface direction matrix. Each of its elements a(i,j,k) has a directional vector (x, y, z). The surface direction matrix is utilized to distinguish the object types from each other. For example, points belonging to a floor have a vertical directional vector (surface normal). Points observed between two floor levels having a horizontal surface normal are considered as columns or walls. Points with arbitrary surface normal indicate a more complex object that does not fit in the category of the first two.

5.3.4 Segmentation of Voxels

The surface direction matrix is classified by elevation. The distribution of the number of voxels that contain as-build data along the vertical direction is obtained from the surface direction matrix. Applying a distribution histogram helps in sorting the objects in respect to the elevation direction.

The top floor of a building under construction that stores many as-built or temporary objects is used as an example. Pending the job site layout, the number of voxels that belong to floor areas is typically significantly larger than the number of voxels that belong to other objects (e.g. columns, walls). The blind spaces to a tower crane operator are generated by obstacles that are in the FOV. Only those objects that limit the FOV are considered for further blind space calculation. These objects are taller than a pre user-defined height (greater than 0.5 meters or equivalent to the highest point once a person is bending).

5.3.5 Data Clustering and Object Classification

A clustering algorithm is implemented on the surface direction matrix in the defined height range to separate the objects from each other. Data clustering is a data mining method in statistics, which divides a set of observations into subsets so that the observations in a subset are similar to each other at one or more properties. There exist several clustering methods, such as hierarchical clustering, partitioned clustering, and spectral clustering [143]. According to the characteristics of the as-built data, a data clustering algorithm called Density-Based Spatial Clustering of Applications with Noise (DBSCAN) was selected. Existing research implemented this data clustering method to

rapidly model work spaces using imaging sensors [144]. DBSCAN finds a number of clusters starting from the estimated density distribution of corresponding nodes [145]. As opposed to other clustering method such as k-means, DBSCAN does not require to know the number of clusters in the data a priori. It requires two parameters: the minimum number of points required to form a cluster and the maximum distance between two points within the same cluster. The algorithm is mostly insensitive to the order of the points in the data set.

The accuracy of the clusters formed by DBSCAN depends on the distances measurement and the point density in each cluster. For example, a small max distance ε will result in a failure and divide an object into multiple parts. A large ε will lead to an error that two adjacent objects fall into one cluster and are merged. In terms of the observed point density, DBSCAN results in bad clusters when large differences in data density exist, because the minimum number of points minPts is static during the computation, and the combination of ε and minPts cannot be chosen appropriately for all clusters with significant variance in point density. Such impacts are insignificant in our case, since the point cloud data collected by laser scanner has a high resolution. This is true, especially because multiple laser scans were gathered and registered. A Euclidean distance measurement metric was implemented. The selection of other distance metric may influence the computational complexity, but such comparison was not part of the objectives of this study.

5.3.6 Computing Boundaries

A convex hull algorithm is applied to construct the boundary of the clustered voxels. The boundaries of the clustered objects are represented by a number of nodes within sequence. Since the voxels are classified into three categories according to the directions, their geometric representations vary. In the case that the clustered voxels have horizontal or arbitrary surfaces, a 3D polyhedron is constructed to represent the geometry of the corresponding object (Figure 21a). In case the cluster consists of only voxels with vertical surfaces, the geometry of the cluster is represented by extruding a 2D polygon. A 2D polygon is created by computing the 2D convex hull on the horizontal cross section of the cluster. The geometry of the clustered object is therefore represented in 2.5D which is

the extrusion of the 2D polygon. The extrusion distance is the height of the cluster (Figure 21b).

Since laser scanning was only performed from the ground/worker level, a full shape representation of all present site objects cannot be guaranteed. For example, laser scanning only captures spatial details of a surface or object within line-of-sight to the scanner. Therefore, the as-built data may form a concave polyhedron. Most 2.5D geometric representations don't significantly deviate from the object's real geometry.

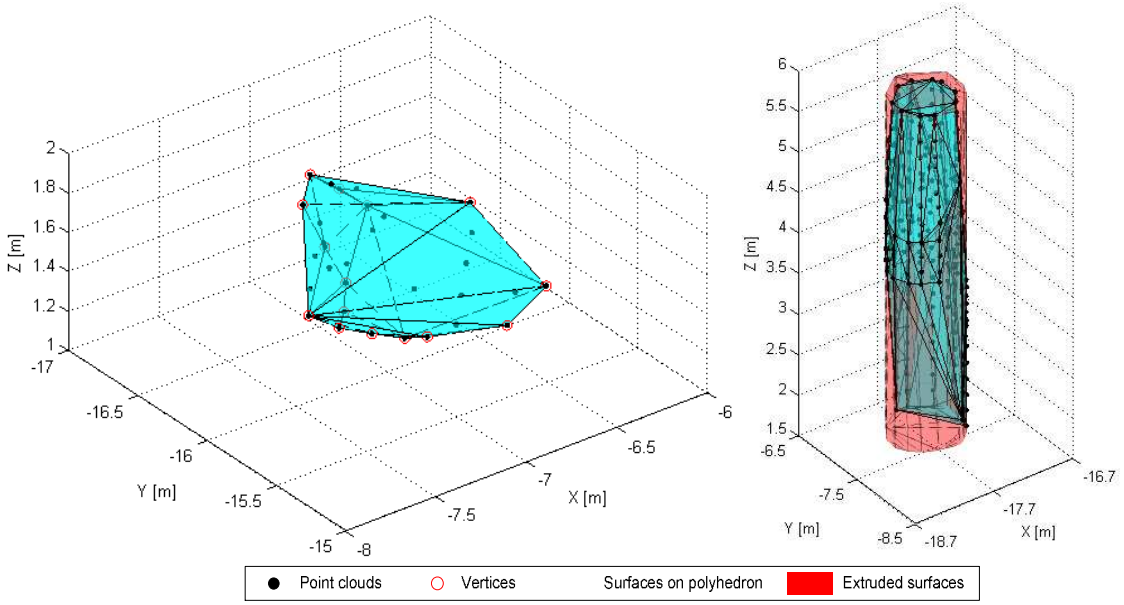

Figure 21 Geometric representations of clustered objects: (a) convex boundary for voxels with horizontal and/or arbitrary directions and (b) 2D extrusion for voxels with vertical directions.

5.3.7 Computation of Blind Spaces

A ray-casting algorithm computes the blind spaces by projecting a line from the position of the tower crane cabin to the vertices on the obstacles. The combination of vertices *i* and their projection to the ground *i** form a convex polygon. The polygon and polyhedron commonly refers to blind spots/areas and spaces, respectively. Figure 22 shows a sketch to a blind spot/area and space caused by a column that obstructs the FOV of a tower crane operator. The size of blind area/spots and spaces can be calculated to each object based on the coordinates of the nodes to each object. The quantitative

measurement of the blind area was used to evaluate how large the obstructions (and potentially safe/unsafe) a tower crane position is. The blind spot caused by an obstacle is calculated using the following steps:

(1) Compute the coordinates of the nodes projected on the ground level

$$x_i^* = \frac{Hx_i - z_i x_c}{H - z_i}, \quad y_i^* = \frac{Hy_i - z_i y_c}{H - z_i} \qquad \text{(Eq. 5-1)}$$

(2) Construct 2D convex hull of the projected nodes

$$(\hat{x}_j^*, \hat{y}_j^*) = convhull\{(x, y) \mid (x, y) \in (x_i^*, y_i^*) \cup (x_i, y_i)\} \qquad \text{(Eq. 5-2)}$$

(3) Compute the area of blind spot based on vertices with known coordinates

$$Blind\ Spot\ Area = \frac{1}{2}\sum_{i=1}^{n-1}(\hat{x}_j^* \hat{y}_{j+1}^* - \hat{x}_{j+1}^* \hat{y}_j^*) \qquad \text{(Eq. 5-3)}$$

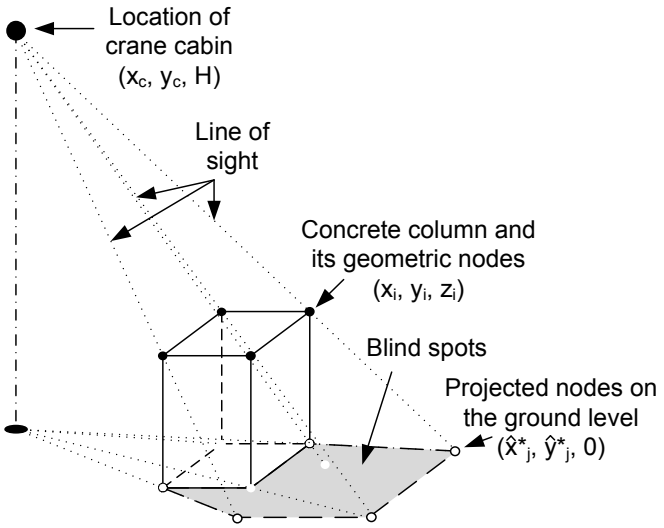

Figure 22 Blind spot caused by a column.

5.3.8 Real-time Location Tracking of Dynamic Resources on the Ground Level

As one of the main motivations for this chapter was to find ways that reduce incidents from cranes swinging over workers, this chapter also measured collected and analyzed the frequency of workers entering such blind areas/spaces. As is mentioned in Chapter IV, a good number of sensing technology is available for real-time tracking of construction resources [58]. Selection of one particular technology depends on the

application, any line-of-sight (LOS) issues between sensors and sensed objects, the desired tracking accuracy, the required signal strength, the format of data that it generates, and the calibration requirements [146].

We used Ultra Wideband (UWB) technology to record the location of the construction resources such as workers, materials, and equipment on the ground level. Earlier research indicated that this technology is capable of recording spatial-temporal data of dynamic objects accurately and in real-time in outdoor construction environments [18]. As little material and equipment moved on the site on the day of observation, only worker locations were recorded though.

The outliers of the tracking data were removed by a Robust Kalman Filter [146]. Worker trajectories were integrated into the 3D site layout map that contained the blind spaces. Intrusion of workers and their frequency in blind spaces became visible. Entry and exit location, distance traveled, speed, moving direction, and duration of workers within blind spaces are measurable. Such data can be used in future studies to conduct in depth analysis of job site layout and travel patterns of resources.

5.4 Experiments and Results

This section presents spatial and tracking data collection at a construction site and testing of the developed ray-casting algorithm and blind space measurement method.

5.4.1 Environment of the Experiment and Instrumentation

The construction of a four-story tall campus building was selected to conduct a case study. The size of the building was approximately 100m by 40m. At the time of the experiment, the second floor was already under construction. Rebar was being placed and some columns for the third floor had been erected. Each floor height was approximately 5m. Most of the work tasks were observed to happen on the second floor. A tower crane had been installed next to the center to one of the longer sides of the building under construction. A range scan with a commercially-available laser scanner determined that the crane cabin was 46.5m high above the ground level.

The same laser scanner also gathered 3D point clouds from two positions which were then registered. Two dark circles in the center of the plan view indicate the location

of the laser scan station (see Figure 23). The color to a range point indicates the reflectivity of each point. Blue and green values indicate high reflectivity and subsequently low errors. Dark areas had no distance measurement. Due to experimental schedule and access constraints, range points to only the second floor were measured. The second floor consisted of a partially finished concrete slab on the floor level, columns which were approximately 4.5m high, and other objects such as material carts in temporary positions, material dumpsters of various sizes and heights (all up to 1.5m tall). Most of the workers present on the site were involved with tying rebar, carpentry such as formwork, and electrical/pipe installation. Some management staff was present as well.

A commercially-available Ultra Wideband (UWB) real-time location tracking sensing (RTLS) technology was utilized to record the location of workers and management present on the second floor. Each worker entering the work zone was tagged. The crane hook was also tagged. Available UWB tags varied from low to high location data refresh rates (1 Hz to 60 Hz) and from low to high power (5 mW to 1 W). The decision on which tag type was applied to each of the resources (workers or hook) was made based on resource type, velocity it was traversing, and type of the closest operational environment it was operating in. Figure 23 and Figure 24 show the plan and elevation view of the point cloud collected of the second floor on the site.

In a manual effort – that takes an experienced laser scanner user only a few minutes – the range point cloud contained data of only the building site and its upper floors. As previously explained, the point cloud was also cleaned manually for some noise such as extreme data outliers, mixed pixels, and other noise. Irrelevant spatial points from adjacent building structures, environmental objects such as trees and bushes, and temporary construction resources such as moving vehicles, workers as well as the crane parts, were all removed. The cleaned data set contained 2,027,763 as-built data points.

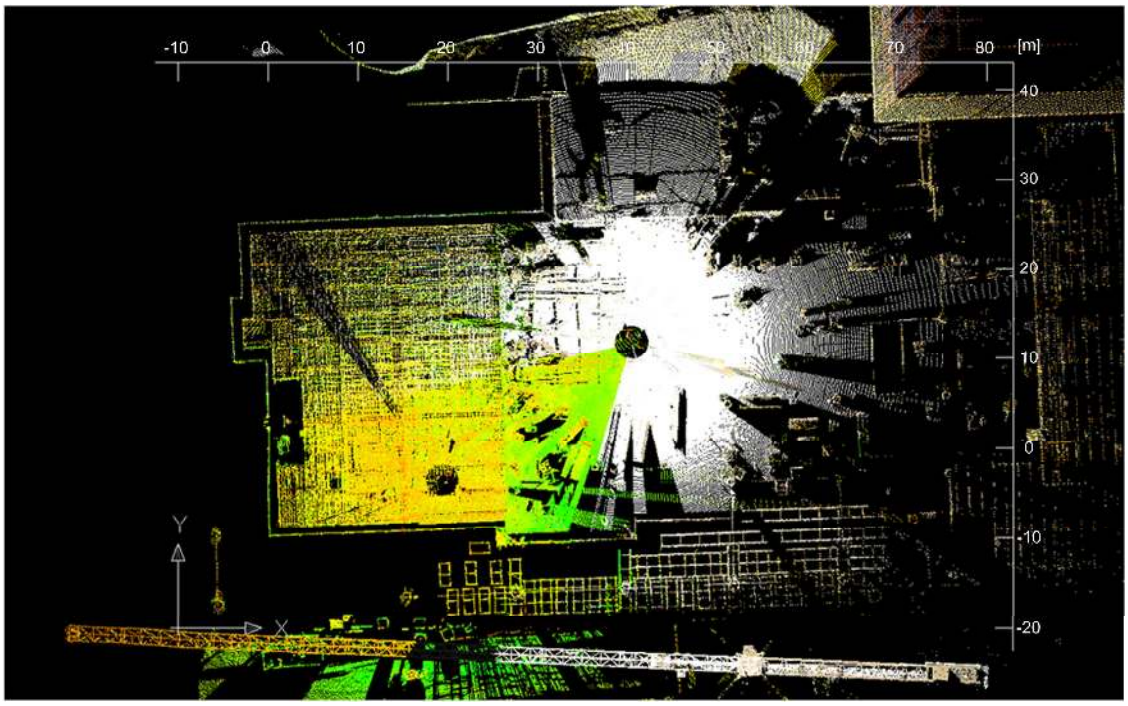

Figure 23 Plan view of the construction site, second floor, and crane location, orientation.

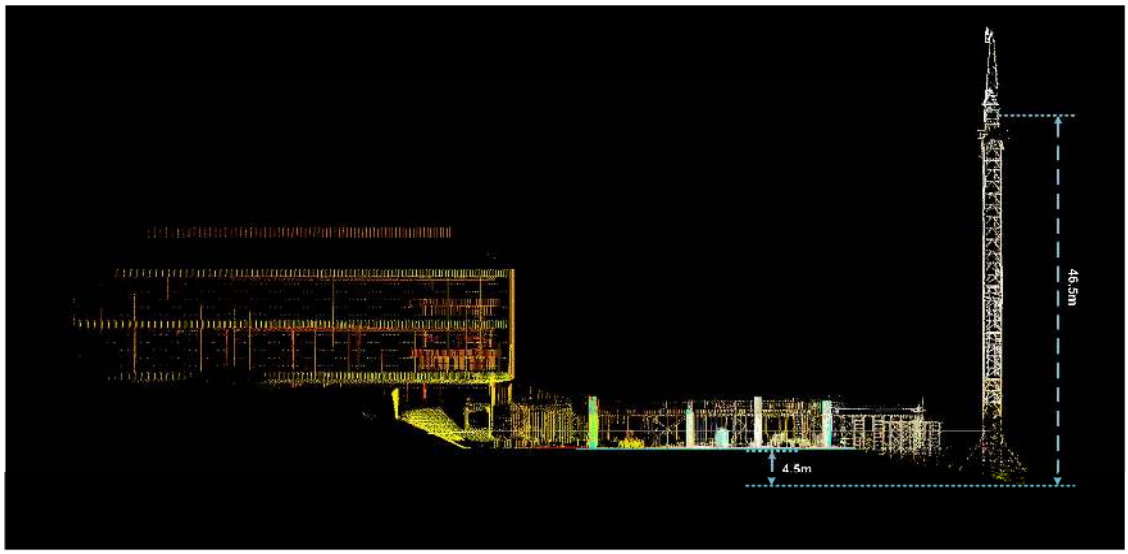

Figure 24 Elevation view of the second floor and the crane location.

5.4.2 Object Detection

The final spatial data were saved in the data format of "x,y,z". The occupancy grid consisted of a series of equal sized voxels, while each voxel was 0.2m x 0.2m x 0.2m long. The size of the voxels can be modified according to the scale of the site scene. The voxel size impacts the level of detail to represent an object. Voxels were filled, if they contained at least three range points. The number of voxels along the elevation was then counted. A total of 64,623 voxels were constructed to store all 2,027,763 as-built data points. Each voxel had on average 31 data points. Therefore spatial data density was sufficient enough for the developed algorithms to work successfully. Figure 25 shows the distribution of the number of voxels along the elevation. Based on empirical judgment the range between -0.2 and 0.2 m was set to be the "ground level" of the second floor. Four major object categories were established (see Figure 25) based on their height. These were objects:

1. *Taller than 1.5 m*: Few voxels were counted that belonged to columns and walls.

2. *Higher than 0.2 m but lower than 1.5 m*: The number of voxels increased. Included were fence material, temporary structures, and other miscellaneous objects.

3. *Between -0.2 m and 0.2 m*: The floor level contained 88.3% of the voxels.

4. *Lower than -0.2 m*: Few voxels which belonged to scaffolding at the leading edges of the floor slab and in areas of rebar installation were counted.

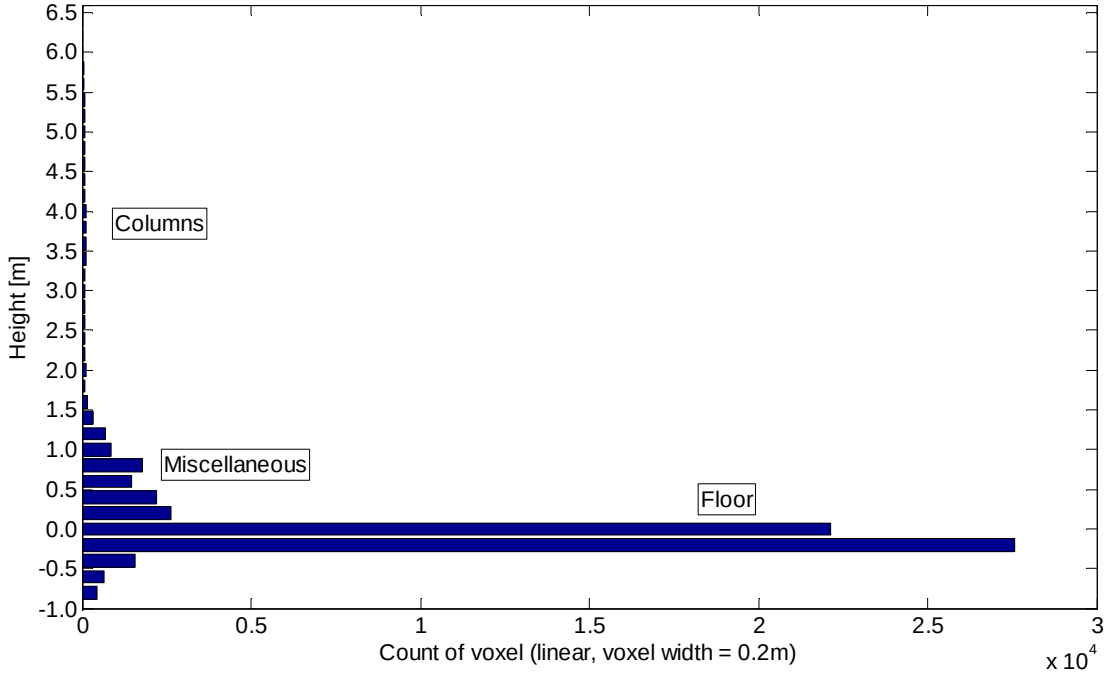

Figure 25 Distribution of the number of voxels along the elevation.

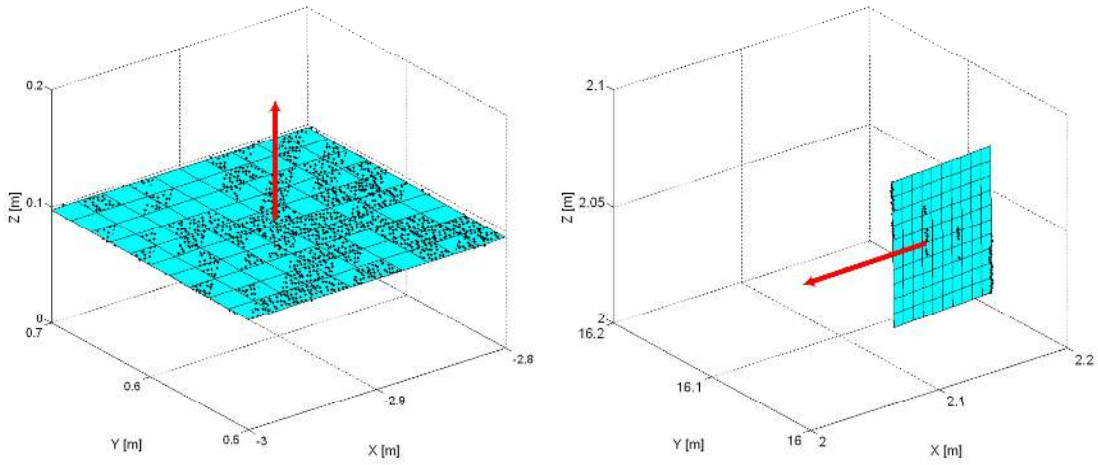

Figure 26 Voxels with horizontal and vertical direction.

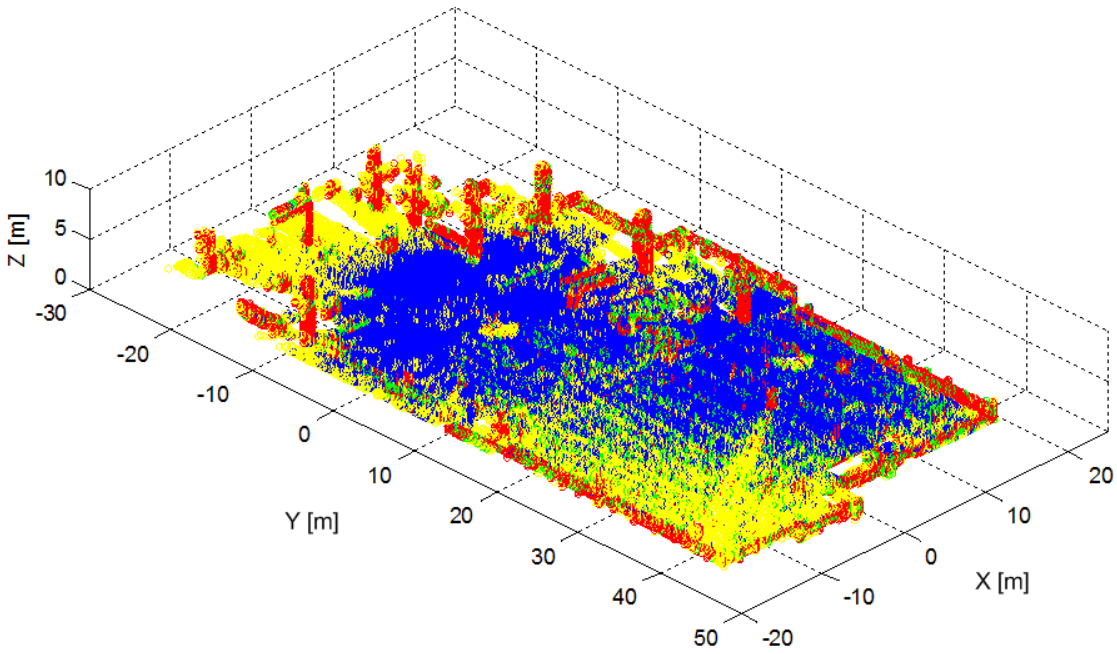

Figure 27 Orientation map of voxels (blue=horizontal, red=vertical, green=arbitrary, yellow=unknown).

The orientation of each voxel was computed to match each voxel with a single object. The range point data to each voxel was fitted to a flat plane. Its normal vector represented the direction of the voxel. Figure 26 illustrates two independent voxels that have vertical and horizontal normal vectors, respectively.

A rule-based approach was taken to classify the object each voxel belonged to. For example, voxels with elevations between -0.2 m and 0.2 m, and vertical orientation were considered to belong to the floor slab. A voxel with locations higher than 1.5 m and a surface normal oriented horizontally was matched to a wall or column. Figure 27 illustrates a voxel-based representation of the construction site.

Each pixel in Figure 27 indicates the location of the center of one voxel. The color shows the orientation to each voxel: Voxels belonging to horizontal surfaces are in blue; voxels belonging to vertical surfaces are in red; voxels that belong to neither horizontal nor vertical surfaces (arbitrary surfaces) are green; and voxels with no or unknown orientation (less than three range points in each voxel) are in yellow.

The voxels were clustered based on the topology and on several elevation ranges. Voxels of the same surface normal direction and with distances to each other less than one meter (ε = 1m) were classified to the same cluster. An additional criterion (to eliminate smaller objects that may not obstruct the FOV of a crane operator) was that each cluster must contain at least eight voxels in order to form a 2 x 2 x 2 cube. Scattered groups which consisted of less than eight voxels were considered as outliers and were not clustered.

The minimum number of voxels to form a cluster can be altered manually according to the density of the point cloud data. The choice of the threshold values, including the size of each voxel and the minimum number of voxel to form a cluster, may vary and depend on site specifications. They depend on the level of detail that a cluster needs to form to satisfy the requirement of classification of an object. Since the clustering process started in the tallest range (objects with heights greater than 1.5m), voxels that had already been assigned to a cluster were removed. This avoided duplicating clusters as well as to increase the computational speed.

The results to clustering are shown in Figure 28 through Figure 30. For visibility reasons, each figure shows the clusters (objects) detected at pre-defined object heights (taller 1.5 m, between 0.7 m and 1.5 m, and between 0.5 m and 0.7 m). The left image in each figure demonstrates the clusters (objects) that were found using the developed algorithm. The numbers of the corresponding objects are projected on the plan view of the point cloud (see right images).

The results show that voxels on large objects whose scale was greater than 0.2 m x 0.2 m x 0.2 m can be clustered. Figure 28 gives an example of clustered objects that were taller than 1.5 m. Thirteen objects including nine columns (No. 2, 3, 4, 5, 7, 8, 10, 12, and 13), a concrete peer (No. 1), a material palette (No. 6), and two big containers (No. 9 and 11) were accurately identified. Similarly, Figure 29 and Figure 30 illustrate the results to 36 clustered objects that had heights between 0.5 m and 1.5 m. A total of 49 clusters were formed. The railing system surrounding the site is clustered in 14 individual parts (see Figure 29: No. 1, 5, 15, 17, 18, 20, 22, 23, and 25; see Figure 30: No. 1, 4, 13, 14, 19 and 21).

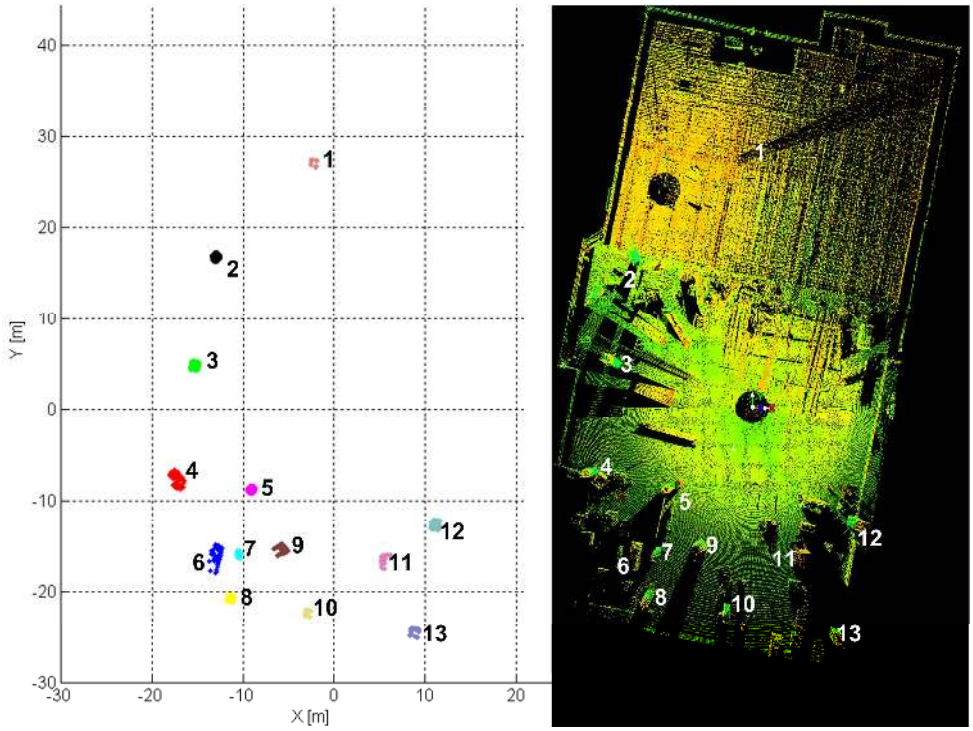

Figure 28 Clustered objects that are higher than 1.5m.

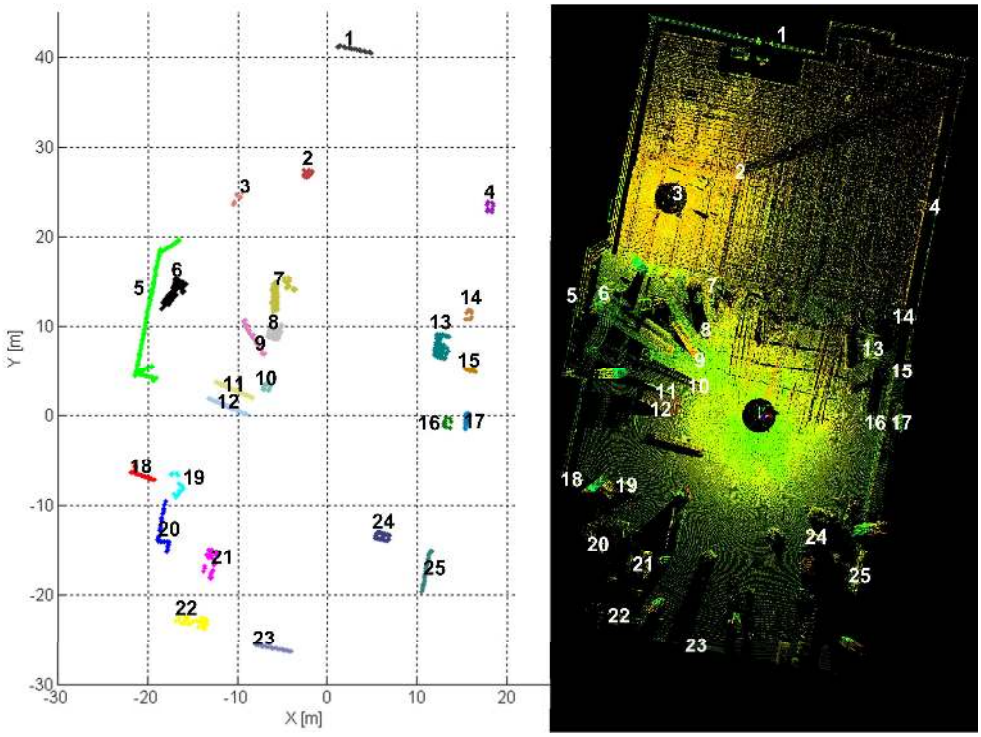

Figure 29 Detected objects with a height ranging between 0.7m and 1.5m.

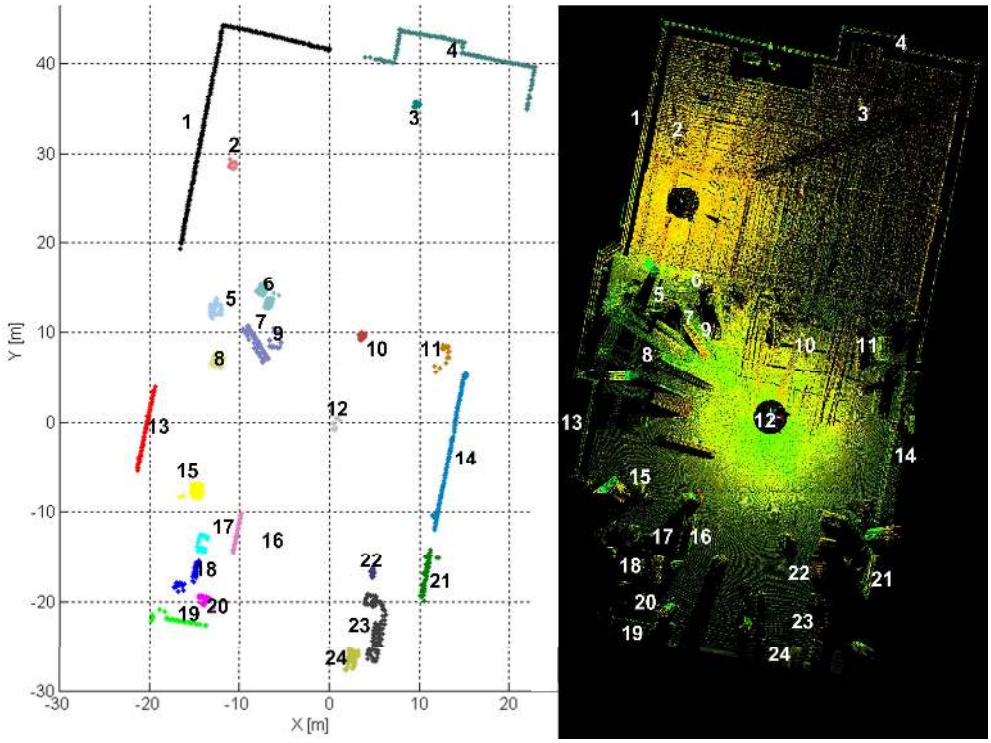

Figure 30 Detected objects with a height ranging between 0.5m and 0.7m.

5.4.3 Calculating the Size and Visualizing Objects and Blind Spaces

Since the position of the crane operator is known, a blind spot/area and space calculation to all the detected clusters (objects) was performed. The boundaries of the detected objects were represented by vertices which resulted from constructing a convex hull to each cluster (e.g., columns, railing, dumpsters, and floor). A ray-casting algorithm helped in detecting the invisible spaces to the crane operator.

Major obstructions on the ground level consisted of columns and structures with vertical surfaces such as box and cylinder shapes. Figure 31 shows the geometric representation of a column which was 5.42 m tall. The blind spaces invisible to a crane operator are marked in red color. The length and area of the blind space were automatically calculated to be approximately 5.1 m and 4.9 m^2, respectively.

The vertices to all objects which were taller than 1.5 m were utilized to automatically generate a blind space map. The isometric view of the blind space map of the entire job site as it relates to columns and floor slabs is illustrated in Figure 32. Blind spaces generated by clusters (concrete columns) that are taller than 1.5 meter and by the

leading edge of the top floor can be seen. Theoretically the blind spaces would go all around the building under construction. However, earth piles and a neighboring building restricted the blind spaces on the lower floor levels to only a portion of the new building.

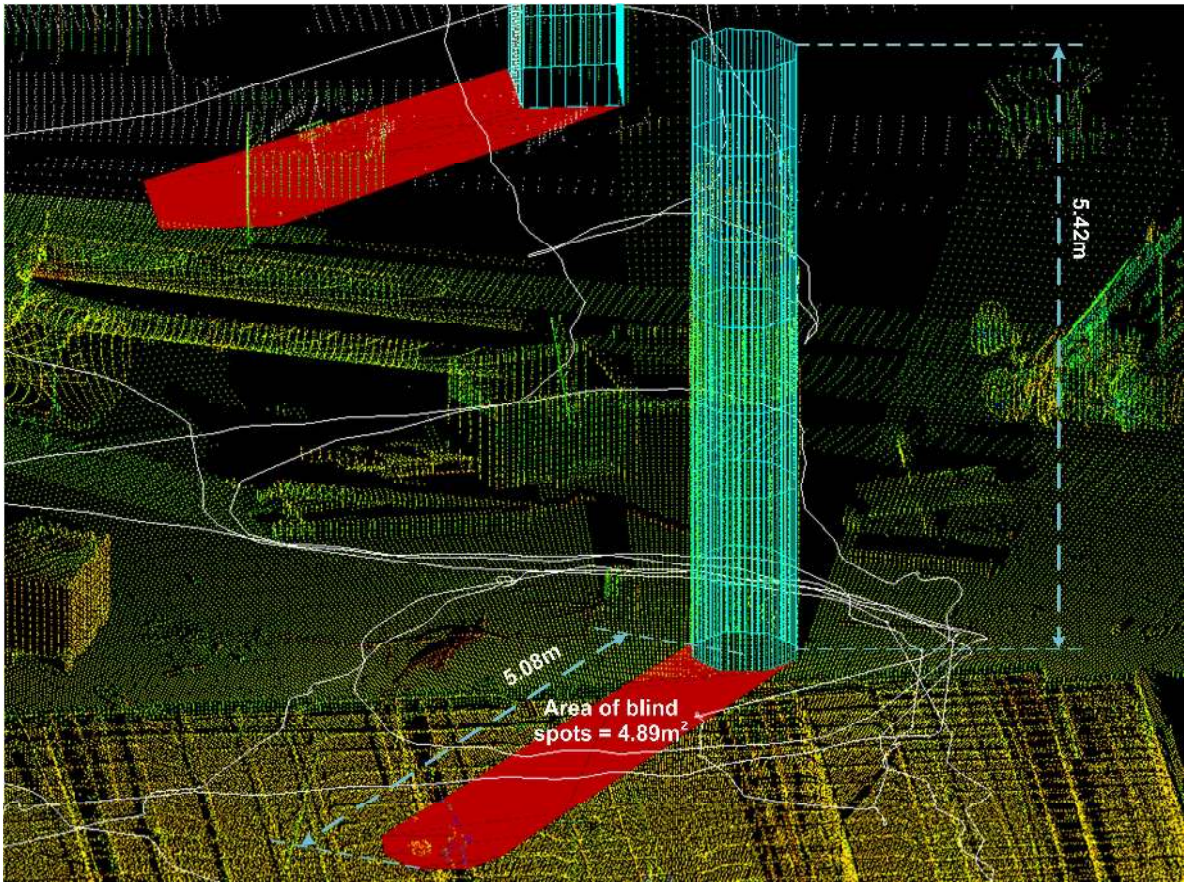

Figure 31 Geometric representation of columns and blind spaces.

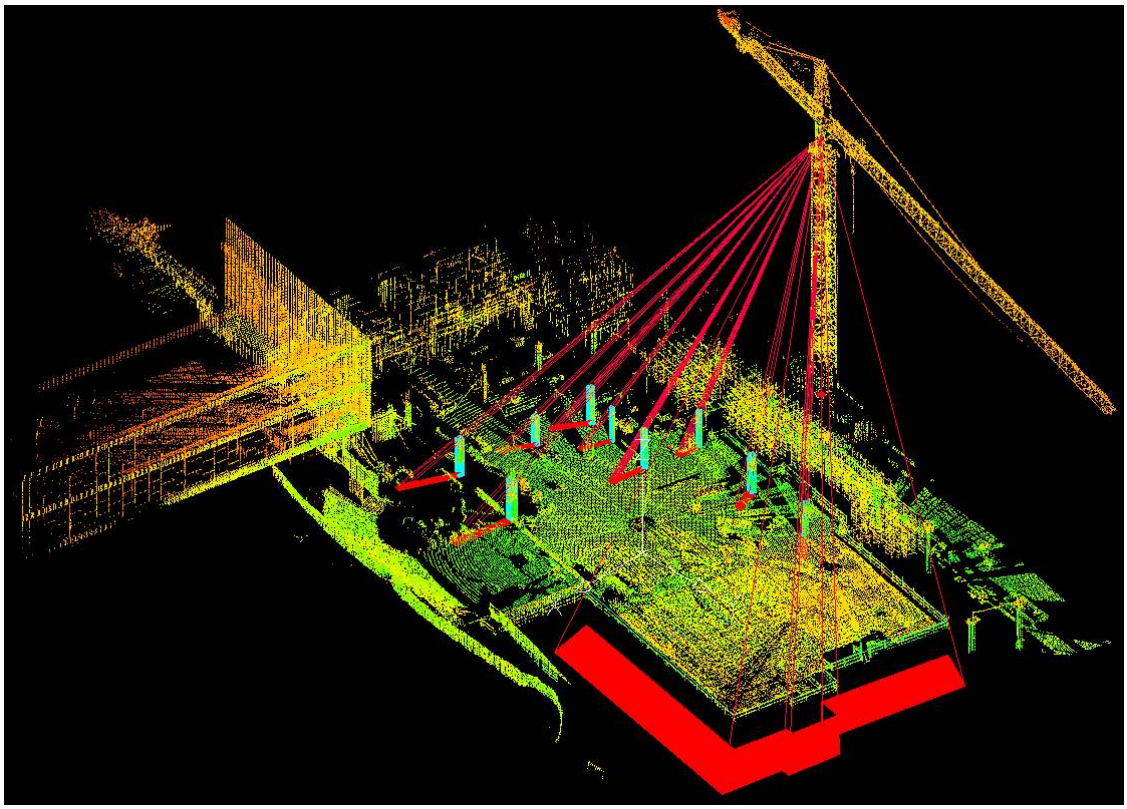

Figure 32 Isometric map of blind spaces to columns and lower level.

Further analysis was done to measure the impact of blind spots by alternating the crane location. Although such a task would make relatively little sense for existing tower crane positions on a project that is already underway, simulating the impact of blind spaces based on crane positions can make a lot of sense for safe and productive construction operations planning. The optimization of crane positions is already a very active research field. Many researchers [147] have recently used BIM to coordinate critical lift planning. However, a lot of projects in the as-built environment do not have a BIM available. They would also first rely on documentation, for example laser scanning, to gather enough 3D information of the environment to generate objects accurately in a BIM. One benefit of the developed algorithm is that it works using the point cloud data and subsequently, does not rely nor require the generation of a BIM.

Seven potential crane locations were manually selected to determine their impact on the size of blind areas. The method then included measuring the size of blind areas for all of the seven crane positions for nine columns on the second floor (work level), four

other objects on the second floor, and areas to lower (ground) level. As the position of the crane cabin (origin for ray-casting) could be virtually moved, the developed algorithm was able to easily measure the sizes of blind spots/spaces for seven different crane cabin locations (all at the same height). The results are shown in Figure 33. Figure 33a visualizes the blind spaces to each crane cabin location in isometric view, and Figure 33b shows the corresponding plan view.

Quantification of the size of blind spots/spaces was also performed. The results are presented in Table 5. Crane position four has the smallest total blind space area that is generated by columns and other major obstructions on the second floor on the job site. As the numbers illustrate, the size of blind spots to individual objects or to the ground level varies based on the location of the crane.

What has been done in the past manually and based on experience can be performed with assistance of data gathering and analysis. Quantitative data in Table 5 indicates that the position of the crane as it was mobilized in the field was ultimately also the best crane position to minimize the blind spots. However, such analysis may vary as site progresses or the shape of building envelope and building elements differs. Further studies are needed to evaluate the developed algorithm for more complex projects and at varying time scales.

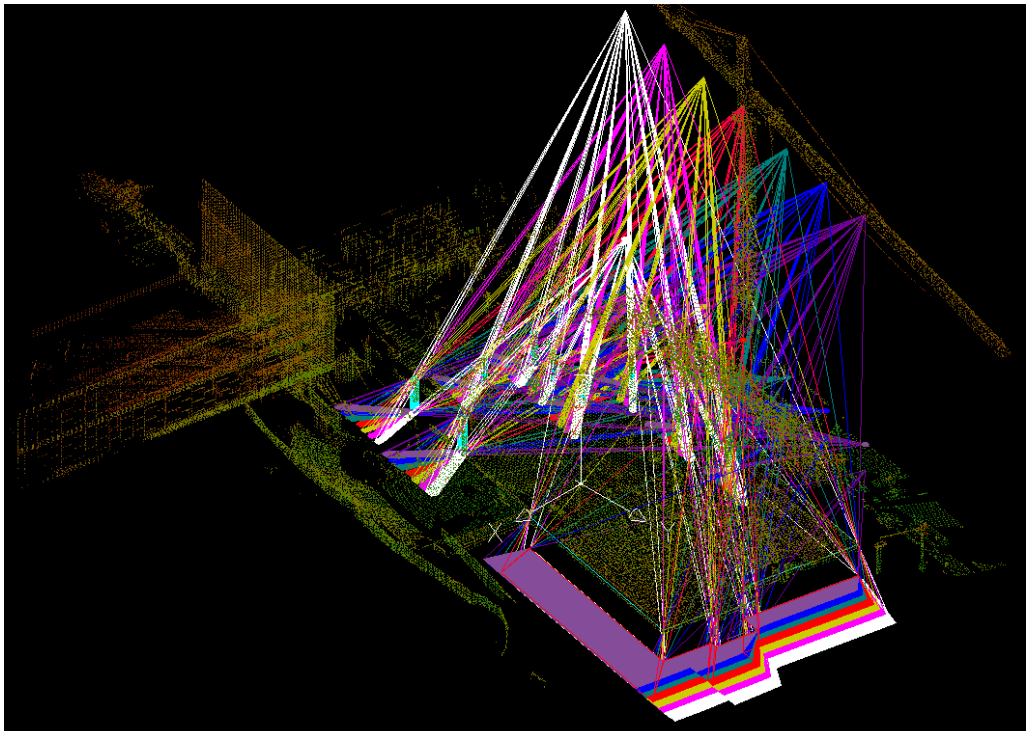

(a) Isometric view of blind spaces at different crane locations.

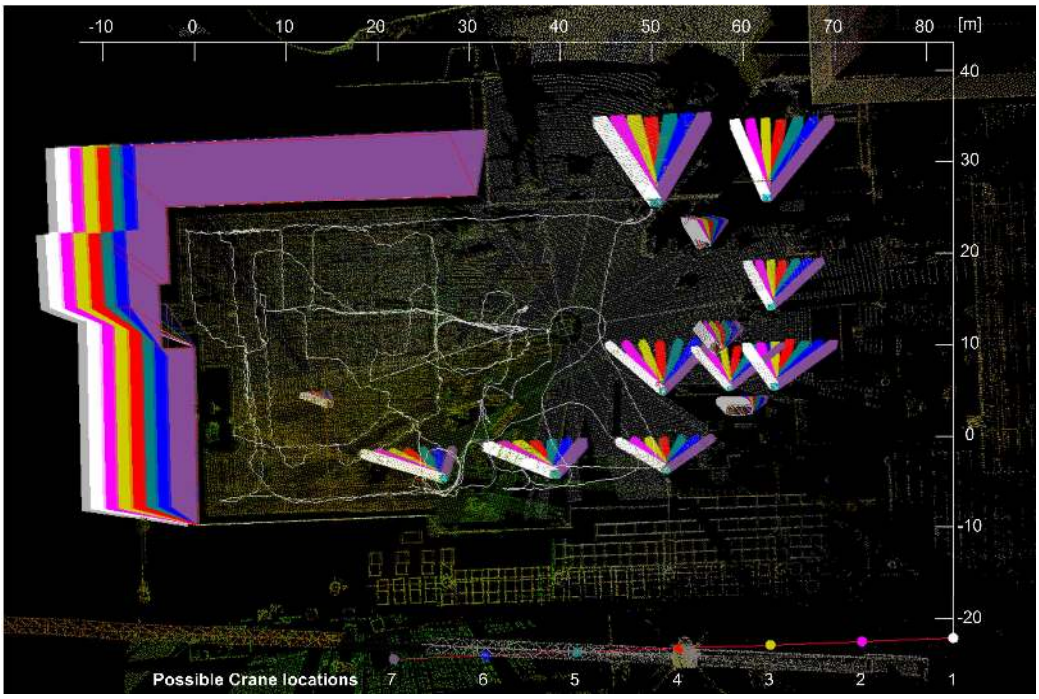

(b) Plan view of blind spaces at different crane locations.

Figure 33 Optimizing the tower crane location to increase crane operator's situational awareness.

Table 5 Comparison of build areas for columns and other objects on the second floor, and to the lower level at different crane positions.

Blind Area [m^2]	Crane Position						
	#1	#2	#3	#4	#5	#6	#7
Column 1	9.24	7.77	6.37	5.04	3.82	3.17	3.31
Column 2	8.41	7.70	5.74	4.43	3.08	3.73	4.99
Column 3	5.28	4.15	3.53	2.97	3.31	4.49	5.82
Column 4	7.17	5.94	5.12	4.84	5.07	6.00	7.11
Column 5	5.06	4.35	3.65	3.31	3.74	4.23	4.72
Column 6	5.59	4.67	3.88	4.95	6.47	7.82	9.18
Column 7	6.60	5.56	4.95	5.88	7.05	8.13	9.22
Column 8	10.14	8.68	7.74	8.98	10.64	12.12	13.59
Column 9	15.67	14.28	12.89	12.04	13.55	15.09	16.64
Sum for Columns	87.04	76.26	66.49	65.16	70.00	78.63	89.51
Object 1	3.95	3.67	3.40	3.31	3.69	4.03	4.37
Object 2	2.98	3.02	3.14	3.26	3.40	3.55	4.19
Object 3	2.77	2.48	2.19	1.90	1.58	1.29	1.00
Object 4	4.19	3.98	3.90	4.23	4.59	4.96	5.36
Sum for Columns and Objects	100.93	89.41	79.12	77.86	83.26	92.46	104.43
Lower Level	681.98	630.29	578.72	513.49	470.16	419.82	370.95

5.4.4 Integration of Blind Spots Measurement with Real-time Location Tracking Data

RTLS data of workers was mapped on the previously generated blind spots/space map. Fusing the data sets allows understanding of inter-relationship among construction resources such as the geometrical distance between moving workers and obstructions that limit the FOV of crane operators.

The spatio-temporal analysis for a single worker is shown in Figure 34. The path of the worker shows where and when the worker was entering/leaving a blind space that was not visible to the crane operator. A detailed view of the trajectory of the worker (white polylines) is illustrated in Figure 34.

Figure 34 Worker trajectories mapped on laser scan with blind areas taller than 1.5m.

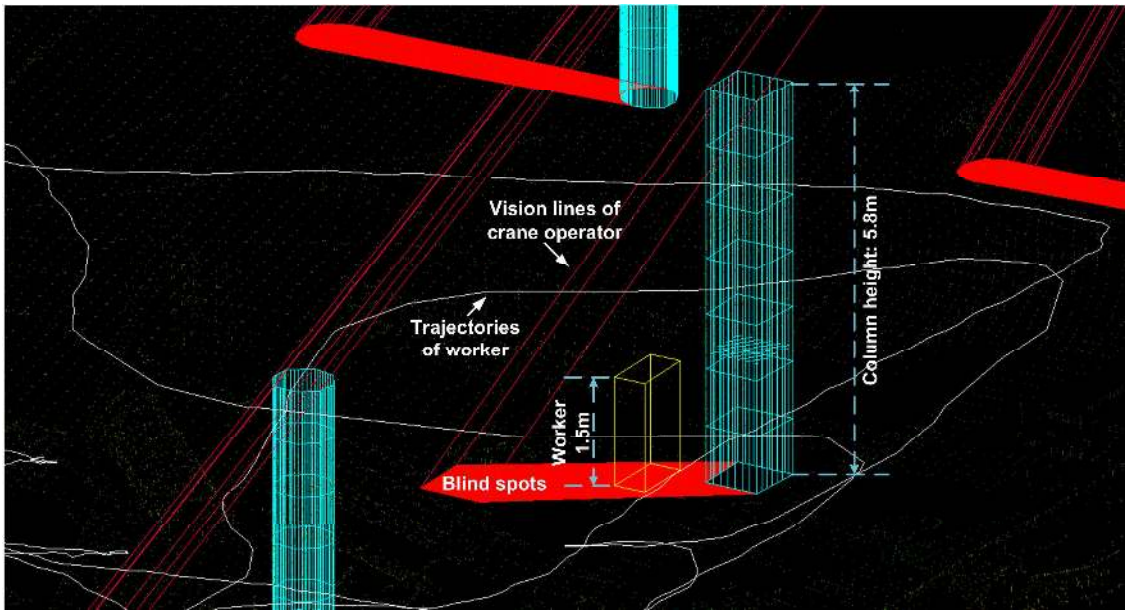

Figure 35 Worker entering blind space.

According the ISO standard (ISO 5006) that measures operator visibility of construction equipment, a 1.5 m tall and 0.6 m wide bounding box should be utilized to simulate a worker near a piece of equipment [69]. Although such a rule may not (yet) be in place for tower cranes, this experiment proceeded with a similar methodology to evaluate if a worker can be seen by the crane operator. A box is placed along the path of the worker to measure visibility to the tower crane operator. As shown in Figure 35, the worker was completely obstructed by a column. Although the duration in the blind space was only for a few seconds, frequency of the same worker traversing blind spaces can be calculated. In total, the same worker entered and left four times the blind space to two columns. The worker spent about 10 seconds total in the blind areas in a five minute long experiment.

Although the demonstrated results to a single worker seem to be very specific and offer no immediate consequence to change the work setting, adding information of (1) location and (2) size of blind spaces, (3) frequency of workers, (4) routes of workers, equipment, and materials, (5) time of workers spent in blind spaces, and (6) where, when, and how close workers get to crane loads, may yield in site layout planning undiscovered potential to design for and execution of safer construction. For the particular site investigated, no major work task was observed in the blind spots detected on the second floor and/or on the ground level. During the time of experiment the tower crane operator had always good situational awareness and workers never were below crane parts or loads, but this again may change on differing (7) site conditions, (8) schedules, (9) structures to build, and (10) tower crane locations.

5.5 Conclusions

Advanced topographic survey technologies (laser scanning) have made it possible to quickly and accurately document as-built conditions. As such technologies become available they lead to novel solutions in identifying and resolving potential design and operational issues, including mitigation of risks associated to safe site layout and equipment operator visibility. This research demonstrated the capability of detecting objects from large as-built spatial data sets collected by a commercially-available laser scanner.

The objective of this chapter was to locate and quantify the blind spots/areas and spaces based on 3D range data. For a large construction setting, multiple scans should be conducted and registered. After removing the noise and outliers of the gathered 3D range data, the developed algorithm detected the location and size of blind spaces that obstruct the field-of-view (FOV) of a tower crane operator. This work has also offered a solution to utilize trajectories of workers to identify (unsafe) locations of workers that are (not) in the FOV of tower crane operators.

The developed approach has great potential to assist jobsite hazard analysis. Once integrated in information models, it can detect potentially dangerous work spaces. During construction, crane activities in conjunction with safe site layout and workers' trajectory can be analyzed and accordingly improved as needed.

Further and more detailed studies are necessary, in particular how well existing safety practices and design can be improved. Long-term experimental validation may also find additional benefits and barriers of the developed approach. A set of standards of evaluating the crane operator's visibility has to be established so that the blind space analysis in different construction site settings can be validated. In addition, current approach considered the worker entering blind spaces as unsafe, but the determination of a real hazardous situation requires the position information from the crane boom and hook. A detailed analysis of proximity hazards among ground workers, crane load, and the corresponding blind spaces need to be investigated in future research. Several limitations were observed, for example, the blind spots analysis and site layout evaluation so far can only be fulfilled offline and is not fully-automated. Especially the point cloud noise removal is accomplished based on a manual process, which could be less efficient. Range scanning and data processing may significantly be improved by scanning from or closer to the tower crane cabin. However, this may add significant complexity in handling the gathered data set, especially if scan speed is slow and ranges are short. In summary, the utilization of as-built documentation and blind spot analysis can detect potentially hazardous work spaces that are related to tower cranes.

CHAPTER VI

EVALUATION OF PROXIMITY HAZARDS OF HUMAN INTERACTING WITH CONSTRUCTION EQUIPMENT AND ENVIRONMENT

The previous two chapters introduced the approaches to retrieve the location information of construction resources and the geometric information of major obstacles on construction sites. Through the analysis of their spatio-temporal relationship, this chapter introduces an approach that can automatically evaluate the proximity hazards of personnel interacting with construction equipment and environment.

6.1 Introduction

Construction sites may have unique size and settings, but a general setting is comprised of similar types of resources involving personnel, equipment and materials. In order to perform highly dynamic construction activities, workers are often required to present at close proximity to traffic, heavy equipment, and various other hazardous substance and conditions. Statistics shows that working proximity to hazards has resulted in a big fraction of construction fatalities. From 2003 to 2010, 3,171 workers were killed due to exposure to various hazardous situations including contacting with objects and equipment, falling from floors, exposing to chemicals and flammable substance, and struck by vehicle. These fatalities accounted for approximately 40% of the total construction fatalities and 6% of the total workplace fatalities experienced during that period.

Existing research summarizes several risk factors that cause worker to be exposed to hazardous situations, which includes [148]: constantly changing job site environments and conditions; unskilled laborers; high diversity of work activities occurring simultaneously; and exposure to hazards resulting from own work as well as from nearby activities. According to these risk factors, the health hazards are grouped as chemical,

physical, biological and ergonomic. Alternatively, this research classifies the hazardous situation into two categories based on the spatio-temporal characteristics of the hazards.

Many hazardous situations occur when dynamic resources such as heavy construction equipment, vehicles and materials are operating in close proximity to ground workers. This type of hazardous situation is always involved in congested working areas. Contact collision between ground workers and these dynamic resources can increase the risk of injuries and fatalities for construction personnel [149]. BLS reported that of the 818 fatalities in construction industry in 2009, 18% (151 fatalities) were caused by workers being struck by an object or construction equipment [15].

Compared to the moving resources, the other type of hazard has relatively constant location and geometry, such as toxic, chemical and flammable substance, high-voltage power line, edge of elevation, and blind space to crane operator. These static hazardous conditions have caused a number of fatal and nonfatal injuries on construction job site. The topical and chemical substance includes dusts, mixtures, and common materials such as paints, fuels, and solvents [150]. Existing of high-voltage power line is always associated to the operating safety of crane and derrick [151]. Fall from floor opening and edge lf elevation has been the leading reason of construction fatalities for the past years [17]. Equipment operator visibility, specifically operator blind spaces, contributes to contact collisions between materials and ground workers [69].

Specific controls including OSHA safety regulations, administrative policies, best practice, and new proactive sensing technologies that have been established and developed are vital to reduce the proximity hazards whenever possible and when workers necessarily have to perform activities in the same area as heavy equipment and harmful substance. However, a deep understanding, evaluation, and monitoring of workers' safety performances under proximity hazards is still lacking, which request scientific analysis of the spatial and temporal relationship between workers and hazards.

6.2 Evaluation of Proximity Hazards

This chapter focuses on analyzing the spatio-temporal relationship between personnel and hazards found on the construction site. As is defined in chapter III, a proximity hazard is

a situation that poses a potential level of threat to a worker's safety, which occurs only when the worker approaches to such a situation. The considered hazards are classified as dynamic and static. The dynamic hazards include mobile ground vehicles and equipment, and cranes. The static hazards include flammable, chemical, and toxic substance placed at fixed position on construction site, floor edge, opens at elevation that are associated to fall hazards, and any pre-defined areas that are only accessible to authorized personnel.

The goal of this chapter is to develop an algorithm that can evaluate and measure the safety performance of construction personnel especially when they conduct activity proximate to the abovementioned hazardous conditions. In order to achieve this goal, several sub-objectives have been defined. The first objective is to automatically generate hazardous areas surrounding the existing static and dynamic hazards on the specific construction site settings. The second objective is to automatically analyze the spatio-temporal conflicts between each worker and each considered hazard. The last objective is to define an indicator that can be utilized to measure the safety performance of workers.

A flowchart of measuring the proximity issue between worker and various hazardous conditions based on real-time location sensing and as-built ranging data is shown in Figure 36. The technologies and techniques implemented for tracking the spatio-temporal data of construction resources and gathering the geometries of major objects on construction site have been introduced in chapter IV and V. This section details the development of an approach that utilizes the known tracking data and geometric information to measure the proximity hazards. The developed approach includes three major parts: generating hazard zones surrounding specific source; analyzing the spatio-temporal relationship between workers and generated hazard zones; computing an indicator that can be used to evaluate the proximity hazard.

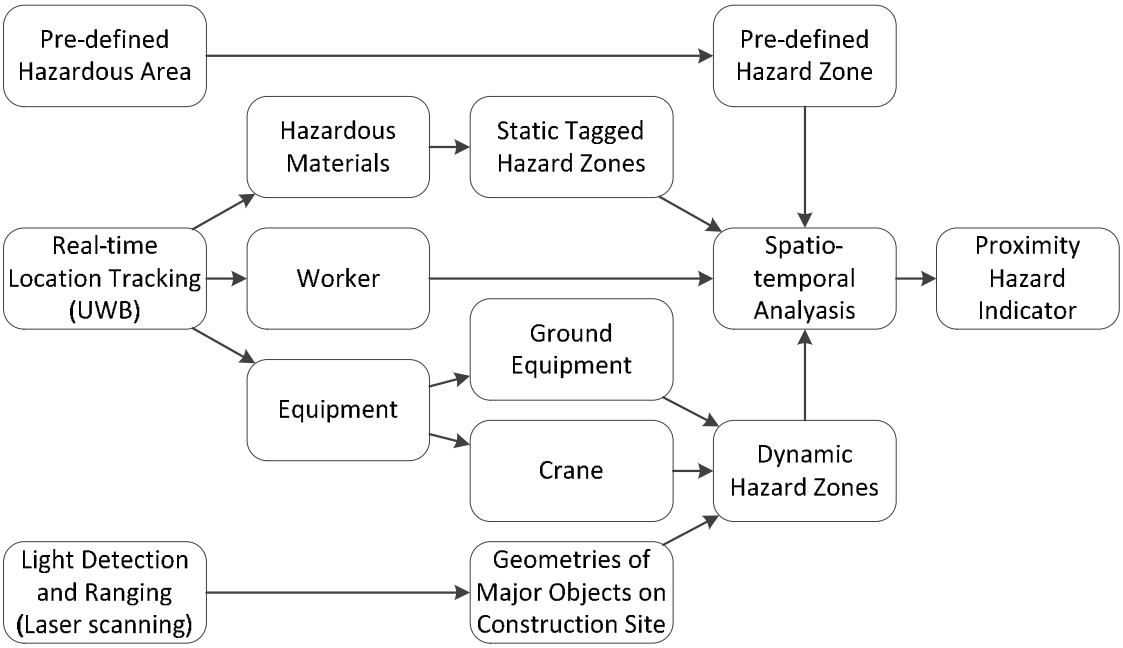

Figure 36 Flowchart of measuring proximity hazard

6.2.1 Hazard Zones

In general, a hazard zone is represented as a polygon that is generated based on the location and geometry information of the potential hazards. The method that is used to generate a hazard zone varies according to the characteristics of the hazardous source. The characteristics of hazardous sources are classified as static and dynamic. In static case, a hazard's is either pre-defined according to the construction environment whose geometry is known (e.g., access-controlled space that only authorized personnel is allowed to enter), or monitored through remote location tracking and sensing technology (e.g., UWB). In dynamic case, the location of a hazard is gathered utilizing real-time location tracking and sensing technology. The following sub-sessions introduce the methods of generating hazard zones in difference situations.

Pre-defined Hazard Zone

As one type of the static hazard zones, pre-defined hazard zones are formed based on the existing construction site settings and structural components. Examples include but are not limited to the following cases:

- *Edge of roof and/or big openings on elevation*
- *High voltage power lines*
- *Unstable excavations and trenches*
- *Confined and other limited-access space*

Since these components always maintain on a construction site and do not change frequently, the hazard zones attached to them have fixed locations and geometries. The locations and geometries of site components are achieved by conducting survey using ranging sensing technologies such as Robotic Total Stations and Laser scanning. Detecting objects' boundaries and retrieving their geometries from as-built data have been introduced in Chapter V, whose results can be directly imported into the algorithm to generate pre-defined hazard zones.

After gathering the geometries of these site components, safety diameters if necessary are utilized to generate pre-defined hazard zones. For example, according to the OSHA standards subpart M 1026.502 [152], the mechanical equipment is not allowed to being used within the 6 feet range from the edge of a roof. In this case, a polygon with 6 feet width along the roof is formed as a pre-defined hazard zone. Operating inside this zone is considered as a hazardous situation.

A pre-defined hazard zone is represented by the boundary of its representing polygon. The polygon's boundary is denoted by the coordinates of its nodes, which are ordered counterclockwise. Figure 37 illustrates a hazard zone represented by a polygon and the corresponding data structure that a hazard zone is stored. Since the coordinates of nodes are either imported from the results of analyzing the as-built ranging data or measured through on-site survey, the shape of the representing polygon can be convex or concave which is only determined by the site conditions and geometries.

In most cases, since a pre-defined hazard zone represents the hazards existing on the same elevation level as the workforces, it is projected into 2D polygon and represented by the centroid of the polygon C and a safety radius r (the maximum distance from polygon nodes to the centroid) which are computed using flowing equations:

$$C_x = \frac{1}{6A}\sum_{i=0}^{n-1}(x_i + x_{i+1})(x_i y_{i+1} - x_{i+1} y_i) \quad \text{(Eq. 6-1)}$$

$$C_y = \frac{1}{6A}\sum_{i=0}^{n-1}(y_i + y_{i+1})(x_i y_{i+1} - x_{i+1} y_i) \quad \text{(Eq. 6-2)}$$

$$r = max(\{i \in [1,n] || Node_i - C|\}) \quad \text{(Eq. 6-3)}$$

where A is the polygon's signed area,

$$A_y = \frac{1}{2}\sum_{i=0}^{n-1}(x_i y_{i+1} - x_{i+1} y_i) \quad \text{(Eq. 6-4)}$$

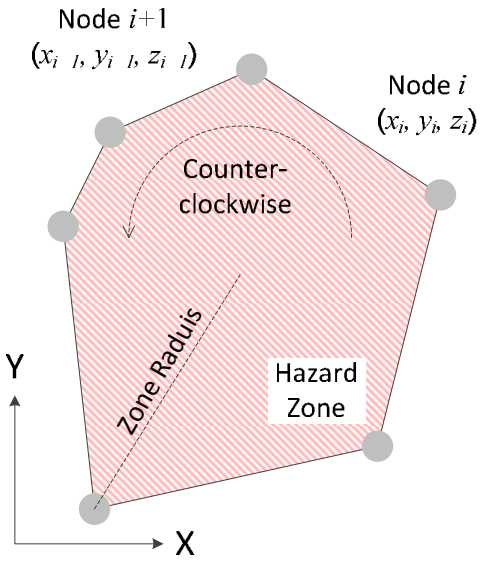

Node ID	X	Y	Z
0	x_0	y_0	z_0
...	...	...	...
i	x_i	y_i	z_i
i+1	x_{i+1}	y_{i+1}	z_{i+1}
...	...	...	...
n	x_n	y_n	z_n
0	x_0	y_0	z_0

Counter-clockwise

Figure 37 A hazard zone represented by a polygon and its data structure.

Static Tagged Hazard Zones

Another type of static hazard zones are generated due to the temporal placement of construction materials or substances that have potential and rapid negative impact to human safety, health and productivity. Examples include but are not limited to the following cases:

- *Flammable liquids, such as petrol, alcohol and welding gas*
- *Chemical and toxic substances, such as acid and alkali solvents*
- *High-voltage power generating unit*

Similar to the pre-defined hazard zones, the generation of a tagged hazard zones requires the location of the hazards as well as a safety diameter. Since these hazardous existences are not counted as permanent resources on a construction site, they only occupy a temporal area and can be moved to support various work tasks during the day. Surveying and ranging technologies which is utilized to determine pre-defined hazard zones are not able to monitor the actual geometry of this type hazards. Instead, this hazardous condition is monitored through the implementation of real-time location sensing technologies. In this dissertation, the hazardous substances and materials are tagged by UWB sensors, so that their location data can be gathered in real-time. The outliers of the location data are removed through Robust Kalman Filter [146], and the filtered data are processed to form a polygon, which represents the geometry of the hazard.

As the geometry of the hazard polygon is known, a hazard zone is represented by extending the hazard polygon using a buffering algorithm. The hazard zone surrounds the hazard and the buffering distance between the circumferences of the hazard zone to the hazard polygon is called safety diameter. This diameter is defined by existing safety regulations. For example, OSHA standard require a 5-foot-clear distance of workers to an individual portable flammable liquid tank when the capacity of the tank exceeds 1,100 gallons [153]. If the safety diameter is not available from the existing safety regulation, user can specify an appropriate factor based on current situation.

Figure 38 illustrates the buffering method that is used to extend a hazard polygon into a hazard zone. A series of buffering circles (black dashed lines) with safety diameter are created on the circumference of the hazard polygon (blue solid lines). The circles are centered at the polygon nodes (blue solid dots) as well as points along the edge. A new polygon which is the hazard zone (red solid lines) of the given hazard is formed by connecting the external tangential point of each buffering circle. The geometry of the

tagged hazard zone is stored in the same data structure as is used for pre-defined hazard zone.

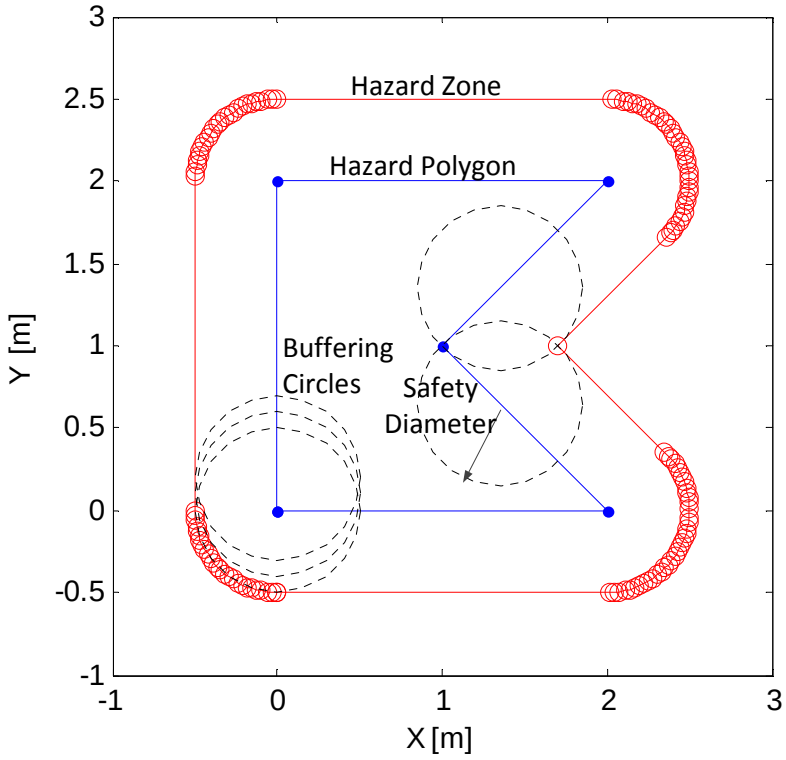

Figure 38 Polygon extension using buffering algorithm

Dynamic Hazard Zone

Besides static hazards, workers on construction site are often continuously exposed to another type of hazardous conditions that keep changing in location, shape, scale and orientation over the time. In this dissertation, this type of hazards is regarded as dynamic hazards. Examples include but are not limited to the following cases:

- *A worker is walking across a traffic road without using the crosswalk while a pieces of construction equipment or vehicle is moving toward him*
- *A worker is performing work tasks behind a piece of equipment or vehicle while it is reversing*

- *A loaded crane hook swings over a crew of ground workers*
- *A worker is performing work tasks inside the blind space of ta crane operator while the operator is maneuvering the load*

The generation of a dynamic hazard zone requires four parameters, which include: scale, function type, location, and velocity of the considered equipment. The equipment's scale influences the size of the hazard zone. The function type defines whether it is a piece of ground equipment or lifting equipment which consists of carrier and a revolving component. The location of a dynamic hazard determines the position where the corresponding hazard zone is centered. The moving velocity determines the orientation and shape of the generated hazard zone.

The scale and the function type are specified by user, which becomes constant parameters. In contrast, a dynamic hazard zone does not have a fixed location and velocity, which are derived by averaging the positions and speed vectors measured by multiple UWB tags mounted on the equipment. Figure 39 illustrates the procedures of deriving location and velocity from the tracking data in a 2D case. The scale of the equipment is denoted by its length L and width W. Multiple UWB tags are mounted on the equipment at various positions which are denoted by α_i, β_i and γ_i, whose values range from -0.5 to 0.5. A positive value indicates that the tag is mounted on the front (left, up) side of the equipment. Assume a piece of equipment is moving along a curve, the positions of tags are collected by the UWB receiver and velocity of each tag is represented by the displacement over a short time (Eq. 6-5). The effective position P_i and velocity V of the entire equipment at the time t is derived using the following equations:

$$\overline{V_i} = \frac{\Delta \overline{P_i}}{\Delta t}, \ \ where\ \overline{P_i} = [x_i, y_i, z_i]^T \qquad \text{(Eq. 6-5)}$$

$$\bar{V} = \frac{\sum_{i=1}^{n} \overline{V_i}}{n} = \left[V_x, V_y, V_z\right]^T \qquad \text{(Eq. 6-6)}$$

$$\bar{P} = \frac{\sum_{i=1}^{n} \overline{P_i'}}{n}, \ \ where\ \overline{P_i'} = [x_i', y_i', z_i']^T \qquad \text{(Eq. 6-7)}$$

$$\overline{P_i'} = \overline{P_i} - \begin{bmatrix} V_y & V_x & 0 \\ -V_x & V_y & 0 \\ 0 & 0 & 1 \end{bmatrix} \begin{bmatrix} \beta_i W \\ \alpha_i L \\ \gamma_i H \end{bmatrix} \qquad \text{(Eq. 6-8)}$$

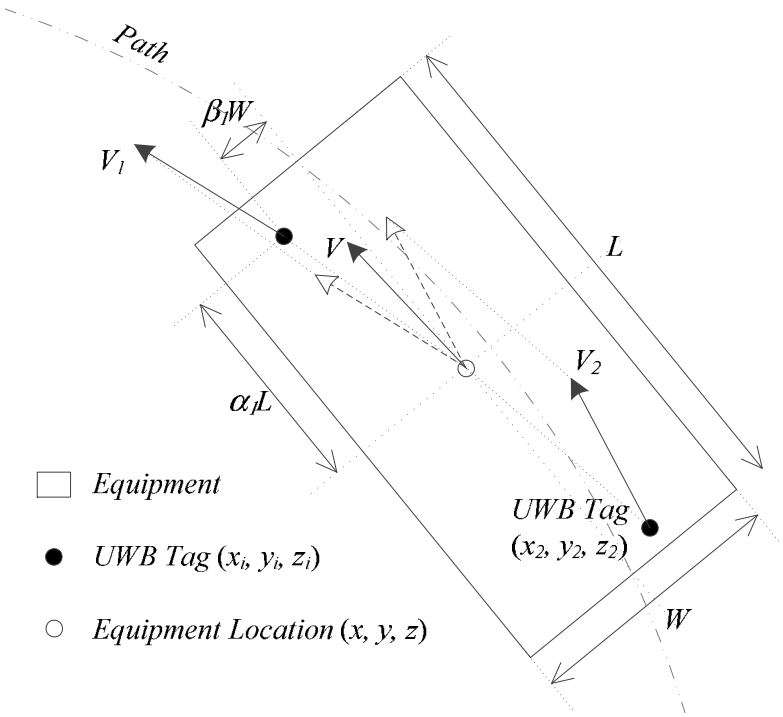

Figure 39 Compute equipment's location using tracking data collected by multiple UWB tags.

When computing the effective position and velocity of the equipment (equation 6-5 to 6-8), the basic idea is using chord to approximate the movement of the equipment on a curve. In Figure 39, the velocities V_i and locations P_i of multiple UWB tags are averaged according to their relative position to represent the equipment's movement as if it travels along the chord. This approach works fine when the equipment moves along a curve that has high curvature. A special case is traveling straight forward or backward, which means the curvature is zero. In this case, since all the UWB tags have an identical moving direction, the overall velocity of the equipment theoretically equals the average of the velocities of all tags. However, this approach has a limitation to estimate the velocity when the equipment is conducting pure revolving actions. One example is a skid-steer loader steers by braking one-side wheels without changing its position. In this case the traveling curvature is infinite, which results in big uncertainty when approximating the arc using its chord.

As the four key parameters (scale, function type, location, and velocity of the considered equipment) are determined, they are used to form dynamic hazard zones. Taking a piece of ground equipment as an instance, Figure 40 illustrates how a dynamic hazard zone is generated. The equipment is tracked by several UWB tags, and each tag is mounted on the various parts of the equipment. The position of the equipment is represented by its center point (*O* in Figure 40), which is derived by computing the geometric average of the tracking data collected by these tags. Besides the location, several input parameters are required to generate a hazard zone around the equipment. These parameters include: the width (*D*) and the length (*L*) of the equipment; a safety buffering diameter (*r*) to the equipment; braking time (Δt) that the equipment operator needs to slow down the equipment before hitting an object; and possible steering angle (σ) when the equipment moves.

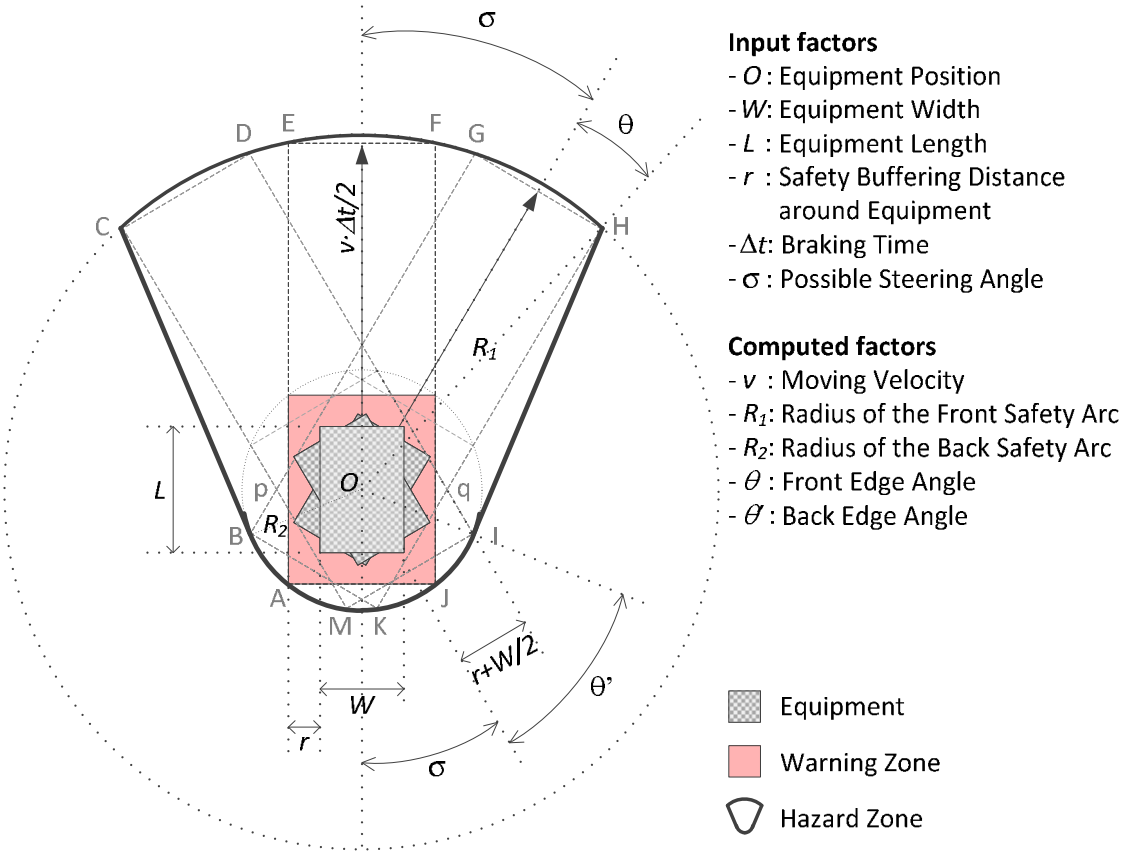

Figure 40 Generation of a dynamic hazard zone surrounding a piece of moving vehicle.

Knowing these parameters, a polygon utilized to represent the hazard zone around the equipment is generated through the following procedures:

1. *Expand the length and width of the equipment using the safety diameter to form a warning zone (hatched area).*

   A warning zone indicates a clearance area such that even though the equipment is not moving, work should still keep a certain distance away from the equipment. This zone is defined in order to avoid potential injury such as worker being hit by the unexpected movement of equipment, or worker being hit by the revolving component of the equipment.

2. *Extend the warning zone by a distance of* $\frac{1}{2}\bar{v} \cdot t$ *on the equipment moving direction to form the box* A-E-F-J. *The velocity* $\bar{v}$ *is computed through the tracking data, and t is the braking time as a given parameter.*

   Zone A-E-F-J represents the area that can be covered by the equipment over the braking time Δt if the equipment is moving straightforward at the speed of $\bar{v}$. The braking distance is $\frac{1}{2}\bar{v} \cdot \Delta t$ when a linear deceleration model is utilized.

3. *Rotate the box* A-E-F-J *with the angle* σ *both clockwise and counterclockwise about the fixed center at O to form two boxes* M-C-D-I *and* B-G-H-K *respectively.*

   Considering the equipment operator may steer during the brake in order to avoid upcoming objects, the moving direction of the equipment may vary. Boxes M-C-D-I and B-G-H-K indicates the area that can be covered by the equipment if the operator steer on both left and right direction from the very beginning till the equipment stops.

4. *Connect nodes* A-B-C-D-E-F-G-H-I-J-K-M *to form a polygon, which is the dynamic hazard zone around this piece of equipment.*

   The dynamic hazard zone is generated based on the current kinematics and geometric status of the equipment. It is also a prediction of the area that can be covered by the equipment over the braking time. The dynamic hazard zone will be stored using the same data structure as it is used for static hazard zones.

Several intermediate parameters are computed using the following equations at the time t when the position of the equipment is $\bar{p} = (x, y)^T$ and the velocity of the equipment is $\bar{v} = (v_x,\ v_y)^T$ on a 2D projection:

$$R_1 = \sqrt{\left(\frac{L}{2} + r + \frac{vt}{2}\right)^2 + \left(r + \frac{W}{2}\right)^2},\ \ where\ v = |\bar{v}| \quad \text{(Eq. 6-9)}$$

$$R_2 = \sqrt{\left(r + \frac{L}{2}\right)^2 + \left(r + \frac{W}{2}\right)^2} \quad \text{(Eq. 6-10)}$$

$$\theta = sin^{-1}\left(\frac{2r + L}{2R_1}\right),\ \ \theta' = tan^{-1}\left(\frac{W + 2r}{L + 2r}\right) \quad \text{(Eq. 6-11)}$$

$$\alpha = tan^{-1}\left(\frac{v_y}{v_x}\right),\ \ \beta = \sigma + \theta,\ \ \gamma = \sigma + \theta' \quad \text{(Eq. 6-12)}$$

In a fixed known Cartesian system XOY, the coordinate of each node is computed using the following equations:

$$Denote\ a\ vector\ Z = Z(\varphi) = (cos\,\varphi,\ sin\,\varphi)^T \quad \text{(Eq. 6-13)}$$

$$F = \left(F_x, F_y\right) = \bar{p} + R_1 \cdot Z(\alpha - \theta) \quad \text{(Eq. 6-14)}$$

$$G = \left(G_x, G_y\right) = \bar{p} + R_1 \cdot Z(\alpha - \sigma + \theta) \quad \text{(Eq. 6-15)}$$

$$H = \left(H_x, H_y\right) = \bar{p} + R_1 \cdot Z(\alpha - \beta) \quad \text{(Eq. 6-16)}$$

$$I = \left(I_x, I_y\right) = \bar{p} + R_2 \cdot Z(\alpha - \pi + \gamma) \quad \text{(Eq. 6-17)}$$

$$J = \left(J_x, J_y\right) = \bar{p} + R_2 \cdot Z(\alpha - \pi + \theta') \quad \text{(Eq. 6-18)}$$

$$K = \left(K_x, K_y\right) = \bar{p} + R_2 \cdot Z(\alpha - \pi - \sigma + \theta') \quad \text{(Eq. 6-19)}$$

Notice that the dynamic hazard zone is symmetric along the central axis, therefore the coordinates of the rest of the nodes can be computed.

Figure 40 and equation 6-9 to 6-19 details the generation of a dynamic hazard zone attaching to a piece of ground equipment such as truck, loader, and dozer. One of the common features of the ground equipment is that the components of the equipment

moves together as a whole. In contrast, the other type of equipment has connected parts that can perform movements separately, such as backhoe, mobile and tower cranes. Since the operation of this type of equipment always involves rotations, the equipment is simplified into translating part and revolving part. Taking mobile crane as an example, the substructure such as the crane's cabin and carrier conducts forward and backward translations while the revolving part is the superstructure including the boom, the hook and the load. In case of the equipment with revolving components, two hazard zones are generated separately: one is a dynamic hazard zone centering at the translating component; the other is another dynamic hazard zone centered at the revolving part. If the substructure of the equipment has to maintain immobile when the superstructure is operating, the substructure's hazard zone becomes static.

To be noticed, two approximations have been performed when forming the hazard zone. First of all, following step 1-3, the hazard zone should have two arcs with radius R1 and R2 on the front and back phase respectively. The arc representation requests a great number of nodes along the arc to be recorded in order to represent a hazard zone, which will significantly increase the computational complexity when later performing spatio-temporal analysis. Therefore, when the dynamic hazard zone is generated, the arcs on the front and end phase are replaced by the chords, so that the coordinates of only limited number of nodes need to be stored. Secondly, instead of using straight edge C-B and H-I on both left and right side, a dynamic hazard zone should have broken edges like C-p-B and H-q-I shown in Figure 38. Nodes p and q are the joints of line C-M and B-G, and K-H and D-I, which make the hazard zone concave. Using broken edge requests significantly computational resources when the algorithm has to repeatedly generate dynamic zones at each time frame and generally the dynamic hazard zone has to be updated 2-5 times every second. Moreover, the difference of generating the dynamic zone using broken edge and straight edge becomes insignificant when the possible steering angle σ is less than 15^{o} and the braking time Δt is smaller than 5 seconds, which covers most of the cases in the human-equipment proximity situations. Therefore, the broken edges are simplified as straight edges when generating a dynamic hazard zone.

Hazard Zones with Blind Spaces

Besides static dynamic and static hazards that have been introduced in the previous paragraphs, a construction site generally consists of numerous multi-sized objects which represent obstacles in the field-of-view (FOV) of an equipment operator and create significant large blind spaces. Ground worker working inside the blind spaces when a part of or the entire piece of equipment is operating close to the same area is considered as a dangerous situation. In this case, a new hazard zone combining equipment movement and blind spaces has to be generated. As the computation of the geometry of blind spaces has been introduced in Chapter V and dynamic hazard zones have been generated in the previous sub session of this chapter, the new hazard zone is generated through Boolean Operations of the blind spaces and dynamic hazard zones.

The hazard zone with blind spaces is formed under two different situations: case of ground equipment and case of equipment with revolving components. In the first case, since the operator moves together with the equipment, the blind space will change accordingly. Figure 41 illustrates the formation of hazard zones of a piece of ground equipment with the blind space generated by an obstacle when the equipment approaches, passes and leave the obstacle. As the equipment approaches and leaves the obstacle, the obstacle itself is outside the dynamic hazard zone. No change will be made to the hazard zone. As the equipment is passing the obstacle, the blind space created by the obstacle overlaps with the dynamic hazard zone. Since it is assumed that operator will not intentionally crash the obstacle, the obstacle here preforms as a protection to the resource behind it. The eventual hazard zone is therefore the dynamic hazard zone minus the blind space. However, it does not necessarily mean that working inside a blind space is safe. Instead, a spatio-temporal analysis has to be conducted which will be explained in the next sub session.

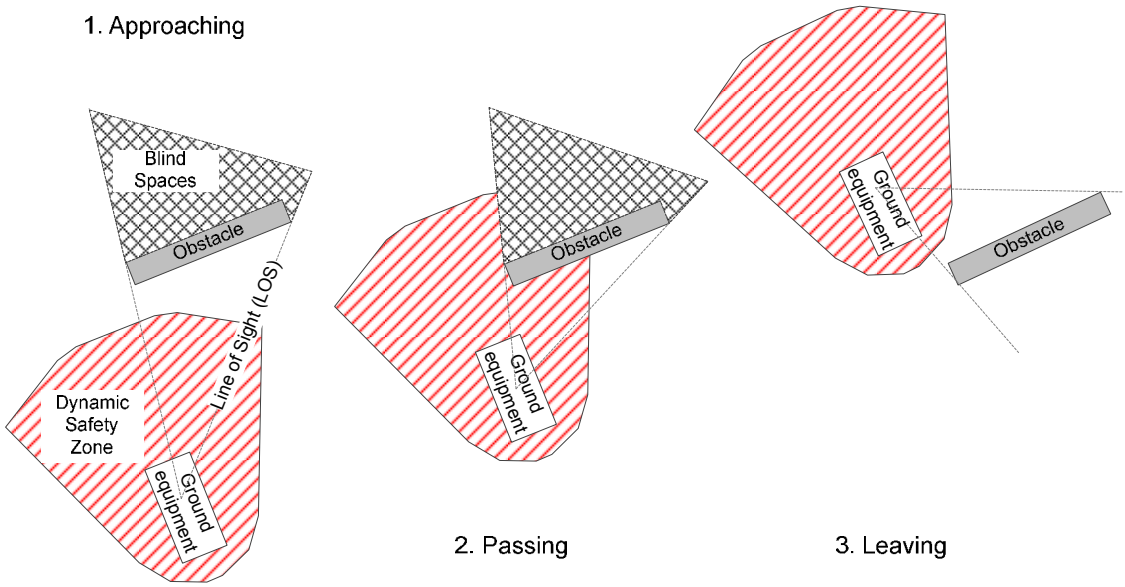

Figure 41 Hazard zones of ground equipment with blind spaces.

In the second case that the operator operates the revolving components at an immobile position, the blind space maintain static. Figure 42 illustrates the formation of the hazard zone in this situation. Taking mobile crane as an example, when no movement is performed, two static hazard zones (shaded in red in Figure 42) are generated around the crane base and crane hook respectively. In addition, the blind space (hatched area) generated by an obstacle is formed within the possible crane coverage area. When the crane boom starts swing, the hazard zone around the hook becomes dynamic. When the crane hook enters the blind space to the operator, a new hazard zone (highlighted in red solid lines) is formed as the joint of the dynamic hazard zone and the blind space.

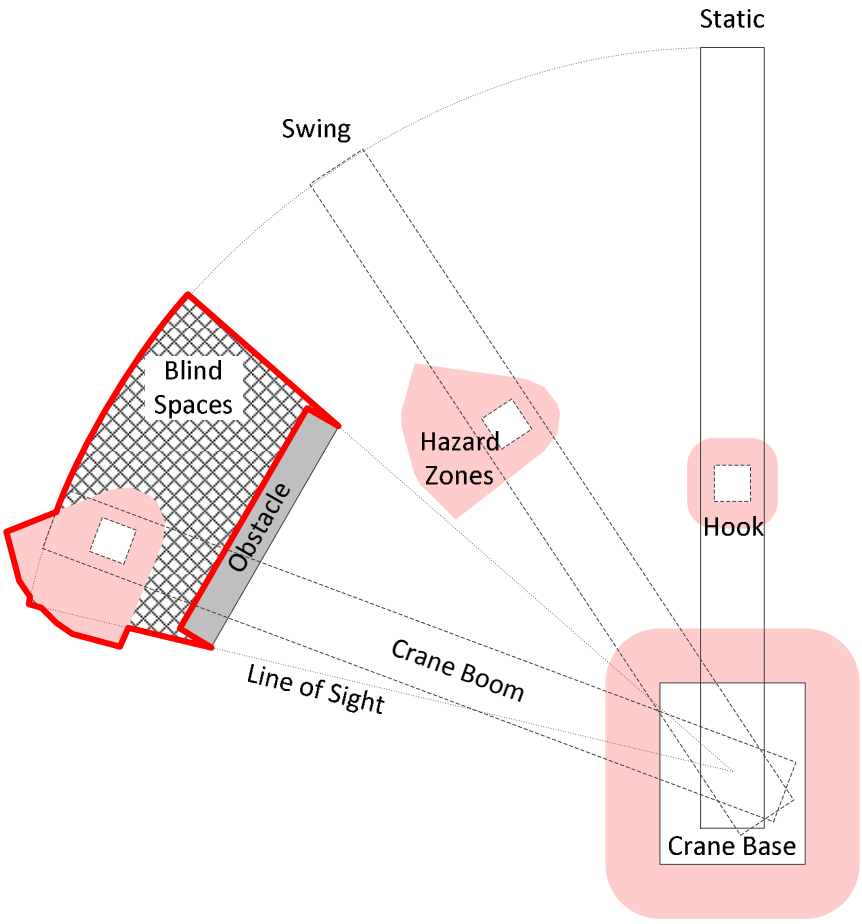

Figure 42 Hazard zones of revolving equipment with blind spaces.

6.2.2 Spatio-temporal Analysis

As worker's location has been tracked in real-time and the hazard zones on construction sites have been defined, their inter-relationships are studied through spatio-temporal analysis. In general, the spatio-temporal analysis examines whether any worker intrudes any existing hazard zone at a given moment t, and predicts the intrusion in a short period at the time $t + \Delta t$. Figure 43 shows the determination of a proximity hazard of one worker. The worker's safety status at current moment (t) is determined by the worker's intrusion status at both current moment (t) and predicted time ($t+\Delta t$). A worker being inside a hazard zone is marked as true intrusion while a worker being outside any hazard zone is marked as false. A worker is safe only if he/she is outside any hazard zone at both current and predicted moment. Therefore, the key to determine the safety status of

a worker lies in checking the geometric and spatial relationship whether the worker's current and next position is inside a safety polygon.

		Current Moment (t)	
		True	False
Predicted Moment ($t+\Delta t$)	True	Proximity Hazard	Proximity Hazard
	False	Proximity Hazard	Safe

Figure 43 Determination matrix of a proximity hazard.

In computational geometry, numerous algorithms have been developed and modified dealing with the point-in-polygon problems. These algorithms are classified into two groups: ray casting algorithm (crossing number algorithm) and winding number algorithm [154]. In this dissertation, the crossing number method is utilized, which counts the number of times a line starting from worker's position crosses the safety polygon boundary edges. The point is outside when this "crossing number" is even; otherwise, when it is odd, the point is inside. The same procedure is repeated on the current and predicted positions of a worker.

The process of detecting proximity hazards can be simplified as two steps: generating hazard zones and conducting point-in-polygon query. As these two steps are expensive in computation, and the algorithm is dealing with several million pieces of tracking data, redundant computing has to be avoided in order to increase the efficiency. Figure 44 presents a flowchart of the spatio-temporal analysis utilizing spatial filtering. The spatial filter makes sure that the zone generation and point-in-polygon computation run only when a worker is close to a hazard. Assuming the algorithm is detecting the proximity hazard of worker i versus equipment j with their known positions *Wpos* and *Hpos* at the time t_k, the worker's position at the next moment is denoted as *Wpos'*.

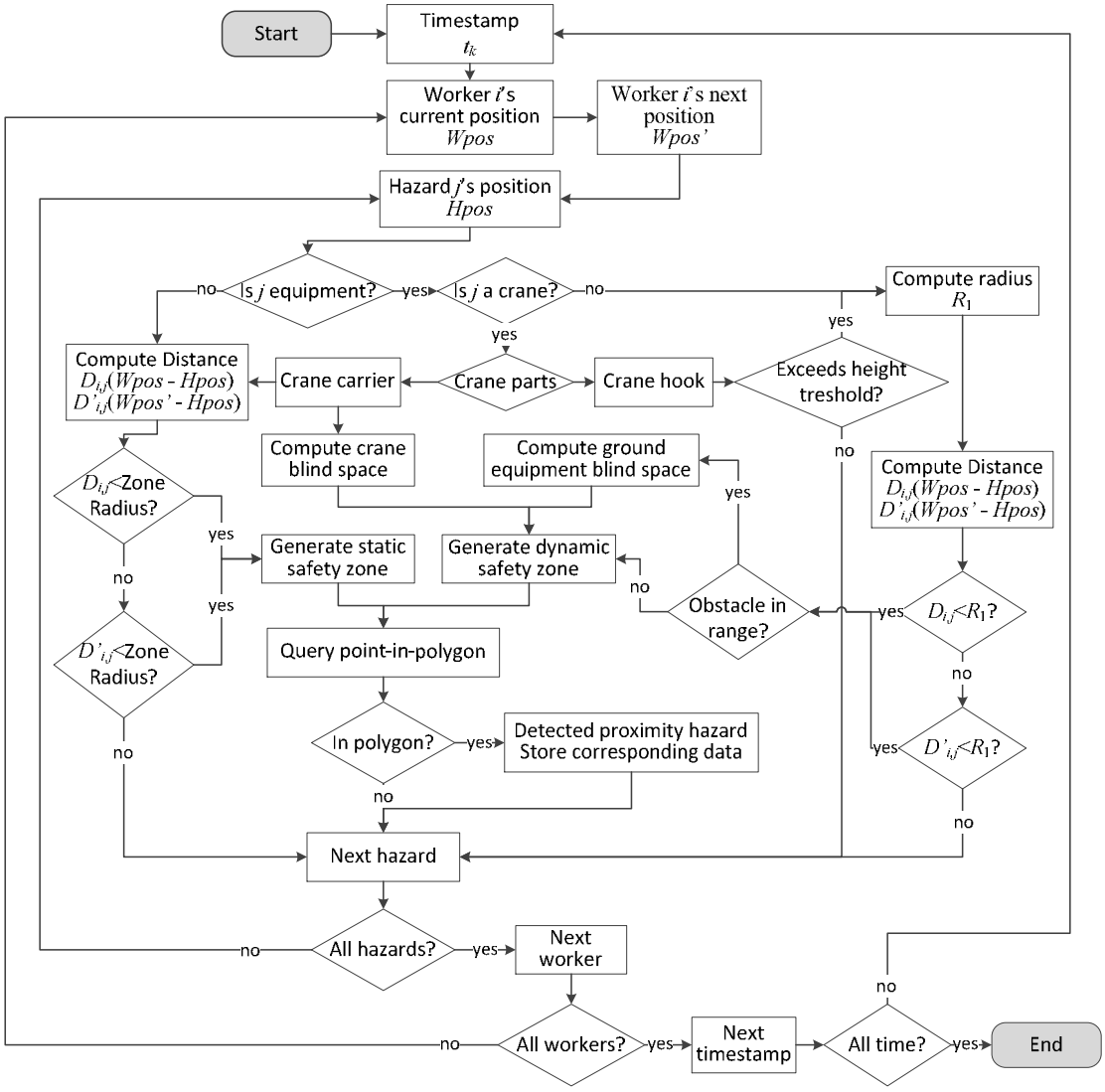

Figure 44 Flowchart of detecting proximity hazard.

When the hazard is not from equipment, it implies a static hazard. The algorithm computes the distances from worker's current/predicted positions to the centroid of the hazard (computed by equation 6-1 and 6-2). If both these two distances are greater than the zone radius (equation 6-4), the worker is considered as safe. If not, the static hazard zone is generated. Either of the worker's current or predicted position is inside the static hazard zone, it is detected as a proximity hazard.

When the hazard is from ground equipment (not crane), the algorithm first computes the equipment safety radius R_1 (equation 6-9). The worker is regarded as safe if

the distances from both the current and predicted positions of the worker to the equipment are greater than R_1. Otherwise, a dynamic hazard zone is generated. In case that an obstacle is inside R_1 range of the equipment, the dynamic hazard zone combines the blind spaces created by the obstacle (Figure 41). Either of the worker's current or predicted position is inside the combined hazard zone, it is detected as a proximity hazard.

When the hazard is from a crane, the algorithm considers the crane carrier as a static hazard and the crane hook as general equipment respectively. In case of crane carrier, the blind space is compute when an obstacle exists inside the crane boom coverage area (Figure 42); in case of crane hook, a dynamic hazard zone is generated only when the hook's elevation is greater than a given threshold, which on-ground hook and load will not be considered as a hazard.

As a case of proximity hazard is detected, the corresponding information including ID of involved entities, location, time, duration, and relative velocity is recorded and stored. The algorithm will iterate the same procedure on the next hazard j+1, next worker i+1, and next timestamp t_{k+1}, respectively, till the entire dataset has been analyzed.

6.2.3 Proximity Hazard Indicator

As a statistic technique, work sampling has been widely used to evaluate the labor productivity by measuring the proportion of time that workers spend in various defined categories of activities [155][156]. The productivity is therefore represented by direct work time rate using the following equation:

$$Direct\ Work\ Time\ Rate = \frac{\sum Time\ of\ Direct\ Work}{Total\ Time} \qquad \text{(Eq. 6-20)}$$

Similarly, the spatio-temporal analysis has sampled the worker's activities and performances into safe and unsafe when the worker(s) is close to considered hazards. Therefore, the worker(s)' safety performance is measured by the Proximity Hazard Indicator (PHI), which is achieved through the similar sampling technique using the following equation:

$$Proximity\ Hazrd\ Indicator\ (PHI) = \frac{\sum_i \kappa_i \times Counts\ in\ Hazardous\ Zone\ i}{Total\ Observing\ Time\ [min]} \qquad \text{(Eq. 6-21)}$$

where i is the index of a hazard zone defined in the previous session and κ_i is the safety factor of each hazard zone. The PHI represents how often the observed target is exposed to various defined hazards within the observing period. The observed target could be a single individual, or a crew of workers.

Compared to traditional work sampling technique and safety inspection which relies on random observation, PHI is achieved based on continues monitoring of the working progress. User can choose appropriate length of observation periods. Within each period, a unique PHI for a specific target can be computed. As the work and monitoring progresses, a series of PHI can be achieved. The distribution of the PHI over the time can be utilized in statistical analyses to find out the target has significantly high rate of unsafe performances. Several examples on computing and using PHI are given in the following session.

6.3 Experiment and Results

This chapter uses three experiments to explain how the proximity hazards are analyzed based on real-time tracking data and site geometric information. The first experiment uses real data in combination with simulated data to demonstrate that the algorithm is able to detect simulated proximity hazards. The second experiment is conducted in a controlled environment, while the participants including personnel and vehicles are performing various safe and unsafe tasks by following pre-scripted scenarios. The third experiment tests the algorithms by using the data collected from uncontrolled real construction site. The results and discussions of each experiment are presented accordingly.

6.3.1 Real Data in Combination with Simulated Data

An experiment was conducted in an outdoor environment to simulate a material handling working scenario (Figure 45). This experiment intended to test the performance of the algorithm when detecting various types of unsafe proximity cases. The experiment occupied a $35\ meter \times 35\ meter$ flat ground area without obstacles. Six UWB receivers were set up on the ground plan and a camera was mounted from a higher vantage point so as to monitor down upon the site. Five participants were recruited and given UWB tags, while one participant also wore the RTS prism and were instructed to keep the prism in

line-of-sight to the RTS station. The purpose of implementing RTS is to measure the error of the tracking data collected by UWB using the approach depicted in chapter IV. In this experiment, 163,007 pieces of UWB data were recorded within the 6 minutes period. The error analysis shows that the UWB data have 0.34 meters as average tracking error and 0.16 meters as standard deviation [157].

The goal of this experiment was to test the algorithm of detecting proximity hazards under abovementioned situations. The current experimental setting consisted of the following components: Two participants were instructed to move several boxes from two fixed source to another two fixed destinies; Another two actors were instructed to approach the previous two participants to simulate a scenario that equipment travels close to ground workers; Two sets of UWB tags were mounted on a red cone and a trolley to simulate static hazards; A series of data was merged into the collected data set to simulate the movement of a crane hook (not shown in photo); besides, a dummy object which was 2 meters high was placed to simulate an obstacle.

Figure 45 showed the experiment setting and the trajectories of participants. 35 unsafe proximity cases were detected whose locations were plotted in the same figure. Figure 46 (a) plotted the details of two cases that one participant walked through a static hazard (small red dots inside purple polygon) and the same participant walked proximate to a dynamic hazard (big red rings inside red polygon). In the second case, the red triangle with black fills represented the position of the equipment at the moment of proximity, and the red polygon represented the dynamic hazard zone. Figure 46(b) plotted the detail of another case that a participant walked from outside into the blind space when the simulated crane hook swung over him. As is discussed in chapter 6.2.2, this case is considered as unsafe proximity.

The results of all the detected unsafe proximity cases were summarized in Table 6. This table counted the total number of unsafe proximity between each pair of worker and hazard. It can be noticed that, none of the participant had exposed himself to static hazard #1 and both of them experienced unsafe proximity to static hazard #2 equipment #2 and the simulated crane hook. Besides, further information including proximity duration, minimum distance, the time when the minimum distance were recorded since the start of the experiment, and the speed at that moment was summarized in this table. In case of

static hazard, the minimum proximity distance was computed as the distance from worker to the centroid of the hazard zone, and the speed was absolute. As a contrast, in case of dynamic hazard, the minimum proximity distance and the speed represented the relative displacement and movement between hazard and worker.

Taking the proximity analysis between worker #2 and crane hook as an instance, more detailed information of the 7 detected unsafe proximity cases was listed in Table 7. In this table, the height of the crane hook was considered when computing the minimum distance. As the result, the distance maintained high when the crane hook was lifted (case 1-6) even though the worker is almost right underneath the crane hook. The entering and exit time indicated the start and end moment of the proximity case. The positions of worker and crane hook as well as their relative velocity were recorded.

The results of this experiment showed that the developed algorithm was able to detect three types of unsafe proximity cases: worker goes through static hazardous zone, worker walks proximately to moving vehicle, and worker stays inside the blind space of crane operator.

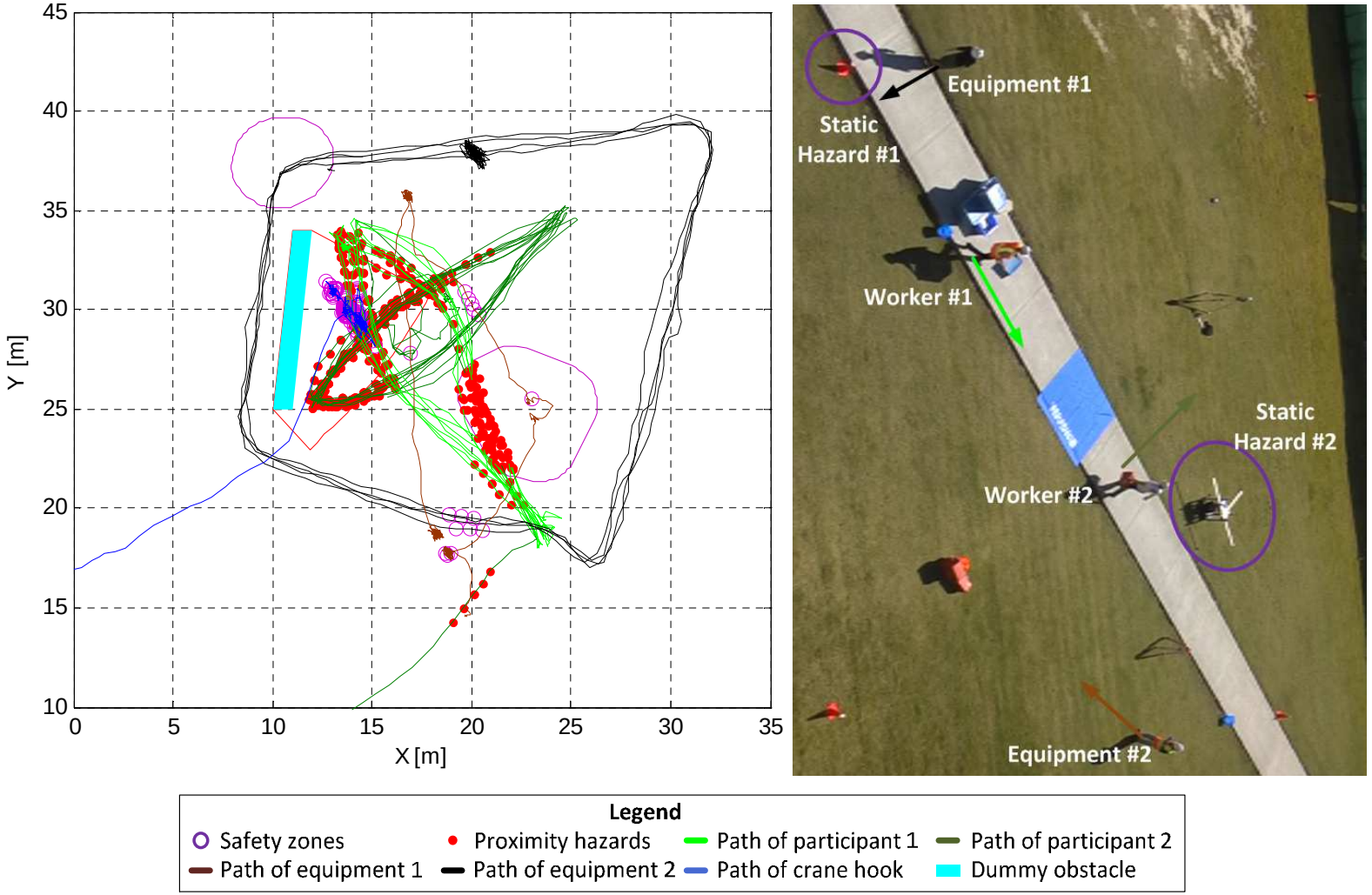

Figure 45 Example 1: Simulated working scenarios.

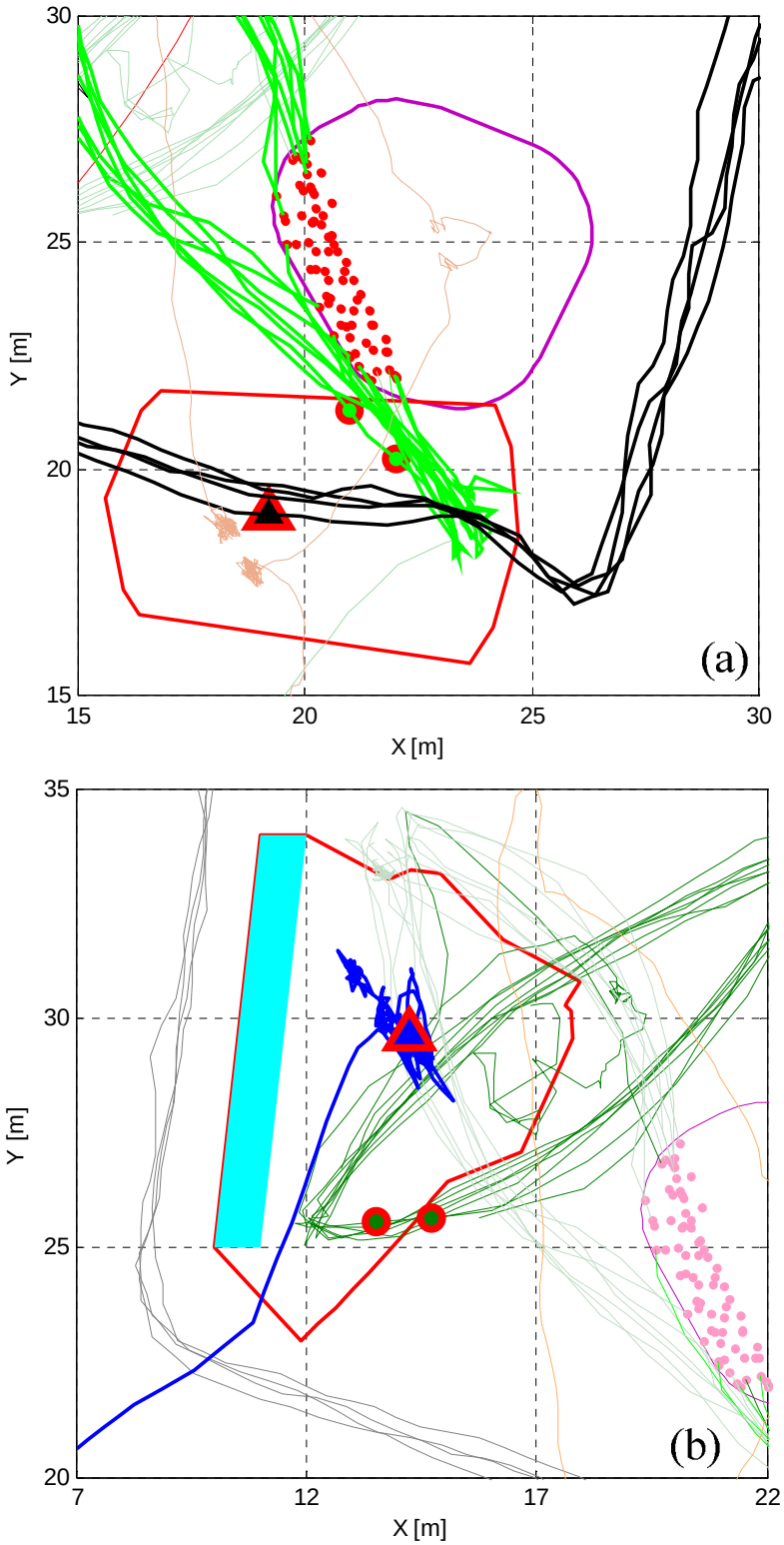

Figure 46 Detected proximity cases, (a) Proximity to a static hazard and a moving vehicle, (b) Proximate to crane hook and inside a blind space.

Table 6 Summary of the result of the simulated working scenario.

		Static hazard #1	Static hazard #2	Equipment #1	Equipment #2	Crane hook
Worker #1	Counts [No.]	0	10	2	2	11
	Duration [mm:ss]	n/a	00:32	00:03	00:02	00:40
	Min. Distance [m]	n/a	1.90	2.57	2.41	12.59
	Time [mm:ss]	n/a	05:17	04:25	02:36	01:54
	Speed [ms^{-1}]	n/a	1.44	4.49	2.90	2.47
Worker #2	Counts [No.]	0	1	0	2	7
	Duration [mm:ss]	n/a	00:04	n/a	00:04	01:07
	Min Distance [m]	n/a	2.10	n/a	1.78	3.33
	Time [mm:ss]	n/a	05:41	n/a	04:01	04:49
	Speed [ms^{-1}]	n/a	1.43	n/a	3.01	3.27

Table 7 Details of each detected proximity case.

		Case #1	Case #2	Case #3	Case #4	Case #5	Case #6	Case #7
Min. Distance [m]		13.07	12.91	13.03	12.60	12.72	12.67	3.33
Duration [mm:ss]		00:09	00:07	00:06	00:09	00:12	00:14	00:12
Enter Time [mm:ss]		02:16	02:47	03:17	03:43	04:03	04:25	04:49
Exit Time [mm:ss]		02:25	02:54	03:23	03:52	04:15	04:39	05:01
Worker position	X [m]	14.55	14.06	14.85	14.20	14.87	14.91	15.58
	Y [m]	25.46	25.57	25.87	29.08	29.23	28.91	29.77
	Z [m]	0.13	0.16	0.24	0.15	0.08	0.10	0.14
Equipment position	X [m]	14.69	15.18	14.59	13.94	13.66	13.70	12.97
	Y [m]	28.97	28.21	29.23	29.38	30.59	29.68	31.09
	Z [m]	12.59	12.59	12.59	12.59	12.59	12.59	1.59
Speed	V_x [ms^{-1}]	-0.91	0.98	-0.91	-0.87	-0.67	0.72	-0.55
	V_y [ms^{-1}]	-0.41	-0.19	-0.42	-0.50	-0.74	0.69	-0.76
	V_z [ms^{-1}]	0.02	0.07	-0.05	0.04	-0.04	0.03	-0.04
	V [ms^{-1}]	2.15	3.56	2.92	3.93	3.58	3.13	3.27

6.3.2 Experiment and Results from Controlled Environment

In order to validate the accuracy and efficiency of the developed algorithm on detecting proximity cases when the subject is continuously exposed to various hazards, another experiment in a fully controlled environment was conducted. By comparing the results of the algorithm to manual observing, the accuracy was measured by the percentage of successfully detected proximity hazards, and the efficiency was measured by the time that was required to achieve the results.

The experiment was conducted on the top floor of a parking deck, which occupied a $50m \times 110m$ rectangular area (Figure 47). The UWB system with multiple tags was deployed to collect the spatio-temporal data from the participants. The RTS system was utilized to set up the UWB infrastructure as well as to collect ground truth tracking data and measure the tracking errors. In this experiment, the tracking error of UWB system had mean as 0.27m and standard deviation as 0.31m [146]. In addition, three video cameras were set up to monitor the entire site when the experiment progressed.

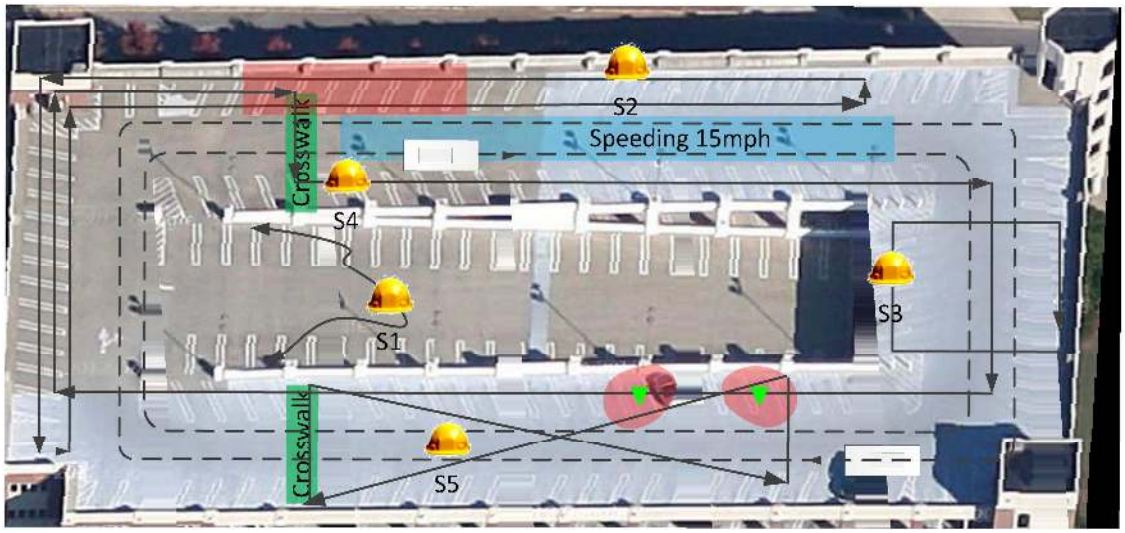

Figure 47 Layout of the controlled experiment with scripted scenarios.

Figure 47 showed a plan view of the site and the scripted experimental scenarios for the participants were plotted. Two static hazard zones (red polygons) were involved in this experiment, one of which was measured by RTS and the other was defined by a static UWB tag (green triangle). Two crosswalks were planned on both sides. The experiment participants included two vehicles (dash lines) and five participants (solid lines). The two vehicles drove following the lanes in clockwise and counterclockwise direction, respectively. On one side of the site, both vehicles were instructed to speed. The five participants were instructed to perform the following scripts during the experiment:

- Scenario #1 (S1) always walked off the traffic, which is considered safe
- Scenario #2 (S2) moved parallel to the traffic lane by keeping a safe distance to the moving vehicles. W2 had to walked across a static hazard zone
- Scenario #3 (S3) regularly crossed the traffic lanes
- Scenario #4 (S4) walked inside the parking area, and cross the traffic lanes using the cross walk. W3 also temporally walked on the traffic lane
- Scenario #5 (S5) crossed the traffic lanes with and without using the crosswalk, and randomly approached to the moving vehicle from arbitrary directions. W4 also entered the UWB tag defined hazard zone

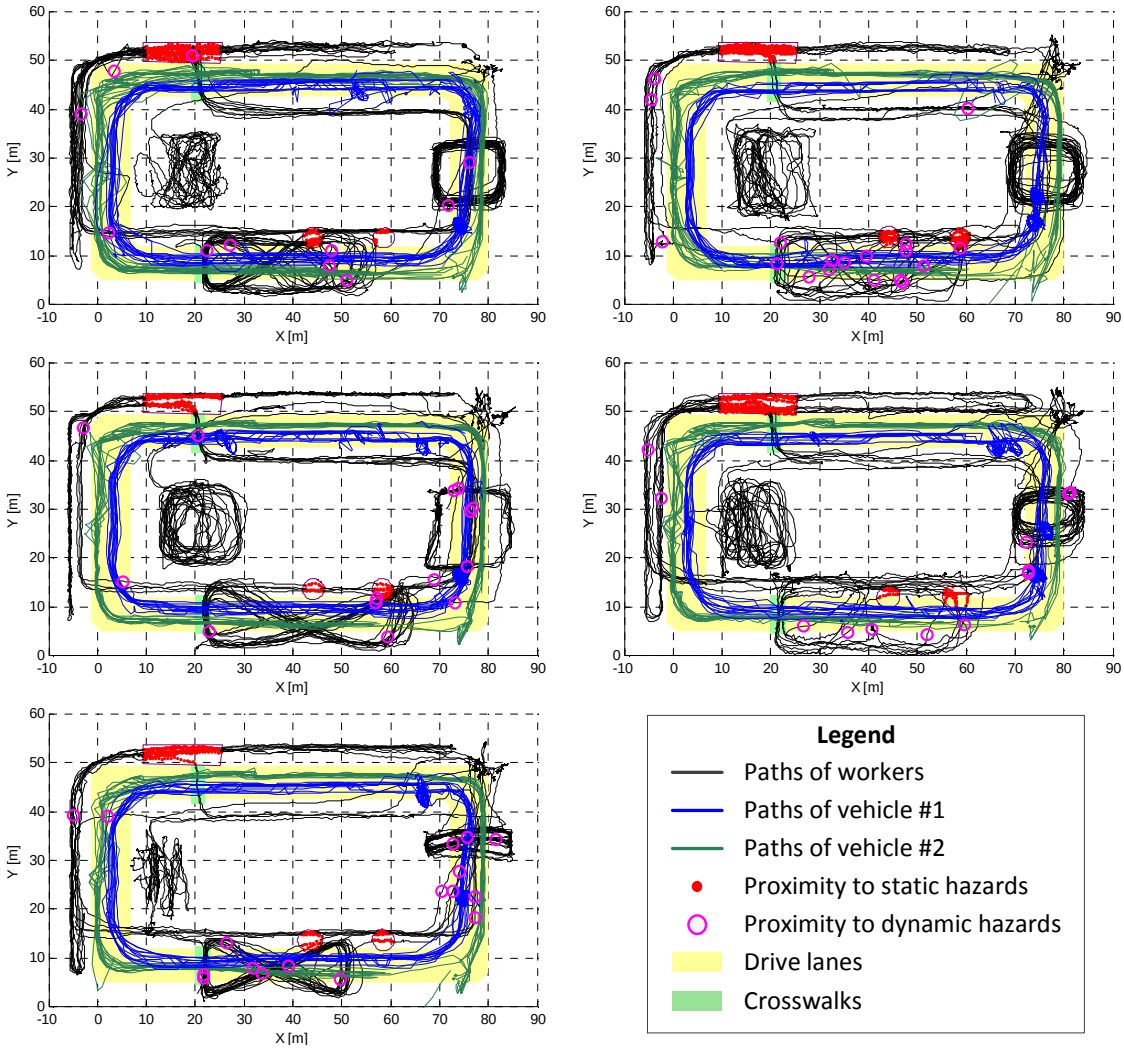

Figure 48 Trajectories and detected proximity cases in the controlled experiment

An extra participant was involved in the experiment to inspect participants' safety performance using behavior-based safety (BBS) technique [38]. The inspector was semi-blind to the experimental scenarios such that he was only instructed on what types of unsafe behavior would occur during the experiment. The inspector had to observe the performances of participants from a fixed location within the inspection period (5 minutes in general), and navigated to another location for the next round of inspection. The BBS technique only recorded the number of participants that were exposed to different hazards without reporting the repetitions of the same participant involved in the same hazard. In addition, the experiment progress was recorded by three video cameras, and the video clips were analyzed by another volunteer who was blind to the developed proximity analysis algorithm. The participants' trajectories, the locations of the proximity cases detected by the algorithm were plotted in Figure 48. Table 8 counted the number of detected proximity cases by manual analysis of video clips and the automated analysis of algorithm, and summarized the number of participants who were found to be exposed to hazards by using BBS.

Table 8 Summary of proximity cases detected by algorithm, on-site behavior based safety inspection, and the analysis of video clips.

No.		Static hazardous zones			Dynamic hazardous zones		Total
		Static 1	Static 2	Static 3	Dynamic 1	Dynamic 2	
Round 1	A*	16	22	22	5	6	71
	C*	16	21	22	5	6	70
	BBS*	2	2	0	1	1	6
Round 2	A	15	4	18	6	8	51
	C	12	4	18	6	7	47
	BBS	0	0	2	1	0	3
Round 3	A	8	10	9	10	7	44
	C	6	8	9	10	6	39
	BBS	2	2	0	2	0	6
Round 4	A	12	12	11	8	10	53
	C	12	10	10	7	7	46
	BBS	0	0	0	1	0	1
Round 5	A	6	6	17	7	5	41
	C	5	5	16	6	5	37
	BBS	0	0	2	0	0	2
Subtotal	A	57	54	77	36	36	260
	C	51	48	75	34	31	239
	BBS	4	4	4	5	1	18
Subtotal	A	188			72		260
	C	174			65		239
	BBS	12			6		18

A*: Algorithm analysis. C*: Video clips analysis. BBS*: Behavior Based Safety

Table 8 showed that the algorithm always detected greater number of proximity cases than the analysis of video clips. Considering the manual video clips as ground truth of detecting unsafe proximity cases, comparisons between the results achieved by these two approaches were detailed in Figure 49. The comparison was performed on the cases of static and dynamic hazards separately.

Total		Algorithm detection	
		Safe	Unsafe
Manual video analysis	Safe	N/a	25 (Improve: 21 Wrong: 4)
	Unsafe	4	235

Precision = 98.3% Recall = 90.3%

Static case		Algorithm detection	
		Safe	Unsafe
Manual video analysis	Safe	N/a	14 (Improve: 14 Wrong: 0)
	Unsafe	0	174

Precision = 100% Recall = 92.5%

Dynamic case		Algorithm detection	
		Safe	Unsafe
Manual video analysis	Safe	N/a	11 (Improve: 7 Wrong: 4)
	Unsafe	4	61

Precision = 93.8% Recall = 84.7%

Figure 49 Results validation by comparing to the video analysis.

Based on the comparison, two types of error were found: miss-detection and over-estimation. A miss-detection meant that a proximity case was recognized in video but was not detected by the algorithm. This type of error was caused by insufficient quality of the tracking data when the tracked target was outside the line of sight of the UWB receivers. In this experiment, four miss-detections happened in the dynamic case and none in the static case. This indicated that 93.4% of the manually recognized dynamic hazardous cases can be accurately detected by the algorithm, and all the static cases can be detected by the algorithm.

Another type of error was over-estimation, which meant that the algorithm detected a proximity case that was considered safe in the manual analysis. Further exploration suggested that the over-estimation should not always be considered as wrong. In some cases, the algorithm was more consistent than the human judgment. For example, in the static hazard situation, as the algorithm automatically generated a dangerous zone based on the given safety diameter, an intrusion into such a zone was considered as unsafe. Since manual video observation relied on a fuzzy process, an intrusion not so close to the hazard can be incorrectly considered as safe. Similarly to the dynamic case, since the manual observation from the video always failed to estimate the moving speed, especially when the vehicle was speeding, the algorithm gave more consistent result. In this experiment, all 14 times over-estimations of the static cases were caused by this reason, which also caused 7 out of 11 times over-estimations of the dynamic cases. The other 4 times over-estimations occurred when the vehicle was steering at high speed,

which were caused due to the limitation of the algorithm. As is mentioned in chapter 6.2.1, the dynamic hazardous zone generated by the algorithm became less reliable when the equipment was performing pure steering, since the velocity vector in this case was uncertain.

As a summary of the results from this experiment, the detection accuracy was 98%, which was the percentage of the unsafe proximity cases can be detected by the algorithm. The algorithm can improve the detection accuracy by 9% by providing more consistent measurements, in spite of that, the algorithm had 2% uncertainty. The above percentages were calculated using the following equations:

$$Accuracy = \frac{No.of\ algorithm\ and\ video\ recored\ hazards}{No.of\ video\ recored\ hazards} \quad (Eq.6-22)$$

$$Improvment\ Rate = \frac{No.of\ Improvements\ by\ algorithm}{No.of\ video\ recored\ hazards} \quad (Eq.6-22)$$

$$Uncertainty\ = \frac{No.of\ Wrong\ detection\ by\ algorithm}{No.of\ unsafe\ case\ according\ to\ algorithm} \quad (Eq.6-22)$$

The participants traversed among the five experimental scenarios until every participant had been involved in each scenario. The Proximity Hazard Index (PHI) of each participant was calculated for every 2 minutes interval using equation 6-21, and the results were plotted in Figure 50. It can be noticed that any participant who performed scenario 4 and 5 had significantly high PHI value, which indicated that these two scenarios requires the workers to be regularly exposed to various hazards.

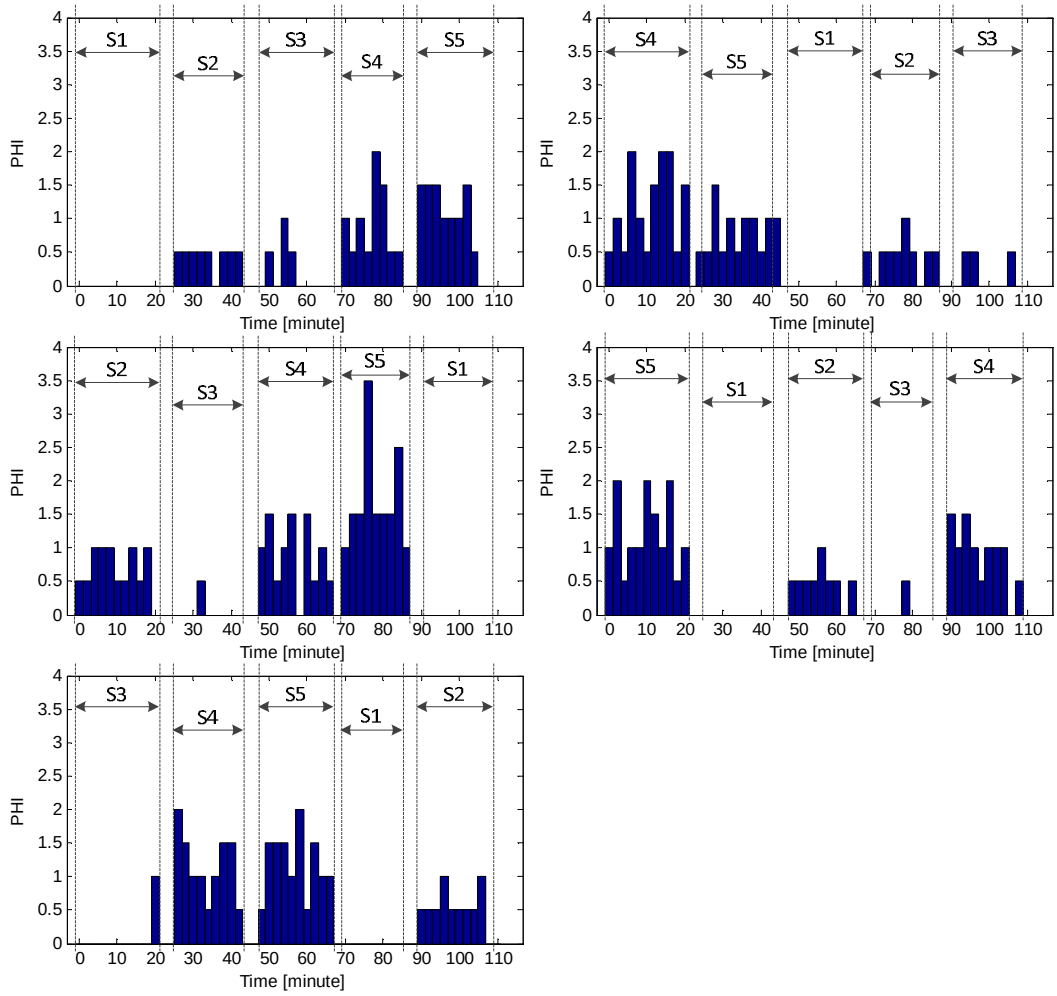

Figure 50 Distribution of the Proximity Hazard Index of all the participants.

6.3.3 Experiment and Result from Real Construction Site

The developed algorithm was tested on an experiment conducted on a construction pit, whose setting has been described in the previous session 4.5.1 and in the author's paper [146]. One crew consisted of a mobile crane operator and 11workers were involved in the work activities.

Several sensing technologies had been involved in this experiment. A Leica laser scanner was utilized to gather the geometric information of the site environment. The collected point cloud data were processed through the method depicted in chapter 5. The results shown in Figure 51 indicated that the hazardous condition on such a site included power lines, and building structures which may create blind spaces to the crane operator.

Moreover, a UWB system was deployed to collect the spatio-temporal data of the crew. The average error of the tracking data in this experiment was 0.34m.

The proximity detection algorithm was utilized to analyze the collected data and the results were plotted in Figure 51. The entire crew worked proximately to the power line 156 times and to crane hook 2 times within the 56 minutes period. Taking every 2 minutes as safety measurement intervals, a distribution of the PHI of the entire crew was illustrated in Figure 52.

According to Figure 52, 73% of the unsafe proximity cases occurred within the last 20 minutes of the experiment. Trajectory analysis implied that the frequent proximity cases were caused by the crane operation. The mobile crane delivered materials into the working area three times and the first delivery started at 37^{th} minute. For each delivery, the ground crew had to yield the crane boom movement, which lasted for 2-6 minutes. During these periods, workers kept safe clearance distance to the lifted load attached to the crane hook. However, they were crowded proximately to the power line, which eventually cause high PHI values.

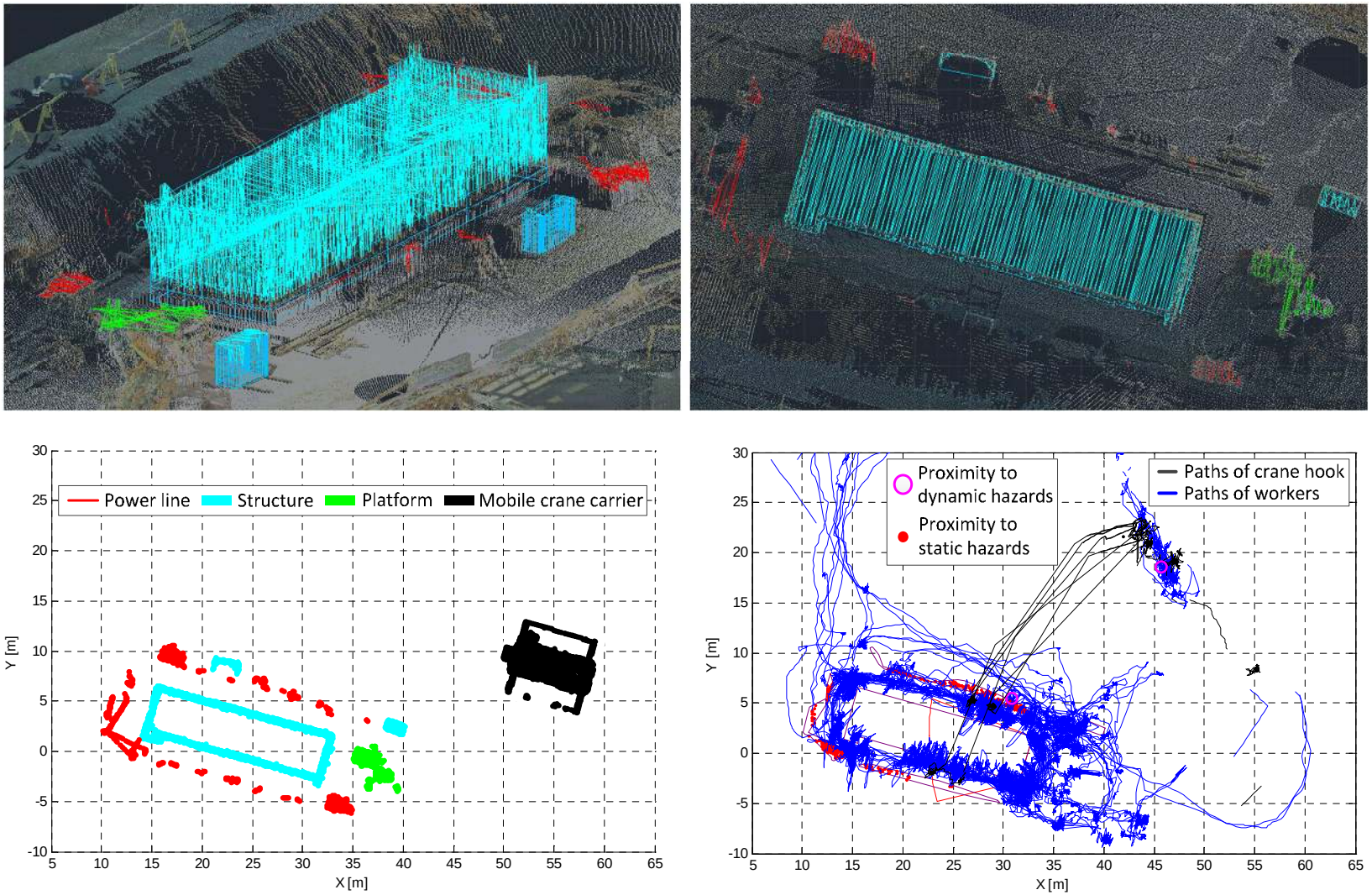

Figure 51 Detecting hazardous conditions and unsafe proximity cases in a construction pit.

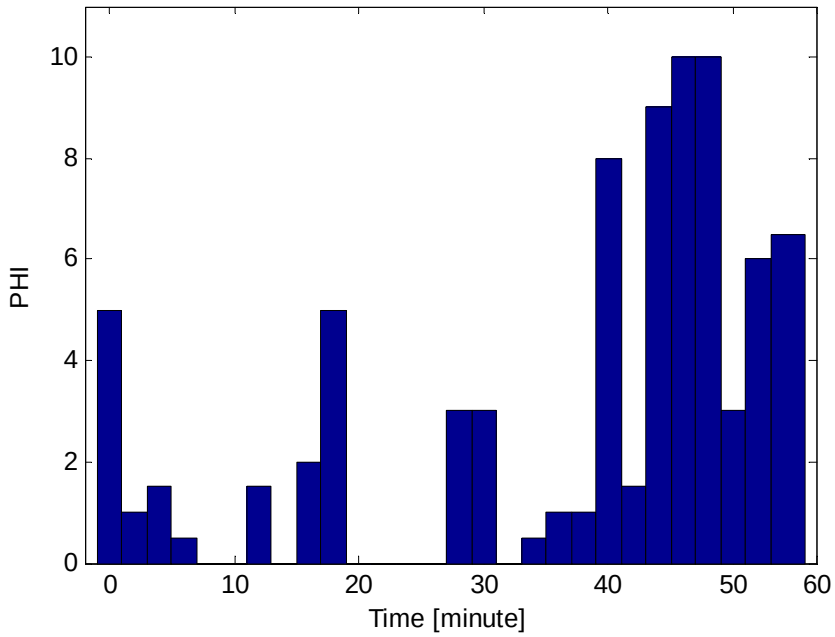

Figure 52 Distribution of the crew's PHI value computed by algorithm

6.4 Conclusion

Advanced real-time location sensing and topographic survey technologies have made it possible to quickly and accurately document spatio-temporal data of the construction resource and environment. As such technologies become available they lead to novel solutions in identifying and resolving potential safety issues, including human-hazards proximity. This chapter demonstrated the capability of measuring the workers' safety performances using existing remote sensing technologies in combination with date processing technique.

The objective of this chapter is to understand, evaluate and monitor workers' safety performances under proximity hazards. This chapter details the development of a proximity detection model. Such model measures the workers' performances based on the analysis of the site geometry, spatial, temporal, and kinematic characteristics of various construction resources. The developed model has been tested in three different environments, and has been validated by comparing to the video records. The results demonstrate that the model can accurately, consistently and reliably detect and measure the workers' safety performance under proximity hazards.

The developed approach has great potential to assist in measuring the construction site safety by using PHI as a leading safety indicator. Once the safety performance of each individual and/or crew has been rated by PHI, it is feasible for the safety manager to identify frequently occurred proximity hazards before any incident could happen. Appropriate safety training and education can be therefore introduced to the individual and/or the crew. In addition, the safety performances of the workers/crew can be automatically, continuously and consistently monitored and tracked, which essentially overcomes the drawback of manual safety inspection.

Further and more detailed studies are necessary, in particular how to eliminate the uncertainty of the algorithm when the equipment performs pure rotary movement. Moreover, the algorithm utilizes several external parameters such as: equipment breaking time and possible steering angle. Since these parameters are currently defined arbitrarily and inappropriate parameter setting may result unreliable measurement, the model can be improved if these parameters are well defined through the further study of construction traffic. Last but not lease, the spatio-temporal analysis developed in this chapter can be extended to other construction management domain such as workers' health and labor productivity analysis.

CHAPTER VII

DATA FUSION OF REAL-TIME LOCATION SENSING AND PHYSIOLOGICAL DATA FOR ERGONOMICS ANALYSIS

Previous chapters have focused on tracking the location of material and equipment and the development of a new measurement for proximity hazards. There is a lack of studies on remote monitoring for improving the health of the construction workforce. This chapter extends the spatio-temporal analysis approach for monitoring ergonomically safe and unsafe behavior of construction workers. The study relies on a methodology that utilizes fusion of data from continuous remote monitoring of construction workers' location and physiological status. This chapter presents the background and need for a data fusion approach, the framework, the test bed environment, and results to some case studies that were used to automatically identify unhealthy work behavior. Results of this chapter suggest a new approach for automating remote monitoring of construction workers safety performance by fusing data on their location and physical strain.

7.1 Introduction

Despite improvements in construction safety and health, the industry is still striving to improve work site conditions and behavior of construction workers. Whereas innovation in working methods and use of technology has eliminated some of the traditional hazards [158], in 2002, construction workers had the second highest job related illness and injury rate of all industries in the U.S., accounting for more than 37% of all illnesses and injuries [159]. In 2008, 28,340 nonfatal occupational injuries resulted in musculoskeletal disorders [160] and 3,020 workers suffered from lower back pain. Several well-known reasons have been suggested to explain these recurring statistics.

Construction work tasks are typically characterized as physically demanding tasks that are often performed in harsh environments. In fact, many construction activities include heavy lifting and carrying, forceful exertions, pushing and pulling, sudden loadings, repetitive motions, vibrations, and awkward work postures [161][162].

According to several researchers, there is a reciprocal relationship between physically demanding work, safety, and productivity [163][164][165][166][167][168]. As a result of the continuous and repetitive exposure to physically demanding work, strains and sprains are the most common type of work-related, nonfatal injuries. Furthermore, the continuous exposure to an excessive level of physical strain can lead to physical fatigue, which may result in decreased productivity and motivation, inattentiveness, poor judgment, poor quality work, job dissatisfaction [169] and increase in the risk of developing worker-related musculoskeletal injuries (MSIs) or cardiovascular disorders [170].

Previous research found that lower back injuries are among the most common MSIs [171]. These occur when the demand of work exceeds the capacity of a worker's body, or the worker repetitively performs heavy activities. MSIs can also be found in other parts of the body, such as the shoulders, wrists, and knees. MSIs are usually caused by overexertion, which is a leading cause of time-loss injury for construction workers [160]. An overexertion occurs when either the demand of work exceeds the capacity of a worker's body or the worker repetitively performs heavy activities. Statistics shows that more than one quarter (25.7%) of the overall disabling workplace injuries are due to overexertion [172]. Overexertion is not only the most common event category, but also the most expensive, resulting in $12.4 billion in direct costs to businesses. In addition, substantial indirect costs are caused through overexertion, such as (temporary) replacement of personnel and the human cost in terms of pain and/or (long-term) disability [173].

Examples of injuries caused by overexertion include those related to inappropriate execution of manual material handling (MMH) tasks, such as lifting, pushing, pulling, holding, carrying, and throwing. The complex interaction of factors that determine physical load or exposure intensity makes it challenging to assess systematically the performance of MMH activities in a dynamic construction environment [174]. Moreover, practitioners are only offered a lifting guide which has been issued by the National Institute for Occupational Safety and Health (NIOSH) [175].

Since heavy load lifting frequently leads to musculoskeletal injuries, the identification and localization of repetitive material handling activities is crucial to better

understand MSI ergonomics. Previous studies suggest that ergonomic- and physiology-related attributes, such as posture, body acceleration, and heart rate can be measured using remote sensing technology. One example is Physiological Status Monitoring (PSM) technology. Commercially-available PSM devices have shown to provide reliable information during dynamic construction activities [176]. The problem with PSM is, however, that it does not record nor relate the location of the worker to the location where unsafe lifting events occur. This shortcoming can be solved by fusing PSM data with data from real-time location sensing (RTLS) devices, such as Global Positioning System (GPS) or Ultra Wideband (UWB) devices. Recent research in construction has shown that sufficient accuracy is provided to track construction personnel with these technologies [146].

In summary, PSM and RTLS devices alone are useful, but research has yet to be performed that integrates data from both approaches (PSM and RTLS) to identify a point of departure from purely location-based or physiological research. To fill this gap, this paper aims at matching physiological and location information of construction workers to detect the workers' physical characteristic in a spatio-temporal relationship in the work environment. The authors have conducted multiple experiments where workers were instructed to perform specific manual material handling tasks of heavy load lifting. These tasks required workers to repeatedly perform awkward posture of squatting and bending. Pursuing data fusion, the authors have synchronized and analyzed the data streams from (1) Physiological Status Monitoring (PSM) (that continuously monitors activity factors of construction workers) and (2) Ultra Wideband (UWB) technology (that records real-time worker location).

7.2 Background

Workers activity factors, including posture, acceleration and heart rate, can be measured by a variety of remote sensing technologies. The capability of PSM to provide reliable information of a worker's vital signs during dynamic activities has been demonstrated in commercial applications. Meanwhile, real-time location tracking technology has emerged that allows tracking resources (e.g., personnel) in harsh

construction environments with sufficient accuracy. Studies have yet to be performed that fuse PSM and location data for advanced safety and health analysis.

7.2.1 Monitoring and Analysis in Ergonomics

Significant improvements have not spared the construction industry from its many challenges for ergonomics, occupational health, and safety. Several researchers have studied ergonomics in construction. Ergonomic risk factors for MSIs during construction activities have been identified and analyzed for the general construction environment [162], concrete formwork construction [177], and carpentry and paving trades [158]. Research has found that ergonomic hazards can be controlled through safe workplace design [178][179].

Similarly, research has shown that excessive body accelerations can be related to muscular-skeletal disorders. Most of these studies have collected data using synchronous (i.e., direct observation) or asynchronous (i.e., videotaping) visual observation techniques, surveys and/or interviews of construction workers, supervisors, or safety and health experts to evaluate worker's ergonomics. They have not focused on a detailed analysis of workers' movements (e.g., body accelerations) and physiological reactions (e.g., heart rate). However, a more detailed worker behavior analysis can provide, if brought into proper context with the work environment, additional important information on ergonomics hazards analysis [180][181].

7.2.2 Location Tracking in Construction

Tracking the location in ergonomic behavior analysis of construction workers is critical if the goal is to identify and correct, unsafe, unhealthy, or unproductive work practices [63][182]. A variety of sensing technologies are available for performing automated location tracking on construction and infrastructure projects [58][56][78], range tracking [80][81], including vision tracking [91][92][93], and GPS [60]. Selection of one particular tracking technology depends on the application area, signal quality, data stream provided, and the calibration requirements [146].

Ultra Wideband (UWB) is an active Radio Frequency Identification (RFID) technology that records location of resources (worker, equipment, and material) in real-

time. UWB employs a tag-to-reader approach [76], where one or more tags can be mounted on a person's helmet or safety vest (see Figure 53 for installation on a construction helmet). The tags communicate with antennas installed within 1,000 m. Research has demonstrated that a commercially-available UWB system is able to provide accurate real-time spatio-temporal data of construction workers, equipment and materials, while the tracking error in a harsh construction environment is lower than 0.5 m [146]. Obstructions, such as thick concrete walls, have been identified as a potential line-of-sight issue for UWB [18][82][83][146]. In addition, conventional GPS data logging technology can provide a cost-effective alternative approach, but only for outdoor applications [146].

7.2.3 Data Fusion in Construction

The Data Fusion Model is a widely-used method for categorizing data fusion-related functions [183][184]. Its applications have been studied in many fields including military command and control, robotics, image processing, air traffic control, medical diagnostics, pattern recognition and environmental monitoring [185][186]. In construction, for example, this model has been implemented in construction material tracking [187] and location estimation utilizing common attributes from multiple sensors [188].

7.3 Research Objectives and Scope Limitations

By fusing data from real-time location trackers (RTLS) and physiological status monitors (PSM) this study attempts to identify and locate unsafe postures by construction workers that can produce Musculoskeletal Injury (MSI). As workers may or may not be aware of unsafe or unhealthy events, the identification of where and when these acts occur is expected to help designing better work environments.

The goal of this research is to measure and analyze ergonomic performance by fusing data on vital signs and location of construction workers involved in repeated manual material handling activities. The first objective is to automatically identify "when" inappropriate postures that are linked to MSIs occur. The second objective is to

automatically locate the “hot-spots” of the improper activities, which indicate a larger repetitive occurrence of ergonomic-related events (i.e., unhealthy postures).

This study is limited to fusing information from two specific sensing technologies (UWB and PSM). All tests were performed in a controlled study environment. Working activities that were recorded with UWB, PSM, and video camera technology occurred indoors and on the same elevation level. This study focuses only on activities associated to the construction personnel, especially, heavy load lifting. Social, legal, or behavioral impacts on workers using UWB and/or PSM technologies were not part of the scope of this study.

7.4 Methodology

Even though several data fusion approaches exist in construction engineering applications, including productivity monitoring and material tracking [187][189][190], data fusion of real-time location tracking data and worker physical information has not been tested in construction. The use of worker physiological data to correct imperfection of purely location-based datasets fills a gap in existing knowledge, since it departs from previous data fusion approaches.

The researchers designed a novel testbed that integrated UWB and PSM technologies to measure and analyze the ergonomic and positioning factors of repeated material handling activities. Results to an experimental approach are presented. Opportunities and barriers using UWB and PSM data recording are discussed.

The components of the experimental test bed are illustrated in Figure 53. For later control measurement, all activities were taped with video cameras. The data analysis process is shown in the flowchart in Figure 54. Data analysis consists of four major components: work sampling, data synchronization, activity identification, and localization. An empirical approach was selected (explained later) for identifying ergonomically unsafe worker motions, for example, lifting heavy loads without bending the knees.

Figure 53 Testbed for experiments

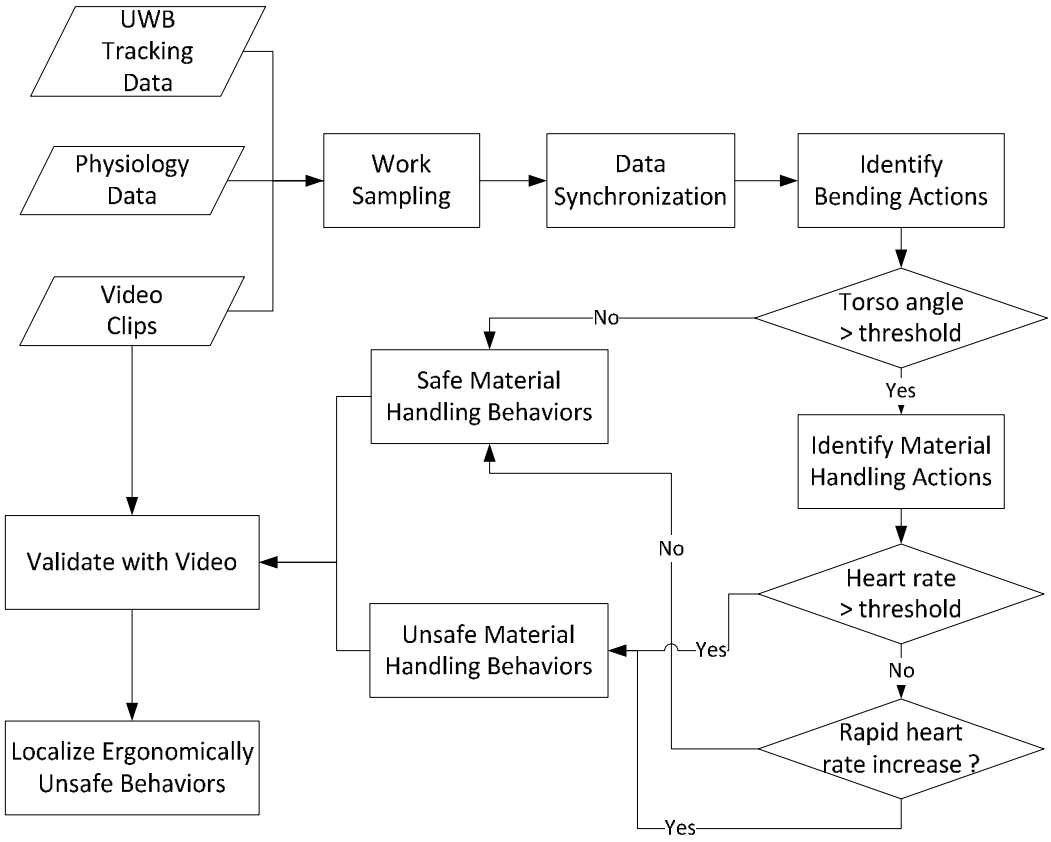

Figure 54 Localizing ergonomically unsafe behaviors

Since the study environment was indoors and little obstructions were present, a commercially-available UWB localization system was selected to track the real-time location of individuals participating in the test cases. UWB tags were placed on the helmets of the individuals, and on relevant static locations in the test scenery (e.g., to identify material bay, rest, and water supply areas). The UWB system itself consists of a central processing hub, which triangulates the position of the incoming radio frequency signal from multiple UWB receivers based on the Time-Distance-of-Arrival (TDoA) principle. These antennas were distributed systematically around the work environment and outside of any of the participating individuals' travel paths. The UWB receivers were connected to the hub via shielded CAT5e cables and a static tag functioning as a reference location was placed in the center of the monitored area.

PSMs can be described as non-invasive ambulatory wireless telemetry systems. A variety of commercially-available PSM systems exist. They can autonomously and

remotely monitor workers' physiological status without hindering or interrupting their routine activities for several hours. The system utilized in the experiment was composed by a chest belt that hosts conductive fabric sensors and an integrated module that includes a mobile transmitter. The selected device had the ability to perform live data transmission wirelessly through a USB radio receiver, which was connected to a data logging PC. As an alternative to real-time transmission, PSMs allow for local data logging. The selected PSM system monitored and recorded physiological and motion data using wearable electrocardiograph (ECG) sensor, breathing rate sensor, and a 3-axial accelerometer. It transmitted the data in real-time to the receiver via a radio frequency signal. Among various parameters, PSM measured the heart rate and the thoracic bending angle. Heart rates were deducted from ECG data. The three-axial (vertical, lateral and sagittal) accelerometer was used to generate the subject's default activity data measured in Vector Magnitude Unit (VMU). VMU was measured as a portion of the gravity acceleration (g). The system built-in module used the VMU values to derive the subject's thoracic bending angles from the 3-axis gravity-compensated value calculated over the previous 1.008 second epoch. The angle was derived as a scalar with positive and negative values, where zero degree represented the vertical right-up posture.

Meanwhile, a network camera was utilized to visually record the experiments. The timeline of the video was regarded as a metric, which means the temporal information from both sensors had to be synchronized to the video time. Visual analysis of the video recording was implemented to establish a ground truth validating the result of the inappropriate posture identification.

7.4.1 Work Sampling

Work sampling is a technique implemented to determine the portion of the time that workers spend in defined category of activities. In this paper, the tracking data collected by UWB are sampled with the workers' speed, indicating travelling and stationary status. The walking speed is derived from the spatio-temporal tracking data. Since the UWB signal can be noisy with occasional outliers, the noises on the spatial location records result in outliners on the derived speed, which violated the assumption of the speed continuity. Thus, the UWB signal was filtered with a Robust Kalman filter [94].

In addition to signal smoothing, the robust Kalman filter rejects outlier measurements so that the outliers do not corrupt the filtered signal estimate.

Meanwhile, PSM posture readings were sampled that indicated a subject's posture status, such as bending, and vertical up-right of the upper body. PSMs are able to measure posture angles within the -90° to 90° range with the 0° angle representing the vertical up-right status; the positive value representing leaning forward, and the negative angle indicating leaning backward. Since the accuracy of the posture angle measurements depends on the way that the PSM chest belt is worn and the feature of the dynamic motions, the PSM signals are noisy with ±10o once it is tested on the vertical up-right status. Thus, a threshold of bending angle is assigned to differentiate the bending and vertical up-right.

7.4.2 Data Synchronization

UWB and PSM technologies collect heterogeneous data sources which have difference levels of detail, data collection rates, data representations, and time reference systems. For example, the utilized UWB system collects the temporal data in UNIX format, while the PSM and video record is in local time format (HH:MM:SS). Data fusion with other sensor signals requires data to be synchronized. The data synchronization process applied in this research is illustrated in Figure 55.

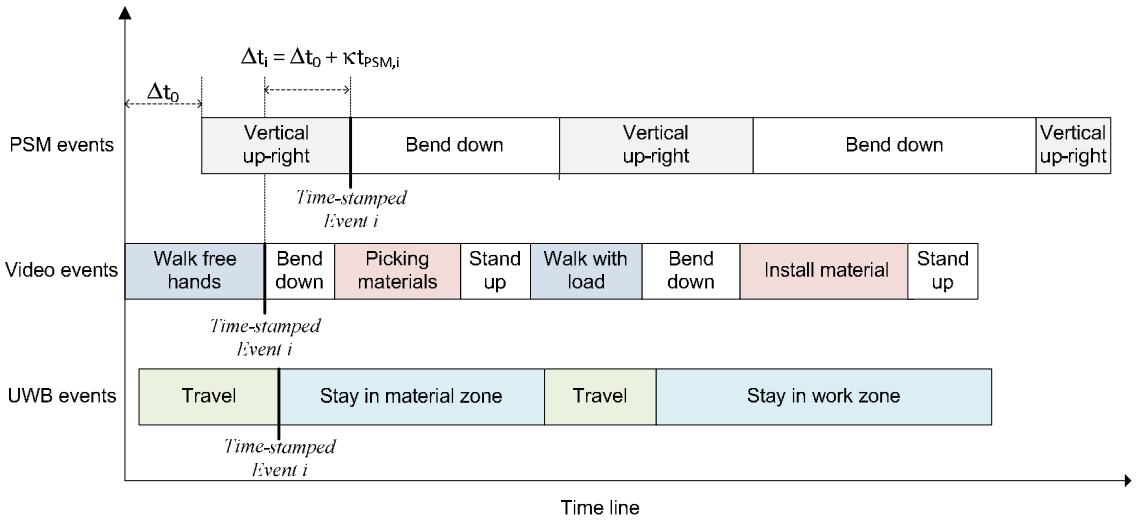

Figure 55 Time lines for multiple sensors.

Firstly, the timestamps are encoded into float numbers starting from the beginning of each experiment with seconds being the unit. The frequency chosen is that of UWB data since it requires up-sampling of the PSM signal (to prevent any loss in information). Secondly, the time-streams are synchronized through a linear time lag propagation model. Since the video time is regarded as the ground truth, it is assumed that the propagation of time difference consists of two parts: initial time shift and continuous time drift (see Figure 55):

$$\Delta t_i = \Delta t_0 + \kappa t_{sensor} \; ; \; \Delta t_i = t_{video\,,i} - t_{sensor\,,i} \quad \text{(Eq. 7-1)}$$

where, Δt_i is the time lag between sensor and video when a specific event i occurs. An event refers to the switching of working behavior, such as bending down, start to move. Term $t_{video,i}\mathrm{t_{video,i}}$ is the video time when event i (e.g., bend down, start to move) is observed. Term $t_{sensor,i}\,\mathrm{t_{sensor,i}}$ is the time recorded by the sensor's clock when the same event $i\mathrm{i}$ takes place. When $i = 0\mathrm{i} = 0$, it refers to the initial status of UWB and PSM sensors when they started recording data. Thus, $\Delta t_0\Delta\mathrm{t_0}$ represent the initial time shift between the sensor and video recordings.

In addition, the built-in timestamps of the sensors may have a clock drift or time drift. For example, the UNIX time used in the UWB system cannot unambiguously represent the Coordinated Universal Time (UTC) as it has approximately a one second drift at every UTC day. Therefore, the sensor clock had to be corrected to match the clock of the video. At the sensor time $t_{sensor}\mathrm{t_{sensor}}$, the drifting time is $\kappa t_{sensor}\kappa\mathrm{t_{sensor}}$ (in seconds). Parameter $\kappa\kappa$ is the time adjustment factor, which corrects each second from the sensor to be equal to the video. A positive κ refers that the sensor clock runs slower than video clock, while the negative value indicates the opposite. To determine parameters $\kappa\kappa$ and $\Delta t_0\Delta\mathrm{t_0}$ $\Delta\mathrm{t_0}$,the linear time lag propagation model was trained on a data set consisting of N random events such that

$$\kappa = \frac{\sum(t_{sensor\,,i} - \bar{t}_{sensor\,,i})\Delta t_i}{\sum(t_{sensor\,,i} - \bar{t}_{sensor\,,i})^2}\,, \Delta t_0 = \overline{\Delta t_i} - \kappa\bar{t}_{sensor\,,i} \quad \text{(Eq. 7-2)}$$

Once the time lag propagation parameters κ and $\Delta\mathrm{t_0}$were computed, the times of sensors and video were synchronized, as follows

$$\hat{t}_j = \Delta t_0 + (1+\kappa) t_{sensor,j} \; ; \; \varepsilon = t_{video,j} - \hat{t}_j \qquad \text{(Eq. 7-3)}$$

where $\hat{t}_j$ $\hat{\mathrm{t}}_{\mathrm{j}}$is the predicted time on the corresponding video timeline. Event *j* jis recorded from the sensor at sensor time $t_{sensor,j}$.$\mathrm{t}_{\mathrm{sensor,j}}$ Index *j*j is the random event index from the testing event set, and ε εis the predicted error. Once the sample size of the testing event *j* jis large enough, the predicting error ε follows Gaussian distribution.

7.4.3 Data Fusion

The data synchronization process aligned the data streams of the UWB and PSM sensors with video data. These multi-sensor data are furthermore fused by implementing a centralized data fusion method. The data fusion architecture (see Figure 56) is based on two stages: estimation of posture status by fusing PSM and video data; and estimation of position using UWB data. Due to the nature of the pre-processed video data – the physical status and location status are of contextual format – a fuzzy representation is implemented to define the observed status from the sensor. The posture status "bending", for example, happens when the corresponding posture angle is greater than a pre-defined threshold and if the subject is "inside a zone". Several sets of observation status are generated at a series of randomly selected times using the data synchronization model (see equation three). The observation noise is implemented to compute the likelihood function using a Bayesian approach that given the data synchronization function the likelihood function is:

$$\ell(A_i \mid S^1_{new} S^2_{new}) = \frac{\prod_{k=1,2} P(A_i \mid S^k_{new}) \, \mathrm{P}(A_i \mid S^1_{old} S^2_{old})}{\prod_{k=1,2} P(A_i \mid S^k_{old})} \qquad \text{(Eq. 7-4)}$$

Where A_i is Observation Status i; S^k_{new} is New Data from Sensor *k*; S^k_{old} is Old Data from Sensor *k*; and $P(A_i \mid S^1_{old} S^2_{old})$ is Prior Estimation in the previous data synchronization model.

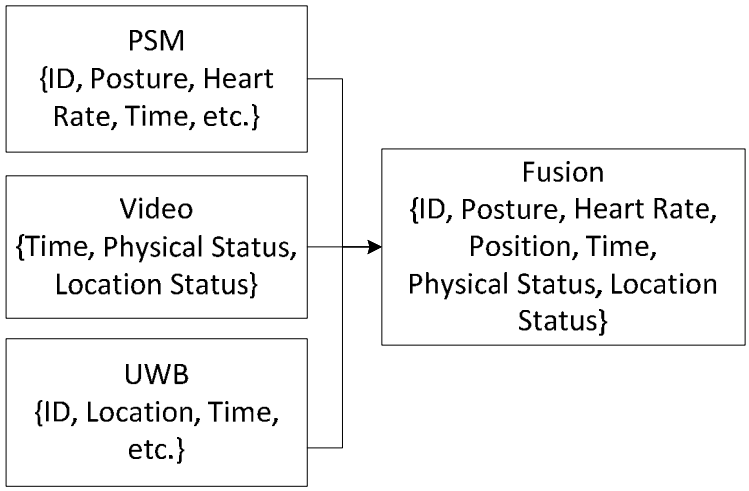

Figure 56 Data fusion architecture.

7.4.4 Activity Identification and Localization

Location (x,y,z, and time) and physiological (bending angle and time) data were utilized to identify those locations where workers bend more than a predefined threshold angle. Although the location and time of an unsafe worker posture can be determined fusing UWB and PSM data, insufficiency in the available data lies in determining what activity type and motion constitutes as unsafe/unhealthy behavior (e.g., lifting a heavy load, and walking). For example, bending more than 25 degrees without lifting a load is typically considered safe, while bending the same angle with a load could be considered unsafe if repeated frequently. Since video data could not be used to answer this fundamental question (video data were gathered only for the control of the experiment), the answer requires an in-depth analysis of a worker's muscular system.

A worker's muscular system is indirectly related to the worker's heart rate. When a worker is conducting physically demanding activities, such as lifting loads, the muscles are undergoing isotonic contractions, which results in a rise of the heart rate. The change of the heart rate may be triggered by various physical and environmental factors, but it may not occur simultaneously when the muscles react. It is therefore very challenging to explore the actual correlation between heart rate change and posture change.

Instead, this paper analyzes the heart rate propagation pattern to identify the type and status of a worker's activity. Two patterns in the heart rate signal differentiate a load

lifting task from normal walking and bending activities. The first pattern uses data from the absolute heart rate. As a heart rate changes based on the type or work a person performs, higher heart rates exceeding a certain threshold indicate isotonic muscle reactions. A threshold has to be defined for every individual by conducting a statistical analysis of his/her absolute and statistical heart rates. Since the absolute heart rate may vary among the population (e.g., occupation, age, and sex) and the average heart rate may also increase on physically demanding activities or with the fatigue level, the second pattern utilize the first differential of the heart rate. Measuring the quickness of change in heart rate of an individual finally allows setting a threshold value for the heart to determine what type of activity is performed.

For example, lifting a heavy concrete masonry unit (CMU) is a physically demanding activity which increases the heart rate. Once the bending threshold and the corresponding heart rate thresholds are set, they can be used to distinguish the moments when physically demanding activities start and end.

7.4.5 Experimental Setting

Three experimental settings were designed to simulate construction tasks. All experiments were conducted in a controlled indoor technology testbed environment. The three simulated construction tasks consisted of (see Figure 57):

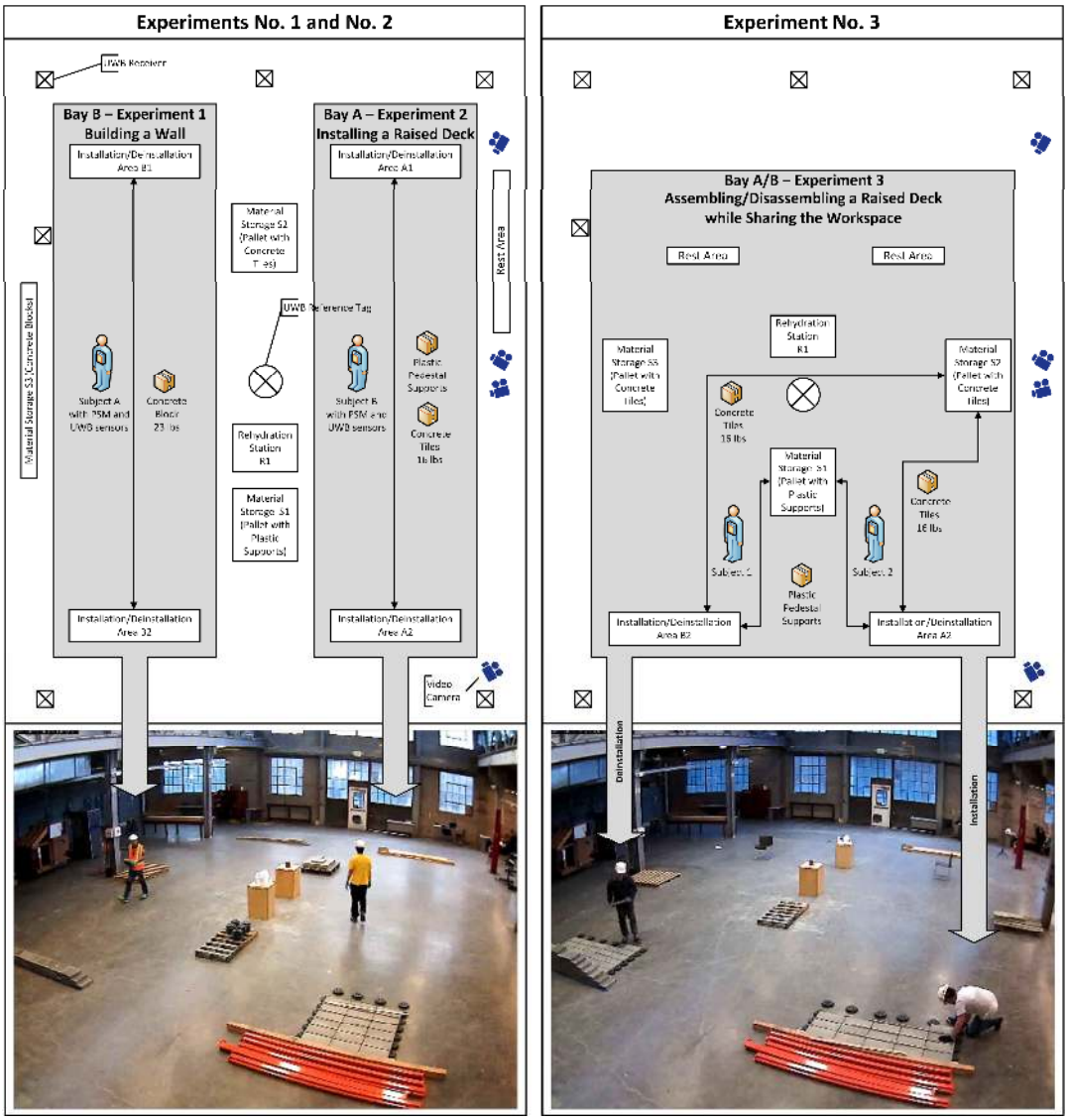

Figure 57 Experiment layout.

- *Experiment No. 1*: Building a wall: one subject builds a wall using 23-lb concrete blocks. One installation and one material area is available;
- *Experiment No. 2:* Assembling a raised deck: one subject assembles a deck using plastic supports and 16-lb concrete tiles. One installation area and two material storage areas exist;
- *Experiment No. 3*: Assembling and disassembling a raised deck: one subject disassembles a deck and stores material in a material laydown area, the other

subject uses the material from the laydown area to assemble a raised deck in a second work area. Assembly and disassembly are spatio-temporal dependent activities. The two subjects share two storage areas, but have their own installation area available.

Three construction tasks were simulated. The first two experiments were conducted simultaneously, since the two subjects worked separately without interfering work spaces. The experimental layout for the first task (building a concrete wall) utilized an installation area, a disassembling area, and a pallet for storing the materials. The layout for the second task was slightly different from the first, and had two pallets containing concrete pavers and plastic pedestals. The third task was performed by two subjects sharing the facilities in an integrated experiment.

Written informed consent was obtained and the subjects were instructed about the experiment by a trained lab technician. The training covered three main topics. First, subjects were trained on how to properly wear and operate UWB and PSM. Secondly, correct material handling techniques and PPE (i.e., gloves, foot guards, knee pads, hard hat, and goggles) utilization were explained. Third, working areas and construction tasks were described.

7.4.6 Performance of UWB and PSM in Experimental Setting

This section analyzes the performance (error rate and reliability) of the utilized sensing technologies UWB and PSM separately. The experimental facility covers an area of about 500 square meters. Based on previous experiences and results of the researchers using UWB [146], the experimental design asked to achieve high fidelity positioning tracking in the order of a few centimeters. Previously performed research in outdoor construction environment [146] indicated that a uniformed tracking error distribution can be observed within the coverage area of UWB receivers. Since the experiments were located indoors, UWB performance tests with three UWB tags (one with 60Hz and two with 1Hz signal refresh rate) were conducted to measure the error rate. The observation period collected 206,190, 2,495, and 3,050 data points, respectively. The average errors of these three tags were 0.28m, 0.31m and 0.27m, respectively. Their standard deviation was 0.16m, 0.35m and 0.12m, respectively. The researchers concluded that the selected

UWB technology and sensor layout was adequate in providing reliable positioning information of workers and decided to progress with the evaluation of the PSM technology.

The PSM system performance test included the subjects' variation in posture and heart rate. There are several limitations of the current physiological data logging sensor. First, posture data are affected by dynamic movement. Fast changes in accelerations prevent the posture from being reliably measured. In fact, posture measurement achieves its maximum accuracy when the subject is in static position and motion. Secondly, the posture angle readings from a subject in a sitting or standing position will depend on the shape of the subject's torso and placement and position of the PSM immediately underneath the garment.

Besides the posture angles, the PSM also records the subject's heart rate. Similar to the posture measurement, the heart rate readings of a subject are derived measurements of subject's Electrocardiogram (ECG) performance. The ECG sensors are connected to the garment's conductive fabric that is touching the subject's skin during the experiment to record data. There are several factors that can affect ECG performance. Though the PSM will perform well with non-moistened sensor surfaces, ECG and heart rate readings can be more susceptible to movement artifact noise under some circumstance. Lack of skin moisture on a subject's skin could produce such effects. The ECG readings could also be affected by Electromyographic (EMG) noise. EMG signals are generated as muscles on the torso contract and relax. The signals can be quite comparable in magnitude with the ECG signals. So, excessive use of these muscles, such as vigorous arm-flapping can affect ECG detection.

Taking the above factors into consideration, both the posture angle and the heart rate performance were collected with (some) noise. Studies on the measurement error analysis of the physiological factors and its impact on the determination of the activity type are outside this paper's scope. Hence, uniformed thresholds determined by the statistics of the measurements are implemented to identify the properties of the subjects' activities.

7.5 Results and Discussions

This section demonstrates the data fusing process and results for the first experiment (No. 1). The same methodology was applied again on the second and third experiments (No. 2 and No. 3). One hour of data taken in the first experiment will explain the data fusion approach and the identification and localization of ergonomically unsafe worker behaviors. The subjects in all experiments were not given instructions (to bend safely or unsafely).

7.5.1 Sampling UWB Data

The tracking data collected from UWB was sampled by the traveling speed, which was implemented to identify several zones where the subjects were static. According to the experimental tasks, the subject had to stop when he was operating in the installation, deinstallation, material bay, rehydration, and rest areas. Hence, it was assumed that ergonomically unsafe behavior, especially bending with heavy loads, only occurs when the subject was standing or moving with very low speeds.

Since the UWB tag was mounted on the subject's helmet, head motions such as nodding and shaking may result in many small to zero movements of the UWB tags (which may lead future research to install location tracking devices on the worker's clothing, preferably the belt). Moreover, subjects moved slowly within the work zone to complete the work task. A speed threshold based on statistical analysis was implemented to determine the subject's walking and staying status.

A histogram illustrates the observed walking speeds of the subject in Figure 58. Two peaks can be noted. The histogram was fitted by two Gaussian distributions with the mean at 0.19m/s and 0.91m/s and standard deviation at 0.01m/s and 0.11m/s, respectively. The first Gaussian relates to a low speed (subject was static) and the second Gaussian relates to a higher speed (subject was moving). The two Gaussians connect at a value of approximately 0.6m/s. This value separates the subject activity in static vs. moving. Consequently, the threshold was set at 0.6m/s to distinguish the subject's stationary from the traveling status.

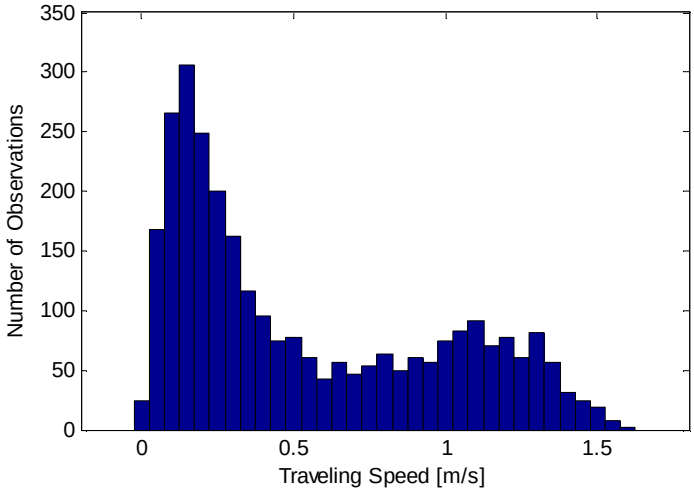

Figure 58 Walking speeds of a worker for one hour experiment.

According to the speed threshold, six clusters of static locations/work zones were identified (see Figure 59). The scattered positioning data were grouped using a convex hull algorithm. Individual polygons denote their geometric boundary. When compared to the testbed layout and video data, the locations of these zones match the installation, material, rest, and rehydration areas. The methodology of separating work from traveling area validates the choice of setting the threshold for this experiment.

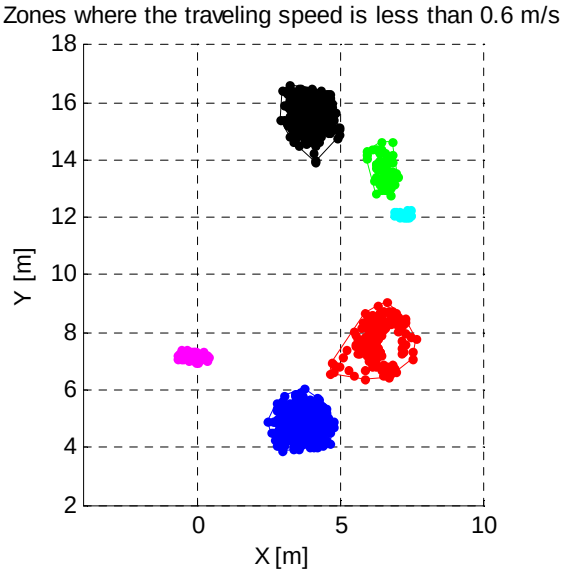

Figure 59 Locations of clusters and work zones where worker is in stationary position.

7.5.2 *Event-Based Data Synchronization*

Sensing data from multiple sensors were synchronized with the video time, where the time clock of the video was considered as the ground truth. The general principle to synchronize timelines among sensors was to compare the time clock of manually set time flags, e.g. when a recognizable event occurred in the UWB data, it should also appear at the corresponding moment in the PSM data set. Examples include entry or exit in a work zone, rapid velocity changes, and/or rapid posture changes such as bending motions.

For the purpose of synchronizing the UWB data to the video data, time flags (control points) were set at all of the 96 times the subject entered/left a static zone. The factors of the time propagation model were determined as $\kappa=3\times10^{-9}$ and Δt_0=1298048273.666s. The parameter κ was close to 0, which means there was almost no time drifting between recorded UWB time and video time. The time shift parameter Δt_0 was high because of the previously described difference in UNIX time and local time format. Though Δt_0 is high (actually refers to January 1, 1970, ~41 years ago) and it can be set to zero. The time propagation model was tested on an additional 40 samples. The mean error synchronization is 0.2 seconds with a standard deviation of 0.6 seconds.

In a process of synchronizing the PSM data with the video data, control points were set to all 29 times bending and vertical behavior occurred. Parameters were κ=0.013 and Δt_0=-9.614s, which means the PSM clock runs one second faster in every 77 seconds of video time. The time propagation model was tested on another 15 samples, and it shows 1.2 seconds error in prediction, with a standard deviation of 0.7 seconds. Since the physiological data were collected at a 1Hz sample rate, the 1.2 seconds error represents on average one measurement shifting during the one hour experiment and it was disregarded in the further data analysis.

7.5.3 *Automatic Identification and Mapping of Ergonomically Unsafe Behaviors*

Since musculoskeletal disorders were accounted for the first reason of nonfatal occupational injuries in construction, a particular emphasis was placed on identifying the ergonomically unsafe behaviors among the dynamic construction activities. Specifically in this experiment, one of the goals was to identify the working behaviors such when the subject was bending (or lifting) with heavy loads. To demonstrate how multiple sensing

technologies can assist the evaluation process of ergonomic behavior, synchronized tracking and physiological data were fused. An analysis of the signal propagation pattern between heart rates and posture angles provides additional reasoning into the subject's behavior.

Safety guidelines for manual material handling state "to reduce the strain on the back, a subject should maintain a posture of the upper body as vertical as possible when lifting or placing heavy loads" [175]. No further official statement has been made on what constitutes a safe bending angle (most likely since a detailed determination depends upon a variety of factors, including work environment and a subject's physical characteristics). In this experiment, the subject's material handling activities are classified into two categories: safe and unsafe (see Figure 60). The individual in this figure was not a subject in the study.

Figure 60 Safe and unsafe work tasks

Using data from experiment 2 (Task No.2), Figure 61 shows the histogram of the posture angle. The average (and coincidently also the median) bending angle is +15.5 degrees. Quite a few of the posture angles were observed at negative level, which was

due to leaning backwards and eventually also the shape of the subject's torso and placement of the PSM immediately underneath the garment. Subsequently, a +25 degree posture angle for the body torso was utilized to distinguish bending from standing. A further but important distinction is whether the subject carries a load while bending. Angles less than +25 degrees without or with load are referred to safe standing/walking activities of the subject. Angles greater +25 degrees with a load are considered unsafe lifting/placing activities. Angles greater +25 degrees without carrying a load in the subject's hand(s) are again safe activities.

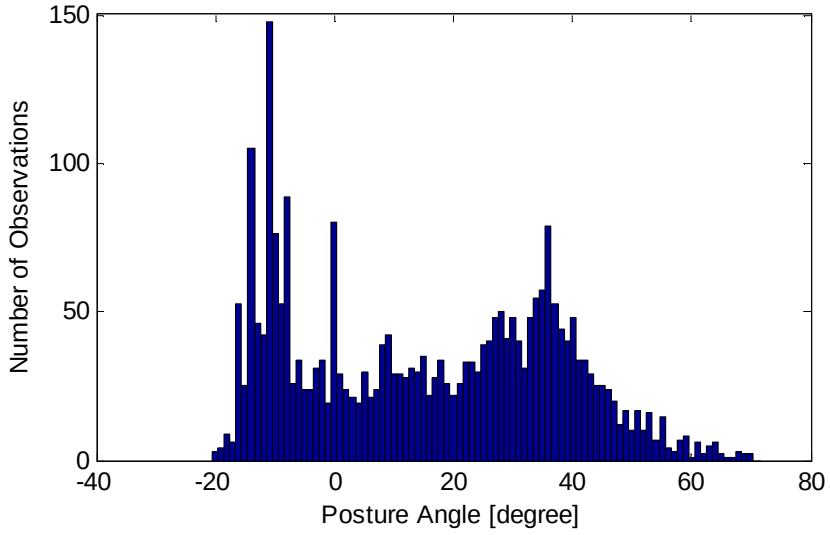

Figure 61 Posture angles from PSM data.

While a subject is conducting physically demanding activities such as lifting and placing loads her/his heart rate is higher than normally. According to rules set by NIOSH (2007), material handling with up-right body posture is safe. A histogram of the subject's heart rate while the bending angle exceeded 25 degrees is shown in Figure 62. Two Gaussian distributions were differentiated. One has the mean at 91 bpm (beats per minute) and the other at 106 bpm. The higher the heart rate value is, the more oxygen a subject consumes. High heart rates in this experiment were directly associated with a subject carrying a load. The two Gaussians connect at 99 bpm, which implies the transition between bending with and without load. The threshold was set slightly higher to 106 bpm to differentiate safe from unsafe lifting/placing motions.

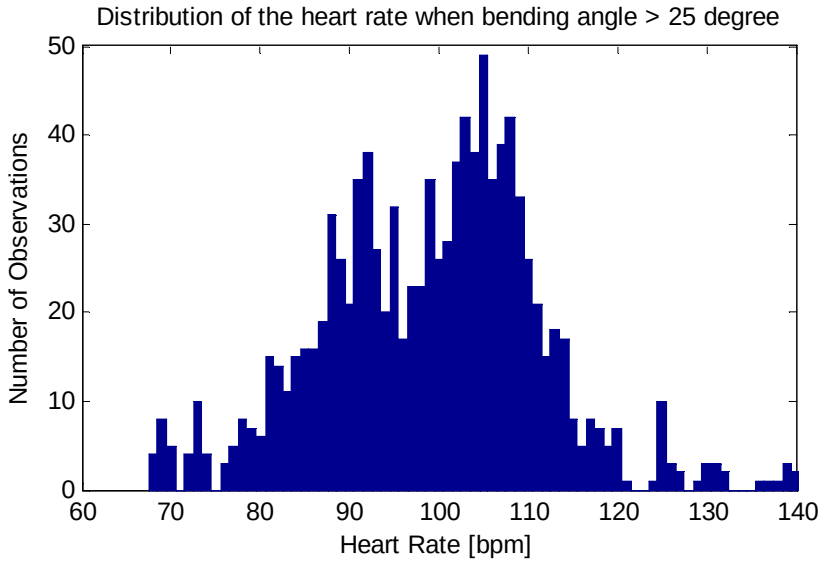

Figure 62 Heart rate from PSM when posture angles are greater than 25 degrees.

Defining and applying only a heart rate threshold probably would not account for other factors that influence the heart rate, for example, subject fatigue or very fast transitions between work activities. Therefore, a pattern analysis for heart rate changes was performed.

The signals of both heart rate and bending angle in a 240 seconds observation period are shown in Figure 63. Two types of the posture angle peaks can be noticed. One with local maximum value greater than +25 degrees (threshold), which always represents the motions observed in the installation zone according to the video. The other one has a local maximum smaller than +25 degrees. It represents the activities performed in the material zone.

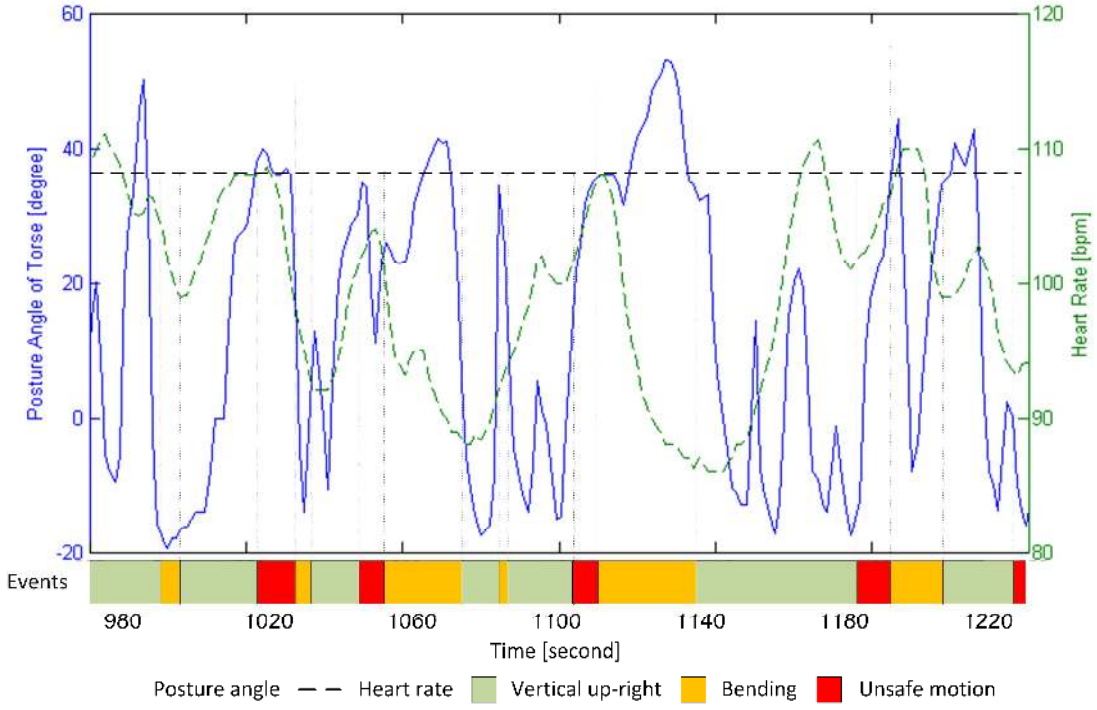

Figure 63 Comparison between posture angles and heart rates.

Several changes in the heart rate pattern can be noticed that correspond to the subject's posture angle: (1) the posture angles were found to be lower than the threshold value when high heart rates were observed (time span from 1,000 sec. to 1,100 sec; the subject might have already been tired due to the rapidly changing motions); (2) both the heart rates and posture angles were found at a low level or less than the threshold value (time span from 1,030 sec. to 1,050 sec.; which implies the subject's torso was in vertical up-right position and recovering to the normal situation); (3) the heart rate maintained at a high level while the posture angle increases and exceeds the threshold value (time span from 1,100 sec. to 1,125 sec.; which indicates bending motions with loads; the heart rate maintained at a high level because the body was not recovered from the previous motion); and finally (4) rapid increments were observed on both heart rate and posture angle (associated with several seconds delay: time span from 1,045 sec. to 1,052 sec.; and simultaneously, time span from 1,105 sec. to 1,110 sec.; these also demonstrate bending motions with loads). The first two patterns have heart rate and posture performance values indicating safe behavior. The last two patterns relate to unsafe work behavior.

An additional consideration to analyze PSM data might be the analysis of the slope change of heart rate values. The changing rate (slope) of the heart pulse when the subject bended more than 25 degrees consists of three isolated peaks: the first one is at 0 bmp/min, the other two peaks were at 1.2 and -1.1 bmp/min. The first peak implies that the subject's heart rate is maintaining, which indicates no physical action or idle status. The other non-zero peaks are symmetrically around the first peak representing the transitional period of the subject's heart rate from the idle status to physical active status or the other way around. Since this research focuses unsafe behavior related to workers bending with heavy loads, the positive peak (1.2 bpm/min) on the changing rate is utilized to differentiate a physically demanding bending from normal activities.

7.5.4 Localization of the Unsafe Behaviors

Fusing the heart rate data and the posture data from PSM provides the capability of differentiating safe from unsafe material handling activities. The next step was to fuse and visualize the spatio-temporal data.

Experiment No. 1

Trajectory and PSM information of one subject performing a concrete wall installation are shown in Figure 64. The weight of each concrete block was 23 lbs. The distance between assemble and disassemble of wall was about 12 meters. The blue color in Figure 64 represents the walking paths of the subject between the installation and de-installation areas, and to/from the rehydration area. The location where the subject squatted safely is shown in green. The red color denotes unsafe bending/lifting events with a heavy load.

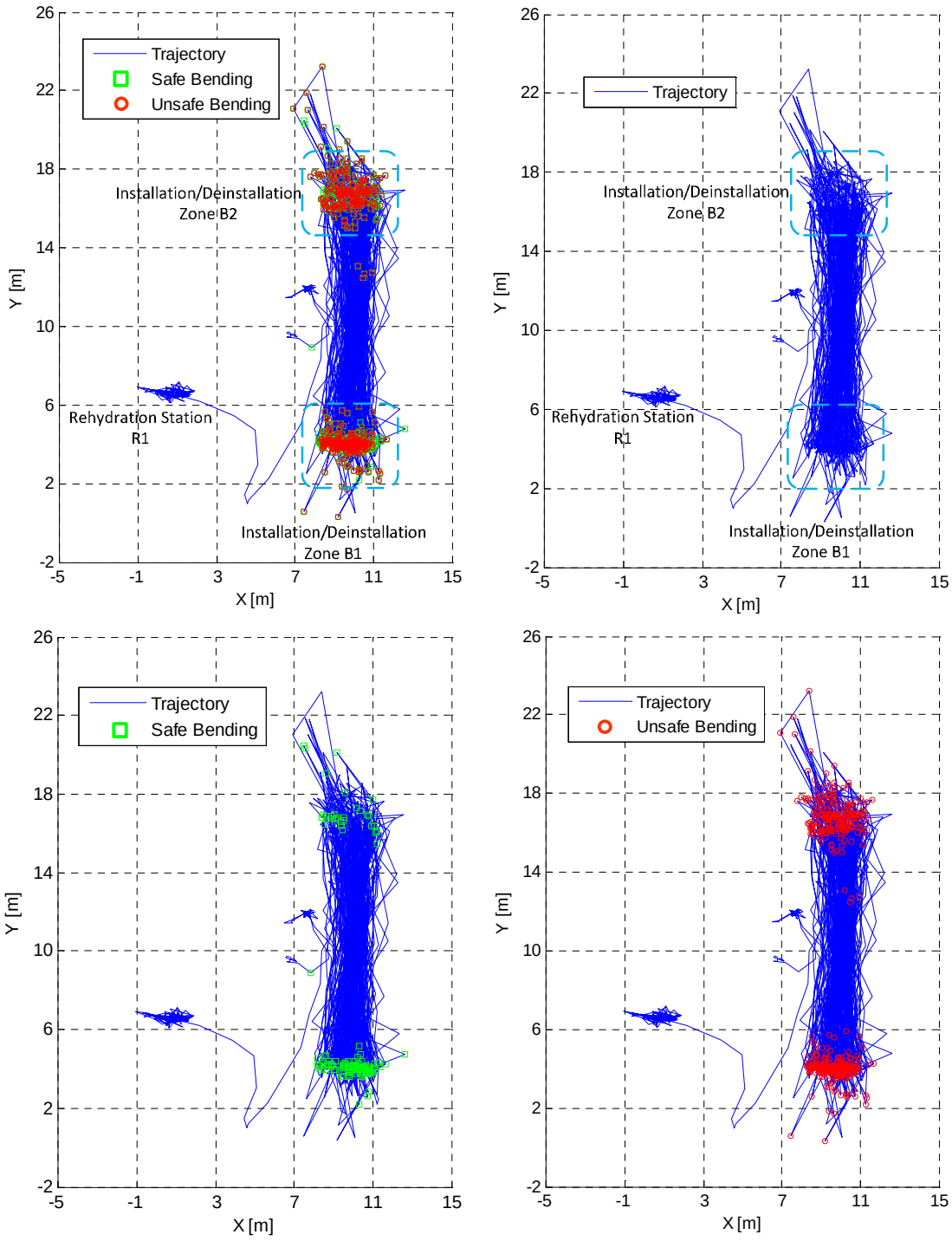

Figure 64 Experiment 1: Localization of safe and unsafe material handling motions.

During the 62 minute long experiment, 105 ergonomically safe and 93 unsafe motions were automatically identified and mapped. Figure 65 shows the analysis of all

unsafe bending/lifting events over the observation time. The unsafe events indicated in red color relate to labor (install a concrete wall) that is physically very demanding and leads to exhaustion. Manual video analysis confirmed that the subject followed more frequently safe bending practices at the beginning of the work shift. The guidelines were followed when handling heavy materials during the first 8 minutes of the experiment. Although the observation time was too short to find statistically significant results for an increase in unsafe acts over time, the number of unsafe lifts slightly increased towards the end of the work shift. Fatigue may have played a role leading to more unsafe lifts at the end of the shift.

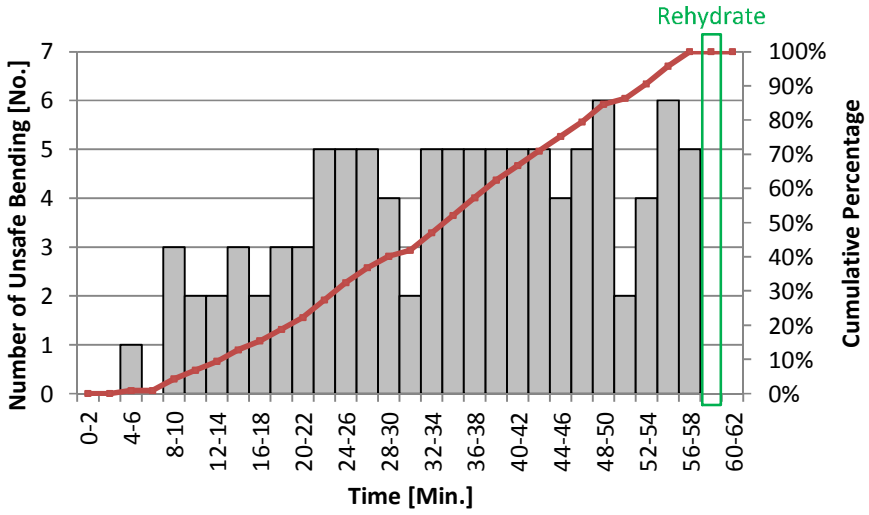

Figure 65 Experiment 1: number of unsafe bending over time.

As the algorithm automatically found, the subject rehydrated only once at the 59 minutes into the experiment, and since the work task had already been completed, spent the remainder of the observation time at the rehydration station. The subject did not take any other break(s).

Experiment No. 2

Trajectory and PSM information of another subject performing a floor installation are shown in Figure 66. The blue line represents the walking paths of the subject. Access/exit points to/from work zone areas (A1 and A2), rest station, dehydration area, and material storage areas (S1 and S2) are also graphically visible. Locations where the

subject squatted safely are shown in green whereas unsafe lifts/placements of heavy load are represented in red color.

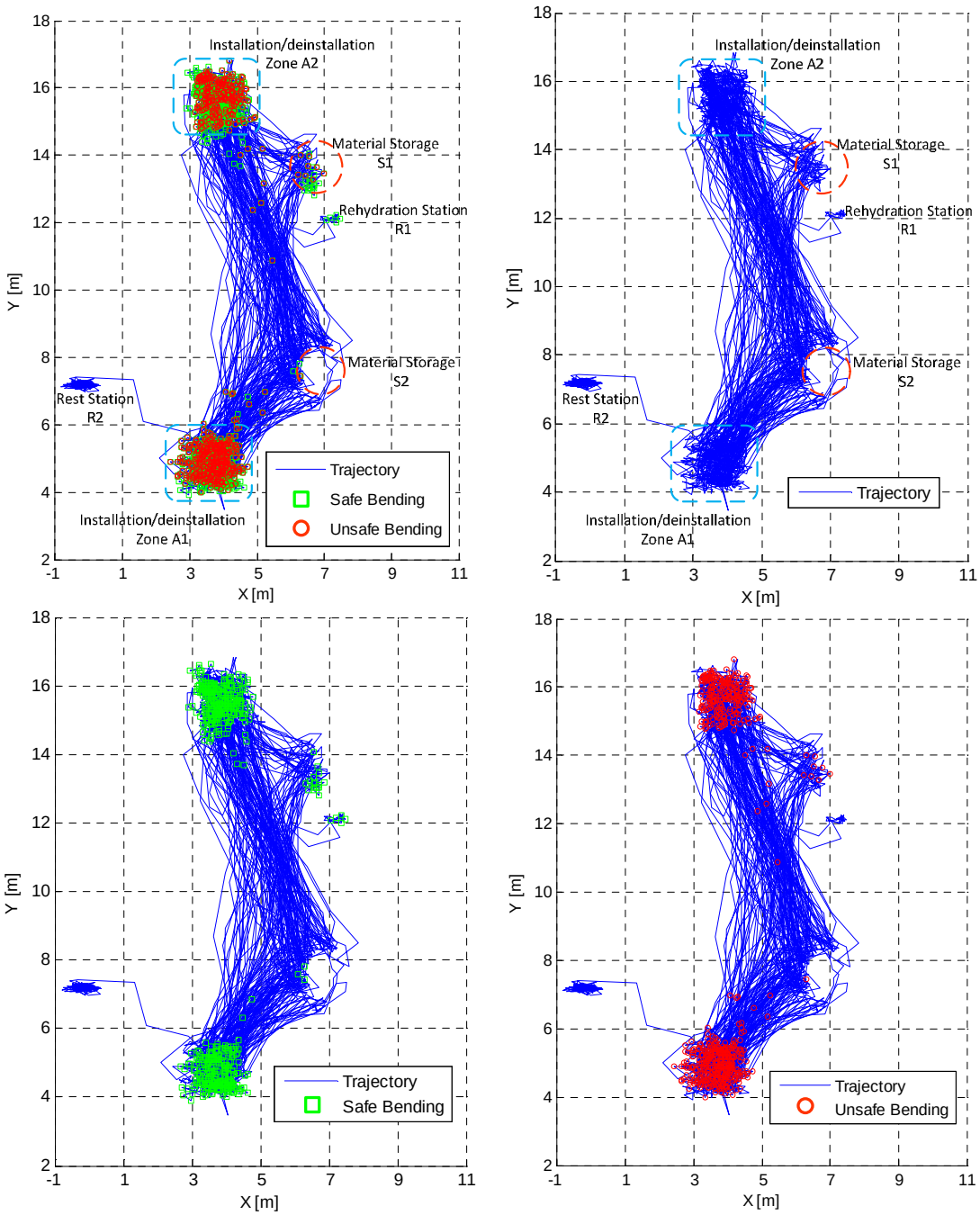

Figure 66 Experiment 2: Localization of safe and unsafe materials handling motions.

During the 45 minutes long experiment, 79 ergonomically unsafe motions were automatically identified and mapped. Figure 67 shows the analysis of unsafe bends over time. Although the observation time was again too short to find statistically significant results, the number of unsafe lifts seemed to be consistent during the work shift. The subject went once to the rehydration station at 27 minutes into the experiment. This visit indicates that the work task was physical demanding and exhausting the subject.

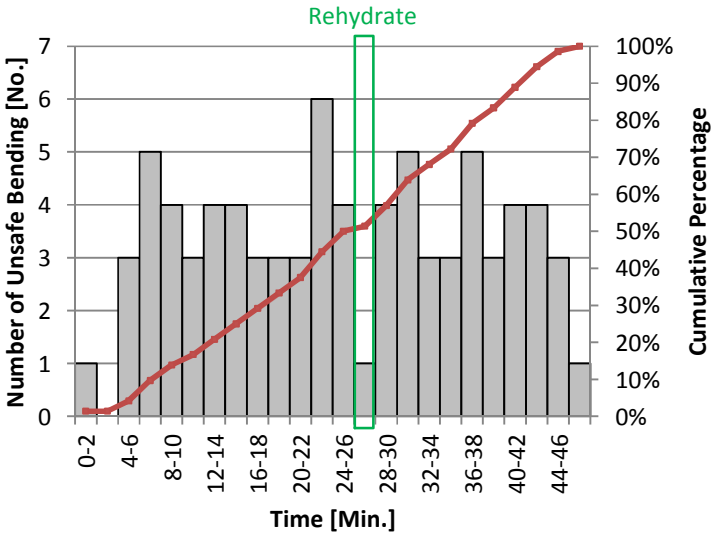

Figure 67 Experiment 2: number of unsafe bending over time.

Experiment No. 3

This experiment included two subjects, one installing and one deinstalling floor materials while they were sharing the same storage areas. Figure 68 and Figure 69, respectively, show the graphic representation of the travel locations of the subjects, and their safe unsafe material handling motions.

During the 1 hour and 30 minutes long experiment, the algorithm identified and mapped 284 ergonomically unsafe motions for subject one and 84 for subject two. Figure 68 and Figure 69 show the trajectory information to subjects to/from work zone areas (A2 and B2), rest areas, dehydration area, and material storage area (S1, S2 and S3). Green and red color marks show the location where the subject squatted safely and unsafely, respectively.

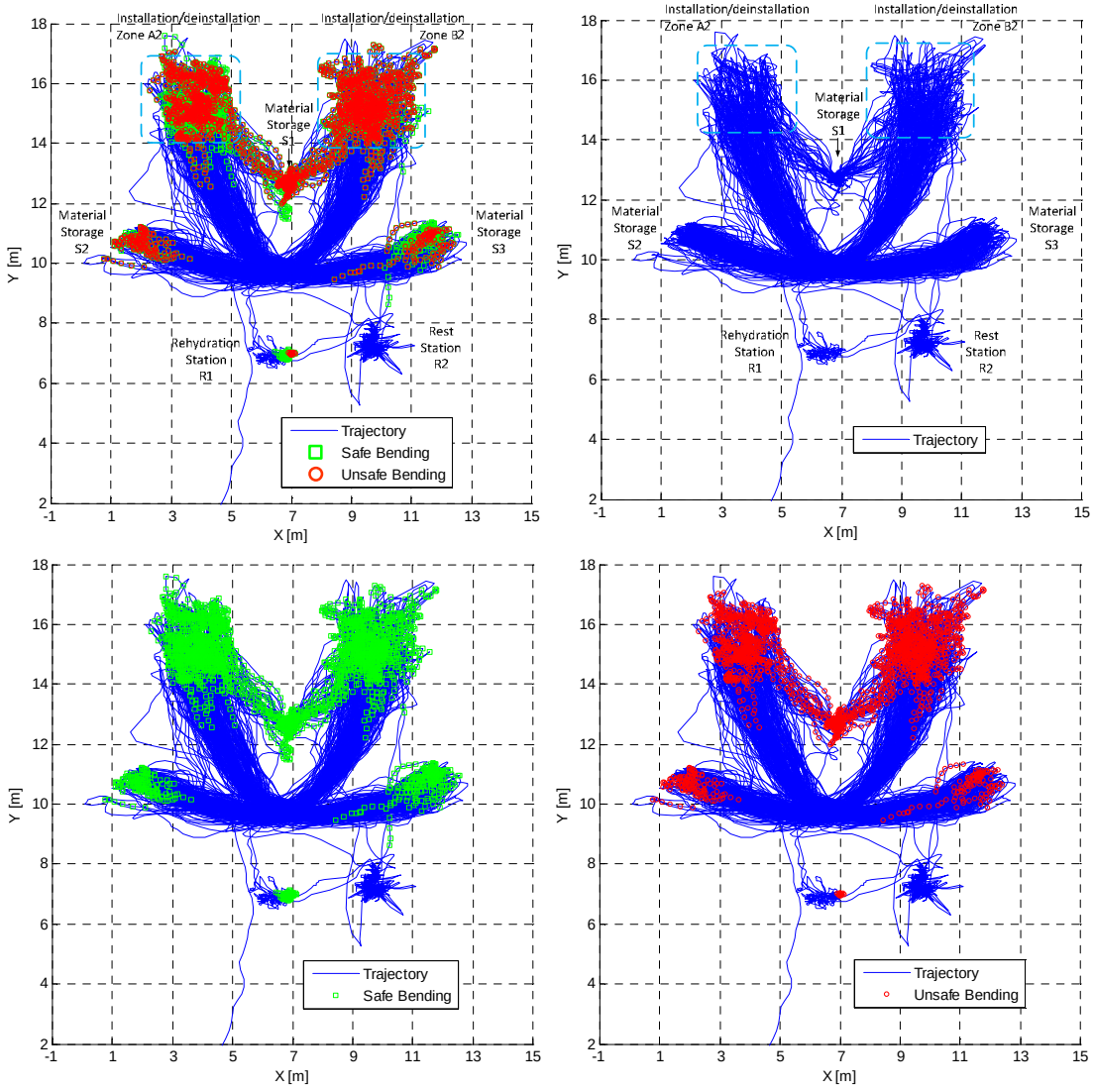

Figure 68 Experiment 3 – subject 1 (deinstalling matertials): location of safe and unsafe material handling motions.

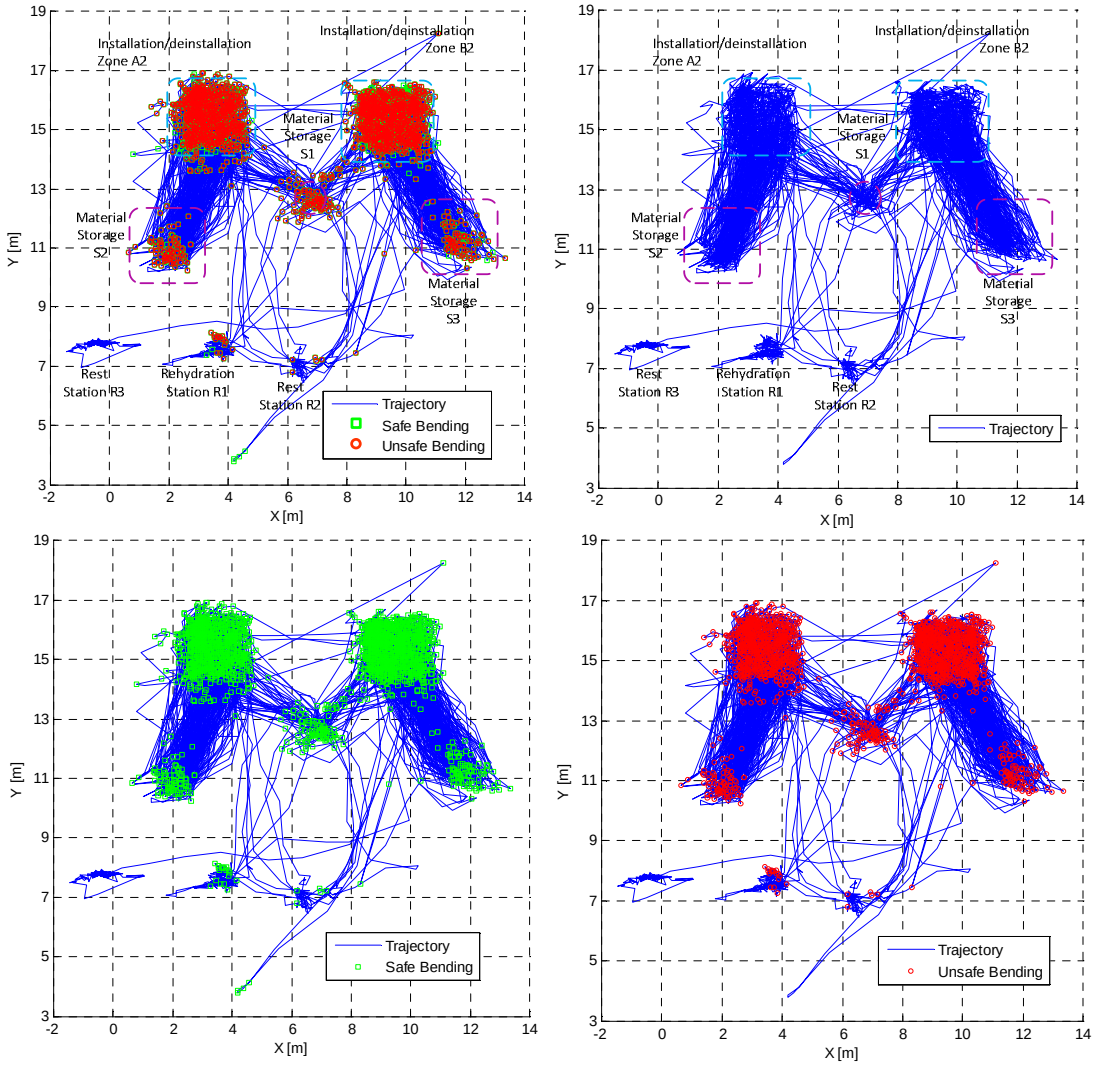

Figure 69 Experiment 3 – subject 2 (installing materials): location of safe and unsafe material handling motions.

The analysis of unsafe bending over time for both subjects is shown in Figure 70 and Figure 71, respectively. Both subjects had consistently unsafe bending throughout the observation period. A difference though is in the frequency of unsafe bending acts. Although the deinstallation work task that Subject 1 performed was very similar to the motions of Subject 2 who was simultaneously installing the floor system, Subject 1 had a significantly higher number of unsafe bending than Subject 2. Focused education and training on subjects (e.g., construction workers) could potentially resolve such behavior.

Compared to experiment one and two, both subjects took more frequently breaks (at least two) and rehydrated at least three times. These breaks were separated roughly evenly over the work task period.

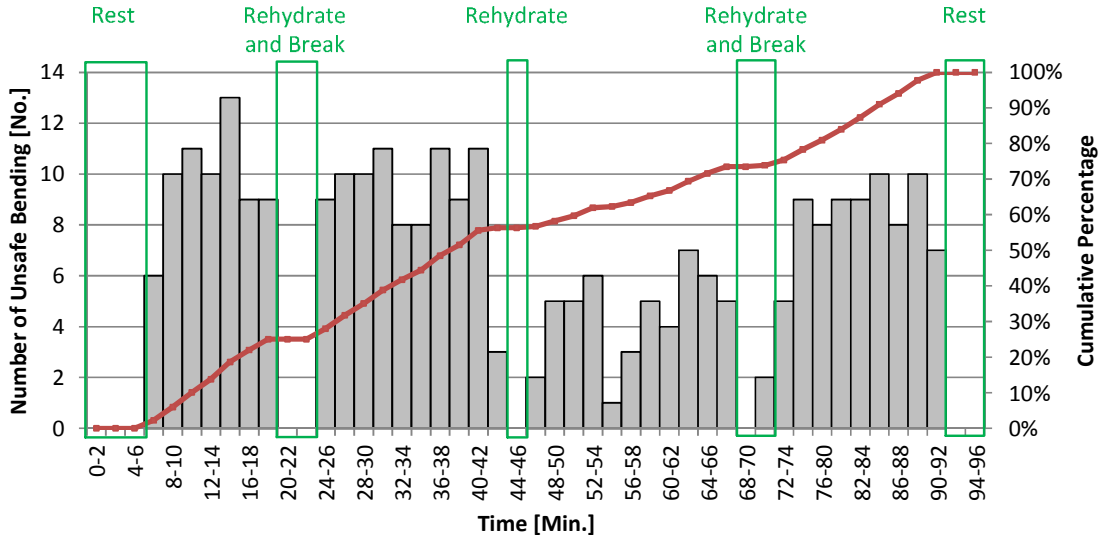

Figure 70 Unsafe lifts over time (Subject 1).

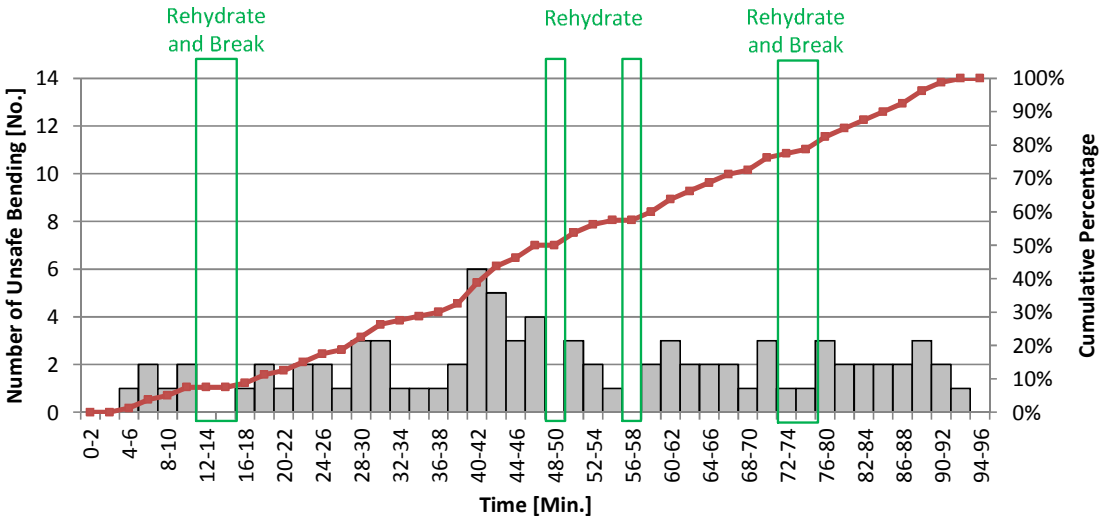

Figure 71 Unsafe lifts over time (Subject 2).

Additional results to the experiments

A tabular analysis for all three experiments was conducted to identify the "hotspots" which present the largest occurrences of ergonomically unsafe lifts.

Comparison is only possible for experiment three which had more than one subject involved.

According to Table 9, most of these unsafe bending occurred in zone A2, B2, S2, and S3. These were the locations were concrete flooring material was either to be stored, removed, or installed. Any of these work areas could be improved by providing elevated work platforms, for example, the storage areas could be elevated in the future to allow a subject (worker) to easily grab or place material.

Table 9 Number of unsafe bending per subject and work area.

	A1	A2	B1	B2	S1	S2	S3	R1	R2	R3	Total
Experiment 1:			57	45				0			102
Experiment 2:	43	29			4	3		0	0		79
Experiment 3: Subject 1		48		94	19	77	45	1	0		284
Experiment 3: Subject 2		35		16	5	15	11	1	1	0	84
Experiment 3: Both Subjects		83		110	24	92	56	2	1	0	348

Secondly, improvements to work environment requires further attention. Area S1, in particular, had relatively small numbers of unsafe bending. The reason is that light and small plastic pedestals were stored in this area. They may not cause as much damage to health over time as would occur when heavy material is placed/lifted. However, even this work area could be elevated to decrease the times a subject is required to squat. Instead of a wooden palette on the ground a forklift temporarily lifting or a fixed palette at raised height might be installed.

Table 9 summarizes the number of unsafe bending events performed by the subjects in each experiment and by specific work area. In experiment 3, a significant difference in the number of automatically detected unsafe bending (squatting) motions between Subject 1 and Subject 2 can be noticed. Subject one performed a total of 284 unsafe bending acts while subject two only had 84. As explained previously, proper education and training might be provided to Subject 1 to stop unsafe bending.

7.5.5 Validation of UWB/PSM Data Fusion Approach with Video Camera Data

The detecting of unsafe/unhealthy material handling activities was validated through a manual analysis of the video data that were recorded for all three experiments. The analysis of work activities using video served as ground truth. The results from the video were also divided into two categories: safe and unsafe bending. Results from video and UWB/PSM data were compared against each other to conclude on the error rate of the developed automatic ergonomics algorithm.

The comparison of video and UWB/PSM data is shown in Figure 72. The figure shows four confusion matrices (one per experiment and subject). These matrices present adequate validation of the comparison. The horizontal direction of each confusion matrix describes the ground truth observation using manual interpretation of video camera footage. The vertical direction of the matrix shows safe/unsafe bending the algorithm automatically detected. The diagonal elements of the matrix represent the true positive cases (squat performed safely) and the true negative (squat performed unsafely) for both video observation and UWB/PSM algorithm. The non-diagonal elements indicate the number of false positive and false negative cases (misidentifications). On average the data fusion approach of UWB and PSM performed accurate detection of unsafe bending with an average success rate of more than 90%.

False positive cases were due to rapidly changing postures. The utilized PSM technology yet has to be adapted to construction environment and may not have always reported a subject's heart rate precisely. A typical example for such an event is when a subject performs several unsafe bending acts in a very short sequence of time (basically one after the other, also called rework or adjustment work to the same concrete block). As the subject does not carry a load during the second time of bending, but the heart rate is still elevated (the body has not recovered yet), the developed algorithm interprets the PSM signal as another unsafe bend.

The false negative cases are another type of error, representing situations where the algorithm considers an unsafe lift as a safe motion. This error occurs because the PSM recordings of a subject are always slightly delayed (up to one second) during physically very demanding activities. A typical example is when a subject bends and lifts

a heavy load, then very rapidly stands up, and walks away. As the subject's torso angle is high at the moment of the lift, the heart rate might still be slow.

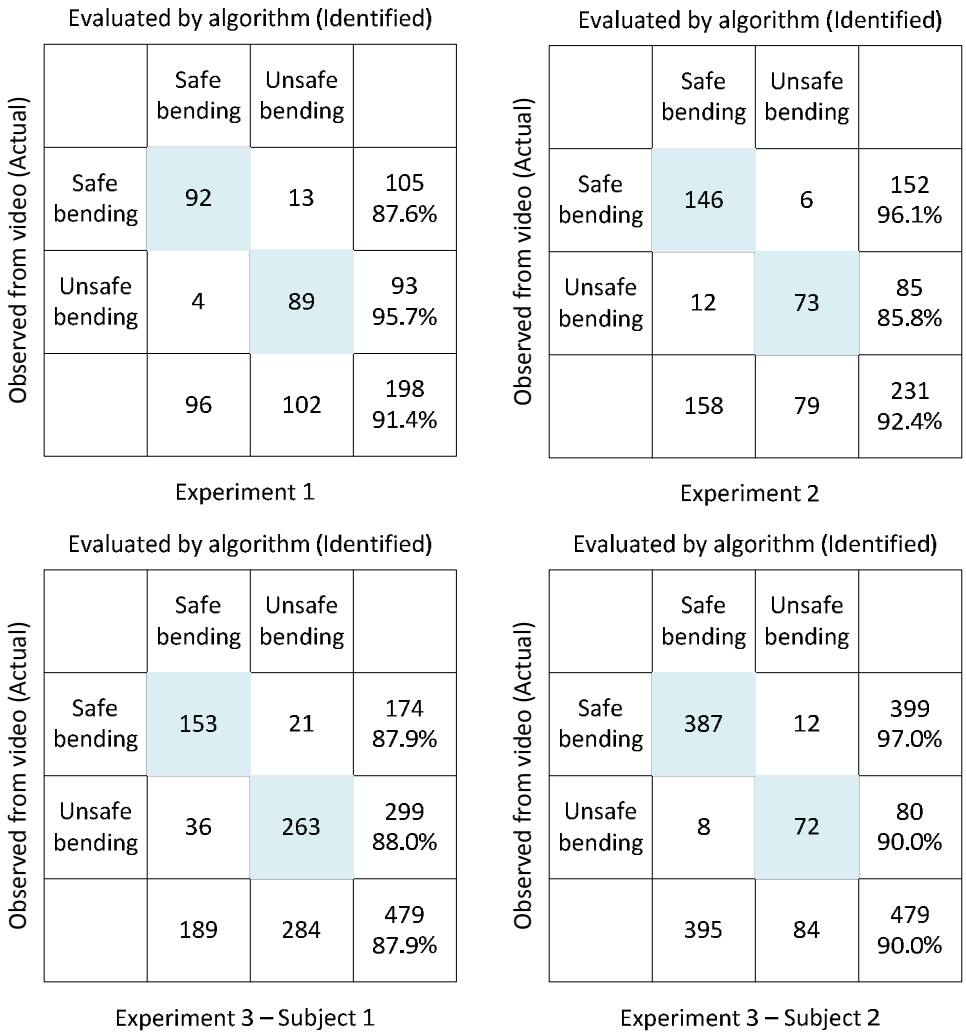

Figure 72 Results validation by comparing manual video data analysis to the approach of fusing UWB and PSM data.

These two types of errors can be reduced by calibrating the physiological factors such as heart rate for each individual. Usefulness of the developed approach may also depend on improvements in technology, for example, existing PSM technology has not been configured to suit construction industry applications. Measurement error can also be solved by increasing the data collection frequency and adding a physiological response function to compensate for signal delays. Since a subject's physiology response

mechanism depends very much on the individual, it will be a future research task to develop a uniform model that fits most users in the construction industry. Further study is necessary on the developed rules, such as the relationship of bending angle and heart rate, thresholds, and their interactions to precisely identify ergonomic hazards.

7.6 Conclusions

Rapid technological advances such as Ultra Wideband (UWB) and Physiological Status Monitoring (PSM) technology have facilitated monitoring the position and physiological status of construction personnel. Traditionally, data from these sources have been independently used and eventually analyzed to infer about the status of entities being observed. However, data collected from various sources can be integrated with the goal of achieving a higher level of knowledge. While possible, the capabilities and benefit of fusing the data from multiple sensors require further study, which is the aim of this investigation. Using a set of experiments conducted in an indoor facility, this paper demonstrated that UWB and PSM data can be fused to automatically identify and localize the ergonomic related unsafe working behaviors.

The results show that current technology is satisfactorily reliable in autonomously and remotely monitoring subjects during simulated construction activities. Partially validated through video analysis, these results suggest that data from these sources can be successfully fused to augment real-time knowledge of construction workers' status. Nevertheless, the selected monitoring technologies show limitations that have to be addressed to fully validate the proposed algorithm. For example, the bending threshold utilized to differentiate the squat from normal posture is ambiguous because of constraints in the existing technology. Therefore, the connection between the bending threshold and the performance of the PSM in dynamic situation requires further study. In summary, the present work showed that potential construction applications of some technologies lie in the integration of various technology-specific data sources.

CHAPTER VIII

AUTOMATED TASK-LEVEL ACTIVITY LEVEL ANALYSIS

Knowledge of workforce productivity and activity is crucial for determining whether a construction project can be accomplished on time and within budget. As a result, significant work has been done on improving and assessing productivity and activity at task, project, or industry levels. Task level productivity and activity analysis are used extensively within the construction industry for various purposes, including cost estimating, claim evaluation, and day-to-day project management. Nevertheless, assessment of task level productivity and activity are mostly performed through visual observations and after-the-fact analyses even though studies have been performed to automatically translate the construction operations data into productivity information and to provide spatial information of construction resources for specific construction operations. This chapter presents an original approach to automatically assess labor activity. Using data fusion of spatiotemporal and workers' thoracic posture data, the authors have developed a framework for identifying and understanding the worker's activity type over time. This information is used to perform automatic work sampling that is expected to facilitate real-time productivity assessment.

8.1 Introduction

As several researchers reported, productivity in the construction industry has been declining over the past decades [191][192][193][194]. These analyses, however, are based on assembled measures from multiple governmental agencies (e.g., Census Value of Construction Put in Place, BLS work-hour data, and BEA structures deflation index) and do not regard the broader concerns regarding the accuracy of such productivity measures [195][196][197][198][199][200]. Up to today, the aggregated productivity performance is not measured for the most part [201] due to the lack of suitable and sustainable approaches to accurately and automatically monitor the actual activity and work output. In addition, an aging and decreasing construction workforce magnifies the

effects of these issues on the predictability of productivity performance. Before the economic recession, the construction industry offered employment to approximately 8% of the total civilian employed population in the United States of America [202]. However, after losing about 2.5 million jobs during the recession, the construction industry workforce only accounts for about 6% of the total domestic employment [203]. In addition, recent studies have highlighted that the recession has produced another effect: the construction industry workforce is aging because workers are delaying retirement [204].

As workforce productivity is a major aspect in determining whether a construction project can be accomplished on time and within budget [205][206], an effective and timely approach to productivity management is crucial to the success of construction projects and construction companies. An extensive literature on construction productivity has confirmed the importance of these concepts to the success of construction projects and companies. Productivity assessment has been found to be crucial in (a) supporting prompt and informed decisions to avoid productivity loss or enhance the productivity in ongoing operations [207], (b) assessing project performance for internal and external benchmarking [208], and (c) creating a basis for future improvement [209]. Even the introduction of lean production techniques to the construction industry while de-emphasizing the focus on productivity improvement [210] has heavily relied on productivity analyses to assess the effectiveness of lean construction approaches [211].

Due to the characteristics of the construction industry, the productivity of this industry can be assessed at three levels: task, project, and industry level [212]. Task level focuses on single construction activities, such as structural steel erection or concrete placing. Task level productivity is used extensively within the construction industry. Different construction tasks are combined at the project level. Obviously, different tasks imply different inputs and/or outputs. Thus, it is necessary to use adjustments to combine the individual task productivity. At the highest cumulative level, industry-level productivity comprises data from all the individual projects. The productivity indices calculated by the Bureau of Labor Statistic (BLS) are examples of industry-level productivity performance measurements. Such indices exist for industry sectors like

manufacturing. For reasons stated by [195][196], the BLS, however, currently does not maintain a productivity index for any sector of the U.S. construction industry.

Productivity assessment at each level can be performed and reported in several separated ways. Each serves as an independent metric for understanding the productivity performance. For example, the majority of metrics to assess the productivity performance at the task level are single factor measures related with labor productivity. However, a standard and universally accepted definition or equation of productivity assessment does not exist in the construction industry. Traditional approaches for productivity analysis includes project-level information systems, direct observation methods and survey/interview based methods [92]. The application of these methods has been constrained by its limitations, including the high cost of performing manual data collection, the risk of interfering with activities under observation, and the tendency to produce inaccurate data. Moreover, these methods are mostly manual intensive, so they result in delayed information analysis and exchange [214][215].

Current practice strongly relies on historical production rates to develop estimates for future projects, but the accuracy of these estimates highly depends on the steadiness of the assumptions while requiring a comprehensive management of productivity records. Whereas on-site productivity analyses provide important information necessary for timely jobsite decision-making, changes in workforce composition are expected to produce uncertainties in historically-based production estimates. Hence, there is a need for data collection and processing approaches that would produce real-time automated productivity assessment.

Gathering relevant data that represent the performance of construction operations is crucial to measure productivity [92]. During the past decades, cutting edge technologies have been introduced and used to raise the efficiency level of engineering and design operations of construction projects. An increasing number of information sources is today available for data collection and analysis, including remote sensing technology that allows for autonomous and remote data collection of construction resources. Data collected from various sources can be integrated with the goal of achieving a higher level of knowledge about the entities being observed [146].

This paper presents an original approach to automatically assess labor productivity. Using data fusion of spatio-temporal and workers' thoracic posture data, the authors have developed a framework for identifying and understanding the worker's activity type over time. This information is utilized to perform automatic work sampling that is expected to facilitate real-time productivity assessment.

8.2 Background

8.2.1 Definition of Productivity

Previous researchers have identified numerous factors that can affect the success of projects. Despite the vast quantity of identified factors, four parameters are usually agreed upon as the most important for determining success of a project: cost, quality, time, and safety. However, obtaining the expected quality, cost, and time is strongly related to the achievement of the expected productivity. Therefore, productivity is widely used as a performance indicator to evaluate construction operations throughout the entire construction phase.

A consensus regarding a common productivity definition as well as standard productivity measurement techniques has not been reached by the construction industry or academia [216][217][218]. A common measurement of productivity describes the ratio between the outputs of a production process over its inputs, which is defined as

$$Factor\ Productivity = \frac{Physical\ Output\ (Unit)}{Labor\ (\$)\ +\ Equipment\ (\$)\ +\ Materials\ (\$)} \qquad \text{(Eq. 8 - 1)}$$

Nevertheless, the selection of how to define input or output is strictly related to the scope of the measure itself and, frequently, to the availability of data. In general, it is possible to define Single Factor Productivity (SFP) or Multi Factor Productivity (MFP) [216][217][218]. SFP, which is also known as partial factor productivity, requires the ratio between a measure of output (e.g., gross value added) and a measure of one input (e.g., number of man-hours). In computing MFP, which is also known as total factor productivity, several parameters (e.g., labor, materials, equipment, energy, and capital)

are considered simultaneously as inputs that influence the output. Factor Productivity is an example of MFP.

Since it is relatively difficult to measure total factor productivity on a typical construction project (the utilization of equipment and materials often remain relatively constant from one project to the next), instead of using MFP, partial factor productivity is widely accepted for productivity assessment [155]. According to the Organization for Economic Co-operation and Development [219], labor productivity is the most frequently used, followed by capital-labor MFP, and capital (K), labor (L), energy (E), materials (M), and services (S) MFP (i.e., KLEMS). This paper adopted the labor productivity metric, which is defined as the number of work hours necessary to complete the unit of physical outputs [220]. As is shown in equation (Eq. 8-2), the labor productivity does not explicitly consider the cost of labor.

$$Labor\ Productivity = \frac{Work\_hours}{Unit\ of\ Physical\ Output} \qquad \text{(Eq.8 - 2)}$$

8.2.2 Productivity Assessment Method

At the end of the 19th century, Frederick W. Taylor started theorizing about scientific management (i.e., Taylorism). Since then, several productivity assessment methods have been created and adopted within the construction industry. In particular, methods can be grouped in two main categories: Productivity Measuring Methods (PMMs) and Productivity Improving Methods (PIMs). PMMs' goal is to measure productivity performances for internal and/or external benchmarking. Examples of PMMs include the Method Productivity Delay Model (MPDM) [221], the Construction Industry Institute (CII) site-level labor productivity assessment [222], the XYZ model [223], and the Construction Productivity Metric System (CPMS) [208]. PIMs aim to evaluate how effectively equipment and workforce utilization are managed. Many PIMs rely on the motion and time study theory, including (a) time studies (also called stopwatch studies); (b) questionnaires and interviews (e.g., questionnaires for craftsmen or foremen; Foreman Delay Survey, FDS; Craftsman Questionnaire Sampling, CQS); and, (c) activity/work sampling.

Work sampling technique, which utilizes alternating Poisson process, has been widely used to understand the characteristics of a work process in industrial settings. In the construction industry, this technique is implemented as an indirect method to measure activity level and productivity. Another PIMs example is activity analysis, which is the evolution of the practice of work sampling [219]. The activity level is defined as the percentage of time that craft workers spend on a particular activity [219]. The productivity is therefore represented by the direct work time rate, which is shown in equation (3). In fact, measuring work rate is not the same as measuring productivity. A strong relationship between these two factors has not been fully established yet. There is some evidence from case studies though that suggests a weak to strong relationship. Reasons for this lack of a strong relationship are the influences of rework, turnover in the labor pool, and of poor work planning [224]. Compared to the traditional work sampling technique, the activity analysis technique includes significantly more detailed observations and is able to provide more descriptive assessment of the effectiveness of the utilization of craft workers' time, and can continuously identify the areas for productivity improvements.

$$Direct\ Work\ Time\ Rate\ =\ \frac{Time\ of\ Direct\ Work}{Total\ Work\ Time} \qquad \text{(Eq. 8 - 3)}$$

8.2.3 Available Sensing Technologies for Productivity Measurement

Even though several existing productivity measurement methods can generate useful information to improve construction activities [207], many of these methods present severe limitations [67][214][215][225], including being manually intensive, involving human judgment, and being ineffective in providing timely and accurate control data. Thus, it is reasonable to assume that automated productivity assessment methods can be very beneficial for the construction industry.

With the development of new information and sensing technologies, it is possible to provide a steady and reliable data stream of construction process. Video recording of construction activities is now commonly used and its benefits have been extensively studied [226][227][228]. However, the process of manually review video-recordings is inefficient. To overcome this limitation, a video interpretation model, which formalizes

key concepts and procedures from the video within construction domain, was developed to automatically translate the construction operations data into productivity information [214]. Nevertheless, automated image and video interpretation requires advanced pattern recognition and computer vision techniques within the construction context [67]. A four-dimensional (4D) reality model based on photograph logs is implemented for automated construction progress monitoring [229]. Automated vision tracking techniques have also been studied to provide spatial information of construction resources for specific construction operations [93][230][231].

Despite of the advantages and achievements of using video cameras, it is still a challenge to monitor multiple targets in the harsh construction environment in real-time. Besides vision technology, sensor-based tracking technologies show potential applications on assisting automated work sampling on material installations [60]. Selection of one particular tracking technology depends on the application area, signal quality, data stream provided, and the calibration requirements [232]. Ultra Wideband (UWB), as an active Radio Frequency Identification (RFID) technology, employs a tag-to-reader approach [76], which allows recording location data of multiple resources (worker, equipment, and material) in real-time. Research has demonstrated that a commercially-available UWB system is able to provide accurate real-time spatio-temporal data of construction workers, equipment and materials, while the tracking error in a harsh construction environment was less than half a meter [146].

8.2.4 Data Fusion Applications for Construction Engineering

Data fusion is a technique that combines data from multiple sources with the purpose of achieving refined identity estimates and inference [183][184]. Data fusion applications span a very wide domain [190] including military command and control, robotics, image processing, air traffic control, medical diagnostics, pattern recognition and environmental monitoring [186][233]. In construction engineering, data fusion has been studied for automated tracking of materials [187], for the identification and localization of engineered components [60], and for the analysis of site operations [93]. Moreover, the implementation of Real-time Location Sensing (RTLS) technologies in

combination with Physiological Status Monitors (PSMs) was used for analyzing ergonomic performance of construction tasks [232].

8.3 Objective and Scope

By integrating data from real-time location sensors (RTLS) and thoracic accelerometers this study attempts to continuously assess task activities of construction worker(s). The goal of this research is to automate the process of activity analysis by fusing information on body posture and positioning factors of repeated manual material handling activities in construction environments. The first objective is to automatically identify and characterize the various site geometries related to different activities including work zone, material zone, and rest zone. The second objective is to automatically measure the direct work time rate by computing the time lapse of both productive and non-productive activities including wrench time, material time, traveling time and rest time.

This study is limited to fusing information from two specific sensing technologies (UWB and PSM). All tests were performed in a controlled study environment. Working activities that were recorded with UWB, PSM, and video camera technology occurred indoors and on the same elevation level. This study focuses only on the labor productivity measurement. All the working activities associate to the construction personnel, especially, those involved in heavy load lifting.

8.4 Methodology

To date, research efforts have not explored the potential of fusing real-time data on construction location tracking and posture to automate activity analysis of multiple targets. This paper proposes a data fusion approach to fill this gap. To test this approach, the authors designed several working scenarios of repeated material handling activities involving multiple workers. The goal of this paper is achieved by integrating and analyzing the location data and thoracic posture information of the workers. The automated data analysis methodology is shown in a flowchart in Figure 73. The methodology consists of three major components: data preparation and site geometry identification, activity identification and sampling, and productivity analysis. Further,

two trained raters accomplished a manual activity analysis based on the experiment video recordings to verify the automated data analysis accuracy level. A description of manual activity analysis protocol is here provided:

- Work: the participant is performing the assigned construction task within a work zone (e.g., assembling the deck).
- Material: the participant is handling construction material within a material zone (e.g., picking up supports/tiles).
- Travel: the participant is moving between, material, and rest zones.
- Idle: any activity that is not work, material, or travel (e.g., staying inside work/material zone with free hands, re-hydrating, talking, and checking PPE).

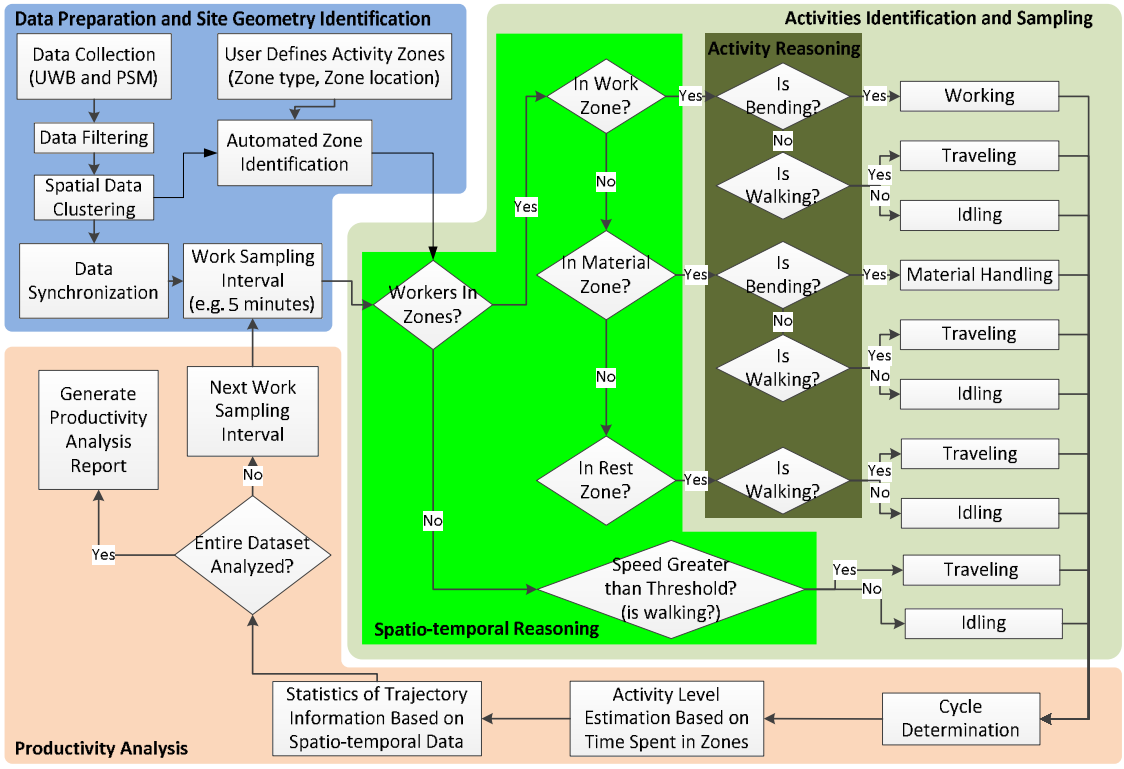

Figure 73 Flowchart of automated activity analysis and productivity measurement by reasoning the workers' spatio-temporal data and posture status.

8.4.1 Data Preparation and Site Geometry Identification

Data Collection and Filtering

This approach is tested in an indoor environment that had a simple site layout and lacked major obstructions. Therefore, a commercially-available UWB localization system is utilized to monitor the real-time spatial and temporal information of the participants in the test case. The UWB system consists of a central processing hub, several receiving antennas and active RFID tags as signal transmitters. The location of the UWB tag is automatically triangulated by computing the Time-Distance-of Arrival (TDoA) of the received radio frequency signal from multiple UWB receivers. The UWB tags are placed on the helmets of the participants for location tracking purpose, as well as at static positions to identify special site geometry, including material, work, and rest zones.

A commercial PSM system was employed to autonomously and remotely monitor the posture of the participants. The selected system is equipped with a wearable 3-axial thoracic accelerometer. The three-axial (vertical, lateral and sagittal) accelerometer is used to generate the participant's posture measurement in Vector Magnitude Unit (VMU). VMU is measured as a portion of the gravity acceleration (g), which is used to derive the participant's thoracic bending angles from the 3-axis gravity-compensated value calculated over the previous 1.008 second epoch. The derived bending angle becomes a scalar with positive and negative values, where zero degree represented the vertical right-up posture.

The location tracking and thoracic posture data of the participant is collected separately, while both data streams carry noises due to various data collection mechanisms. The noises of the spatial data collected by the UWB system may result in unexpected outliers of travelling speed, which is derived from the first differential of the spatiotemporal data. Since the traveling speed determines the moving status of the participant which directly link to the result of identification of the participant's activity type, it is necessary to smooth the UWB signals and remove the unexpected outliers. Thus, the location tracking data are filtered with a Robust Kalman filter [146]. The UWB data error analysis as well as PSM/UWB data synchronization has been explained in detail in [232].

Identifying Work, Idle, Travel, and Material Handling Zones

The UWB tracking system is setup based on a known local Cartesian coordinate system established at the workface. Several task-related zones represented by polygons are initially identified by the user based on the site layout and work plan. The task-related zone categories include work, material handling, and rest zones. Since the site layout may change as work activities advance, zones need to adapt to match the participant's spatiotemporal pattern accordingly. Filtered spatial data are implemented to dynamically update each zone's geometrical properties (location and shape) by reasoning the workers' moving statuses. Whereas zones were initially defined by the user, each zone's location and shape may change over time, and a new zone may have to be assigned. For example, an initially defined material zone may shrink and furthermore disappear when the materials inside the corresponding area have been removed; or a new rest zone has to be defined if a worker takes frequent stops in the middle of traveling.

Data Synchronization

Since the PSM and UWB systems monitor the work activities on two different aspects and independent timelines of the same experiment, the attributes of the location tracking and posture information have to be fused. Fusing these two data streams requires the data to be synchronized. As a network camera was utilized to visually record the experiments, the temporal information from both sensors is synchronized to the video time. The two data streams are then transformed (down-sampled or up-sampled) into a uniformed data log frequency to perform data fusing.

The synchronized data streams from UWB and PSM sensors are fused through probabilistic inference. A fuzzy representation is implemented to define the results of spatiotemporal reasoning and activity status reasoning. The spatio-temporal status is therefore described as "inside" or "outside of a zone", and the activity status is represented as "bending" and "walking". The likelihood function using Bayesian approach is computed at a specific reasoning status A_i at a given data synchronization function, such that

$$\ell(A_i \mid S^1_{new} S^2_{new}) = \frac{\prod_{k=1,2} P(A_i \mid S^k_{new})\, \mathrm{P}(A_i \mid S^1_{old} S^2_{old})}{\prod_{k=1,2} P(A_i \mid S^k_{old})} \qquad \text{(Eq. 8 - 4)}$$

where S^k_{new} is new datum from sensor *k*, S^k_{old} is old datum from sensor *k*, and $P(A_{i|} \mid S^1_{old} S^1_{old})$ is the prior estimation in the previous data synchronization model.

8.4.2 Activity Sampling

The fused data stream including location and posture attributes is utilized to assess the work activities based on defined data query rules. In order to achieve an accurate work activity assessment, it is crucial to define a set of proper activity categories, which must suit the need and the objective of the study and the feature of the work tasks that are being monitored. In addition, the defined categories must be able to involve all activities that might be observed. In this paper, the activities are sampled into four work categories: direct, material handling, travel, and idle. Then the activity sampling characterizes the proportion of time that the participant performed on specific activities. This process uses a two-step reasoning mechanism: spatio-temporal reasoning and activity reasoning.

Categorize activities by spatiotemporal reasoning

The fused data stream is firstly queried on the spatial and temporal aspect. The geometrical relationship between the participant's trajectories and the updated zone definition is checked, and the relevant data are extracted such that the location tracking data are intersected with zones. Three zone types are assigned by the user including work zone, material zone, and rest zone. Trajectories of the participant presenting inside zones are classified and characterized with specific zone type.

Categorize activities by activity status reasoning

The extracted location tracking data that intersect with various zones are further reasoned by the thoracic posture of the participant. Staying in a specific zone will not be identified as a corresponding activity unless a motion change of the participant's thoracic posture status is observed. The fused data are then classified and characterized with identified activity status including working, traveling, material handling, and idling. The

identification of direct work activity requires the behaviors of the participant to meet two criteria: the participant has (1) to be present in the work zone; and (2) to have a high posture angle. Activities in the work zone with up-right posture will be considered as either traveling or idling according to the participant's moving speed. Similarly, the material handling activities are identified through the posture status and movement of the participant inside and/or outside the specific zones. For example, the trajectories outside zones are regarded as traveling or idling according to the moving speed.

8.4.3 Productivity Analysis

As the activity type has been identified, the work cycle information such as the start time, end time and the duration that a participant conducts each identified activity can be determined. The activity level, which is represented by the rate of direct work time versus total time (equation 8-5), can be therefore automatically computed.

To be noticed, the estimated direct work time rate (equation 8-5) computed by this approach might be an over-estimation of the actual activity level due to the accuracy of activity identification. Under the approach adopted in this paper, a work activity is determined from the participant staying inside the work zone while assuming a possible working posture. This approach cannot accurately identify whether a participant is actually performing the work activity or mimicking it. For instance, a participant could bend down inside the work zone while waiting material to be delivered. Whereas this should be recorded as idling, the approach would instead record it as direct work. However, inaccuracy of visual observations is expected to be higher due to a combination of inconsistent judgment of the work activity across raters and individual rater's test-retest subjectivity. Therefore, the activity level measured by the proposed approach can be utilized as the upper bound of the actual case, such that

$$Estimated\ Direct\ Work\ Time\ Rate = \frac{Time\ of\ Identified\ Direct\ Work}{Total\ Time}$$

$$\geq Actual\ Direct\ Work\ Time\ Rate = \frac{Time\ of\ Direct\ Work}{Total\ Time} \qquad \text{(Eq. 8 - 5)}$$

8.5 Experiment and Results

The researchers designed a set of experiments to measure and analyze the productivity performance of several crafts when they conduct repeated material handling activities. Experimental data were used to test the proposed approach, and results are presented in this section. This section also presents the work cycle information that can be generated from fusing location tracking and thoracic posture data.

8.5.1 Experimental Setting

A total of three experiments were performed to simulate construction tasks. These experiments were conducted in a controlled indoor environment without major obstructions to avoid risk of interferences in the propagation of the wireless signal. Figure 74 shows a layout of the experimental testbed. A description of these simulated construction tasks is also provided:

- *Experiment No.1 (assembling a raised deck):* one participant assembles a deck using plastic supports and 16-lb concrete tiles; one installation area and two material storage areas.
- *Experiment No.2 (building a wall):* one participant builds a wall using 23-lb concrete blocks; one installation area and one material storage area.
- *Experiment No.3 (assembling and disassembling a raised deck):* one participant disassembles a deck and store material, another participant uses this material to assemble a raised deck in a different work area. Assembling and disassembling are dependent activities; two storage areas used by both participants and two installation areas used separately.

Three simulated construction tasks were performed in the same space using a similar experimental layout (see Figure 74). Four video cameras were installed on the perimeter of the experimental area. The first two experiments were conducted simultaneously, since the two participants worked separately without interfering paths. The experimental layout for the first construction task (right on Figure 74) consisted of an installation area, a disassembling area, and a material storage bay area. The layout for the second task was slightly different from the first, which had two material storage areas

containing concrete blocks and plastic footings. The third task had interaction of both participants in the entire work area.

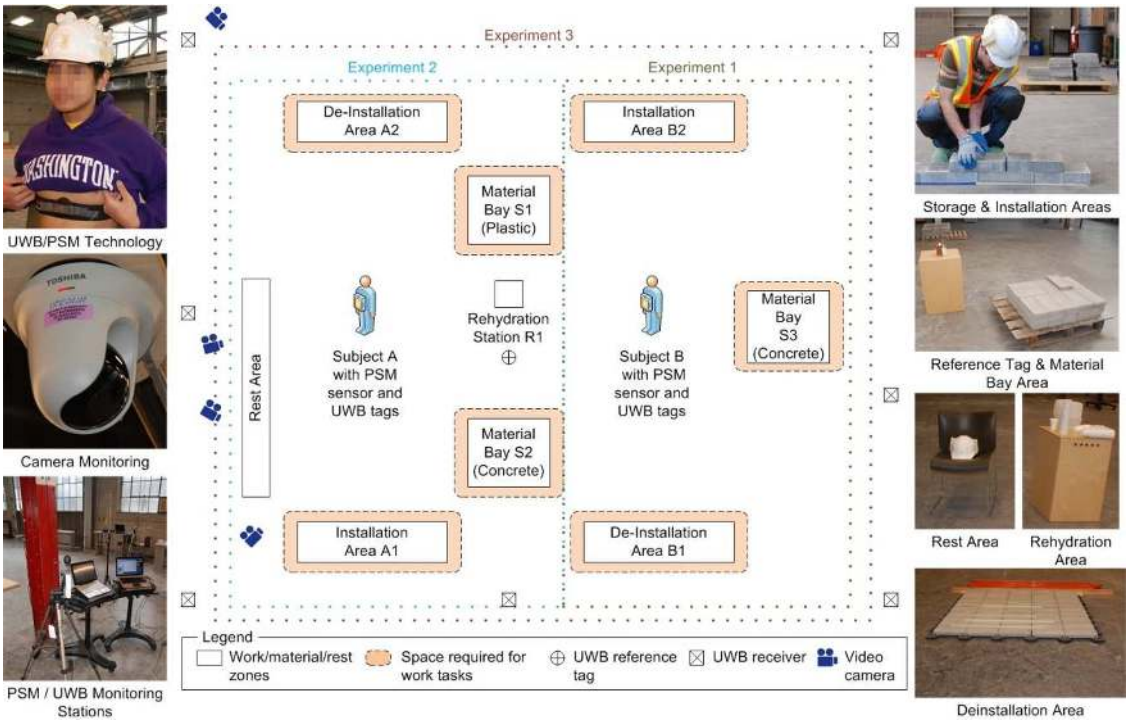

Figure 74 Experiment settings.

The participant's location and thoracic posture status is monitored by a UWB and a PSM system. The error of the UWB system was calibrated using three specific spots with known coordinates. Three additional UWB tags with multiple frequencies (one 60 Hz and two 1 Hz) were placed on the same spot as the reference tag was located. All tags maintained stationary during the error calibration. The three reference tags collected 206190, 2495 and 3050 data points, respectively. The average error to each tag was 0.28m, 0.31m, and 0.27m, respectively. The error associated with standard deviations was 0.16m, 0.35m, and 0.12m, respectively. The computed errors demonstrated that the UWB infrastructure layout in this experiment setting had capacity to provide reliable location tracking data. This technique confirmed previous research that indicated that a uniform location estimation error distribution can be observed within the coverage area of

UWB receivers [146]. In further experiments, these tags supplied ground truth data to moving UWB tags inside the experimental setting.

In addition to the location data that were gathered by UWB, the participants' variation in posture status was determined by an accelerometer. The accelerometer was embedded in a PSM device that was mounted on a chest belt that a worker wore. The utilized PSM system had also the capability to transmit live data wirelessly through a USB radio receiver, which was connected to a data logging PC. The PSM's data stream included data from several sensors, including a three-axial (vertical, lateral, and sagittal) accelerometer, with which the device generates the participant's default activity data measured in Vector Magnitude Unit (VMU, which is measured in portion of the gravity acceleration: g). The participant's instant posture data are derived through the PSM system's built-in module using readings from the accelerometer. The posture data carry a scalar with positive and negative values, where 0 degree represents vertical right-up posture(s).

8.6 Results

This section demonstrates the results of the activity level estimation and the work cycle analysis from the three experiments. Experiment No. 1 and No. 2 were conducted by a participant whereas two participants were involved in Experiment No. 3. This last experiment was designed to assess if the proposed approach was able to analyze the productivity performance of multiple participants. Further, this section presents the manual activity analysis output and compares it with the automated activity analysis estimation.

Experiment No. 1

In experiment 1, the speed distribution of the participant was fitted by two Gaussians with the mean at 0.19m/s and 0.91m/s and the standard deviation at 0.01m/s and 0.11m/s, respectively. The two Gaussians joint at 0.60m/s, which was set to be the speed threshold to distinguish the participant's moving and stationary status. The speed threshold was utilized to classify various task-related zones. In Figure 75, two work zones (A1 and A2), two storage zones (S1 and S2), and two rest zones (R1 and R2) were

clustered from the trajectory data. Four types of activities including direct work, traveling, material handling, and idling were classified from the fused data. Their paths and locations are plotted in Figure 75.

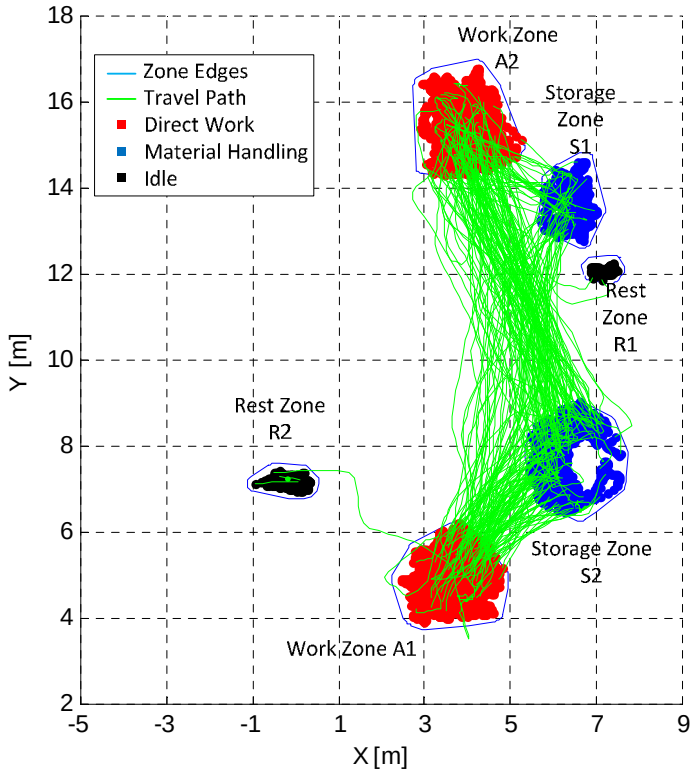

Figure 75 Experiment 1: results of classified activities of the first participant.

Table 10 to Table 15 show the results to the first participant in experiment 1. The tables include number of trips between zones (e.g., Table 10), total and average duration of the trips between zones (e.g., Table 11 and Table 12), total and average traveling distance (e.g., Table 13 and Table 14), and average traveling speed (e.g., Table 15). The diagonal elements (*i, i*) in each table represents the corresponding information when the participant stayed inside the same zone. The non-diagonal element (*i, j*) of the matrix represents a cycle from zone *i* to *j*.

Table 10 represents the count of traveling cycles among specific zones, which exposes the travel pattern of the participant. The travel pattern is determined by the layout of the experimental settings as well as the designed work plan. The values in the non-diagonal elements in Table 10 represent the frequency that that participant traveled

from the origin (row) to the destiny (column), and vice versa. To be noticed, the diagonal elements of the table have significantly greater value than the non-diagonal elements. The high value in the diagonal element in Table 10 does not mean that the participant entered and exited the same zone very often. Instead, the values in the diagonal elements of this table represent how many times the participant bends down to perform related work such as installation, de-installation, and picking up materials. In this experiment, the participant bends down 65 and 66 times to install materials in work zones A1 and A2, respectively. This participant stayed a total of three times ({R1, R1}=1 and {R2, R2}=2) in the rest zone to take breaks.

The graphical interpretation of Table 10 in Figure 75 is a bit more difficult. Table 10 shows that the participant travels from A2 to R2 once, but in Figure 75 the only path entering zone R2 is from A1. As a matter of fact, the participant starts traveling from A2, passes through A1, and eventually arrives at R2. Since the participant does not stop on the route and the algorithm computes a new cycle only when the participant changes kinematic status, passing through a zone without stopping will not be identified as an entering or exiting activity. Therefore, in this particular instance, the participant traveled from A2 to R2 and not from A1 to R2.

Table 10 Number of stays within one zone and number of travel cycles between zones.

Number of cycles [No.]	A1	A2	S1	S2	R1	R2
A1	65	3	12	43		
A2	3	66	12	35	1	1
S1	13	13	26			
S2	42	35	1	80		
R1		1			1	
R2						2

Table 11 and Table 12 represent the total and average duration of the trips that the participant made between zones. Similarly to Table 10, the diagonal elements have significantly greater value than the non-diagonal elements, since they represent the total time that the participant spent in each specific zone.

Table 11 Total time spent within a zone and traveling between two zones.

Total Time [MM:SS]	A1	A2	S1	S2	R1	R2
A1	15:25	00:28	01:42	02:40		
A2	00:29	14:26	00:46	04:15	00:12	29
S1	01:34	00:44	01:33			
S2	02:34	03:57	00:08	03:17		
R1		00:06			00:33	
R2						03:42

Table 12 Average time spent within a zone and traveling between two zones.

Avg. Time [MM:SS]	A1	A2	S1	S2	R1	R2
A1	00:14	00:09	00:08	00:04		
A2	00:09	00:14	00:04	00:07	00:12	00:29
S1	00:07	00:02	00:04			
S2	00:04	00:07	00:08	00:03		
R1		00:06			00:33	
R2						01:51

Table 13 and Table 14 list the total and average travel distances between zones. Non-diagonal elements that represent the movement between work zones and material zones such as {A1, S1} and {A1, S2} have relatively high values, which could be interpreted as long traveling distances. Since the zones are relatively small, these high values stem from small movements (e.g., small side steps back and forth) a worker performs inside a zone. Additional distance errors might be added from UWB reading accuracy (e.g., UWB tag positions on helmet might move more frequently than if installed on the worker's belt) and tag refresh rate (e.g., 60Hz vs. 1 Hz). Since the participant spends most of the time inside a zone in this experiment and UWB location data were collected at 15Hz, the cumulative measured travel distance inside a zone over a longer period is therefore higher than expected.

Table 13 Total traveling distance within a zone and between two zones.

Total Traveling Distance [m]	A1	A2	S1	S2	R1	R2
A1	279.25	33.65	105.77	132.82		
A2	32.26	254.14	33.04	259.86	6.65	20.35
S1	112.60	34.63	37.96			
S2	139.84	255.52	6.59	88.87		
R1		6.74			4.73	
R2						46.01

Table 14 Average traveling distance within a zone and between two zones.

Average Traveling Distance [m]	A1	A2	S1	S2	R1	R2
A1	4.30	11.22	8.81	3.09		
A2	10.75	3.85	2.75	7.42	6.65	20.35
S1	8.66	2.66	1.46			
S2	3.33	7.30	6.59	1.11		
R1		6.74			4.73	
R2						23.00

Table 15 Average traveling speed within a zone and between two zones.

Average Traveling Speed [m/s]	A1	A2	S1	S2	R1	R2
A1	0.37	1.19	1.06	0.87		
A2	1.14	0.36	0.74	1.03	0.53	0.69
S1	1.14	0.79	0.52			
S2	0.91	1.07	0.84	0.51		
R1		0.88			0.15	
R2						0.23

Table 15 shows the average travel speed of the participants during the experiment. The speeds on the diagonal elements of the table are significantly smaller that on the non-diagonal elements. The low speed is caused by the fact that the participants do not move very often inside specific zone when certain tasks such as direct work and material handling are conducted.

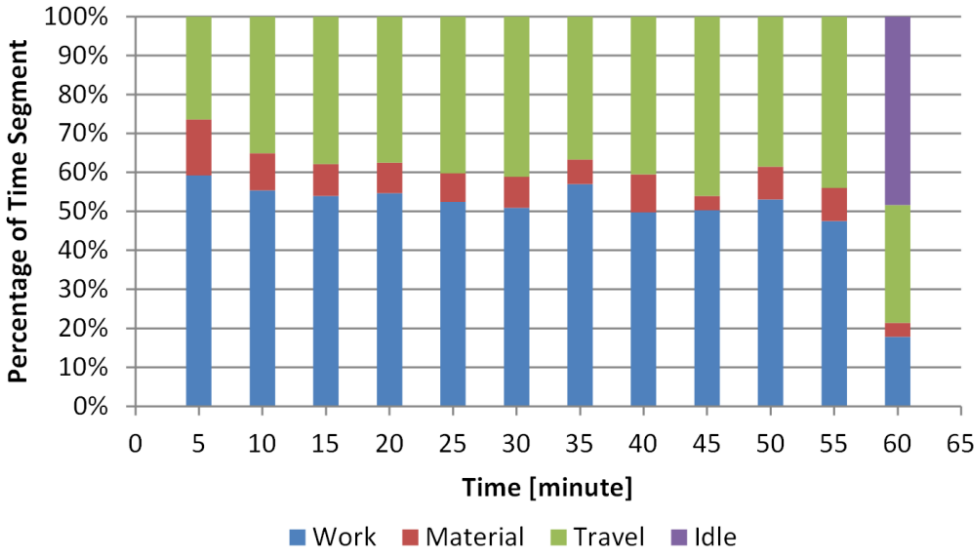

Figure 76 Result of automated work sampling for every 5 minutes (experiment 1, Participant 1).

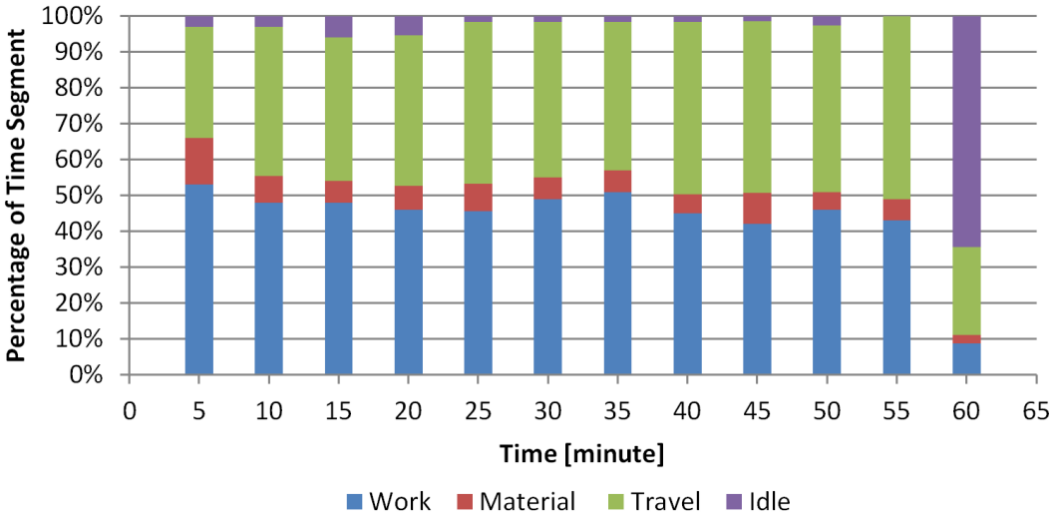

Figure 77 Result of manual work sampling (Experiment 1, Rater 1).

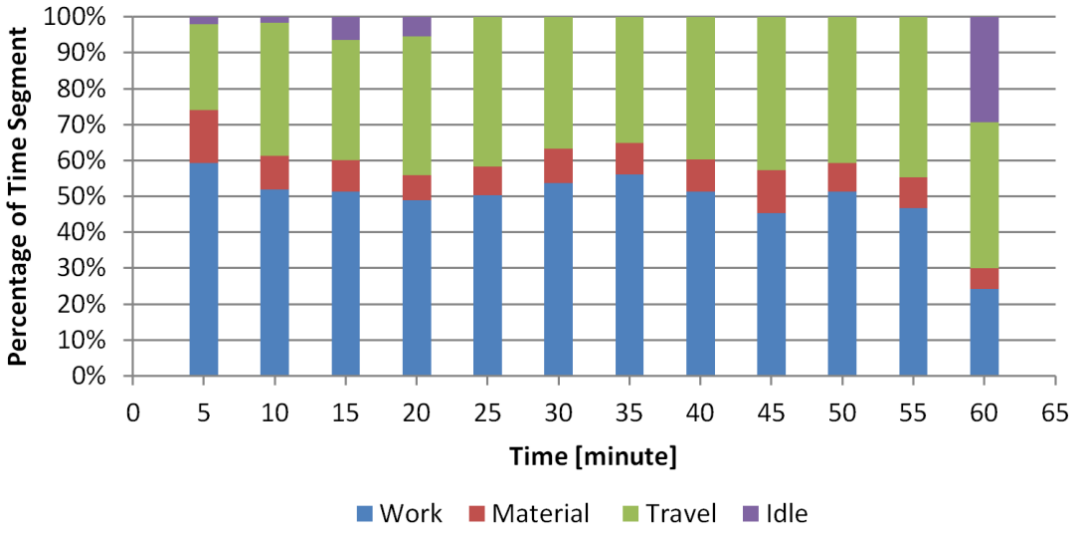

Figure 78 Result of manual work sampling (Experiment 1, Rater 2).

Results of the automated and manual activity analysis for experiment 1 are shown in Figure 76 to Figure 78. Table 16 presents the average difference and the standard deviation of the differences between the automated and manual activity analysis. The activity level of the participant is assessed every 5 minutes, which is represented by the ratio of direct work time to the observation time. In this experiment, the productivity level maintained at 50% for the most of the experimental period, and it decrease at the end of the experiment due finishing up the work and a longer rest.

Table 16 Average and standard deviation of the difference between automated and manual activity analysis (Experiment 1).

	Rater 1				Rater 2			
	Work	Material	Travel	Idle	Work	Material	Travel	Idle
Average difference	6.4%	1.3%	-4.0%	-3.7%	0.9%	-1.2%	-0.1%	0.3%
Stand. dev. of differences	2.0%	2.3%	3.7%	4.2%	3.4%	2.5%	4.1%	6.3%

Experiment No. 2

The same analysis method was repeated for the second experiment. The results to the second experiment are plotted and listed in Figure 79 to Figure 82 and Table 17 to

Table 22. In Figure 79, a user marked the initial work zones (B1, B2, and R2). The developed algorithm automatically identified two additional zones (Idle Zones 1 and 2) based on the trajectory analysis. Both of these two zones were clusters that corresponded to speeds of the participant that were slow. The convex hull to each of these zones is represented by a series of ordered nodes, while the consecutive nodes form a polygon. Entering the polygon triggered the data recording for the particular zone. In this particular case, the slow speed and no direct work activity in these zones indicate either a rest or idle zone. Manual analysis of the video recordings confirmed this observation.

No material handling activity was observed (see Figure 80). Since the work tasks of the participant is to de-install the concrete block from one work zone and use the same materials to install another concrete slab inside the other work zone, the algorithm determines both activities as productive work.

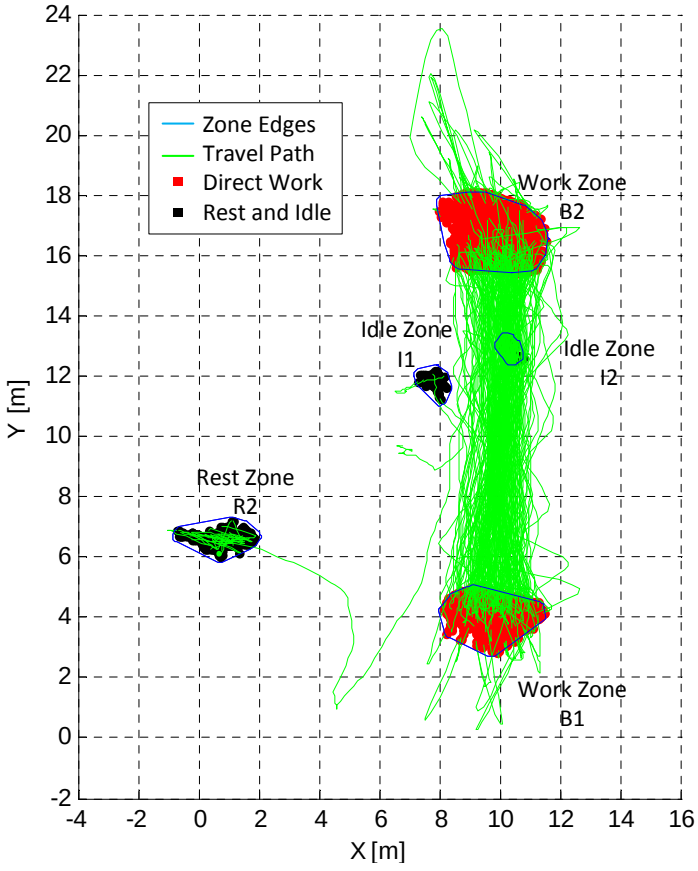

Figure 79 Experiment 2 – work zones and trajectories of travel cycles of the second participant.

Table 17 Number of stays within one zone and number of travel cycles between zones.

Number of cycles [No.]	B1	B2	R2	I1	I2
B1	108	98	1	1	
B2	98	118			1
R2			32		
I1	1			3	
I2	1				3

Table 18 Total time spent within a zone and traveling between two zones.

Total Time [MM:SS]	B1	B2	R2	I1	I2
B1	11:03	17:51	00:38	00:10	
B2	18:51	08:31			00:04
R2			02:23		
I1	00:07			00:53	
I2	00:13				00:21

Table 19 Average time spent within a zone and between two zones.

Avg. Time [MM:SS]	B1	B2	R2	I1	I2
B1	00:07	00:11	00:38	00:10	
B2	00:12	00:05			00:04
R2			00:05		
I1	00:07			00:18	
I2	00:13				00:07

Table 20 Total traveling distance within a zone and between two zones.

Total Traveling Distance [m]	B1	B2	R2	I1	I2
B1	218.81	1239.88	39.84	8.10	
B2	1224.03	261.43			3.34
R2			34.87		
I1	7.37			9.21	
I2	10.78				4.03

Table 21 Average traveling distance within a zone and between two zones.

Avg. Traveling Distance [m]	B1	B2	R2	I1	I2
B1	2.03	12.65	39.84	8.10	
B2	12.49	2.22			3.34
R2			1.09		
I1	7.37			3.07	
I2	10.78				1.34

Table 22 Average traveling speed within a zone and between two zones.

Avg. Traveling Speed [m/s]	B1	B2	R2	I1	I2
B1	0.52	1.15	1.05	0.86	
B2	1.08	0.62			0.97
R2			0.38		
I1	1.06			0.19	
I2	0.86				0.28

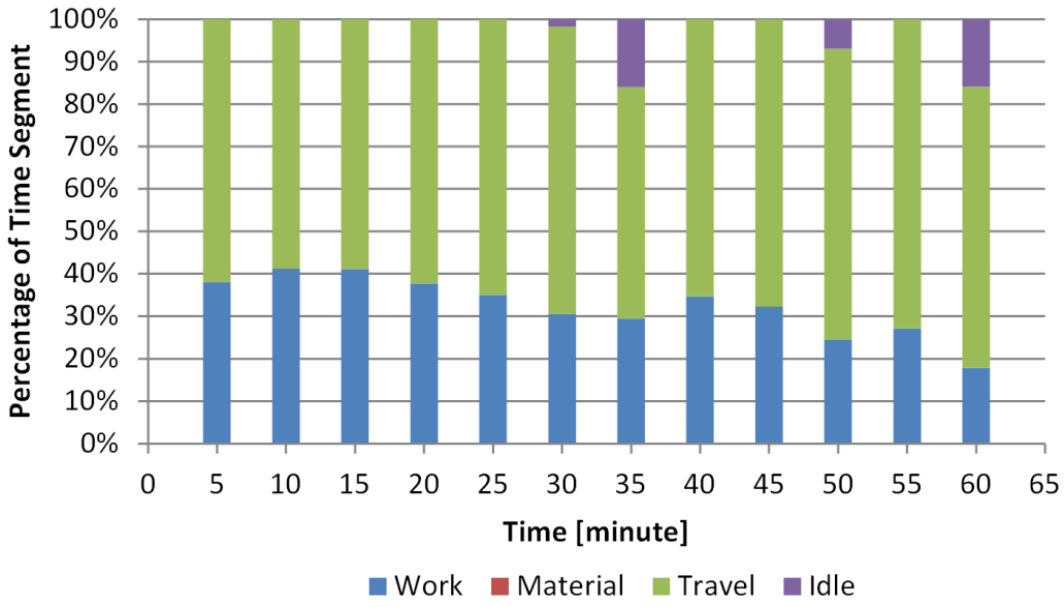

Figure 80 Result of automated work sampling for every 5 minutes (Experiment 2).

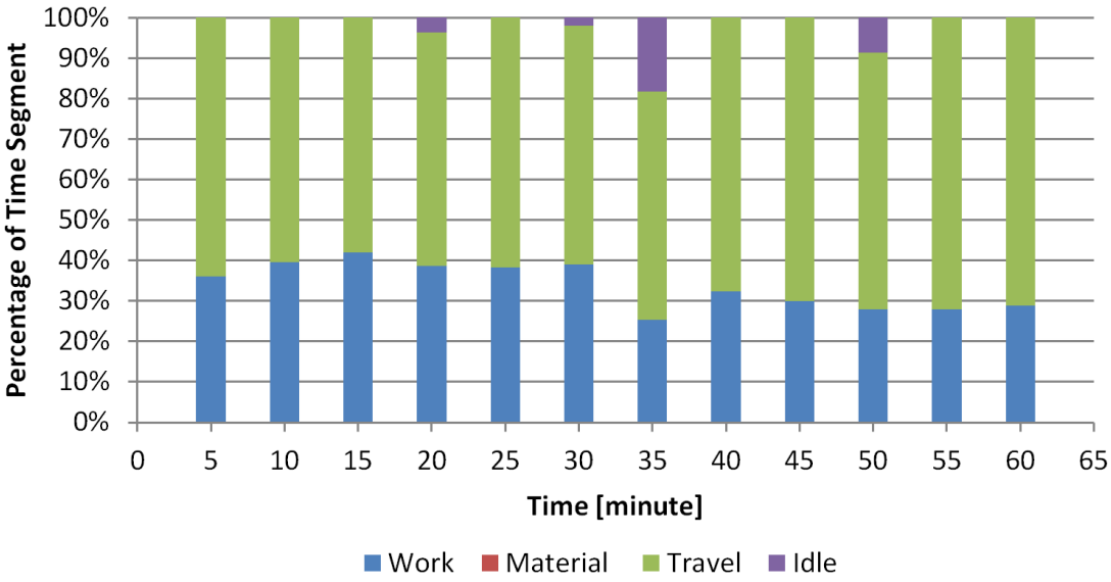

Figure 81 Result of manual work sampling (Experiment 2, Rater 1).

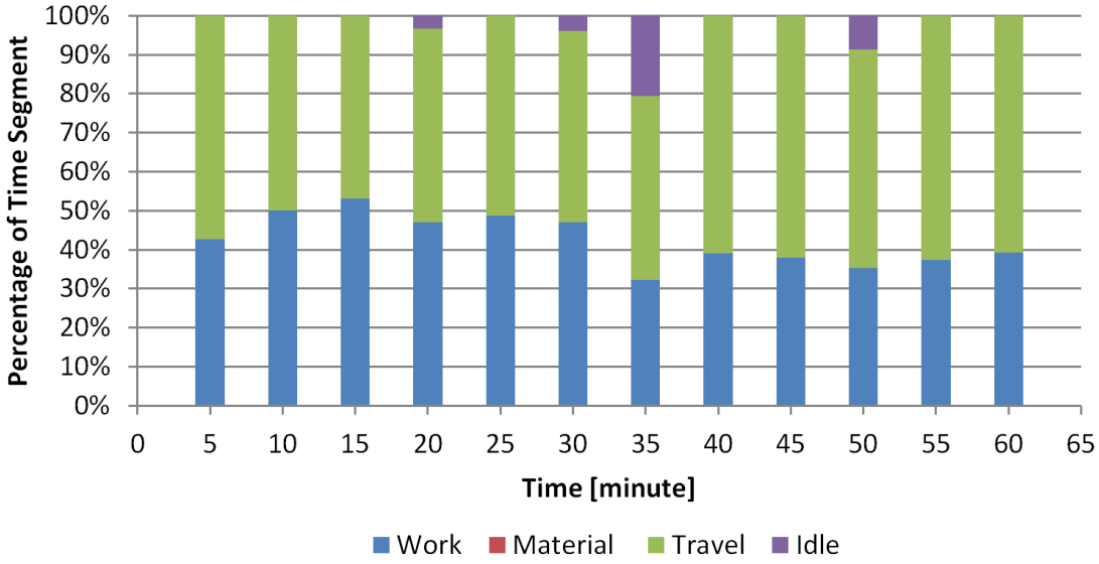

Figure 82 Result of manual work sampling (Experiment 2, Rater 2).

Table 23 Average difference and standard deviation of the differences between the automated and manual activity analysis (Experiment 2).

	Rater 1				Rater 2			
	Work	Material	Travel	Idle	Work	Material	Travel	Idle
Average difference	-1.4%	NA	0.7%	0.7%	-10.0%	NA	9.7%	0.3%
Stand. dev. of differences	4.6%	NA	4.0%	5.0%	5.4%	NA	4.4%	5.2%

Experiment No. 3

The results of the activities that were automatically detected of the two participants in the third experiment are plotted in Figure 83 and Figure 84. Two work zones (A2 and B2), three material zones (S1, S3, and S4), and four rest zones (R1 to R4) as well as the corresponding activities in and in between them were identified. The two participants worked as a team. While the first participant's duty was to de-install material from one work zone and deliver the material to the storage zones, the task of the second participant was to use the material available at the storage zones to install a floor system in another work zone.

Table 24 to Table 30 list and compare the statistics of the work cycle from both participants. Numbers to each participant are listed in the tables. Both participants were conducting activities simultaneously. Data analysis similar to the previous two experiments can be conducted.

Data in Table 24 show how often the participants stayed in a work zone. For example, Participant 1 stayed in A2 99 and in B2 115 times. Similar information can be generated to any of the zones.

Table 25 can be analyzed in the following way: Participant 1 spent less time inside a work zone, because the task was material removal (which was quick and easy to do). The time spent on traveling from one zone to another is therefore significantly higher than the ones of Participant 2. In contrast, Participant 2 who had to accurately install the floor material and had to be concerned of the quality of the

final product significantly spent more time in the work zones. For example, adding the values in

Table 25 for work zone A2 and B2 for Participants 1 and 2 equals to 11 minutes and 32 seconds and 32 minutes and 36 seconds, respectively. The travel time of Participant 1 to areas S1, S3, S4 equals 26 minutes and 31 seconds, while Participant 2 spent 10 minutes and 52 seconds traveling to the same areas. Other data in the table can be calculated and used for travel cycle analysis.

Table 26 to Table 29 relate to travel speed and distances within and to each zone. As previously explained, some values in these tables can become more useful for practitioners than others, e.g. in assessing work productivity, site layout, ergonomics analysis. Many more applications exist where such technology could be applied and become useful, e.g., how often do workers take (required) breaks.

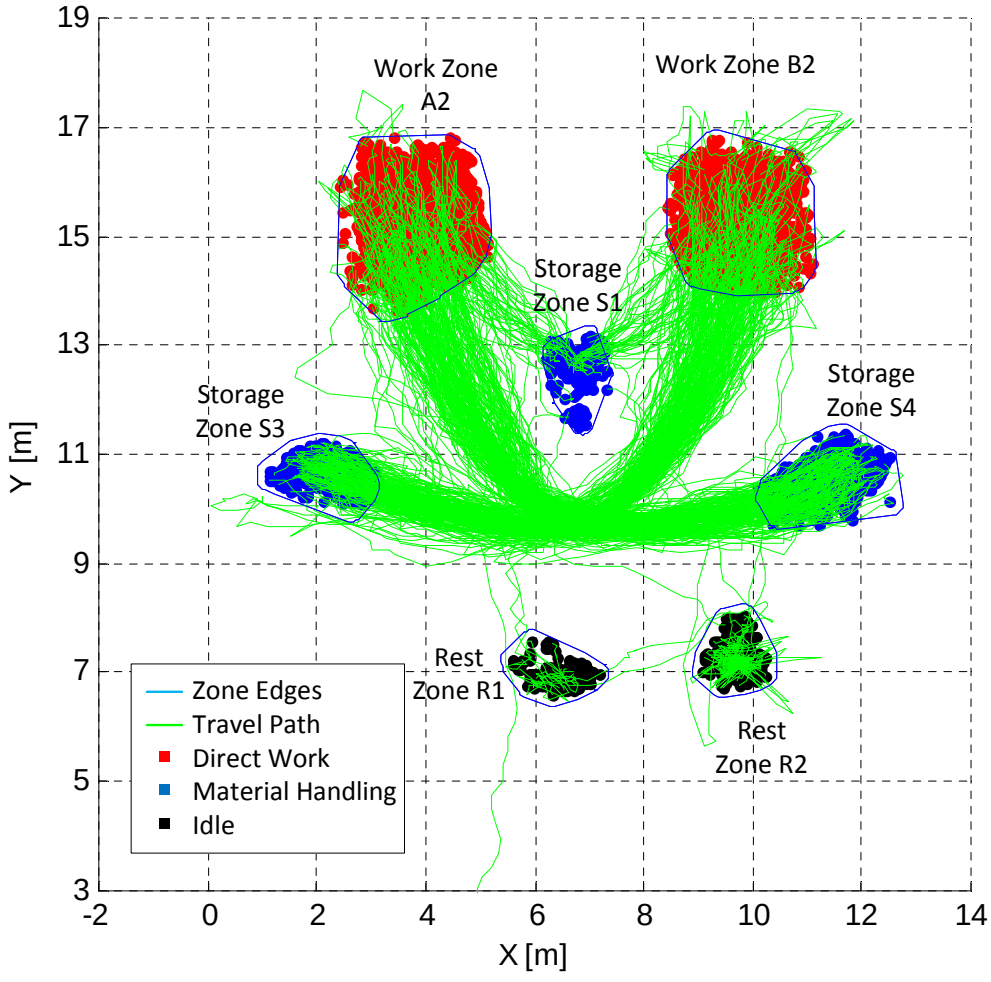

Figure 83 Experiment 3 – Work zones and trajectories of travel cycles of Participant 1.

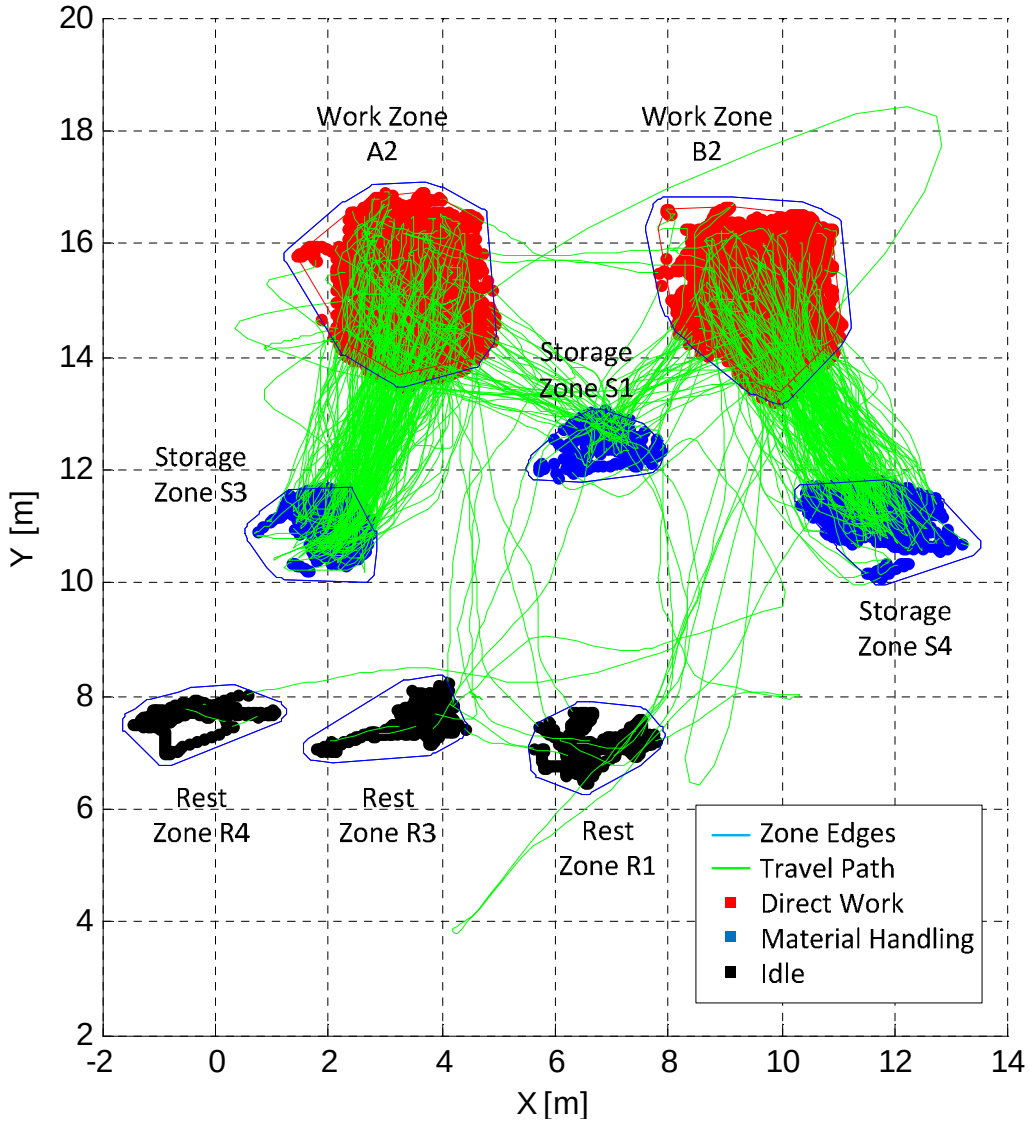

Figure 84 Experiment 3 – Work zones and trajectories of travel cycles of Participant 2.

Table 24 Number of stays in one zone and number of travel cycles between zones.

Number of Cycles [No.]		A2	B2	S1	S3	S4	R1	R2	R3	R4
A2	Participant 1	99		20		74				
	Participant 2	233		11	86		1		2	
B2	Participant 1		115	19	82					
	Participant 2	1	254	15		91			4	
S1	Participant 1	16	17	39	1	2	2	1		
	Participant 2	14	20	35						
S3	Participant 1		83		88			1		
	Participant 2	86			90					
S4	Participant 1	76			1	88				
	Participant 2		91			95				
R1	Participant 1						7	2		
	Participant 2			3			4			
R2	Participant 1	1	1			1		20		
	Participant 2									
R3	Participant 1									
	Participant 2			4			2		6	
R4	Participant 1									
	Participant 2			1						1

Table 25 Total time spent within a zone and traveling between two zones.

Total Time [MM:SS]		A2	B2	S1	S3	S4	R1	R2	R3	R4
A2	Participant 1	06:38		01:04		11:37				
	Participant 2	15:11		00:38	05:07		00:39		00:22	
B2	Participant 1		04:54	00:56	12:54					
	Participant 2	00:03	17:25	00:36		04:31			00:56	
S1	Participant 1	00:48	00:58	01:18	00:15	00:50	00:15	00:07		
	Participant 2	00:47	00:58	01:31						
S3	Participant 1		12:11		02:00			00:39		
	Participant 2	05:23			03:18					
S4	Participant 1	13:06			00:11	02:27				
	Participant 2		05:34			03:40				
R1	Participant 1						01:20	00:10		
	Participant 2			00:23			03:45			
R2	Participant 1	00:08	00:07			00:03		09:33		
	Participant 2									
R3	Participant 1									

	Participant 2			00:27			00:05		02:03	
R4	Participant 1									
	Participant 2			00:11						02:11

Table 26 Average time spent within a zone and traveling between two zones.

Avg. Time [MM:SS]		A2	B2	S1	S3	S4	R1	R2	R3	R4
A2	Participant 1	00:04		00:04		00:10				
	Participant 2	00:04		00:04	00:04		00:39		00:11	
B2	Participant 1		00:03	00:03	00:10					
	Participant 2	00:03	00:04	00:03		00:03			00:14	
S1	Participant 1	00:03	00:04	00:02	00:15	00:25	00:08	00:07		
	Participant 2	00:04	00:03	00:03						
S3	Participant 1		00:09		00:02			00:39		
	Participant 2	00:04			00:03					
S4	Participant 1	00:11			00:11	00:02				
	Participant 2		00:04			00:03				
R1	Participant 1						00:12	00:05		
	Participant 2			00:08			00:57			
R2	Participant 1	00:08	00:07			00:03		00:29		
	Participant 2									
R3	Participant 1									
	Participant 2			00:07			00:03		00:21	
R4	Participant 1									
	Participant 2			00:11						02:11

Table 27 Total traveling distance within a zone and between two zones.

Total. Traveling Distance [m]		A2	B2	S1	S3	S4	R1	R2	R3	R4
A2	Participant 1	269.81		69.12		933.20				
	Participant 2	454.93		37.44	311.98		22.65		17.29	
B2	Participant 1		297.85	60.83	1037.57					
	Participant 2	3.16	546.72	40.71		290.63			44.28	
S1	Participant 1	52.37	68.03	51.68	16.49	60.48	14.62	7.72		
	Participant 2	47.25	53.21	51.41						
S3	Participant 1		999.10		118.08			38.48		
	Participant 2	309.18			129.11					
S4	Participant 1	1057.24			17.12	139.21				
	Participant 2		332.32			150.14				
R1	Participant 1						31.70	10.16		
	Participant 2			23.11			47.86			
R2	Participant 1	9.22	7.49			3.84		200.71		
	Participant 2									

R3	Participant 1									
	Participant 2			28.19			3.83		27.80	
R4	Participant 1									
	Participant 2			11.29						25.85

Table 28 Average traveling distance within a zone and between two zones.

Avg. Traveling Distance [m]		A2	B2	S1	S3	S4	R1	R2	R3	R4
A2	Participant 1	2.73		3.46		12.61				
	Participant 2	1.95		3.40	3.63		22.65		8.65	
B2	Participant 1		2.59	3.20	12.65					
	Participant 2	3.16	2.15	2.71		3.19			11.07	
S1	Participant 1	3.27	4.00	1.33	16.49	30.24	7.31	7.72		
	Participant 2	3.38	2.66	1.47						
S3	Participant 1		12.04		1.34			38.48		
	Participant 2	3.60			1.43					
S4	Participant 1	13.91			17.12	1.58				
	Participant 2		3.65			1.58				
R1	Participant 1						4.53	5.08		
	Participant 2			7.70			11.96			
R2	Participant 1	9.22	7.49			3.84		10.04		
	Participant 2									
R3	Participant 1									
	Participant 2			7.05			1.92		4.63	
R4	Participant 1									
	Participant 2			11.29						25.85

Table 29 Average traveling speed within a zone and between two zones.

Avg. Traveling Speed [m/s]		A2	B2	S1	S3	S4	R1	R2	R3	R4
A2	Participant 1	1.08		1.10		1.35				
	Participant 2	0.58		1.01	1.08		0.59		0.81	
B2	Participant 1		1.19	1.12	1.34					
	Participant 2	1.04	0.65	1.20		1.20			0.89	
S1	Participant 1	1.10	1.18	0.80	1.13	1.20	1.00	1.23		
	Participant 2	1.04	0.94	0.62						
S3	Participant 1		1.37		1.04			1.00		
	Participant 2	1.00			0.72					
S4	Participant 1	1.36			1.68	1.01				
	Participant 2		1.11			0.75				
R1	Participant 1						0.47	1.01		
	Participant 2			0.99			0.22			
R2	Participant 1	1.26	1.14			1.28		0.41		

	Participant 2									
R3	Participant 1									
	Participant 2			1.05			0.78		0.25	
R4	Participant 1									
	Participant 2			1.08						0.20

Participant 1 took four breaks during the experiment (see Figure 85). The total resting time was over 7 minutes in a work task that took about 90 minutes. More than 70% of the time was spent on traveling since the participant's duty was to deliver materials to the storage areas that the second participant used. The direct work time rate was therefore significantly smaller than in any of the two previous experiments. Manual study of video material and in particular measuring the times the first participant was traveling confirmed this observation.

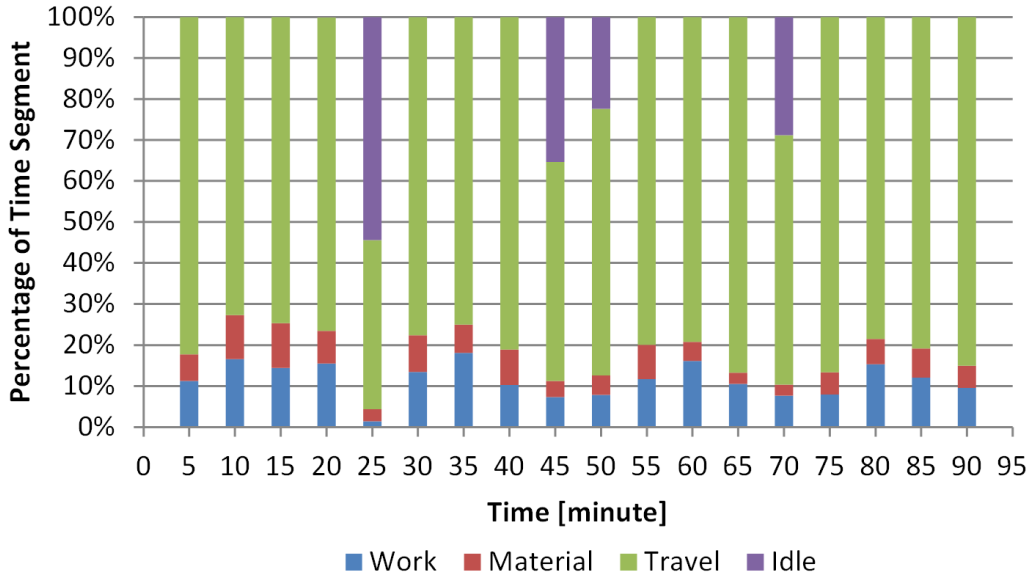

Figure 85 Result of automated work sampling for every 5 minutes (Experiment 3, Participant 1).

Figure 86 shows the direct work rate of Participant 2 in the same experiment. Since both participants were conducting the activities at the same time, a correlation of the productivity performance can be noticed by the comparing the results with the direct work time rate. At the beginning of this experiment, Participant 2 (installing material) had to wait more than 40% of the first time segment for his team member (Participant 1) to set up the materials. Participant 1 (de-installing material) took two breaks during the

20-25 and 76-70 minute time segments since limited materials were available for de-installation (or in other words, Participant 1 completed the first de-installation task within approximately 22 minutes). Based on the information in Figure 85 and Figure 86, Participant 2 had significantly more bending tasks to perform and took more frequently breaks. The reason is very likely the intense of the installation work that Participant 2 had to perform.

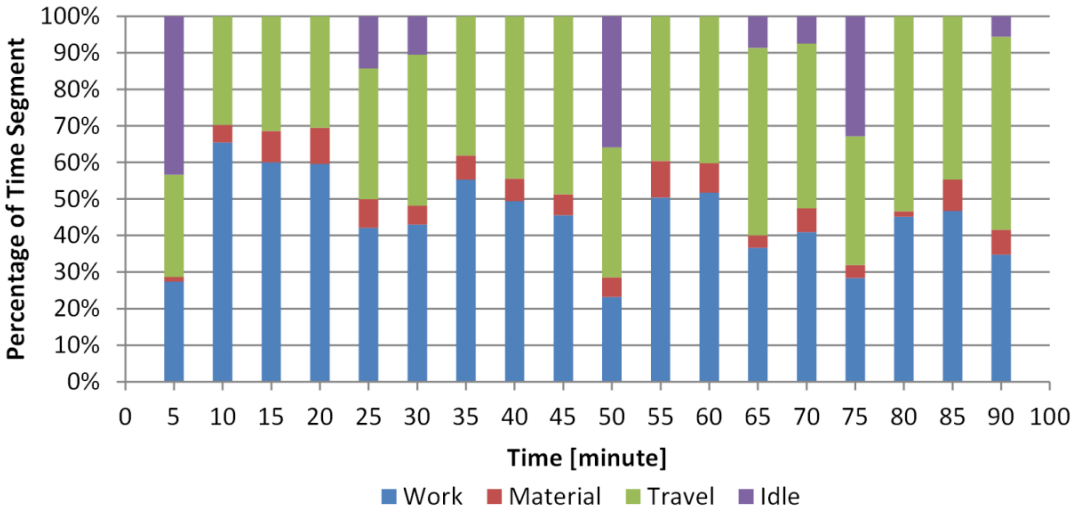

Figure 86 Result of automated work sampling for every 5 minutes (Experiment 3, participant 2).

Results of the manual activity analysis for Participant 1 and 2 are shown in Figure 87 to Figure 90. Table 30 and Table 31 present the average difference and the standard deviation of the differences between the automated and manual activity analysis.

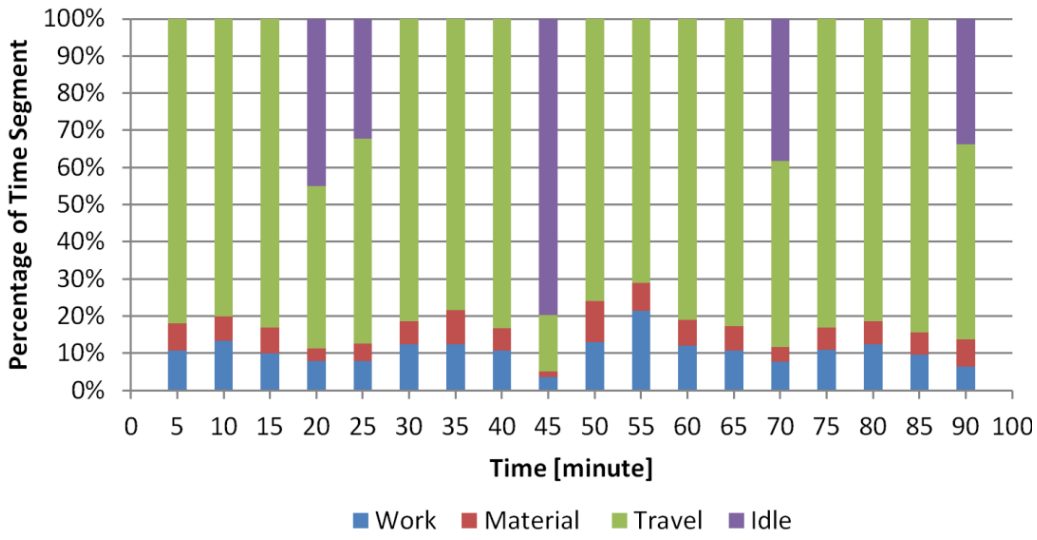

Figure 87 Result of manual work sampling (Experiment 3, Participant 1, Rater 1).

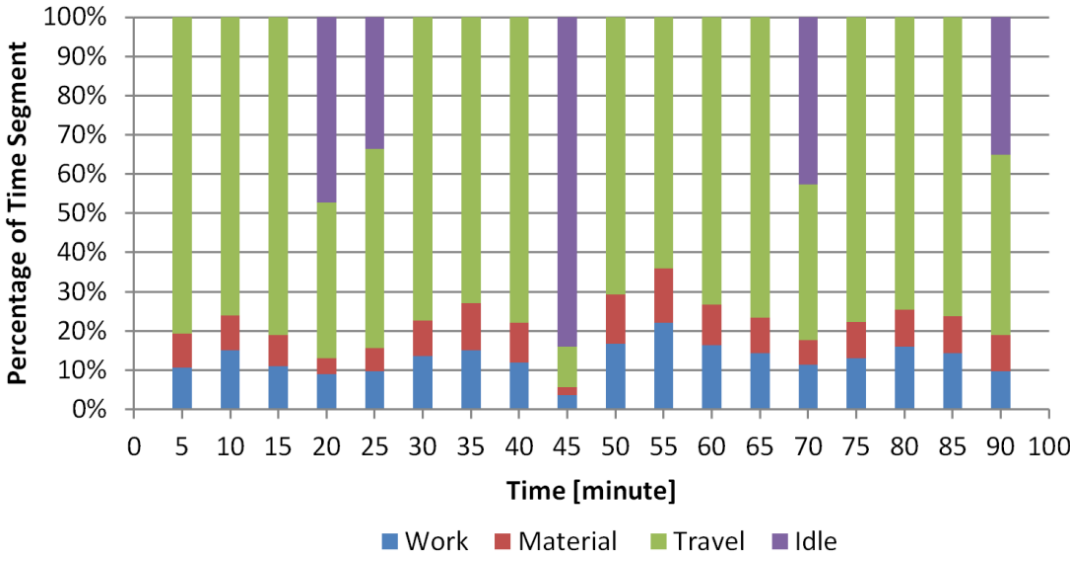

Figure 88 Result of manual work sampling (Experiment 3, Participant 1, Rater 2).

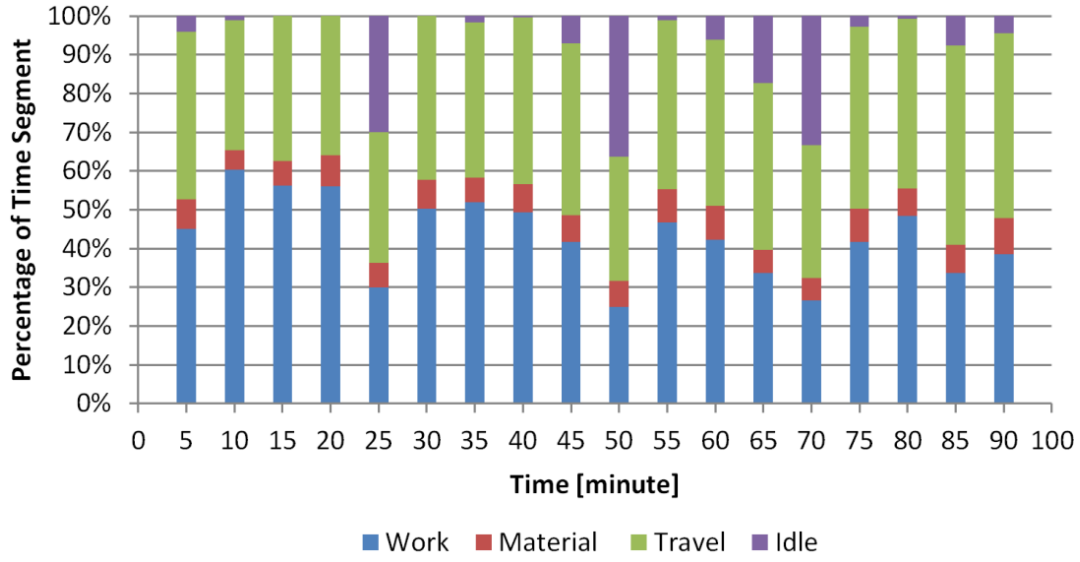

Figure 89 Result of manual work sampling (Experiment 3, Participant 2, Rater 1).

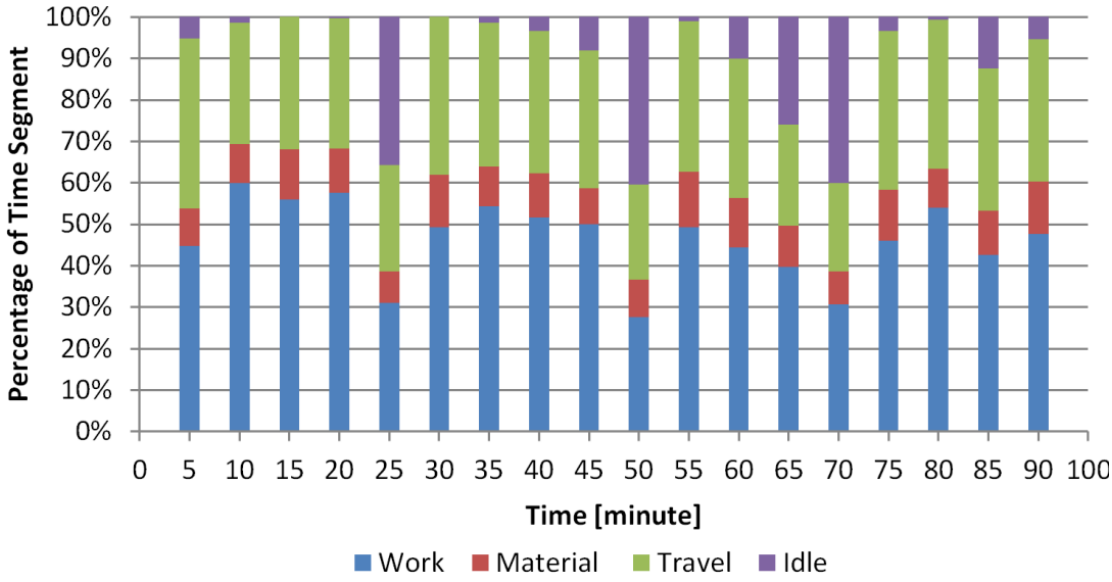

Figure 90 Result of manual work sampling (Experiment 3, Participant 2, Rater 2).

Table 30 Average and standard deviation of the differences between the automated and manual activity analysis (Experiment 3, Participant 1).

	Rater 1				Rater 2			
	Work	Material	Travel	Idle	Work	Material	Travel	Idle
Average	0.8%	0.0%	4.1%	-4.9%	-1.5%	-2.4%	9.5%	-5.6%

difference								
Stand. dev. of the differences	4.5%	3.0%	15.3%	18.4%	4.6%	3.4%	15.8%	19.4%

Table 31 Average and standard deviation of the differences between the automated and manual activity analysis (Experiment 3, Participant 2).

	Rater 1				Rater 2			
	Work	Material	Travel	Idle	Work	Material	Travel	Idle
Average difference	1.5%	-1.1%	-0.8%	0.3%	-1.7%	-4.3%	8.0%	-2.0%
Stand. dev. of the differences	8.5%	2.6%	7.1%	14.8%	8.6%	2.6%	10.1%	16.3%

8.7 Conclusions

Previous research has found that remote and rapid sensing such as Ultra Wideband (UWB) and Physiological Status Monitoring (PSM) technology can effectively facilitate automatic monitoring of the position, posture, and physiological status of construction personnel. However, these technologies have not been used to improve productivity and activity assessment. Potentially, data from these sensing technologies can be integrated with the goal of achieving a higher level of knowledge of work productivity and activity performance. This paper describes results of a study that was designed to test the capabilities and benefit of fusing the data from these sensors. Using a set of experiments conducted in an indoor facility at the University of Washington, this paper demonstrated that UWB and PSM data can be fused to automatically identify the dynamic zones associated to the work activities as well as to categorize the work activities for the purpose of activity assessment.

The results show that current technology is satisfactorily reliable in autonomously and remotely monitoring participants during simulated construction activities. In addition, the authors have found that data from various sensing sources can be successfully fused to augment real-time knowledge of construction activity (and potentially productivity) assessment, which would reduce, if not avoid, the shortcomings of traditional visual observation and estimation of productivity rates. The output of the proposed approach could be used by contractors to evaluate the maximum actual production against the

planned production as a way to automatize project control functions and perform true real-time “productivity and activity assessment”. The real-time productivity and activity assessment will enable project managers to accurately determine the progress of construction operations and easily share the information with all project parties.

Nevertheless, at this time, the proposed approach is only able to estimate the upper boundary of the actual activity due to technological constraints, such that the fusion of the location tracking data and thoracic posture data are not able to provide accurate information of activity details. Moreover, the approach is currently more oriented to assess the labor activity that is involved in repetitive work tasks such as assembling work in prefabrication shops. To ensure accurate and rapid spatio-temporal data collection a more sophisticated sensor infrastructure setting is required for large deployment on a construction site. In summary, the presented work has shown the potential of technologies lies in the integration of various technology-specific data sources. While technology manufactures are quickly improving the level of integration and the richness of data collected, research as the one described in this paper advances knowledge of data fusion for construction applications.

CHAPTER IX

DATA VISUALIZATION FOR CONSTRUCTION SAFETY AND ACTIVITY MONITORING APPLICATIONS

Data on construction resources (personnel, equipment, materials) as they operate in the field are vast, but the effort to collect, analyze, and visualize even parts of it is hardly taken. Considering how well the quality of decision making can be improved once real-time data collection, processing, and visualization technology become available, the use of any such enabling technology becomes a priority, especially in construction-related resource intensive operations. Although recent developments in remote data sensing and intelligent data processing have been made to supplement manual data recording and analyses practices, few data visualization tools in construction exist that accept data from dynamic resources and stream it to a field-realistic real-time virtual reality environment. This chapter presents a new framework that focuses on streaming data from real-time remote location sensing technology to a real-time data visualization platform. Results demonstrate that some important construction information related to both safety and activity in field operations can be automatically monitored and visualized in real-time, thus offering benefits such as increased situational awareness to workers, equipment operators, or decision makers anywhere in the field or world.

9.1 Introduction

The distributed nature of construction project information and the presence of multiple teams performing on site are well known characteristics of a typical construction project. Communication of essential information among construction project stakeholders is considered a key for successful construction engineering and management. Traditionally, an enormous amount of site information has been communicated among project team members by means of paper-based documents including two-dimensional drawings or verbal communication. A significant deficiency in the traditional information

delivery process has been that the project team is not always in the position to make rapid and correct decisions because of unavailable or insufficient information [234].

For the purpose of making more timely and more accurate decision during construction, at multiple timescales, and for multiple entities, a deeper understanding of construction activity information is needed in real-time and additionally in a visually appealing format. In addition, it is believed that a more effective use of gathered and distributed real-time site information would generate new knowledge that can assist project stakeholders in making more effective and efficient decisions on-site or even from a remote location [146].

Important site information such as the location of construction resources (personnel, equipment and materials), including their inter-relationships and temporal information on specific work tasks, is currently mostly manually monitored and recorded [146]. Such observation tasks require typically experienced observers but many observations remain error prone as they are very labor intensive and subjective. Moreover, manual observations are made through the viewpoint of the observer and the particular perspective can often not be shared with a project team in or near real-time. These are some limitations of current practices that can become a bottleneck for fast and accurate decision making on a busy construction site. Especially, large capital facility projects require more oversight, and one of the primary application areas is safety and construction site monitoring.

Effective construction safety and site monitoring start at the front-end of a project. Several approaches have been taken in the past to coordinate design and planning of construction with site organization and layout. One way of finding potential clashes or hazards is using walkthroughs in virtual reality (VR) models. VR is a method of visualization, aligning the virtual objects with the real world. Many applications of VR technology have been found in building science covering both project design and construction operation levels. Immersive VR systems also have wide applications in practice and education of architects, engineers, and contractors who deal with design and construction of buildings. The main reason of its rising implementation is that immersive VR has the unique capability of giving users a sense of presence and scale, as if they

were observing a realistic world. By immersing the user in a computer generated synthetic environment, VR learning and training offers an active learning experience where the user is in control and is required to deliberate proper actions. VR also facilitates the understanding of complex construction processes by the interaction within the VR environment [235].

Tracking and visualizing dynamic resource data in a field-realistic virtual environment in real-time has additional benefits to a project team [146]. For instance, spatial constraints of a work environment, workers themselves, and their safety behavior can be improved once their inter-related risks have been identified and are assessed properly. Such risks often have the origin in the motivation to achieve higher levels of productivity that pushes workers to work 'near the edge' and beyond the zone of control or recovery [210]. One alternative is to prevent putting workers in such risky environments by educating and training designers or planners at the front-end of projects [114]. As they can eliminate most hazards before workers are sent into the field to carry out work tasks, it would be useful for them to have information available what impact design has on hazards. Monitoring equipment and workers in a design model may give further conclusion on how to design or plan construction work more safely. Most importantly real-time safety data visualization will benefit safety engineers and managers to react in real-time to an accident, and even coordinate search and rescue efforts more effectively. Another potential benefit of real-time data gathering and visualization is that data can be documented and used afterwards to establish more efficient and effective safety best practices, education, and training methods.

This paper focuses on one of the key research challenges in real-time pro-active construction safety and site activity monitoring: Gathering and processing construction resource data in real-time and visualizing relevant safety and activity performance information to a decision maker in real-time. After a literature review, remote sensing and visualization technologies are introduced that monitor, record, and visualize safety-critical data of construction resources (personnel, equipment, and materials) in real-time and within a realistic and rapid virtual immersive visualization environment. The developed framework and results to case studies follow before the paper finishes with a conclusion and an outlook for future research.

9.2 Background in Data Visualization Technology

Many efforts have implemented virtual environments for the purpose of visualizing architectural designs and facilitating building construction and project management level. The use of virtual mockups to replace existing physical models by developing a virtual reality (VR) environment for a courthouse project was investigated by [236]. Another study was conducted to describe the barriers that impact the practical implementation of VR, such as management support, degree of business competition, coordination of design resources and participation of end users [237]. An immersive large scale VR projection system was developed for students in the architectural engineering program in order to experience and experiment with three-dimensional (3D), full scale virtual models of construction projects [238]. VR applications were also used in an architectural design studio to coordinate and critique student work within a collaborative virtual environment (CVE) [239][240]. A Virtual Reality Modeling Language (VRML) [241] was developed to represent the steel structure and construction equipment with online project information access.

Visualization technology has been a widely applied tool even in construction management. Virtual construction allows stakeholders to detect and inspect construction problems early in the design phase and enables contractors to manage projects more efficiently [242][243][244][245]. 4D graphics for construction planning and site utilization were developed to assist planners to deal with daily activities and site management [109][246]. Researcher also worked on site layout optimization [109]. It is suggested that a 4D VR model increases the comprehensibility of the project schedule and allows users to detect potential problems such as scheduling conflicts prior to the construction [243]. They have suggested that the planner using 4D simulation is likely to allocate resources more effectively. The use of 4D CAD also assists the planner in avoiding schedule conflicts, examining constraints, and evaluating alternative construction methods.

As the literature review shows, most of the recent research focused on cost, scheduling, and the extent of architectural design. VR technologies have since then been implemented successfully in Building Information Models (BIM) and resulted in

significant cost savings in particular when applied to complex projects. To date, there is little VR research focusing on factors such as real-time pro-active safety and activity monitoring, or any analysis that focuses on the construction task level. Few have so far addressed adequate real-time data visualization and use of it. As other research literature states “a clear agenda for use of real-time construction site data collection visualization is missing” [146].

Real-time safety hazard recognition, reporting, and visualization prompted researchers to investigate these topics at the earliest possible stage in the construction process [51]. Traditional safety hazard identification in construction has been using a combination of site drawings and project schedules. Up to today, very often decisions are being made based on visual site inspection(s). Since field drawings are mostly in 2D, safety managers have often difficulty understanding the spatial constraints in the environment [247]. The application of VR has so far not been very common at the construction task level since most VR models are based on simulated data or prerecorded data. Such models or data cannot represent or reproduce the changing nature of a construction site. In addition, existing VR tools require expert knowledge to handle and customize the intensive graphical and dynamic characteristics of construction task modeling [248]. Immersive VR at the operational level also focuses on displaying resources (personnel, equipment, materials, terrain, building objects) over time. Researchers formalized a descriptive language to facilitate automated communication of simulated dynamic construction scenarios that can visualize construction operations in a 3D virtual environment [249]. They also developed dynamic 3D visualization and simulation of articulated construction equipment, such as a crane or excavator, by using the principles of forward and inverse kinematics [250]. Their research proposed an approach to achieve smooth, continuous motion of virtual construction resources based on discrete and simulated information. Recent research investigated the generic and scalable techniques to accurately represent 3D motion paths in dynamic animation of operations simulated using discrete-event simulation by using the VITASCOPE visualization system [251]. Others presented accurate and high-speed animation of simulated models [252].

Apart from the implementation in the engineering practice, many efforts have been invested in the application of information technology especially advanced VR and VE technologies in building science education such as school teaching and learning. Researcher studied the use of digital imagery and visualization materials to improve student understanding and assessment of civil and building engineering by applying distributed performance support systems of construction events in the form of a visualized electronic course [253]. Others evaluated the impact of multimedia-based education on students and found that visualized, self-paced learning offers distinct advantages over traditional, instructor-led classroom learning [254]. However, these early adoptions of VR in education utilized simulated data in a simulated environment. A similar simulated but immersive VR environment was created by for construction training and education [255]. This effort shows that a real-time visualization can enhance the memory retention and increase the learning gains of the trainees of learners. Other researchers developed an attribute-based risk analysis method to help designers and preconstruction planner to identify potential struck-by hazards in the building models [256]. A preliminary safety rule checker system was developed to automatically visualize and identify fall hazards in the existing Building Information Models (BIM) [114].

Besides the construction industry and education disciplines, VR and VE have already been widely used in other engineering fields. An application of VR tools was introduced that integrated near-real-time visualization with publish and subscribe mechanisms to achieve remote monitoring and control of dynamic objects in underwater construction and maintenance operations [257]. They created a virtual training system as an integrated system consisting of a training visualization suite, an interface model, and instruction module [258]. Fully immersive training environments for the manufacturing industry have received some initial attention.

In summary, one of the important challenges of (immersive) VR lies in the integration of realistic and real-time field data. Along with spatial information of the as-built scene, such gathered data sets can become, once filtered for errors and processed to become information, very valuable input parameters for VR environments. Tracking a dynamic object's 3D position accurately and recognizing orientation is crucial for any real-time VR applications [259]. Sensing technologies such as Radio Frequency

Identification (RFID) in combination with Global Positioning Systems (GPS) or Ultra Wideband (UWB) are able to provide unique spatio-temporal information to construction resource locations [60][258]. Each of the tracking technologies comes with unique advantages and limitations that have already been recognized [146].

9.3 Methodology

The main research objective was to create technology that increases the situational awareness for construction site stakeholders of dynamic construction site operations. The application was safety in outdoor and indoor construction site environments. The research scope was limited to explore the potential of the developed technology and to see what application it can have on workers-on-the-ground who work nearby heavy equipment. In order to accomplish this objective, one of the selected research methods was to collect live field data of dynamic construction resources, filter it for errors and process it, and finally stream in real-time valuable safety information to an immersive virtual reality world that represents the accurate construction site. The assumption was that any project stakeholder (equipment operator, worker on the ground, safety control command) with access rights and who could view live and processed field data in an immersive VR could make more informed decisions in shorter times and at lower cost.

To accomplish the research goals, an accurate spatial world of the construction environment (e.g. site layout and terrain) was created using commercially-available laser scanning and modeling techniques. The immersive VR world then integrated data from real-time location tracking sensors (GPS and/or UWB) that collected trajectory data of resources present within the construction site. A user was then able to create safety rules [5]. And based on the information output, the user can see and observe results, and even interact within the immersive world but from a safe distance.

This research integrated some of the emerging remote sensing technology that is capable of collecting live field data from construction resources and a real-time visualization technology that produces accurate and timely information for distributed decision makers (stakeholders at all project levels, from workers, to equipment operators, to engineers on site, management and ownership off-site). The proposed technical

solution consisted of four central research phases: (1) data collection, (2) data processing, (3) information visualization, and (4) decision making and application in the field, education, and training.

Since different types of information are required by various stakeholders, proper selection of data gathering technologies can solve their demands. Based on data from [34], the scope of this research was limited to proximity issues between construction workers-on-the-ground and nearby heavy equipment.

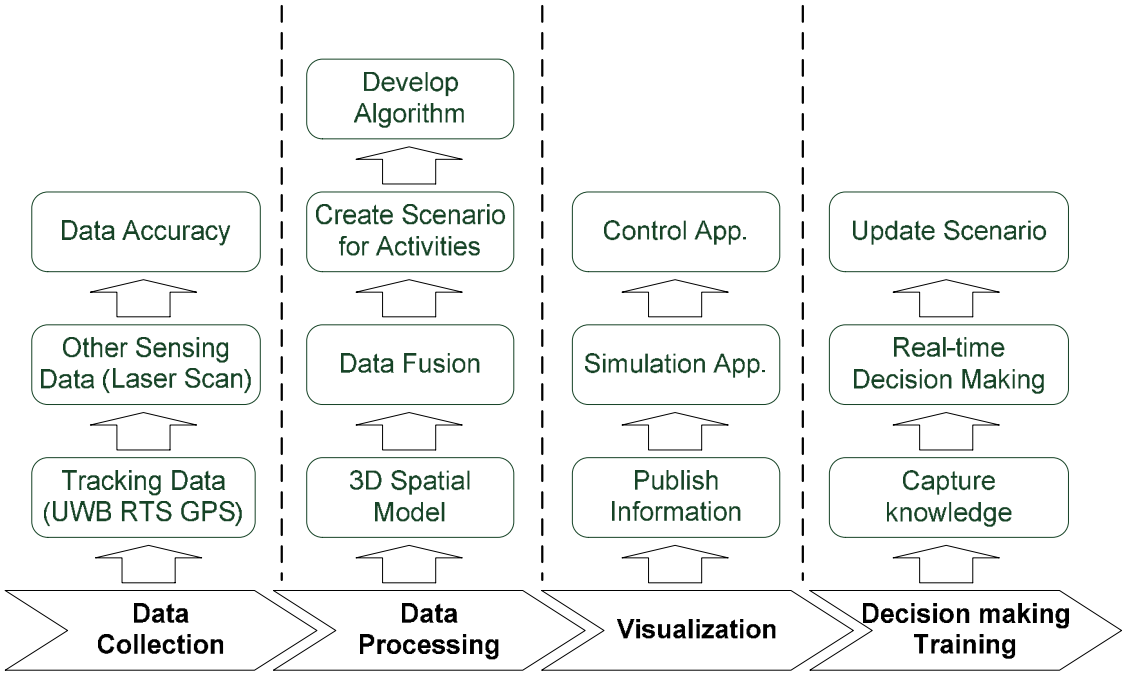

Figure 91 Flowchart of real-time data visualization.

As shown in Figure 91, raw data were collected using commercially-available location tracking sensors. Aspects to accuracy and implementation are further detailed in. The gathered spatial and temporal trajectory attributes to each of the resources in the field had to be processed before they were delivered in the form of an information package to a decision maker. At the same time the data were geospatially referenced to a terrain model that was created using commercially-available modeling software. Especially in construction applications such as safety and health, real-time feedback is necessary. Since the scope was limited to investigate initially only proximity issues of resources, real-time data acquisition and processing included a basic rule set that a user had to provide before

any information could be visualized. In this case, too close proximity of any two resources was defined as being closer than a few meters to the hazard. A hazard was defined as a worker being too close to equipment or below a load that was lifted. Further alarms or alerts were visualized in the VR should any of the pre-defined proximity events take place. Data were recorded and could be replayed at any time, which is especially useful in education and training settings. Real-time data visualization was the integral part of the research. It has the function of building a rich and realistic VR model that can visualize the extracted information. With the help of robust data distribution, stakeholders can make their decision in an interactive immersive 3D environment.

9.3.1 Real-time Location Tracking of Resources

There is immense interest and potential in systems that provide users the location of project critical resources (workforce, equipment, materials). Knowing the location of construction resources and identifying and measuring the status of work tasks helps to improve the project (safety) performance. Several real-time sensing technologies such as GPS, UWB, and vision tracking can be implemented to collected 3D/4D (spatio-temporal) data. However, in most construction tasks, data are scattered across several systems, many of which are isolated from each other. High deviated choices of sensor technologies make the data consolidation and data fusion a challenge. One alternative is to apply a protocol that adapts to any data stream. Another alternative is to constrain the input data into a uniformed data pattern even if it comes from different sources, including databases.

The scope of this research was limited to only one real-time data source from a specific tracking technology. Although any of the mentioned tracking technologies could have been selected to monitor the trajectories of construction resources, a technology that is capable of studying the location of workers, equipment, and materials at the same time and at high update rates was preferred. Preference was mainly given to a technology that is small in size and can be worn by workers, is rugged, and reliable enough to withstand a harsh construction environment, and is capable of accurately and precisely recording the activities that are associated to the selected work task: material handling.

In addition, most of the raw data the sensor collected contains noise that must be filtered for errors. Furthermore, the performance of the selected technology was impacted

by the complex environment of the jobsite. The authors applied techniques they have developed in [146].

9.3.2 Visualization in Virtual Reality (VR) World

The VR world applied in this paper uses an efficient data structure called "world data model". It consists of a list of entities and properties designed to represent their real-world counterparts. The entities are the basic element of the virtual world, which involves scene, surfaces, light, objects, cameras, properties, relations and labels.

The scene in visualization tools is a collect of interfaces and modular components that define the elements of a virtual environment. Examples are surface, static and dynamic objects, cameras, lights, and indicators. The surface and static objects are reproduced based on the application of surveying technologies. Laser scanning was used in the survey of the construction site. The collected range point clouds were converted to a triangular mesh. The surface is therefore represented by rendered polygons.

The survey of site surface and static objects was accomplished by a set of scans. Each scan will create an individual scan world which contains a large number of point clouds. Since every scan world has a unique coordinate system, a registration process is implemented which connects a set of scan worlds into a uniformed coordination, called a project's scan world. The integration is derived by a set of constraints, e.g. pairs of equivalent tie-points or overlapping point clouds that exist in both scan worlds. The registration process computes the optimal overall alignment transformations for each scan world. The registration is complete when constraints are matched as closely as possible. Even though the point clouds are coordinated, the registered scan world still contains several point clouds from scan worlds. Triangular meshes cannot be created across different point clouds. Therefore, the point clouds from each scan are unified into one single point clouds through a unification process. In addition, some features on the surface such as edges and corners have to be preserved when a triangle mesh is created. Therefore, several polylines termed "breakline" are implemented to represent a curb on the edge between different surfaces (see Figure 92). Breaklines assist in the generation and decimation of the mesh in that they will preserve geometric features. Based on specified breaklines and unified point clouds, a TIN mesh is generated where there are no

overlapping triangles with respect to the vertical direction. In sum, a surface model was produced by rendering the TIN mesh that was built from point clouds.

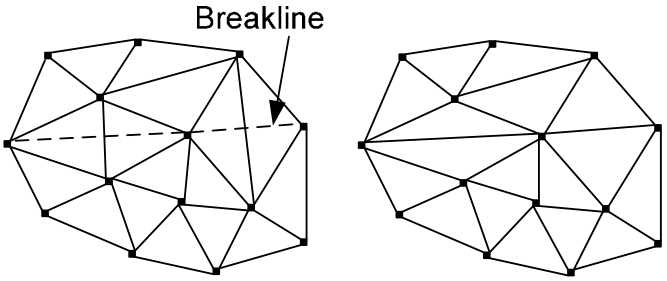

Figure 92 Breakline on point clouds.

Another feature of most virtual environments is lighting. Light is not always constant in the real world, but in simulated environments it is often directional. Spot and/or conical lights are widely implemented to represent light in VR tools.

Objects in VR are commonly created using CAD geometry or basic shapes. Examples can be cubes, cylinders, spheres, and cones. Complex objects are represented by using level of details (LODs), whose definition consists of several geometry descriptions with different levels of detail. Therefore, they are sensitive to proximity of the viewing camera (perspective of the VR user).

The viewing camera module defines various viewing points in the scene that responds to several input devices. A virtual camera can be attached to any moving objects to provide multiple vantage points. Relations are applied to connect entities in the scene, which represent the interdependency between elements existing in the real world. Several viewing cameras can be applied in a scene. An example is the distance between two objects or a projected distance between an object and a surface. Applied scenarios are watching from inside of an equipment cabin, through the eyes of a ground worker or virtual perspectives such as fly-through.

The properties of dynamic objects are updated through a data server which receives real-time data from the sensing technology. The data are bond to the various properties of objects to be visualized. However, most relevant information is not explicitly defined in the original data source. Location-characteristic information of

tracking data from construction resources (people, equipment, materials) including velocity, orientation, proximity of two or more resources and the frequency that resources interact with each other, can be derived from location tracking data. The velocity vector (direction, orientation, and speed) of resources is calculated through the comparison of its current and previous location or if multiple sensor tags are deployed on a single resource. The orientation of object is typically determined via multiple sensor tags placed on the resource.

A label visualizes the result of an algorithm that process data to information. An example related to the scope of the research (proximity) is computing the relation of a distance between several dynamic objects and simulating the equipment and its subcomponents. Compared to raw data, the derived information is more valuable for the stakeholders to make effective decision. Specific algorithms can be defined by a user and are discussed later.

A more detailed view of the architecture of the developed real-time tracking and visualization system is shown in Figure 93.

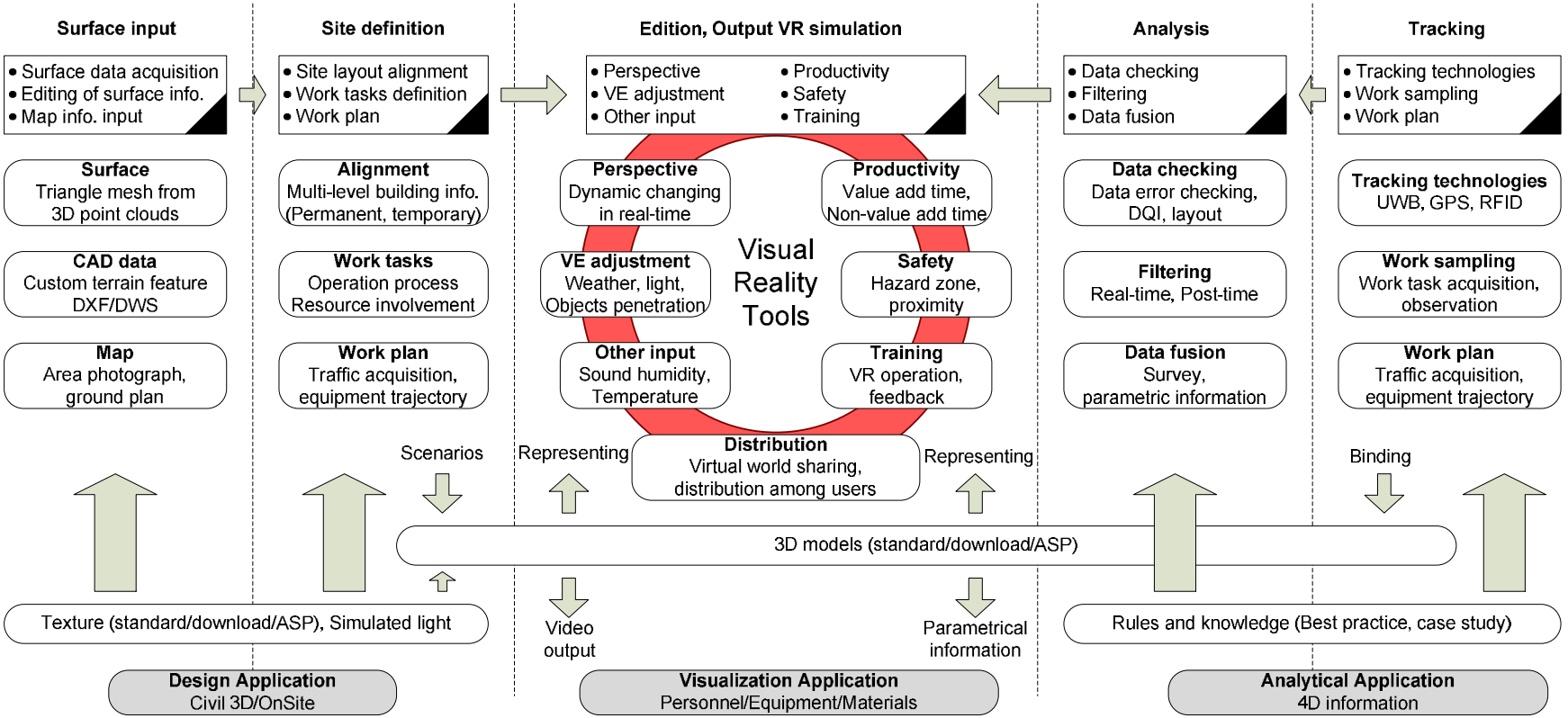

Figure 93 Architecture of real-time data tracking and visualization.

9.3.3 Real-time Data Distribution

In order to satisfy the information requirement of distributed project team, relevant information must be delivered not only to a local server but preferably must also be visualized on a remotely located 3D viewer. It requires that the data server of the proposed visualization system has not only the mechanism of data subscribing and publishing but also takes advantage of the currently available internet and intranet infrastructure. Figure 94 shows the developed architecture of data collection, distribution, processing, and visualization. All local information can be shared with multiple users via internet or intranet access.

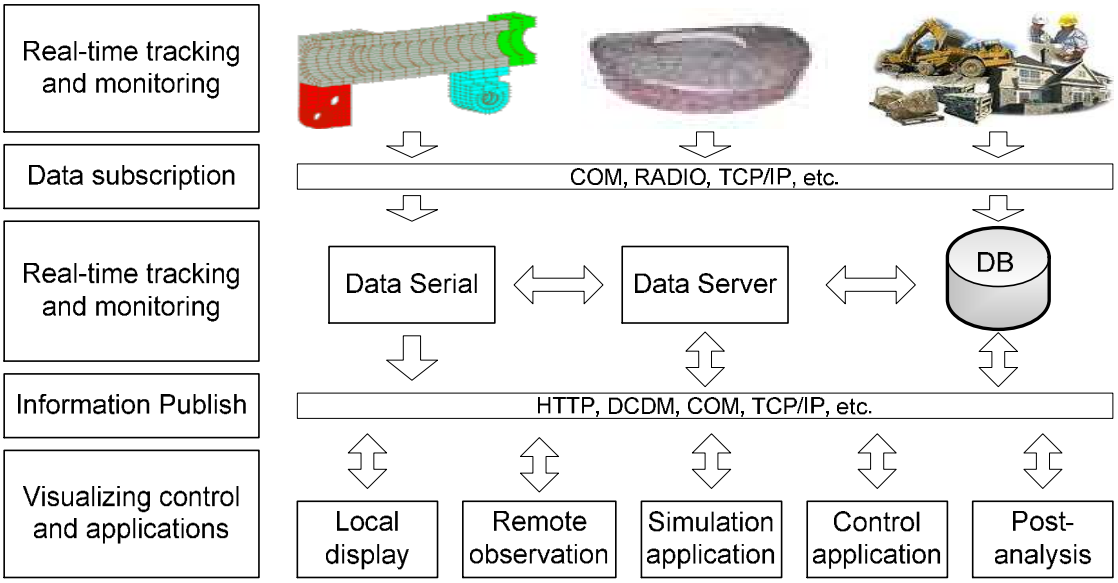

Figure 94 Architecture of the distribution of data and virtual world model.

An elaborate world model includes complex static structures and dynamic objects, such as buildings, equipment, materials and personnel, which assist and improve the perception and understanding of the construction site. When the elements of the virtual world are linked with real-time sensor data, updates from sensors must be made available using a subscribing mechanism and a local real-time data server. A real-time data server is responsible for maintaining an accurate representation of all dynamic and static elements that compose the construction site scene. Relevant information for users such as resource localization, distance, velocity, acceleration, and/or orientation is retrieved from the local server. The server also stores the job-site scene using an efficient data structure,

which consists of a list of entities (surfaces, objects, light, camera, and relations) with their properties designed to represent the counterpart in the real world.

The publishing and subscribing mechanism allows other application or data collectors to synchronize updates and query information from the virtual world model. Users with internet or intranet access can subscribe to any real-time data field being published. They also receive updates every time the information changes, allowing them to monitor and log events of the construction site into a database at the same time they are taking place in reality.

The information is published to a server and distributed to multiple user at both local and remote location in real-time through the data visualization module that facilitates fast and corrected decision making. The application allows the operators and users to observe and interact with the real world model through the virtual environment that increases the awareness of a distributed project team. Moreover, the users are able to share and track feedback with the project team.

The virtual reality system can also be applied as an education, training, and teaching tool. Real-time visualization helps the trainees and students in gaining an intuitive understanding of construction site complexity including potential hazards that exist. Since all the sensing data published to the server is logged, a reconstruction of the working activities and operations can be accomplished after it took place in reality and/or replayed.

9.4 Case Studies

Several experiments have been conducted to test the implementing of real-time data collection and visualization technology in live construction operations. The experiments concentrate on proximity relations in a simulated scene (first scenario), and working in an outdoor and indoor environment (second and third scenario, respectively). The first experiment illustrates a common construction site scenario. It was simulated since safety violations on construction site may not occur. This scenario was used to validate that the developed approach would work during live tests in the field. The first scenario also helps to explain the procedure that leads from field data collection to the

real-time visualization world. The focus of the first scenario is: a worker is approaching heavy equipment and walks underneath a load a crane carries. The second experiment shows results to live construction data: a worker faces a hazard of walking underneath an elevated load. The third scenario records and visualizes events in a training sequence for ironworkers. Data in the three scenarios will be analyzed for proximity issues in construction.

9.4.1 Simulation of Proximity of Worker to Hazards

The method to create the virtual world is illustrated in Figure 95. The scene consists of five major objects: a dozer, a loader, a worker, a crane with load, and a building. The scene surface is generated using point cloud data from spatial surveying equipment, e.g. a laser scanner. The 3D object models represent construction site resources. To each of the resources data are recorded. The real-time data acquisition is linked via object relations to the 3D object models. The relations also allow representation of safety rules, e.g. too close proximity.

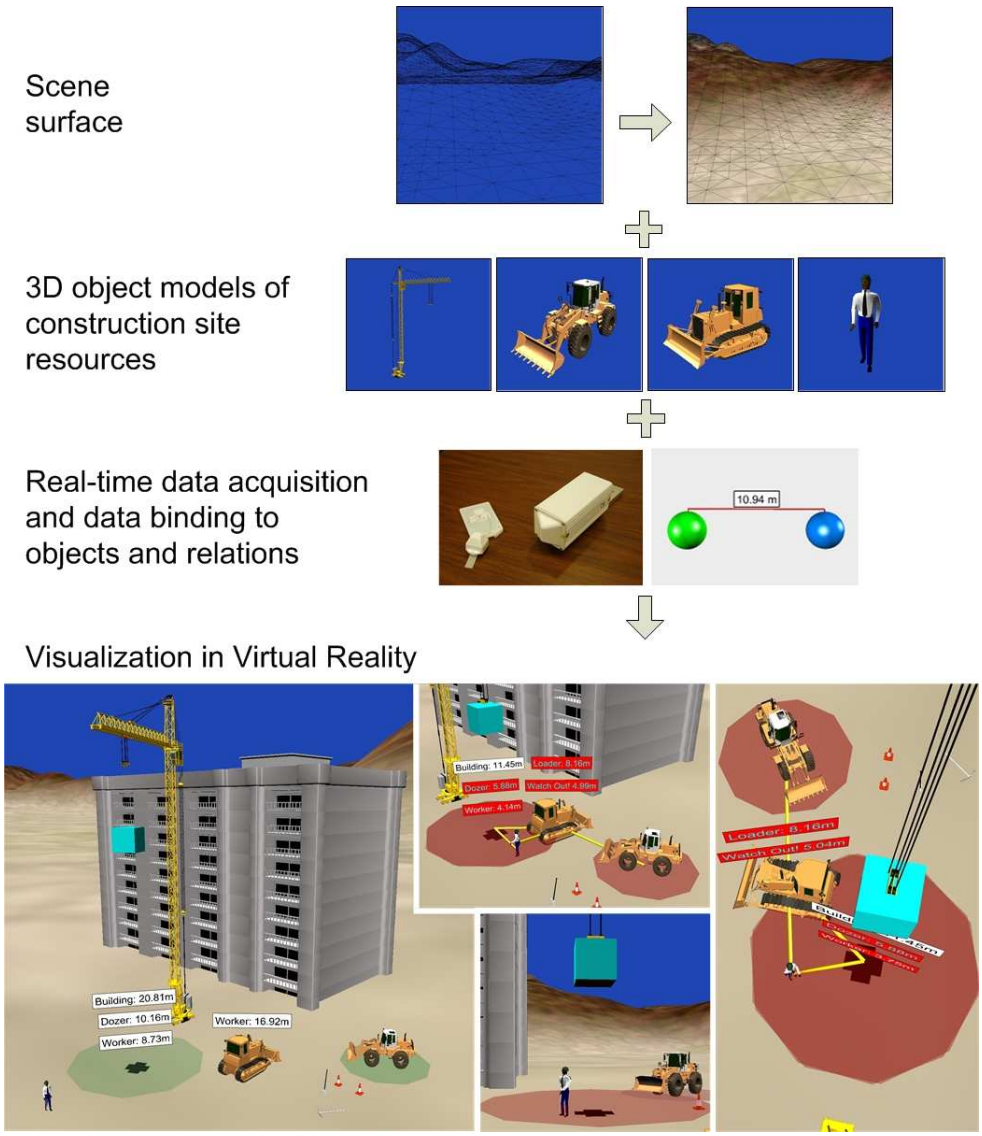

Figure 95 Visualization of proximity hazards using simulated data.

The spatial data are subscribed to the server and the processed information is published in a 3D viewer. Two preliminary defined dangerous zones are denoted by green circles around the static loader and projected from the crane load onto the ground. The distance between each pair of entities is computed automatically from the spatial data. In this scenario, the calculated distances are shown in the labels. When virtual proximity zones and labels turn red they indicate severe risk to a resource. Both circular regions maintain in green when all resources are outside the virtual proximity zone. Zones switch to red when other tracked objects are approaching below a pre-defined

threshold value that a user has set. The size of dangerous zones can be defined according to safety rules or guidelines, e.g. OSHA standards or other best safety practices. Several incidents are shown in the lower portion of Figure 96. The images show several cases that a worker or piece of equipment or both are within proximity to a hazard. Some of these hazards are overhanging load and being too close to (other) equipment. As events are flagged, alerts can be issued and data be logged.

The trajectory of the resources can be extracted from the collected data. The headings of resources are determined by their tangential direction along the trajectories which change over time. These must be calibrated using at least two spatial points along the path. In order to determine the heading of a dynamic object, at least two sensor tags must be mounted on a resource with a large enough distance from each other. Location data to both tags is then collected simultaneously and therefore the heading information becomes available by calculating the tangential angle of the vector formed by the two most recent location records.

Another challenge in this model is to simulate the activity of the tower crane. The crane has two degrees of freedom: the heading of the crane arm along the base axis and the elevating of the load. Since data from the positioning sensor can only provide absolute spatial information (same as the derivative of worker's heading), multiple sensors are necessary. The crane structure is broken into three major subcomponents (see Figure 96): crane base, crane boom, and the pulley attached to the boom that connects to the hook.

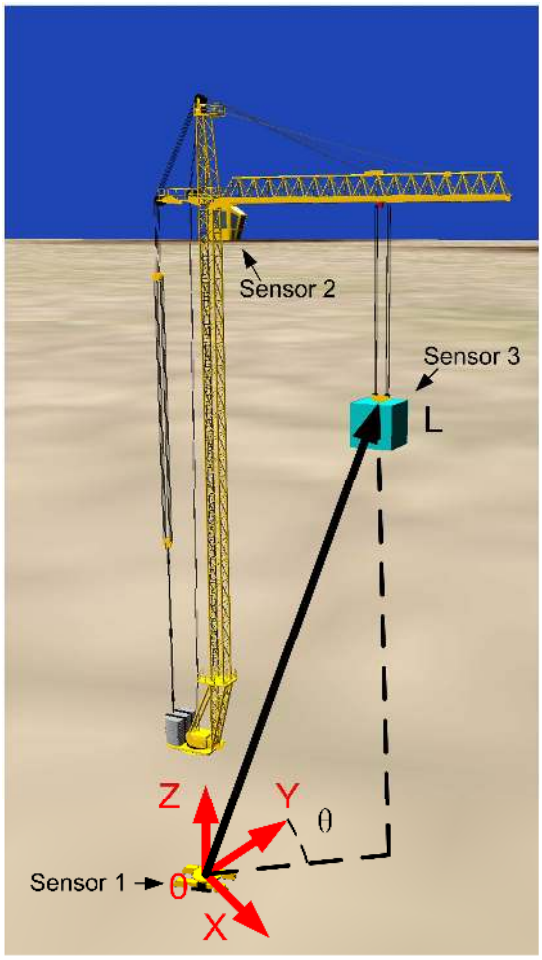

Figure 96 Simulation of the tower crane activities.

The further discussion of this particular scenario assumes that the load does not swing when the crane boom is rotating. Three sensor tags are attached on each subcomponent to collect absolute location data. Sensor tag 1 is attached on the crane base on the ground level which gives reference location of the crane. Sensor tag 2 is attached on the crane body. The connecting vector between sensor tags 1 and 2 is perpendicular to the ground which forms a reference axis parallel to Z axis. Sensor tag 3 is attached at the crane hook to record the location of the load. The local coordinate has an origin on sensor tag 1 and the Y axis is randomly defined as the zero heading direction. The heading of the crane boom is therefore determined by the following formula:

$$\theta = \cos^{-1}\left(\frac{\overline{OZ} \times \overline{OL} \cdot \overline{OX}}{\|\overline{OL}\|}\right) \qquad (Eq. 9-1)$$

where OL is the vector of crane load.

This scenario has shown the method and potential benefits of visualizing unsafe proximity event. In sum, proximity of resources can be recorded and visualized in real-time. Risks can be easily defined using proximity zones. Warnings or alerts can be effectively communicated by displaying dangerous situations in color. The relation between resources can be quantified and updated automatically in real-time. Real-time in this scenario means images in the VR world are updated every second at least once. Collection of real-time location tracking data and streaming to the local server, however, can be at update rates of up to 60 Hz. A user can also view detailed information of ongoing construction site activities by monitoring it form any preferred viewpoint in an interactive manner. For instance, the user's view can be changed from the crane cabinet and moved to the one an equipment operator has sitting in the dozer's cabin. Even the view of a worker can displayed spontaneously and simultaneously. In addition, the visualization of relevant information can be prioritized by a user and limited so that only the most urgent and most necessary information is displayed. This greatly limits overwhelming users with too much information.

9.4.2 Visualization of Live Construction Activities in a Construction Pit

This scenario presents data that were collected using laser scan and location tracking technology. The experiment was conducted in an active construction pit of a large capital facility project. The observation area of the experiment was approximately 1,800 m^2. A commercially-available laser scanner collected the as-built-conditions of the pit including earthwork material, embankments, ramp for vehicles to enter, egress/exit for workers from the pit, protective safety equipment such as guardrails, already built formwork and rebar/concrete structures, and temporary laydown yard with obsolete materials. The laser scans were performed after a mobile crane took its position within the pit to perform several lifting tasks. The point clouds of all scans were registered and used to create a virtual scene. A 3D model of the mobile crane was designed and placed in the exact same position as the original location. Figure 97 shows a photo, the registered point cloud, a mesh of the scene, and the final 3D model before trajectory data were added to the virtual world.

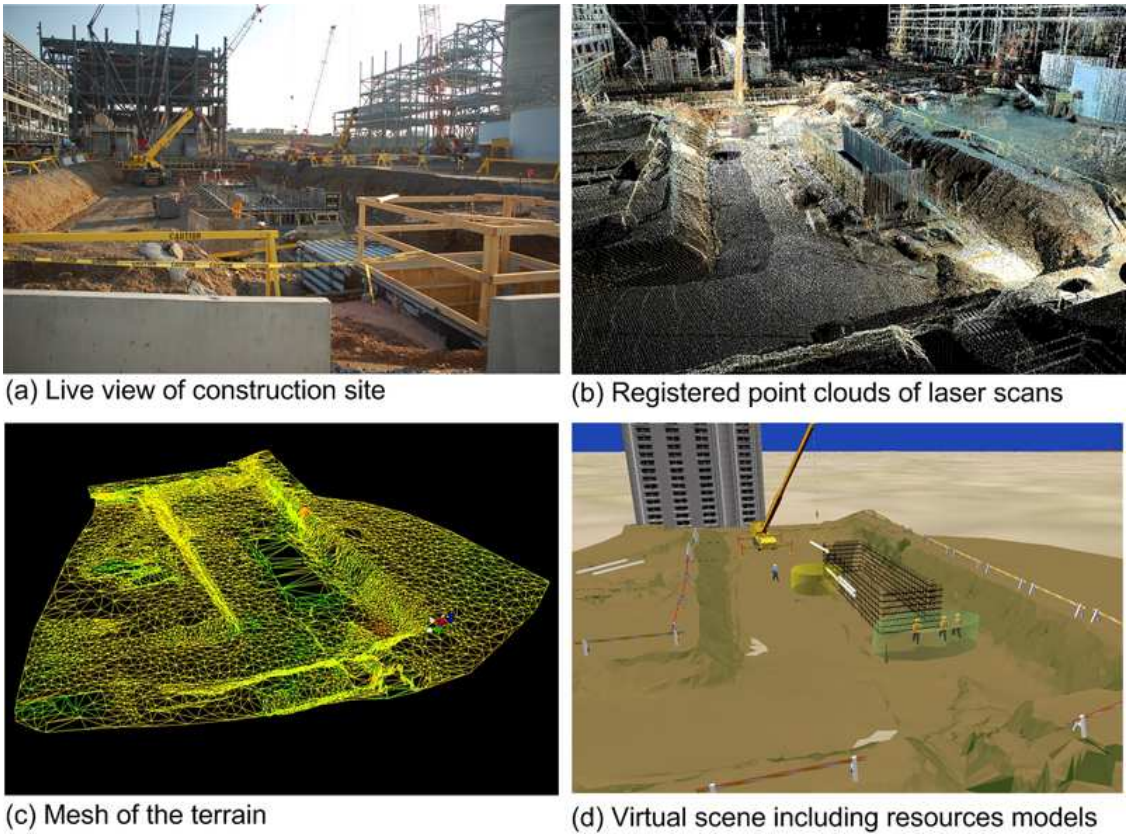

Figure 97 Sequence to build a 3D virtual world.

An active Radio Frequency Identification (RFID) technology called Ultra Wideband (UWB) was used to track the resources in the pit. The resources that were tagged were all workers entering the pit, the mobile crane and its four outrigger positions, and any temporary vehicles entering pit. The method that was used to tag the resources was the same as in [146]. The accuracy of the trajectories of all resources was measured. Since the error rate of the tracking technology was not the focus of this experiment, results are presented in [146]. The focus, however, was to take the real-time positioning data (with up to 60 Hz update rate) of the tagged resources and visualize it in the virtual world. In sum, positioning data of a rebar and carpentry crew and the activities of a mobile crane and other vehicles entering/leaving the pit were tracked and monitored using UWB technology.

Each worker from the rebar crew was outfitted with at least one UWB tag. Each tag collected spatio-temporal data and subscribed the data to the local server. Task-

related information such as position, speed, heading to each resource was calculated by the server. The processed information was then published to the virtual environment, and linked to the corresponding 3D model with unique object ID.

The activities of the mobile crane were captured by multiple UWB tags. Four tags were mounted on the outriggers; one UWB tag was mounted on the structural frame of the crane cabin; and another UWB tag was mounted on the crane hook. The heading of the crane boom was calculated using the location of UWB tags on the crane (see Figure 98).

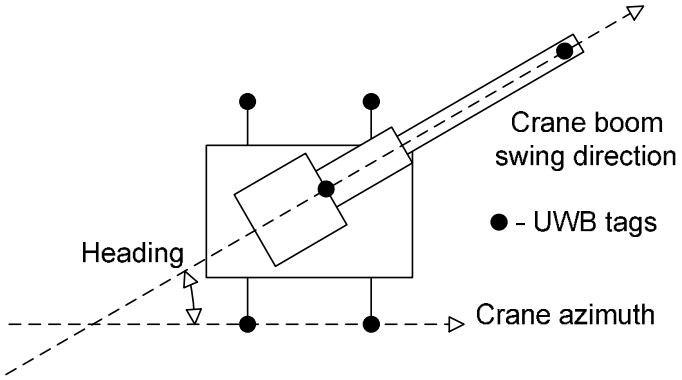

Figure 98 Determination of the heading of the boom of a mobile crane.

The focus of this experiment was to record and analyze the behavior of construction resources in the pit. In particular, results to proximity events of workers being close to a crane load are presented next.

The general view of a construction pit is shown in Figure 102a. All resources in the pit are tagged. Their location is known at any given time. The labels indicate the distance of the workers to the bottom of the crane load. Turns a label red means the resource the label belongs to is at risk (e.g., worker below or within range of the crane load). The proximity zone of the crane is yellow when no warning or alert has been issued. A virtual partially transparent yellow cylinder visualizes the proximity zone of the crane. When a worker invaded the proximity zone of the crane load it turned red. The proximity zone of a worker stays green if the worker is not at risk. The proximity zone of the crane load was set to 2.5 meters; and respectively, to 1 meter for workers. Several

relationships between workers and the crane load were established based. The distance between the resources were computed in real-time and labeled in the virtual world.

The visualization environment allows analysis of operator visibility. Figure 102b demonstrates the limited visibility (dark areas) the equipment operator has from a crane cabin. In the event that a load has to be placed behind an as-built structure (indicated through formwork, rebar, and concrete in Figure 102c), the crane operator can switch in the virtual world to camera position that allows to "see" the location from an optimized view (Figure 102d). The same camera view may assist a tower crane operator whose field-of-view is also obstructed (see Figure 102e).

In another event (see Figure 102f), a worker triggers an alert (proximity area of crane load and worker's label turn red) being below a crane load. Other calculations, e.g. the distance of the foreman to a work gang, can be visualized. The white lines in the image indicate the distance measurement.

(a) Construction pit – general view

Figure 99 Visualization of terrain, 3D model and real-time trajectory data in the virtual world.

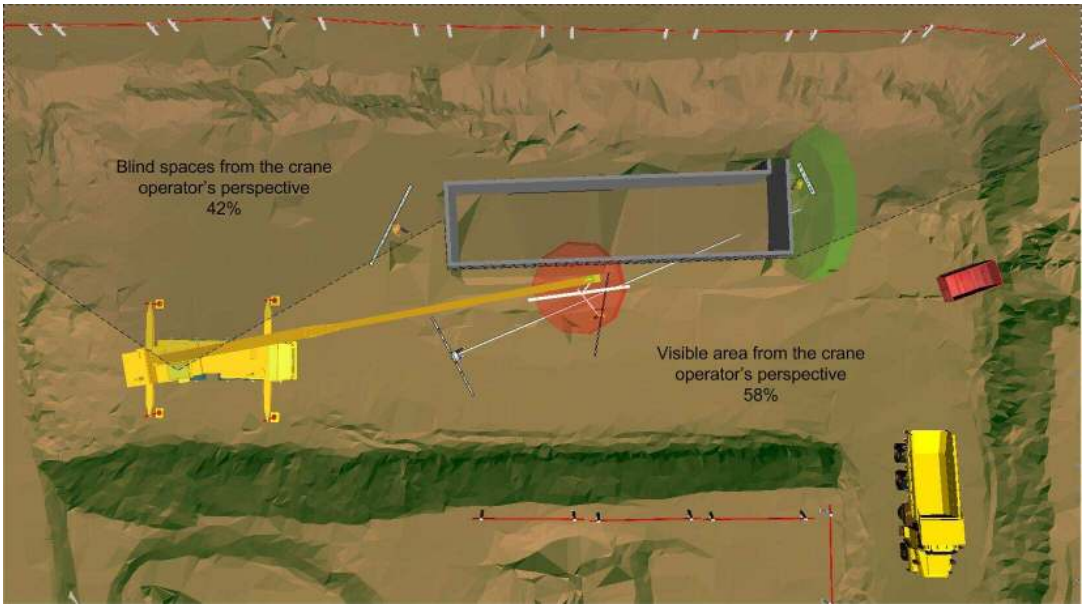

(b) Limited visibility and blind areas of the crane operator (plan view)

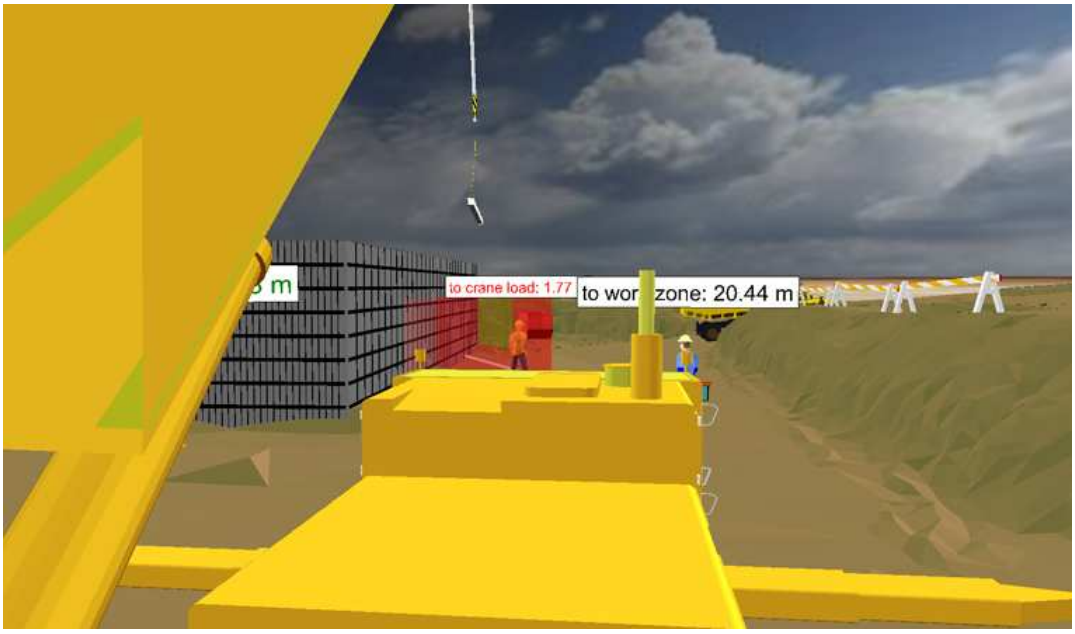

(c) Limited field-of-view of crane operator due to the crane boom and as-built structures

Figure 100 Visualization of terrain, 3D model and real-time trajectory data in the virtual world (Continue).

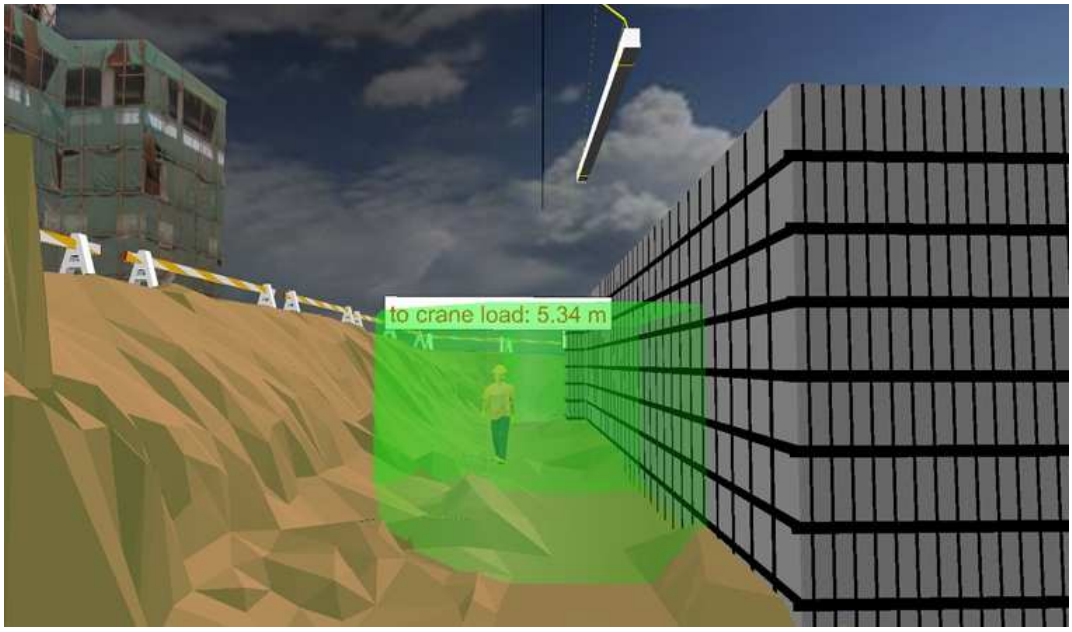

(d) Changing the field-of-view in the virtual world allows a crane operator to "see" behind obstacles

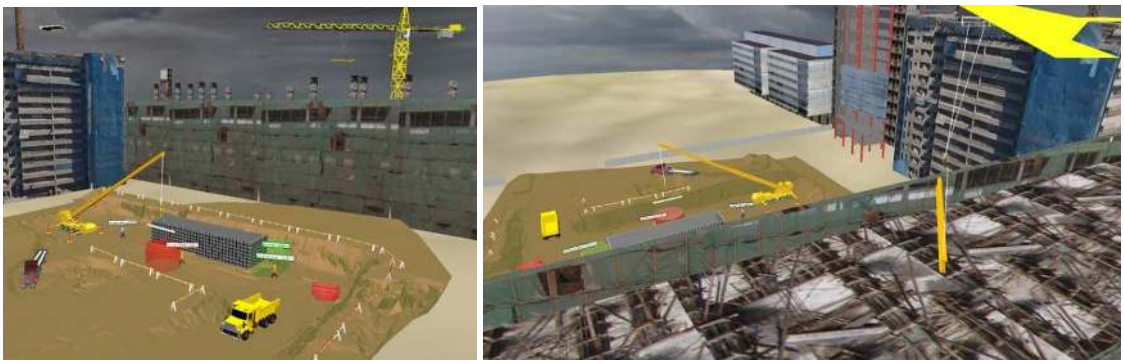

(e) Limited field-of-view of a tower crane operator

Figure 101 Visualization of terrain, 3D model and real-time trajectory data in the virtual world (Continue).

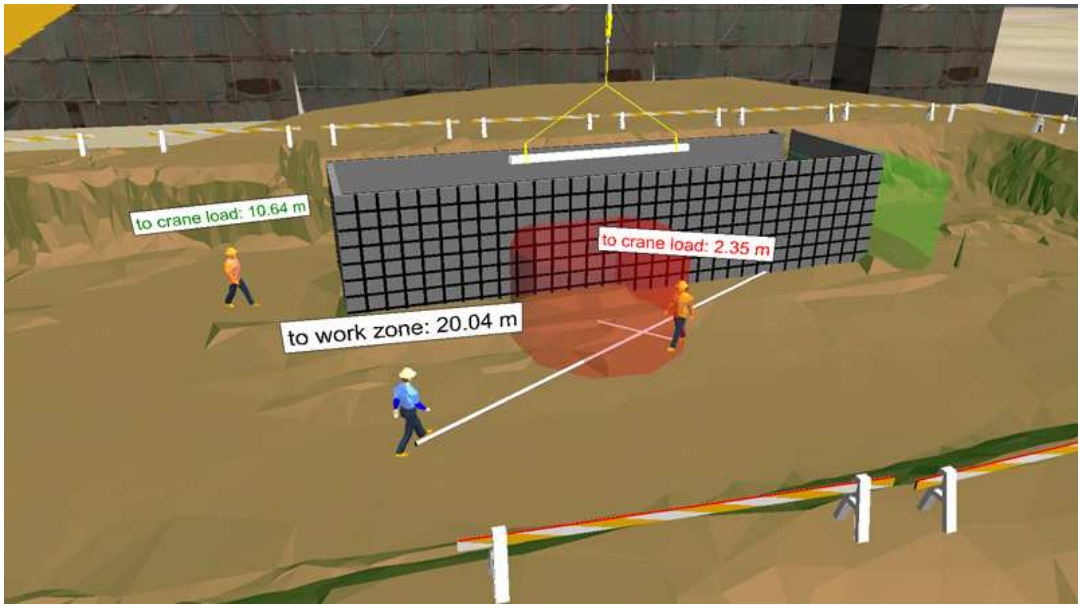

(f) Proximity alert (red label and zone) when intrusion occurs

Figure 102 Visualization of terrain, 3D model and real-time trajectory data in the virtual world (Continue).

9.4.3 Visualization of Recorded Activities in an Ironworker Training Facility

The purpose of the next experiment was visualizing both the safety performance and working efficiency of ironworkers in a training facility. Skilled crafts arte interested in boosting their work performance, however, advanced location tracking and visualization technology has yet to be applied in their training environment to facilitate potentially more effective and effective learning. Applying such technology in a training environment provides several advantages. Examples are: Capacity to replay work activities; objective assessment of safety and productivity performance; demonstration of situational awareness; group discussions in live and classroom setting; study of trainee and trainer performance in complex and dynamic construction processes; interaction of trainees in an immersive virtual world; visualization and more engaging feedback for all training participants and future generations of trainees.

An experiment was conducted in the Southeast Regional Ironworker Training Facility in Atlanta, Georgia. The objective was to test the applicability of the location tracking and visualization system in a compact environment with the goal to provide

(real-time) feedback to trainers and trainees. After the environment was modeled (see Figure 103), the spatio-temporal information of the trainees, crane, and materials was collected.

Five ironworkers that participated in a training session to connect steel girders and a trainer were outfitted with UWB tags. Their locations were tracked. The ironworkers (apprentices) were rigging, hoisting, and connecting steel girders on a two story mock-up structure that is located within the training facility. The girders were first rigged to the crane hook and then hoisted from the material deposit area to their final destination. Two connectors (both apprentices) were tasked to connect the girders. Two connectors stayed on the steel structure while two riggers and one crane operator walked on the ground level.

Figure 103 The real and virtual world of ironworker a training facility.

Similar to the previous experiment, data were analyzed. Data were collected for the entire time of the training session (total 4 hours). Algorithms identified close-calls by measuring the proximity of resources to each other. Only one event was found. It is shown in Figure 104 where a worker navigates below a load. This event was visualized and presented to the trainer and trainers. Analysis was performed to understand how it came to the close-call. Multiple views were generated to understand who was at fault and what the best mitigation strategy would be to avoid such an instance in the future. According to a replay and the visuals, the rigger stepped into the pre-defined dangerous zone from the left, and walked across the dangerous area. Eventually, the rigger left the area. The shortest distance between rigger and the center of the hazard zone was 2.04 m and the rigger stayed within this dangerous area for a total of 8 seconds.

Figure 104 Visualization of a proximity case.

The developed algorithm also calculated the time an ironworker apprentice needed to connect all 14 steel girders in the training session. Although it was not possible to track and measure the connecting time of more than one apprentice, the result for one connector is shown in Figure 105. The time is shown on the vertical axis while the girders are shown on the horizontal axis. Girders had all dimensions and travel and wait times were excluded from the analysis. The connecting time indicates a "learning curve" of the apprentice. At the beginning of the training session the ironworker needed about 500 seconds to connect the first girder, towards the end it is about 100 seconds only. Participants in the experiment were very interested in technology and results. The majority of their opinion-based feedback supported further evaluation of the technology.

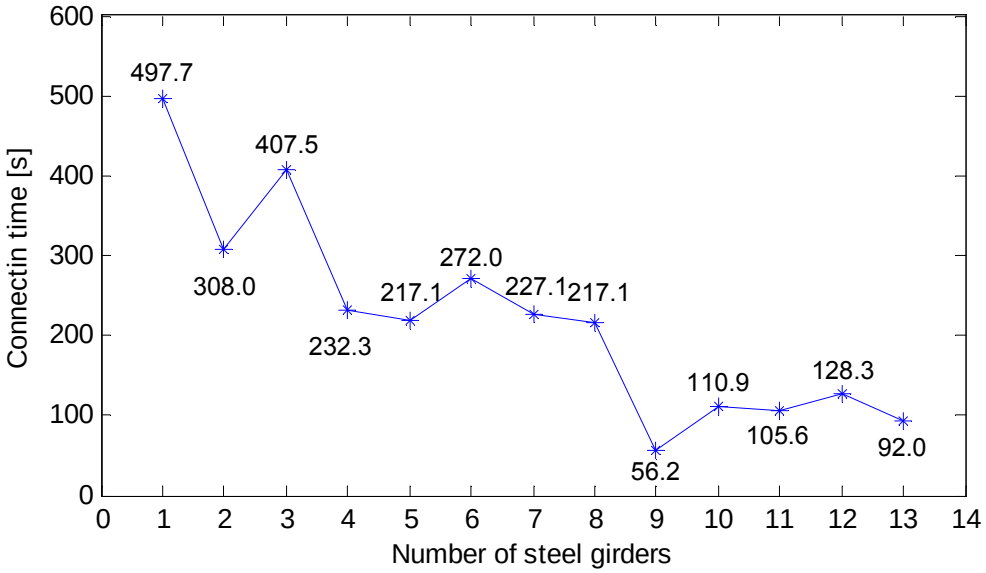

Figure 105 Time needed to connect steel girders.

9.5 Conclusions

Although virtual reality (VR) technology has already been widely used in construction, limited research has focused on the application of real-time VR technology in combination with emerging sensing. A method of implementing real-time (location) data collection and visualization technology in construction safety and monitoring applications was presented and tested.

The developed real-time tracking and visualization system contains real-time data collection, data processing, visualization, and application in live and training environments in construction. Although the effectiveness of the system was tested, further analysis to measure its impact on existing work and training practices are needed. Relevant information was derived from the collected data and visualized. The information represents the state of construction resources and their inter-relations. Such valuable information was transmitted to other distributed decision makers. Stakeholders were provided with real-time information in an interactive virtual environment that enables them to inspect and make fast decision.

Several experiments of data collection and visualization have been conducted to test its applicability. The view provided by the 3D display improved situational awareness of viewers and allowed views from multiple resource locations in relation to other resources.

Future research or development may also focus on providing visual warning and alert mechanisms to workers, operators, or any other decision maker. The use of the gathered data may also lead to shutdowns of equipment or other alert functions, e.g. (semi-) automated safety data analysis or reporting systems. Long-term studies to measure the effectiveness need to be conducted.

CHAPTER X

CONCLUSIONS AND RECOMMENDATIONS

This chapter summarizes the results of this research and relates them to the research questions addressed. The major findings, some limitations and future potential are explained.

10.1 Conclusion Remarks

Applications of real-time monitoring and controlling of construction site progress is of both managerial and technological interests. From a management perspective, accurate and emerging remote sensing technology, with a particular emphasis on real-time detection and tracking of construction resources (personnel, equipment, and material), can provide critical spatio-temporal information. Once gathered data are processed, information has the potential to advance the understanding of construction processes, for example, the level of safety and productivity performance. From a technical perspective, the development and evaluation of various electronic sensors for applications in the harsh construction environment, as well as the exploration of their potential as a valuable aid in project management, enables tighter control of project progress.

In the first chapter of this dissertation, five research questions are raised. These questions are addressed throughout the dissertation, which is summarized as follow:

1. *What hazards exists on construction site?*

   Chapter II synthesized the historical fatality data in construction industry in the past decades, which indicated that approximately 40% of the fatalities were directly and indirectly caused by worker being proximate to various hazardous conditions. Especially, one of the distinct safety problems has been identified as the proximity of workers-on-foot to heavy construction equipment. Further revision on safety management technique indicated that the current operation level safety measurements are inconsistent, subjective and error-prone, since they

highly rely on manual observation and survey. Therefore, the goal of this research is to design, test, and validate new methods that improve construction safety and productivity measurement for a more sustainable construction process. A special emphasis of this research focuses on measuring the proximity hazards that construction personals are exposed to various hazardous conditions, which are omnipresent in complex construction environments.

2. *Can technologies be used to reliably collect data from construction resources?*

   Rapid technological advances have made it possible to implement Ultra Wideband (UWB) real-time localization and tracking systems in construction applications. Chapter aims to evaluate the capabilities and benefits of UWB deployment. It has been demonstrated that, in field trials, a commercially-available UWB system is able to provide real-time location data of construction resources thereby resolving the capability question. Validation occurred through performance measurements utilizing a Robotic Total Station (RTS) for ground truth measurements.

3. *What type of hazards can be detected using remote sensing technology?*

   Advanced topographic survey technologies (laser scanning) have made it possible to quickly and accurately document as-built conditions. As such technologies become available they lead to novel solutions in identifying and resolving potential design and operational issues, including mitigation of risks associated to safe site layout and equipment operator visibility. Chapter V demonstrated the capability of detecting objects from large as-built spatial data sets collected by a commercially-available laser scanner. This Chapter also located and quantified the blind spots/areas and spaces based on 3D range data. For a large construction setting, multiple scans should be conducted and registered. After removing the noise and outliers of the gathered 3D range data, the developed algorithm detected the location and size of blind spaces that obstruct the field-of-view (FOV) of a tower crane operator. This work has also offered a solution to utilize trajectories of workers to identify (unsafe) locations of workers that are (not) in the FOV of tower crane operators.

4. *How to detect and measure the interactions between workers and identified hazards?*

   Advanced real-time location sensing and topographic survey technologies have made it possible to quickly and accurately document spatio-temporal data of the construction resource and environment. As such technologies become available they lead to novel solutions in identifying and resolving potential safety issues, including human-hazards proximity. Chapter VI demonstrated the capability of measuring the workers' safety performances using existing remote sensing technologies in combination with date processing technique. This chapter details the development of a proximity detection model. Such model measures the workers' performances based on the analysis of the site geometry, spatial, temporal, and kinematic characteristics of various construction resources. The developed model has been tested in three different environments, and has been validated by comparing to the video records. The results demonstrate that the model can accurately, consistently and reliably detect and measure the workers' safety performance under proximity hazards.

5. *How to reproduce the detected unsafe behavior share the information among project participants?*

   Chapter IX demonstrated a method of implementing real-time (location) data collection and visualization technology in construction safety and monitoring applications. The developed real-time tracking and visualization system contains real-time data collection, data processing, visualization, and application in live and training environments in construction. Relevant information was derived from the collected data and visualized. The information represents the state of construction resources and their inter-relations. Such valuable information was transmitted to other distributed decision makers. Stakeholders were provided with real-time information in an interactive virtual environment that enables them to inspect and make fast decision. Several experiments of data collection and visualization have been conducted to test its applicability. The view provided by

the 3D display improved situational awareness of viewers and allowed views from multiple resource locations in relation to other resources.

As a summary, the major scientific contributions of this doctoral research include the following:

- This research creates a model that can automatically analyze spatio-temporal data of construction resources (workers, equipment and materials), and automatically identify, evaluate, and visualize their safety, health, and productivity performance.
- This research creates a test-bed to evaluate the performance of various real-time tracking technologies when they are implemented in harsh construction environment.
- This research creates a data processing algorithm to automatically detect object from the large point cloud dataset collected by Light Detection And Ranging (LADAR) technology, and furthermore identify potential hazards, especially the blind spaces from the equipment operators' perspective on construction sites.
- This research creates a new measurement to continuously and consistently assess hazardous situation that workers are proximate to various identified hazards.
- This research constructs a framework to combine real-time tracking data with a virtual environment for construction safety monitoring purpose.

10.2 Limitations and Future Research

This current research in this dissertation focuses on post-time data analysis, which is not able to provide real-time estimating and warning of the workers' unsafe and unhealthy behaviors. Existing research has discussed and tested a RFID based real-time waning technology [149], but such technology has not taken construction site setting and movements of construction resources into consideration. Connecting this doctoral research to the real-time warning technology is the future direction of developing proactive safety monitoring strategy.

Besides, several limitations of this doctoral research have been identified on the data collection, data processing and information interpretation stages, which are briefly listed as follow:

Ultra Wideband technology, as the selected data collection method, requires the installation of infrastructure. Chapter IV has demonstrated that strict layout of the system infrastructure is necessary in order to achieve acceptable data logging accuracy. However, in most of the construction site, sensor's setup is always constrained, which may eventually result in mistakes of safety and productivity measurements. The developed model should be advanced and compactable to other alternative data collection techniques.

Chapter V evaluates the construction site layout and computes the blind spaces of a tower crane operator. This session was not fully automated. Especially the point cloud noise removal is accomplished based on a manual process, which could be less efficient. Range scanning and data processing may significantly be improved by scanning from or closer to the tower crane cabin. However, this may add significant complexity in handling the gathered data set, especially if scan speed is slow and ranges are short. In summary, the utilization of as-built documentation and blind spot analysis can detect potentially hazardous work spaces that are related to tower cranes.

Chapter VI details the development of a proximity detection model. Such model measures the workers' performances based on the analysis of the site geometry, spatial, temporal, and kinematic characteristics of various construction resources. This model utilizes several external parameters whose accurate definition requires further study of construction traffics.

REFERENCES

[1] Bureau of Economic Analysis. "Value added by industry as a percentage of Gross Domestic Product." <http://www.bea.gov/newsreleases/industry/gdpindustry/2012/pdf/gdpind11_ adv.pdf>, (Accessed, July 2, 2012).

[2] United States Census Bureau, "American Community Survey 2010, 1-year estimates." <http://www.census.gov/acs/www/data_documentation/2010_release/> U.S. Department of Commerce, (Accessed, July 2, 2012).

[3] Bureau of Labor Statistics. "National census of fatal occupational injuries in 2010. <http://stats.bls.gov/news.release/pdf/cfoi.pdf>, (Accessed, July 2, 2012).

[4] Bureau Of Labor Statistics, "Census of fatal occupational injuries charts, 1992-2010", <http://www.bls.gov/iif/oshwc/cfoi/cfch0009.pdf >, (Accessed, July 2, 2012)

[5] Centers for Disease Control and Prevention, (2006). "NIOSH fatal occupational injury cost fact sheet: Construction." NIOSH Publications and Products, 2006-153.

[6] International Labor Organization, (2003). "Safety in numbers." Rep. No.061.

[7] CII Research Summary, (2010). "Real-time proactive safety in construction". Construction Industry Institute, Research summary 269-1, July 2010.

[8] PRATT, M.P., and BONNESON, J.A., (2010). "Development of safety performance monitoring procedures." Taxes Transportation Institute, Report 0-4703-7, Feb. 2010.

[9] HINZE, J., and GODFREY, R., (2003). "An evaluation of safety performance measures for construction projects." Journal of Construction Research, 4(1): 5-15.

[10] SULLIVAN, A., and SHEFFRIN, S.M., (2003). Economics: Principles in action. Upper Saddle River, New Jersey 07458: Pearson Prentice Hall.

[11] United Kingdom Health and Safety Executive. "A guide to measuring health and safety performance." Released on December 2001. <http://www.hse.gov.uk/opsunit/perf meas.pdf>. (Accessed, July 2, 2012)

[12] HINZE, J. "Leading indicator of construction safety performance." Presented on ConocoPhillips Downstream Construction Network – Face to Face Meeting, Los Angeles, CA, September 20, 2006.

[13] TOOLE T.M. (2002). "Construction site safety roles." Journal of Construction Engineering and Management, 128(3): 203-211.

[14] PEGULA, S. (2011). "Work zone- fatal occupational injuries at road construction sites, 2003-2010." Bureau of Labor Statistics, 2011 National Occupational Injury Research Symposium, Morgantown, West Virginia. Oct. 18-20, 2011.

[15] BUREAU OF LABOR STATISTICS, "National census of fatal occupational injuries in 2008." Released on Aug. 20, 2009. <http://www.bls.gov/news.release/archives/cfoi_08202009.pdf> (Accessed, July 30, 2012).

[16] BUREAU OF LABOR STATISTICS, "Workplace injuries and illness in 2008." Released on Oct. 29, 2009. <http://www.bls.gov/news.release/archives/osh_10292009.pdf> (Accessed, July 30, 2012).

[17] National Safety Council, "Injury facts, 2008 edition." Itasca, IL, ISBN 978-0-87912-278-2. <https://www.usw12775.org/uploads/InjuryFacts08Ed.pdf>. (Accessed, July 30, 2012).

[18] TEIZER, J., VENUGOPAL, M., and WALIA, A., (2008). "Ultra Wideband for automated real-time three-dimensional location sensing for workforce, equipment, and materials positioning and tracking." Transportation Research Record: Journal of the Transportation Research Board, Washington D.C., No. 2081: 55-64.

[19] TEIZER, J., ALLREAD, B.S., FULLERTON, C.E., and HINZE, J., (2010). "Autonomous pro-active real-time construction worker and equipment operator proximity safety alert system." Automation in Construction, 19(5): 630-641.

[20] FOSBROKE, D.E., (2004). "NIOSH report! Studies on heavy equipment blind spots and internal traffic control." 2004 Roadway Work Zone Safety and Health Conference, Baltimore, MD, 2004. <http://www.workzonesafety.org/files/documents/news_events/wz_conference_2004/heavy_equipment.pdf> (Accessed, July 5, 2012).

[21] Construction Industry Institute, "Measuring safety performance with active safety leading indicators." CII Research Summary 284-1, July 2012.

[22] HECKER, S., CAMBATESE, J., and WEINSTEIN, M. (2005). "Designing for worker safety: moving the construction safety process upstream." Professional Safety, 32-44.

[23] Occupational Safety and Health Administration, Definitions, basic program elements for federal employees OSHA. 1960.2. <http://www.osha.gov/pls/oshaweb/owadisp.show_document?p_id=11264&p_table=standards> (Accessed, July 6, 2012).

[24] American Bureau of Shipping, (2012). "Guidance notes on safety culture and leading indicators of safety." January 2012. <http://www.eagle.org/eagleExternalPortalWEB/ShowProperty/BEA%20Repository/Rules&Guides/Current/188_Safety/Guide> (Accessed, July 6, 2012).

[25] LAUFER, A. and LEDBETTER, W.B., (1986). "Assessment of safety performance measures at construction safety." Journal of Construction Engineering, 112(4): 530-543

[26] American National Standards Institute, (1973). "Method of recording and measuring injury experience." Z-16.1, New York, American National Standards Institute.

[27] HINZE, J., and HARRISON, C., (1981). "Safety programs in large construction firms." Journal of the Construction Division, 107(3): 455-467.

[28] LINDSAY, F.D., (1992). "Successful health and safety management: The contribution of management audit." Safety Science, 15:387-402.

[29] Construction Owners Association of Alberta, (2004). Leading indicator – best practice. <http://www.coaa.ab.ca/Portals/0/Downloads/BP%20Safety/LEADING%20INDICATORS%20BEST%20PRACTICES.PDF> (Accessed, July 6, 2012).

[30] GRABOWSKI, M., AYYALASOMAYAJULA, P., MERRICK, J., HARRALD, J., and ROBERTS, K., (2007). "Leading indicators for safety in virtual organizations." Safety Science, 45(10): 1013-1043.

[31] BERGH, V.D., (2003). "Leading and trailing indicators: occupational safety." Proceedings of ISSA/Chamber of Mines Conference 2003 – Mines and Quarries Prevention of Occupational Injury and Disease, Sandton Convention Center, Sandton, South Africa, 2003.

[32] Construction Industry Institute, "Implementing active leading indicators." CII Implementation Resource 284-2, July 2012.

[33] Construction Industry Institute, "The owner's role in construction safety." CII Research Summary 190-1, March 2003.

[34] HINZE, J., THURMAN, S., and WEHLE, A. (2012). "Leading indicators of construction safety performance." Safety Science, doi:10.1016/j.ssci.2012.05.016.

[35] Cambridge Center for Behavior Studies, "Introduction to Behavioral Safety", < http://www.behavior.org/resource.php?id=330 > (Accessed, July 6, 2012).

[36] CHHOKAR, J.S., and WALLIN, J.A., (1984). "Improving safety through applied behavior analysis." Journal of Safety Research, 15(4): 141-151.

[37] FANG, D.P., XIE, X.Y., and HUANG, H.L., (2004). "Factor analysis-based studies on construction workplace safety management in China." International Journal of Project Management, 22(1): 43-49.

[38] LINGARD H., and ROWLINSON, S., (1997). "Behavior-based safety management in Hong Kong's construction industry." Journal of Safety Research, 28(4): 243-256.

[39] CHOUDHRY, R.M. and FANG, D.P., (2008). "Why operatives engage in unsafe work behavior: Investigation factors on construction site." Safety Science, 46(4): 566-584.

[40] ZOHAR, D., and LURIA, G., (2003). "The use of supervisory practices as leverage to improve safety behavior: A cross-level intervention model." Journal of Safety Research, 34(5): 567-577.

[41] Occupational Safety and Health Administration, (2002). "Job hazard analysis." OSHA-3071. < http://www.osha.gov/Publications/osha3071.pdf > (Accessed, July 6, 2012).

[42] GADD, S., and COLLINS, A.M., (2002). "Safety culture: A review of the literature." Health and Safety Laboratory, Human Factor Group, U.K. <http://www.hse.gov.uk/ research/hsl_pdf/2002/hsl02-25.pdf > (Accessed, July 6, 2012).

[43] AGNEW, J., and DANIELS, A., (2011). "Development high-impact leading indicator for safety." The Performance Management Magazine, Accelerating Business Performance. <http://aubreydaniels.com/pmezine/developing-high-impact-leading-indicators-safety> (Accessed, July 6, 2012).

[44] KENNEDY, R., and KIRWAN, B., (1998). "Development of a hazard and operability-based method for identifying safety management vulnerabilities in high risk systems." Safety Science, 30: 249-274.

[45] GLENDON, A.L., CLARKE, S.G., and McKENNA, E.F., (2006). "Human safety and risk management", CRC Press, Taylor and Francis Group. ISBN: 0-8493-3090-4.

[46] HINZE, J. (2005). Construction Safety. Prentice-Hall, Inc. ISBN: 0-1311-8651-5.

[47] SURAJI, A., DUFF, A.R., and PECKITT, S.J., (2001). "Development of causal model of construction accident causation." Journal of Construction Engineering and Management, 127(4): 337-345.

[48] REASON, J., (1990). Human error, Cambridge University Press, New York. ISBN: 0-521-31419-4.

[49] HINZE, J., (1996). "The distraction theory of accident causation." Proceedings of International Conference on Implementation of Safety and Health on Construction Sites, CIB Working Commission W99: Safety and Health on Construction Sites, Balkema, Rotterdam, Netherlands, 1996; 357–384.

[50] RASMUSSEN, J., (1982). "Human errors: taxonomy for describing human malfunction in industrial installations." Journal of Occupational Accidents, 4: 311-313.

[51] FURNHAM, A. (1994). Personality at work: the role of individual differences in the workplace. Routledge, New York. ISBN: 0-415-03547-3.

[52] CACCIABUR, P.C., (1997). "A methodology of human factors analysis for systems engineering: theory and applications." IEEE Transactions on Systems, Man, and Cybernetics-Part A: System and Humans, 27(3), May 1997.

[53] ROWLINSON, S.M., (2004). Construction safety management systems. Taylor and Francis, ISBN: 0-4153-0063-0.

[54] NAVON, R., and BERKOVICH, O. (2006). "An automated model for materials management and control." Construction Management and Economics, 24 (6):635–646.

[55] SONG, J., HAAS, C.T., CALDAS, C.H., ERGEN, E., and AKINCI, B. (2006). "Automating the task of tracking the delivery and receipt of fabricated pipe spools in industrial projects." Automation in Construction, 15 (2):166–177.

[56] SONG, J., HAAS, C.T., CALDAS, C.H. (2006). "Tracking the location of materials on construction job sites." ASCE, Journal of Construction Engineering and Management 132 (9):911–918.

[57] SONG, J., HAAS, C.T., CALDAS, C.H. (2007). "A proximity-based method for locating RFID tagged objects." Journal of Advanced Engineering Informatics 21:367–376 Elsevier.

[58] AKINCI, B., ANUMBA, C. (2008). "Editorial — Sensors in construction and infrastructure management." ITcon, Special Issue Sensors in Construction and Infrastructure Management 13:69–70.

[59] GRAU, D., CALDAS, C.H., HAAS, C.T., GOODRUM, P.M., and GONG, J. (2009). "Assessing the impact of materials tracking technologies on construction craft productivity." Automation in Construction, 18: 903–911.

[60] GRAU, D., and CALDAS, C.H. (2009). "Methodology for automating the identification and localization of construction components on industrial projects." ASCE Journal of Computing in Civil Engineering 23(1):3–13.

[61] BOHN, J.S., and TEIZER, J. (2009). "Benefits and barriers of construction project monitoring using hi-resolution automated cameras." Journal of Construction Engineering and Management. 136(6): 632-640.

[62] TUCHMAN, J., (2009). "Owners join effort to improve industry productivity." Engineering News Record, December Issue, 12.

[63] LUNDBERG, E.J., BELIVEAU, Y.J. (1989). "Automated lay-down yard control system — ALYC." ASCE Journal of Construction Engineering and Management 115(4):535–544.

[64] GOODRUM, P.M., HAAS, C.T., CALDAS, C.H., ZHAI, D., YEISER, J., and HOMM, D. (2011). "A model to predict a technology's impact on construction productivity." ASCE Journal of Construction Engineering and Management, 137(9):678-688.

[65] NASIR, H., HAAS, C.T., YOUNG, D.A., Razavi, S.N., Caldas, C.H., and Goodrum, P.M. (2010). "An implementation model for automated construction materials tracking and locating." Canadian Journal of Civil Engineering 37(4):588–599.

[66] Construction Industry Institute, (2011). Leveraging Technology to Improve Construction Productivity. The University of Texas at Austin, College of Engineering, 240–241, RS.

[67] NAVON, R., and SACKS, R., (2006) "Assessing research issues in automated project performance control (APPC)." Automation in Construction, 16(4):474–484.

[68] HINZE, J.W., and TEIZER, J. (2011). "Visibility-related fatalities related to construction equipment." Journal of Safety Science, 49(5):709–718 Elsevier.

[69] TEIZER, J., ALLREAD, B.S., and MANTRIPRAGADA, U. (2010). "Automating the blind spot measurement of construction equipment." Automation in Construction, 19(4):491–501 Elsevier.

[70] BORCHERDING, J., (1976). "Improving productivity in industrial construction." Journal of the Construction Division, 102(4): 599-614.

[71] WANG, Y., GOODRUM, P.M., HAAS, C.T., GLOVER, R.W. (2009). "Analysis of observed skill affinity patterns and motivation for multi-skilling among craft workers in the U.S. industrial construction sector." ASCE, Journal of Construction Engineering and Management 135(10):999–1008.

[72] Construction Industry Institute, (2010). Guide to Activity Analysis, the University of Texas at Austin, College of Engineering, Implementation Report 252–2a.

[73] NAVON, R., and GOLDSCHMIDT, E. (2003). "Monitoring labor inputs: automated-data-collection model and enabling technologies." Automation in Construction, 12(2):185–199 Elsevier.

[74] EASTMAN, C.M., and SACKS, R. (2008). "Relative productivity in the AEC industries in the United States for on-site and off-site activities." ASCE Journal of Construction Engineering and Management, 134(7):517–526.

[75] TEIZER, J., CALDAS, C.H., and HAAS, C.T. (2007). "Real-time three-dimensional occupancy grid modeling for the detection and tracking of construction resources." ASCE Journal of Construction Engineering and Management 133(11):880–888.

[76] TEIZER, J., LAO, D., and SOFER, M. (2007). "Rapid automated monitoring of construction site activities using ultra-wideband." Proceedings of 24th International Symposium on Automation and Robotics in Construction, IAARC, Cochin, Kerala, India, 2007.

[77] KHOURY, H.M., KAMAT, V.R. (2009). "Evaluation of position tracking technologies for user localization in indoor construction environments." Automation in Construction, 18(4):444–457.

[78] BOUSHABA, M., HAFID, A., and BENSLIMANE, A. (2009). "High accuracy localization method using AoA in sensor networks." Computer Networks 53:3087–3088.

[79] RABAEY, J.M., AMMER, J., da SILVA Jr., PATEL, J.L., and SHAD, D.R. (2000). "Picoradio supports ad hoc ultra-low power wireless networking." IEEE Computer 33(7):42–48 D.

[80] BAHL, P., and PADMANABHAN, V. (2000). "RADAR: an in-building RF-based user location and tracking system." Proceedings of InfoCom, 2:775–784, V.

[81] NICULESCU, D., and NATH, B. (2003). "DV based positioning in ad-hoc networks." Telecommunication Systems 22 (1–4):267–280 B.

[82] CHO, Y., YOUN, J., and MARTINEZ, D. (2010). "Error modeling for an untethered ultra-wideband system for construction indoor asset tracking." Automation in Construction, 19(1):43–54 Elsevier.

[83] SAIDI, K.S., TEIZER, J., FRANASZEK, M., and LYTLE, A.M. (2010). "Understanding static and dynamic localization performance of commercially-available ultra wideband tracking systems." Automation in Construction, 20(5):519-530, Elsevier.

[84] FONTANA, R.J., AMETI, A., RICHLEY, E., BEARD, L., and GUY, D. (2002). "Recent advances in ultra wideband communications systems." IEEE Conference on Ultra Wideband Systems and Technologies, 129–133.

[85] FONTANA, R.J., RICHLEY, E., and BARNEY, J. (2003). "Commercialization of a ultra wideband precision asset location system." IEEE Conference on Ultra Wideband Systems and Technologies, 369–373.

[86] FONTANA, R. (2004). "Recent system applications of short-pulse Ultra-Wideband (UWB) Technology." IEEE Transactions on Microwave Theory & Techniques 52(9):2087–2104.

[87] ERGEN, E, AKINCI, B., and SACKS, R. (2007). "Tracking and locating components in a precast storage yard utilizing radio frequency identification technology and GPS, Automation in Construction, 16 (3):354–367, Elsevier.

[88] COSTIN, A., SEDEHI, A., WILLIAMS, M., LI, L., BAILEY, K., and TEIZER, J. (2010). "Leveraging passive radio frequency identification technology in high-rise renovation projects." 27th International Conference on Applications of IT in the AEC Industry, Cairo, Egypt, November 16–18, 2010.

[89] SKIBNIEWSKI, M.J., and JANG, W.S. (2009). "Simulation of accuracy performance for wireless sensor based construction asset tracking." Computer-Aided Civil and Infrastructure Engineering, 24(5):335–345.

[90] BRILAKIS, I., and SOIBELMAN, L. (2008). "Shape-based retrieval of construction site photographs." ASCE Journal of Computing in Civil Engineering 22(1):14–20.

[91] BRILAKIS, I., CORDOVA, F., and CLARK, P. (2008). "Automated 3D vision tracking for project control support." Proceedings of the Joint US-European Workshop on Intelligent Computing in Engineering, Plymouth, UK, 487–496.

[92] GONG, J., CALDAS, C.H. (2010). "Computer vision-based video interpretation model for automated productivity analysis of construction operations." ASCE Journal of Computing in Civil Engineering 24(3):252–263.

[93] TEIZER, J., and VELA, P.A. (2009). "Workforce tracking on construction sites using video cameras." Advanced Engineering Informatics, 23(4):452–462, Elsevier.

[94] DUROVIC, Z., and KOVACEVIC, B. (2009). "Robust estimation with unknown noise statistics." IEEE Transactions on Automatic Control, 44(6):1292–1296.

[95] BEVINGTON, P. Data Reduction and Error Analysis for the Physical Sciences, 3rd edition, McGraw-Hill, 2002.

[96] GOODRUM, P.M., ZHAI, D., and YASIN, M. (2009). "The relationship between changes in material technology and construction productivity." ASCE Journal of Construction Engineering and Management 135(4):278–287.

[97] KNOBLAUCH, R.L., PIETRUCHA, M.T., and NITZBURG, M. (1996). "Field studies of pedestrian walking speed and start-up time." Transportation Research Record, 1538:27–38.

[98] SACKS, R., NAVON, R., GOLDSCHMIDT, E. (2003). “Building project model support for automated labor monitoring.” ASCE Journal of Computing in Civil Engineering 17(1):19–27.

[99] Center to Protect Workers' Right (CPWR). (2009). “Crane-Related Deaths in Construction and Recommendations for Their Prevention.” <http://www.cpwr.com/research-cranereport.html>, (Assessed, September 6, 2012).

[100] Bureau of Labor Statistics (BLS), (2008). “Crane-related Occupational Fatalities.” <http://www.bls.gov/iif/oshwc/osh/os/osh_crane_2006.pdf>, (Assessed, September 6, 2012).

[101] Engineering News Record (ENR), (2012). “Why every Pick Needs a Plan.” Engineering News Record, McGraw-Hill Companies, New York, p.8-9.

[102] AL-HUSSEIN, M., ALKASS, S., and MOSELHI, O. (2005). “Optimization algorithm for selection and on site location of mobile cranes.” Journal of Construction Engineering and Management, 131(5):579–590.

[103] ROSENFELD, Y., and SHAPIRA, A. (1998). “Automation of existing tower cranes: economic and technological feasibility.” Automation in Construction, 7(4):285-298.

[104] LEE, G., CHO, J., HAM, S., LEE, T., LEE, G., YUN, S.H., and YANG, H.J. (2012). “A BIM and sensor-based tower crane navigation system for blind lifts.” Automation in Construction, <http://dx.doi.org/10.1016/j.autcon.2012.05.002>, (Assessed, September 6, 2012).

[105] LI, Y., and LIU, C. (2012). “Integrating field data and 3D simulation for tower crane activity monitoring and alarming.” Automation in Construction, <http://dx.doi.org/10.1016/j.autcon.2012.05.003>, (Assessed, September 6, 2012).

[106] NEITZEL, R.L., SEIXAS, N.S., and REN, K.K. (2001). “A review of crane safety in the construction industry.” Journal of Application Occupation Environment Hygiene, 16(12):1106–1117.

[107] Nationwide Crane Training, (2009). “Qualifying Rigger/Signal Person Training.” <http://www.nationwidecranetraining.com/post/qualifying-rigger-signalperson-training>, (Assessed, September 6, 2012).

[108] MARX, A., ERLEMANN, K., and KOONIG, M. (2010). “Simulation of construction processes considering spatial constraints of crane operations.” Proceedings of the International Conference on Computing in Civil and Building Engineering, Nottingham, UK.

[109] AKINCI, B., FISCHER, M., and KUNZ, J. (2002). “Automated Generation of Work Spaces Required by Construction Activities.” Journal of Construction Engineering and Management, 128(4):306-315.

[110] SHAPIRO, H. I., SHAPIRO, J. P., and SHAPIRO, L. K. (2000). “Cranes and derricks.” 3rd edition, McGraw-Hill, New York.

[111] PEURIFOY, R. L., and SCHEXNAYDER, C. J. (2002). “Construction Planning, Equipment, and Methods.” McGraw-Hill, New York.

[112] RODRIGUEZ-RAMOS, W. E. and FRANCIS, R. (1983). “Single crane location optimization.” Journal of Construction Engineering and Management, 109(4):387-398.

[113] HUANG, C., WANG, C.K., and TAM, C.M. (2011). “Optimization of tower crane and material supply locations in a high-rise building site by mixed-integer linear programming.” Automation in Construction, 20(5):571-580.

[114] ZHANG, S., TEIZER, J., Lee, J.-K., EASTMAN, C.M., VENUGOPAL, M. (2012). “Building Information Modeling (BIM) and Safety: Automatic Safety Checking of Construction Models and Schedules.” Automation in Construction, Elsevier, < http://dx.doi.org /10.1016/j.autcon.2012.05.006>, (Assessed, September 6, 2012).

[115] TAM, W.Y., and FUNG, W.H. (2010). “Tower crane safety in the construction industry: A Hong Kong study.” Journal of Safety Science, 10:1016-1024.

[116] FAIR, H.W. (1998). “Crane safety on construction sites: An introduction.” Crane Safety on Construction Sites, ASCE Manuals and Reports on Engineering Practice No. 93, Task Committee on Crane Safety on Construction Sites, ASCE, Reston, Va., 1–18.

[117] HÄKKINEN, K. (1993). “Crane accidents and their prevention revisited.” Journal of Safety Science, Elsevier, 16(2):267–277.

[118] HINZE, J., PEDERSEN, C., and FREDLEY, J. (1998). “Identifying root causes of construction injuries.” Journal of Construction Engineering and Management, 124(1):67–71.

[119] ABDELHAMID, T.S., and EVERETT, J.G. (2000). “Identifying root causes of construction accidents.” Journal of Construction Engineering and Management, 126(1):52–60.

[120] BEAVERS, J.E., MOORE, J.R., RINEHART, R., and SCHRIVER, W.R. (2006). “Crane-related fatalities in the construction industry.” Journal of Construction Engineering and Management, 132(9):901–910.

[121] SHAPIRA. A., and SIMCHA, M. (2009). “AHP-Based weighting of factors affecting safety on construction sites with tower cranes.” Journal of Construction Engineering and Management, 135(4):307-318.

[122] SHAPIRA. A., and SIMCHA, M. (2009). “Measurement and risk scales of crane-related safety factors on construction sites.” Journal of Construction Engineering and Management, 135(10):979-989.

[123] SERTYESILISIK, B., TUNSTALL, A., Mclouglin, J. (2010). “An investigation of lifting operations on UK construction sites.” Safety Science, Elsevier, 48:72–79.

[124] KANG, S.C., CHI, H.L., MIRANDA, E. (2009). “Three-Dimensional simulation and visualization of crane assisted construction erection processes.” Journal of Computing in Civil Engineering, 23(6):363-372.

[125] PARK, T., KIM, M.K., KIM, C., and KIM, H. (2009). “Interactive 3D CAD for effective derrick crane operation in a cable-stayed bridge construction.” Journal of Construction Engineering and Management, 135(11):1261-1270.

[126] EVERETT, J.G., and SLOCUM, A.H. (1993). “CRANIUM: Device for improving crane productivity and safety.” Journal of Construction Engineering and Management, 119(1):23–39.

[127] SHAPIRA. A., ROSENFELD, Y., and MIZRAHI, I. (2008). “Vision system for tower cranes.” Journal of Construction Engineering and Management, 134(5):320-332.

[128] JOHNSON, A.E., and HEBERT, M. (1999). “Using Spin Images for Efficient Object Recognition in Clustered 3D Scenes.” IEEE Transactions on Pattern Analysis and Mechine Intelligence, 21(5):433-449.

[129] EL-OMARI, S., MOSELHI, O. (2008) “Integrating 3D Laser Scanning and Photogrammetry for Progress Measurement of Construction Work”. Automation in Construction, 18(1):1-9

[130] DU, J.C., and TENG, H.C. (2007). “3D Laser Scanning and GPS Technology for Landslide -Earthwork Volume Estimation.” Automation in Construction, 16:657-663.

[131] KIM, H., RAUCH A. F., and HAAS, C. T. (2004). “Automated Quality Assessment of Stone Aggregate Based on Laser Imaging and a Neural Network.” Journal of Computing in Civil Engineering, 18(1):58-64.

[132] BOUKAMP, F., and AKINCI, B. (2007). “Automated Reasoning about Construction Specification to Support Inspection and Quality Control.” Automation in Construction, 17(1):90-106.

[133] BOSCHE, F., HAAS, C. T., and AKINCI, B. (2009). “Automated Recognition of 3D CAD Objects in Site Laser Scans for Project 3D Status Visualization and Performance Control.” Journal of Computing in Civil Engineering, 23(6):311-318.

[134] WANG, H., AKINCI, B., ERGEN, E., TANG, P., and GORDON, C. (2008). “Technological Assessment and Process implications of Field Data Capture Technologies for Construction and Facility Infrastructure Management” Journal of Information technology in Construction (ITcon), Special Issue Sensors in Construction and Infrastructure Management, 14:134-154.

[135] CHENAVIER, F., REID, I., and BRADY, M. (1994). “Recognition of Parameterized Objects from 3D data: A parallel Implementation.” Image Visualization and Computation, 12(9):573-582.

[136] DAI, F. RASHIDI, A., BRILAKIS, I., and VELA, P.A. (2012). “Comparison of Image- and Time-of-Flight-Based Technologies for 3D Reconstruction of Infrastructure”, ASCE Construction Research Congress, West Lafayette, Indiana, United States, May 21-23, 2012, <http://dx.doi.org/10.1061/9780784412329.094>, (Assessed, September 6, 2012).

[137] GOLPARVAR-FARD M., BOHN J., TEIZER J., SAVARESE S., and PEÑA-MORA F. (2011). “Evaluation of image-based modeling and laser scanning accuracy for emerging automated performance monitoring techniques.” Automation in Construction, 20(8):1143-1155.

[138] TANG, P., AKINCI, B., and HUBER, D. (2009). “Quantification of Edge Loss of Laser Scanned Data at Spatial Discontinuities.” Journal of Automation in Construction, 18(8):1070-1083.

[139] WEYRICH, T., PAULY, M., KEISER, R., HINZLE, S., SCANDELLA, S., and GROSS, M. (2004). “Post-processing of scanned 3D surface data.” Proceedings of IEEE Eurographics Symposium on Point-Based Graphics, ETH Zurich, Switzerland, June 2-4, 2004.

[140] ZWICKER, M., PAULY, M., and GROSS, M. (2002). “Pointshop 3D: An interactive system for point-based surface editing.” Proceedings of Computer Graphics SIGGRAPH 2002, pages 322-329, San Antonio, TX, July 2002.

[141] ALEXA, M., BEHR, J., COHEN-OR, D., FLEISHMAN, S., LEVIN, D., and SILVA, C. (2001). "Point set surfaces." Proceedings of IEEE Visualization, page 21-28, San Diego, CA, October 2001.

[142] TEIZER, J., HAAS, C.T., CALDAS, C.H., and BOSCHE, F. (2006). "Applications for real-time 3D modeling in transportation construction." Proceeding on 9th International Conference on Applications of Advanced Technology in Transportation, Chicago, Illinois, 123-128.

[143] TAN, P., STEINBACH, M., and KUMAR, V., (2006). Introduction to data mining. Chapter 8: Cluster analysis: basic concepts and algorithm. Pearson Addison Wesley, ISBN-0321321367.

[144] GONG, J., and CALDAS, C.H. (2008). "Data processing for real-time construction site spatial modeling." Automation in Construction, 17:526-535.

[145] ESTER, M., KRIEGEL, H. P., SANDER, J., and XU, X. (1996). "A density-based algorithm for discovering clusters in large spatial databases with noise". Proceedings of the Second International Conference on Knowledge Discovery and Data Mining (KDD-96). AAAI Press. pp. 226–231. ISBN 1-57735-004-9.

[146] CHENG, T., VENUGOPAL, M., TEIZER, J., and VELA, P.A. (2011). "Performance evaluation of Ultra Wideband technology for construction resource location tracking in harsh environments." Automation in Construction, Elsevier, 20(8):1173-1184.

[147] AL-HUSSEIN, M., ALKASS, S., and MOSELHI, O. (2005). "Optimization algorithm for selection and on site location of mobile cranes." Journal of Construction Engineering and Management, 131(5):579–590.

[148] Division of Occupational Safety and Health, (2011). "Health hazards in construction", Washington State Department of Labor and Industries. May 2011. <wisha-training.lni.wa.gov/training/presentations/HealthHaz.pps>, (Accessed, August 23, 2012).

[149] MARKS, E., and TEIZER, J., (2012). "Proximity sensing and warning technology for heavy construction equipment operation." Proceedings of Construction Research Congress, West Lafayette, USA, pp. 981-990.

[150] Occupational Safety and Health Administration, "Hazardous and toxic substances." <http://www.osha.gov/SLTC/hazardoustoxicsubstances/index.html>, (Accessed, August 23, 2012)

[151] LEVINE, L., (2008). "Worker safety in construction industry: The crane and derrick standard." Congressional Research Services Report for Congress. Released on November 21, 2008. <http://www.fas.org/sgp/crs/misc/RL34658.pdf>, (Accessed, August 23, 2012)

[152] Occupational Safety and Health Administration (OSHA). Fall protection. Construction Safety and Health Outreach Program, U.S. Department of Labor, OSHA office of Training and Education, May 1996. <http://www.osha.gov/doc/outreachtraining/htmlfiles /subpartm.html > (Accessed, September 17, 2012).

[153] Occupational Safety and Health Administration (OSHA). Fire protection and prevention – flammable liquids. Safety and Health Regulations for Construction. Part-1926.152. <http://www.osha.gov/pls/oshaweb/owadisp.show_document?p_id=10673&p_table=STANDARDS> (Accessed, September 18, 2012).

[154] HECKBERT, P. (1994). Graphics Games IV. Academic Press Professional, ISBN 0-12-336156-7. Boston, 1994.

[155] THOMAS, H.R. (1991). "Labor productivity and work sampling: the bottom line." Journal of Construction Engineering and Management, 117(3):423-444.

[156] CHENG, T., TEIZER, J., MIGLIACCIO, G., and GATTI, U. (2013). "Automated task-level activity analysis through fusion of real-time location sensors and worker's thoracic posture data." Automation in Construction, 29(1):24-39.

[157] YANG, J., CHENG, T., TEIZER, J., VELA, P.A., and SHI, Z.K. (2011). "A performance evaluation of vision and radio frequency tracking methods for interacting workforce." Advanced Engineering Informatics, 25:736-747.

[158] VAN DER MOLEN, H. F., SLUITER, J. K., and FRINGS-DRESEN, M. H. W. (2009). "The use of ergonomic measures and musculoskeletal complaints among carpenters and pavers in a 4.5-year follow-up study." Ergonomics, 52(8), 954-63.

[159] CENTER TO PROTECT WORKER'S RIGHTS (CPWR) (1999), The construction chart book, The US construction industry and its workers, 3rd Edition, CPWR, Silver Springs, MD.

[160] Bureau of Labor Statistics (BLS) (2008). Case and demographic characteristics for work-related injuries and illnesses involving days away from work, U.S. Department of Labor, Washington, DC.

[161] HARTMANN, B., and FLEISCHER, A. G. (2005). "Physical load exposure at construction sites." Scandinavian Journal of Work Environment and Health, 31(2), 88-95.

[162] SCHNEIDER, S., and SUSI, P. (1994). "Ergonomics and construction: a review of potential hazards in new construction." American Industrial Hygiene Association Journal, 55(7), 635-649.

[163] ABDELHAMID, T. S., and EVERETT, G. J. (1999). "Physiological demands of concrete slab placing and finishing work." Journal of Construction Engineering and Management, 125(1), 47-53.

[164] ASTRAND, P., RODAHL, K., DAHL, H. A., and STROMME, S. B. (2003). Textbook of work physiology, Human Kinetics, Champaign, IL.

[165] BOUCHARD, D. R., and TRUDEAU, F. (2008). "Estimation of energy expenditure in a work environment: Comparison of accelerometry and oxygen consumption/heart rate regression." Ergonomics, 51(5), 663-674.

[166] BROUHA, L. (1967). Physiology in industry, Pergamon Press, New York, NY.

[167] GARET, M., BOUDET, G., and MONTAURIER, C., (2005), "Estimating relative physical workload using heart rate monitoring: a validation by whole-body indirect calorimetry." European Journal of Applied Physiology, 94(1), 46-53.

[168] RAMSEY, J.D. (1985). "Ergonomic factors in task analysis for consumer product safety." Ergonomics, 26(5), 495-504.

[169] ABDELHAMID, T. S., and EVERETT, G. J. (2002). "Physiological demands during construction work." Journal of Construction Engineering and Management, 128(5), 427-438.

[170] MATHIASSEN, S. E., WINKEL, J., SAHLIN, K., and MELIN, E, (1993). "Biochemical indicator of hazardous shoulder-neck loads in light industry." Journal of Occupational and Environmental Medicine, 35(4), 404-413.

[171] HOOTMAN, J.M., MACERA, C.A., AINSWORTH, B.E., ADDY, C.L., MARTIN, M., and BLAIR, S.N. (2002). "Epidemiology of musculoskeletal injuries among sedentary and physically active adults." Medicine and Science in Sports and Exercise, 34(5), 838-844.

[172] ZAIDMAN, B. (2008). Workplace Safety Report 2006. Minnesota Department of Labor and Industry, St. Paul, MN.

[173] LIBERTY MUTUAL RESEARCH INSTITUTE FOR SAFETY (2008). "Liberty mutual workplace safety index." <http://www.libertymutualgroup.com/researchinstitute> (Accessed, Mar. 2, 2011).

[174] TAK, S.W., BUCHHOLZ, B., PUNNETT, L., MOIR, S., and PAQUET, V. (2011). "Physical ergonomics hazards in highway tunnel construction: overview from the construction occupational health program." Applied Ergonomics, 42(5), 665-671.

[175] WATER, T.R., ANDERSON, V.P., and GARG, A. (1994). Applications manual for the revised NOISH lifting equation, U.S. Department of Health and Human Services Public Health Service. National Institute for Occupational Safety and Health, Atlanta, GA.

[176] GATTI, U.C., MIGLIACCIO, G.C., and SCHNEIDER, S. (2011). "Wearable physiological status monitors for measuring and evaluating worker's physical strain." Proc., 2011 ASCE Workshop of Computing in Civil Engineering, ASCE, Miami, FL, 24.

[177] SPIELHOLZ, P., WIKER, S. F., and SILVERSTEIN, B. (1998). "An ergonomic characterization of work in concrete form construction." American Industrial Hygiene Association journal, 59(9), 629-35.

[178] HINZE, J. W., and WIEGAND, F. (1992). "Role of designers in construction worker safety." Journal of Construction Engineering and Management, 118(4), 677-684.

[179] HECKER, S., and GAMBATESE, J. A. (2003). "Safety in design: a proactive approach to construction worker safety and health." Applied Occupational and Environmental Hygiene, 18(5), 339-342.

[180] HESS, J. A., HECKER, S., WEINSTEIN, M., and LUNGER, M. (2004). "A participatory ergonomics intervention to reduce risk factors for low-back disorders in concrete laborers." Applied Ergonomics, 35(5), 427-41.

[181] ALPHIN, M. S., SANKARANARAYANASAMY, K., and SIVAPIRAKASAM, S. P. (2010). "Experimental evaluation of whole body vibration exposure from tracked excavators with hydraulic breaker attachment in rock breaking operations." Journal of Low Frequency Noise Vibration and Active Control, 29(2), 101-110.

[182] GOODRUM, P.M., HAAS, C.T., CALDAS, C.H., ZHAI, D., YEISER, J., and HOMM, D. (2010). "A model to predict a technology's impact on construction productivity." Journal of Construction Engineering and Management, 137(9), 678-688.

[183] WHITE, E.F. (1987). "Data fusion lexicon", Joint Directors of Laboratories, Technical Panel for C3, Data Fusion Sub-Panel, Naval Ocean Systems Center, San Diego, 1987.

[184] STEINBERG, A.N., and BOWMAN, C.L. (2011). Revision to the JDL data fusion model, Handbook of Multisensor Data Fusion, CRC Press, 2011, pp. 18.

[185] VARSHNEY, P. K. (1997). "Multisensor data fusion." Electronics and Communication Engineering Journal, 9(6), 245-253.

[186] HALL, D.L., and LLINAS, J. (1997). "An introduction to multisensor data fusion." Proceedings of the IEEE, 85(1), 6-23.

[187] RAZAVI, S. N., and HAAS, C. T. (2010). "Multisensor data fusion for on-site materials tracking in construction." Automation in Construction, 19(8), 1037-1046.

[188] RAZAVI, S. N., and HAAS, C.T. (2011). "A reliability-based hybrid data fusion method for adaptive location estimation in construction", ASCE Journal of Computing in Civil Engineering, doi: 10.1061/(ASCE)CP.1943-5487.0000101.

[189] PRADHAN, A., AKINCI, B., and HAAS, C. T. (2011). "Formalisms for query capture and data source identification to support data fusion for construction productivity monitoring." Automation in Construction, 20(4), 389-398.

[190] SHAHANDASHTI, S. M., RAZAVI, S. N., SOIBELMAN, L., BERGES, M., CALDAS, C. H., BRILAKIS, I., TEIZER, J., VELA, P. A., HAAS, C., GARRETT, J., AKINCI, B., and ZHU, Z. (2011). "Data-fusion approaches and applications for construction engineering." Journal of Construction Engineering and Management, 137(10), 863-869.

[191] TEICHOLZ, P. "Labor productivity declines in the construction industry: causes and remedies." AECbytes Viewpoint, http://www.aecbytes.com/viewpoint/2004/issue_4.html (Accessed, October 15, 2011).

[192] ALLMON, E., BORCHERDING, J.D., and GOODRUM, P.M. (2000). "U.S. construction labor productivity trends 1970-1998." ASCE Journal of Construction Engineering and Management, 126(2): 97-104.

[193] GU, W. and HO, M.S. (2000). "A comparison of industrial productivity growth in Canada and in the United States." American Economic Review, 90(2): 172-175.

[194] ARDITI, D. and Krishna, M., (2000). "Trends in productivity improvement in the US construction industry." Construction Management and Economy, 18:15–27.

[195] ALLEN, S.G. (1985). "Why construction industry productivity is declining." The Review of Economics and Statistics, 67(4): 661-669.

[196] PIEPER, P. (1989). "Why construction labor productivity is declining: Comment." The Review of Economics and Statistics. 71(3): 543-546.

[197] GULLICKSON W. and HARPER, M.J. (1999). "Possible measurement bias in aggregate productivity growth." Monthly Labor Review, 122(2): 47-48.

[198] TRIPLETT J.E. and BOSWORTH, B. (2004). Productivity in the U.S. Services Sector: New sources of economic growth, Brookings Institution Press, 2004.

[199] DYER B.D. and GOODRUM, P.M. (2009). "Construction industry productivity: omitted quality characteristics in construction price indices." Proceedings of the 2009 Construction Research Congress, Seattle, WA, 2009.

[200] HARRISON, P. (2007). "Can measurement error explain the weakness of productivity growth in the Canadian construction industry." Research Report by the Center for the Study of Living Standards for the Construction Sector Council, April 2007, Ottawa, ON, Canada.

[201] GOODRUM, P.M. and HAAS, C.T. (2002). "Partial factor productivity and equipment technology change at activity level in U.S. construction industry." ASCE Journal of Construction Engineering and Management, 128(6): 463-472.

[202] Bureau of Labor Statistics (BLS), (2012a). American Community Survey 2006.

[203] Bureau of Labor Statistics (BLS), (2012b). American Community Survey 2010, 1-year estimates, 2012b.

[204] SCHWATKA, N.V., BUTLER, L.M., and ROSECRANCE, J.R., (2011). "An aging workforce and injury in the construction industry." Epidemiologic Reviews, 34, 156-167.

[205] GHANEM, A.G., and ABDEL RAZIG, Y.A., (2006). "A Framework for real-time Construction project progress tracking." Proceeding of the 10th Biennial International Conference on Engineering, Construction, and Operations in Challenging Environments pp. 1-8. Reston, VA. 2006.

[206] JENKINS, J.L. and ORTH, D.L., (2004). "Productivity improvement through work sampling." Cost Engineering, 46(3), 27-33.

[207] CALDAS, C.H., GOODRUM, P.M., and CHASTAIN, D., (2009). "Effortless productivity tracking, Construction Industry Institute (CII)." Retrieved from <https://www.construction-institute.org/scriptcontent/btsc-pubs/CII-BTSC-121.doc> (Accessed, October 28 2009).

[208] PARK, H.S., THOMAS, S.R., and TUCKER, R.L., (2005). "Benchmarking of construction productivity." ASCE Journal of Construction Engineering and Management, 131(7), 772.

[209] CHANG, L., (1991). "A methodology for measuring construction productivity." Cost Engineering, 3(10), 19-25.

[210] HOWELL, G.A., BALLARD, B., TOMMELEIN, I.D., and KOSKELA, L., (2004). "Discussion of Reducing Variability to Improve Performance as a Lean Construction Principle." ASCE Journal of Construction Engineering and Management.130:299-308.

[211] BALLARD, G., and Howell, G., (2003). "Lean project management." Building Research and Information, 31(2), 119-133.

[212] CHAPMAN, R.E., BUTRY, D.T., and HUANG, A.L., (2010). "Measuring and Improving U.S. Construction Productivity." CIB W117 Performance Measurement Special Track, Proceedings of 18th CIB World Building Congress, May 2010, Salford, UK, 1-12.

[213] GONG, J., and CALDAS, C.H., (2010). "Computer vision-based video interpretation model for automated productivity analysis of construction operations." ASCE Journal of Computing in Civil Engineering, 24(3): 252-263.

[214] MCCULLOUCH, B., (2010). "Automating field data collection in construction organizations." Proceeding of the 5th Construction Congress: Managing Engineered Construction in Expanding Global Markets, ASCE, Reston, VA., 957-963, 2010.

[215] CHEOK, G S., STONE, W.C., LIPMAN, R.R., and WITZGALL, C., (2000). "Ladars for construction assessment and update." Automation in Construction, 9(5), 463–477.

[216] CRAWFORD, P. and VOGL, B. (2006). "Measuring productivity in the construction industry." Building Research and Information, 34(3): 208-219.

[217] LIU, C. and SONG, Y.U. (2005). "Multifactor productivity measures of construction sectors using OECD input-output database." Journal of Construction Research, 6(2): 209-222.

[218] THOMAS, H.R. and MATHEWS, C.T. (1986). "An analysis of the methods for measuring construction productivity." the University of Texas at Austin: Source Document 13, Construction Industry Institute (CII), 1986.

[219] Organization for Economic Co-operation and Development (OECD), (2010). Measurement of Aggregate and Industry-Level Productivity Growth, OECD Manual, 2010.

[220] Construction Industry Institute (CII), (2010). "Guide to activity analysis, Craft Productivity Research Program Research Team." Implementation Resource 252-2a. July 2010.

[221] ADRIAN, J.J., and BOYER, L.T., (1979). "Modeling method productivity." Journal of the Construction Division, 102(1), 157-168.

[222] Construction Industry Institute (CII), (1990). "Productivity measurement: an introduction - research summary 7-1." Austin, TX, 1990.

[223] CHITESTER, D.D. (1992). "Model for analyzing jobsite productivity, Transactions of the American Association of Cost Engineers, 1, C.3.1-C.3.5." American Association of Cost Engineers – AACE.

[224] GOUETT, M., HAAS, C., GOODRUM, P., and CALDAS, C., (2011). "Activity analysis for direct-work rate improvement in construction." ASCE Journal of Construction Engineering and Management. 137(2): 1117-1124.

[225] IBRAHIM, Y., LUKINS, T., ZHANG, X., TRUCCO, E., and KAKA, A., (2009). "Towards automated progress assessment of work package components in construction projects using computer vision." Advanced Engineering Informatics, Elsevier, 23(1), 93-103.

[226] ABEID, J., and ARDITI, D., (2002). "Linking time-lapse digital photography and dynamic scheduling of construction operations." Journal of Computing in Civil Engineering, 16: 269-279.

[227] BOLIVAR, A., and MEE, A.S., (1997). "Activity analysis using computer-processed time lapse video." Proceeding of 1st Congress held in conjunction with A/E/C system, ASCE, Reston, VA, 1405-1411.

[228] EVERETT, J.G, and PEÑA -MORA, F., (2007). "Application of visualization techniques for construction progress monitoring." Proceeding of 2007 International Workshop in Civil Engineering, ASCE, Reston, VA, 216-223.

[229] GOLPARVAR-FARD, M., PEÑA-MORA, F., and SAVARESE, S., (2012). "Automated Progress Monitoring Using Unordered Daily Construction Photographs and IFC ‐ Based Building Information Models." ASCE Journal of Computing in Civil Engineering, http://dx.doi.org/10.1061/(ASCE)CP.1943-5487.0000205, in press.

[230] BRILAKIS, I., PARK, M.W., and JOG, G., (2011). "Automated vision tracking of project related entities." Journal of Advanced Engineering Informatics, Elsevier, 25(4):713-724.

[231] YANG, J., ARIF, O., VELA, P.A., TEIZER, J., and SHI, Z., (2010). "Tracking multiple workers on construction sites using video cameras." Advanced Engineering Informatics, Elsevier, 24(4):428-434.

[232] CHENG, T., MIGLIACCIO, G.C., TEIZER, J., and GATTI, U. C., (2012). "Data fusion of real-time location sensing (RTLS) and physiological status monitoring (PSM) for ergonomics analysis of construction workers." ASCE Journal of Computing in Civil Engineering, http://dx.doi.org/10.1061/(ASCE)CP.1943-5487.0000222, in press.

[233] SAMARASOORIYA, V. and VARSHNEY. P K., (1997). "Decentralized signal detection with fuzzy information." Optical Engineering, 36, 685-694.

[234] HAMMAD, A., WANG, H., and MUDUR, S. P. (2005). "Distributed augment reality for visualizing collaborative construction tasks." Journal of Computing in Civil Engineering, 23(6):418-427.

[235] Setareh, M., Bowman, D., and Kalita, A. (2005). "Development of VSAP, a virtual reality structural analysis system." Journal of Architecture and Engineering, 11(4): 156-164.

[236] MALDOVAN, K., MESSNER, J.I., and FADDOUL, M. (2006). "Framework for reviewing mockups in an immersive environment." Proceeding in 6th International Conference on Construction Applications of Virtual Reality, (2006) Aug. 3-4, Orlando, FL.

[237] FERNANDES, J.K., RAJA, V., WHITE, A., and TSINOPOULOS, C. (2006). "Adoption of virtual reality within construction processes: a factor analysis approach." Technovation 26(1):111-120.

[238] MESSNER, J. and HORMAN, M. (2003). "Using advanced visualization tools to improve construction education." Proceedings in Conference on Construction Applications of Virtual Reality (CONVR) (2003), Blacksburg, VA., 145-155.

[239] KALISPERIS, L., OTTO, G., MURAMOTO, K., GUNDRUM, J., MASTERS, R., and ORLAND, B. (2002). "An affordable immersive environment in beginning design studio education." Proceedings on Annual Conference of the Association for Computer Aided Design in Architecture, Pomona, CA, Va., 49-56.

[240] MOLONEY, J. and AMOR, R. (2003). "StringCVE: Advances in a game engine-based collaborative virtual environment for architectural design." Proceeding in Conference on Construction Applications of Virtual Reality (CONVR), Blacksburg, VA., 156–168.

[241] LIPMAN R. and REED, K. (2000). "Using VRML in construction industry applications." Proceedings of the Annual Symposium on the Virtual Reality Modeling Language, VRML, 119-124.

[242] MCKINNEY. K. and FISCHER. M. (1998). "Generating, evaluating and visualizing construction schedules with CAD tools." Automation in Construction, 7:433–447.

[243] KOO, B., and FISCHER, M. (2000). "Feasibility study of 4D CAD in commercial construction." Journal of Construction Engineering and Management, 126(4):251–260.

[244] HUANG, D., TORY, M., SRAUB, S., and POTTINGER, R. (2009). "Visualization techniques for schedule comparison." IEEE-VGTC Symposium on Visualization, (28).

[245] BANSAL, V.K. and PAL, M. (2008). "Generating, Evaluating, and visualizing construction schedule with geographic information systems." Journal of Computing in Civil Engineering. 22(4):233-242.

[246] CHAU, K.W., ANSON, M., and ZHANG, J.P. (2003). "Implementation of visualization as planning and scheduling tool in construction." Building and Environment, 3:713-719.

[247] HADIKUSUMO, B.H.W. and ROWLINSON, S. (2002). "Integration of virtually real construction model and design-for safe-process database." Automation in Construction, (11):501-509.

[248] ISSA, R., FLOOD, I., and O'BRIEN, W.J. (2003). "4D CAD and visualization in construction: Developments and applications." Balkema, Rotterdam, The Netherlands, 281–284

[249] KAMAT, V.R. and MARTINEZ, J.C. (2003). "Automated generation of dynamic, operations level virtual construction scenarios." Electronic Journal of Information Technology in Construction (ITcon), (8) Special Issue on Virtual Reality.

[250] KAMAT, V.R. and MARTINEZ, J.C. (2005). "Dynamic 3D visualization of Articulated Construction Equipment." Journal of Computing in Civil Engineering, 19(4):356-365.

[251] KAMAT, V.R. and MARTINEZ, J.C. (2008). "Generic representation of 3D motion paths in dynamic animations of simulated construction processes." Automation in Construction, 17(2): 188-200.

[252] REKAPALLI, P.V., MARTINEZ, J.C., and KAMAT, V.R. (2008). "VR. Algorithms for accurate three-Dimensional scene graph updates in high speed animations of simulated construction operations." Journal of Computer-Aided Civil and Infrastructure Engineering, 24 (3): 1-13.

[253] BOUCHLAGHEN, N., WILSON, A., and BEACHAM, N. (2002). "Computer imagery and visualization in built environment education: The CAL-Visual approach." Innovations in Education and Teaching International,39(3):225-236.

[254] ISSA, R.R.A., COX, R.F., and KILLINGSWORTH, F.C. (1999). "Impact of multimedia-based instruction on learning and retention." Journal of Computing in Civil Engineering 13(4):281-290.

[255] LIAW, Y.L., LIN, K.Y., LI M., and CHI, N.W. (2012). "Learning assessment strategies for an educational construction safety video game." Proceeding in Construction Research Congress, May 21-23, West Lafayette, IN.

[256] ESMAEILI B., and HALLOWELL, M. (2012). "Attribute-based risk model for measuring safety risk of struck-by accidents." Proceeding in Construction Research Congress, (2012), May 21-23, West Lafayette, IN.

[257] SANTAMARIA C.J. and OPDENBOSCH. A. (2002). "Monitoring underwater operations with virtual environments." Proceedings in 2002 Offshore Technology Conference, Houston TX.

[258] FERNANDES, J.K., Raja, V., and EYRE, J. (2003). "Immersive learning systems for manufacturing industries." Computers in Industry, 51:31-40.

[259] AZUMA, R., BAILLOT, Y., BEHRINGER, R., FEINER, S., JULIER, S., and MACINTYRE, B. (2001). "Recent advances in augmented reality." IEEE Computer Graphic Application, 21(6):34-37.

VITA

Tao Cheng received his Ph.D. from the School of Civil and Environmental Engineering at the Georgia Institute of Technology. His research areas included Construction Engineering, Construction Safety and Productivity Measurement, Real-time Remote Sensing Technology, Real-time Visualization Technology, and Data Mining. His research aimed to enhance the measurements of the safety and productivity performance of construction workers. Tao completed his Bachelor of Science degree in Theoretical and Applied Mechanics from the Peking University, Beijing, China, in 2003. Since then, he pursued the first Master degree in Space Physics at the Chinese Academy of Science (CAS), and completed it in 2006. In the same year, he started his second Master degree in Civil Engineering at the Technische Universität Dresden, Germany. After receiving the second Master degree in 2008, he joined the Real-time Automated Project Information and Decision Systems (RAPIDS) lab at the Georgia Institute of Technology to pursue his doctoral research titled *Automated Safety Analysis of Construction Site Activities Using Spatio-Temporal Data*. At Georgia Tech, Tao was directly responsible for conducting experiments with various technologies including laser scanning, Radio Frequency Identification (RFID), Ultra-Wideband (UWB), Global Positioning System (GPS), and Building Information Modeling (BIM). With the implementation of these technologies, he has played a leading role in the development of new techniques for pro-active construction safety. His research was recognized by Construction Research Council and Construction Industry Institute, as two of the largest research organizations of construction engineering and management in North America. By the time of graduation, his research findings have been published in ten journal papers and numerous conference proceedings.